« As they sailed up the River Nile, the ancient Greeks noticed that it became warmer. Being logical in their search for explanation, they assumed that the Earth must slope towards the sun. »
The word 'climate' traces its roots from this now discredited deduction, being derived from a Greek word meaning 'slope'.

Climate change is an inherent characteristic of climate. What is normal now may turn out to be very abnormal when a longer time perspective is employed. This implies a need for establishing the range of climate conditions existing in the past.

Palaeoclimate work is the only reliable tool to reconstruct climate conditions in the past and to evaluate how fast natural systems can change.

This thesis investigates past climate change in the mid-latitudes (30-60°S) of the Southern Hemisphere. These latitudes are wedged inbetween two major climate drivers: the Antarctic system and the Tropics. The region itself is lashed by the howling Southern Westerly winds, an important global wind system that is still poorly understood. The main focus of this research is attempting to better understand the behaviour of this Southern Westerly wind system through time and to unravel which climatic driver is the puppeteer pulling these winds' strings.

RCMG

Faculteit Wetenschappen

UNIVERSITEIT GENT

FWO VLAANDEREN

Katrien Heirman

'A Wind of Change':

'A Wind of Change':

Changes in Position and Intensity of the Southern Hemisphere Westerlies during Oxygen Isotope Stages 3, 2 and 1

Katrien Heirman

'A Wind of Change':

Changes in the Position and Intensity of the Southern Hemisphere Westerlies during Oxygen Isotope Stages 3, 2 and 1

'Een Wind van Verandering':

Wijzigingen in de Positie en Intensiteit van de Westenwinden in het Zuidelijke Halfrond gedurende Zuurstofisotoopetages 3, 2 en 1

Katrien Heirman

2011

Thesis submitted to the degree
of Doctor of Science: Geology

Fonds Wetenschappelijk Onderzoek
Research Foundation – Flanders

Research funded by FWO - Vlaanderen

Members of the reading committee:

Prof. Dr. Marc De Batist (Ghent University, Belgium): Supervisor
Prof. Dr. Nathalie Fagel (Université de Liège, Belgium)
Dr. Santiago Giralt (Institut de Ciències de la Terra Jaume Almera, Spain)

Members of the examination committee:

Prof. Dr. Jacques Verniers (Ghent University, Belgium): chair
Prof. Dr. Marc De Batist (Ghent University, Belgium): Supervisor
Prof. Dr. Nathalie Fagel (Université de Liège, Belgium)
Dr. Santiago Giralt (Institut de Ciències de la Terra Jaume Almera, Spain)
Dr. Stephen Roberts (British Antarctic Survey, United Kingdom)
Prof. Dr. Stephen Louwye (Ghent University, Belgium)
Prof. Dr. David Van Rooij (Ghent University, Belgium)
Prof. Dr. Wim Vyverman (Ghent University, Belgium)

Katrien Heirman carried out the research with financial support of the Research Foundation - Flanders (FWO - Vlaanderen).

This research project was conducted at the Renard Centre of Marine Geology, Ghent University (Ghent, Belgium).

To refer to this thesis: Heirman, K., 2011. 'A Wind of Change': Changes in Position and Intensity of the Southern Hemisphere Westerlies during Oxygen Isotope Stages 3, 2 and 1. PhD thesis, Ghent University, Belgium.

I've been climbing rocks and stones
been collecting broken bones
I've been swimming across the lakes
just to find this perfect place

I got lost into the woods
I've been covered up in mud
I've been going through a lot
just to find this perfect spot

(Lycris from "Treehouse", I'm from Barcelona)

Table of Contents

List of Figures

List of Tables

List of Abbreviations

AAO: Antarctic Oscillation
ACC: Antarctic Circumpolar Current
ACR: Antarctic Cold Reversal
AD: Anno Domini (Since Birth of Jesus)
AF: Alternating Field
ALST: Annual Lake Surface Temperature
AMOC: Atlantic Meridional Overturning Circulation
AMS: Accelerator Mass Spectrometry
ARM: Anhysterestic Remanent Magnetization
ASL: Above Sea Level
AVZ: Austral Andean Volcanic Zone (49-55°S)
BIT: Branched vs. Isoprenoid Tetraether Index
BP: Before Present (Before 1950 AD)
CBT: Cyclisation Index of Branched Tetraethers
CTD: Conductivity-Temperature-Depth sensor
CVZ: Central Andean Volcanic Zone (14-27°S)
D: Declination
D-O: Dansgaard-Oeschger event
ENSO: El Niño - Southern Oscillation
EPICA: European Project for Ice Coring in Antarctica
GDGT: Glycerol Dialkyl Glycerol Tetraethers
H: Heinrich Events
I: Inclination
IRM: Isothermal Remanent Magnetization
ITCZ: Intertropical Convergence Zone
k: low field Magnetic Susceptibility
LGM: Last Glacial Maximum
LIA: Little Ice Age
LOI: Loss-On-Ignition
LSCE: Laboratoire des Sciences du Climat et de l'Environnement
MAAT: Mean Annual Air Temperature
MAD: Maximum Angular Deviation
MBT: Methylation Index of Branched Tetraethers
MCA: Medieval Climate Anomaly
MS: Magnetic Susceptibility
MSCL: Multi-Sensor Core Logger

NGRIP: North Greenland Ice Core Project
NIOZ: Nederlands Instituut voor Onderzoek der Zee (Royal Netherlands Institute for Sea Research)
NOCS: National Oceanography Centre Southampton
NRM: Natural remanent magnetization
NVZ: Northern Andean Volcanic Zone (5°N-2°S)
OIS: Oxygen Isotope Stage
PAE: Protistology and Aquatic Ecology
PSA: Particle Size Analysis
RCMG: Renard Centre of Marine Geology
RPI: Relative Palaeointensity
SEM: Scanning Electron Microscope
SST: Sea Surface Temperature
SV: (geomagnetic) Secular Variations
SVZ: Southern Andean Volcanic Zone (33-46°S)
SWW: Southern Westerly Winds
TEX86: Tetraether Index of Tetraethers with 86 carbon atoms
TN: Total Nitrogen
TOC: Total Organic Carbon
TWT: Two-Way Travel Time
XRD: X-Ray Diffractometry
XRF: X-Ray Fluorescence Scanning
YD: Younger Dryas
2D: Two-dimensional
3D: Three-dimensional

Thank You!

Tist, Jasper, Maarten, Anita, Evelien, Steve, Alejandro, Sébastien, Koen, Mario, Roberto, Robert, Javiera, Manuel, Paulina, Alvaro, Rolf, Marcelo, Franz, Carolina, Rodrigo, Patricio, Jean-Pierre, Estéban, Lorena, Rolo, Mieke, Jeroen, Tuco, Dries, Fabien, Roland, Ricardo Luís, Sebastián, Andres, Nathalie, Dirk, Danielle, Michael, Nicole, Veerle, Sabine, Jan, Aurelia, Philippe, Adrian, Gerald, Flavio, Dierk, Ursula, Vera, Jens, Rineke, Rik, Jord, Jaap, Veerle, Eddy, Michael, Willem, Sofie, Wouter, Anouk, Camille, Ben, Mieke, Hans, Matthias, Rindert, Marc, Sonia, Andres, Lieven, Jean-Pierre, Wim, Jeroen, David, Tine, Arne, Kristien, Els, Isabelle, Mario, Lies, Peter, Vera, Thomas, Anneleen, Davy, François, Kurt, Elie, Wim, Margo, Catherine, Camille, Stephanie, Heleen, Victor, Kirsty, Dave, Jenny, Liam, Cat, Ling, Holly, Adam, Clara, Luke, Phil, Yolanda, Sam, Chris Julie, Ann, Thomas, Jan, Koen, Kenneth, Jan, Marijn, Tim, Ines, Liesbet, Mieke, An, Eva, Kobe, Stijn, Annelies, Annelies, Maarten, Carolien, Eveline, Dominique, Helena, Hans, Wendi, Mira, Marijke, Manu, David, Johan, Axelle, Katleen, Toon, Kaat, David, Dries, Lotte, Anna, Sara, Maarten, Sander, Diederik, Ana, Caroline, Tip, Klong, Kirra, Ryoko, Jonny, Kim, Krystyna, Gabrielle, Rocio, Michael, Nick, Rachel, Olga, Howie, Laura, Debra, Yuribia, Irene, Fabio, Nicoletta, Lorenzo, Marinella, Teo, Alessandra, Laila, Manu, Silke, Oma, Opa, Oma, Opa, Tantes, Nonkels, Neefjes, Nichtjes, Melissa, Sieglien, Gert, Toon, Mama & Papa

My sincere apologies to everyone I might have forgotten

Summary

Climate has varied continuously on all timescales. Irrespective of the extent to which human activities lead to changes in the global climate system, it will continue to vary in the future. This is unquestioned; doubts surround only the nature of change and future variability and the degree to which the consequences of human activities will influence or perhaps even dominate it.

In many parts of the world the public has become highly aware of the issues concerning climate change in recent years as individual extreme events have forced a reappraisal of what is meant by 'normal'. In the past, it was common for a few decades of meteorological observations to be taken as indicative of the likely range of conditions which would be experienced at a certain place. But all this inherently assumed a stable climate, one for which a baseline established on data from the past could be relied upon to provide safe guidance for the future. If the climate is changing, such an approach is fundamentally flawed.

Palaeoclimate work is the only reliable tool to reconstruct climate conditions in the past and to evaluate how fast natural systems can change.

The focus for much of this work has centred on the termination of the last ice age. The primary reason for this is that the warming associated with this termination is of similar or even larger magnitude than the human-induced climate modification expected under future greenhouse-gas scenarios, although the rate of change was much slower.

Climate encompasses the statistics of temperature, humidity, atmospheric pressure, wind, rainfall, atmospheric particle count and other meteorological elemental measurements in a given region over long periods of time. Variations and changes in these parameters are orchestrated by changes in solar radiation and the five interrelated climate components: atmosphere, hydrosphere, cryosphere, biosphere and geosphere. Regardless of man's efforts to understand these five components and how they affect each other, the comprehension of this system is as sensitive to change as current climate. Even though many decades of palaeoenvironmental research have gone by, we still do not have adequate understanding of the patterns of change over huge swatches of the globe's surface, and, in particular, the Southern Hemisphere.

An important Southern Hemisphere climate component are the Southern Westerlies. These are the prevailing winds in the southern mid-latitudes (30-60°S) of Earth's atmosphere, blowing from west to east between the high-pressure areas of the subtropics and the low-pressure areas near Antarctica. This wind system exhibits considerable variability on intra- and inter-annual time scales.

Until the early 1990s, the Westerlies were generally not regarded as a particularly important component of the global climate system. Now, it is assumed that the Southern Westerlies, in conjunction with the Antarctic Circumpolar Current, regulate meridional heat flux and the concentration of atmospheric carbon dioxide, and rapidly transmit climatic signals like El Niño-Southern Oscillation (ENSO). Changes in Westerly intensity over time will enhance or diminish these climatic controls.

This thesis investigates past climate change in the southern part of the world, more

particularly in the mid-latitudes of the Southern Hemisphere using lake sediments. Being relatively small bodies of water in comparison with the oceans, lakes can respond relatively quickly to an external forcing variable such as climate. The response of the lake system to such change will leave traces in the sediment which accumulates on the bottom of the lake. The main focus of this research is to better understand the behaviour of this Southern Westerly wind system during the last 45000 years of the Earth's history.

Two types of techniques were used to study these sediments. First of all a seismic survey was performed. With this technique an acoustic image of the entire lake basin infill is created. This allows a quasi three dimensional reconstruction of the sediment accumulation in the basin. Consequently the evolutionary history of this basin can be reconstructed. The resolution of this technique is, however, rather low (e.g. millenial time scale). Therefore, short term variations will not be represented in such a record. To bypass this limitation, sediment cores can be taken of the same lake sediment. A sediment core record will not span the same large time span as a seismic record, nor will it allow a three dimensional reconstruction, but it will allow the reconstruction of climatic variations on a high resolution time scale (centennial to decadal scale). Combining both techniques the climatic history of a region can be unravelled in all of its aspects.

The seismic stratigraphy of four lakes was studied in detail: three lakes in the Chilean Lake District (Lago Villarrica, Lago Calafquén, Lago Panguipulli and Lago Riñihue at 39-40°S) and one lake in the Kerguelen Archipelago (Lac d'Armor at 49°S). In most parts of the lake basins the high-resolution seismic reflection surveys exposed the complete lake-basin infill allowing a good reconstruction of the evolution of the different lake basins.

The high-resolution reflection seismic profiles of four lakes in the Chilean Lake District revealed the presence of four important seismic unconformities in each lake basin. All four unconformities in the Chilean lakes were probably created by glacial activity. The fact that such unconformities are present indicates that the last advances and retreats of the glaciers in each of these four basins were less extensive, less powerful and probably not as long lasting than the glacial advances which created the oldest unconformity. This information can be considered as a sign that the climatic situations in the mid-latitudes of the Southern Hemisphere were different from the Northern Hemisphere were the glacier advances during OIS 2 were the most extensive of the entire last glacial period. Since no absolute ages are available for the four unconformities, it is difficult to create a time frame for these events. Advances of the glaciers in the Southern Andes during the last century, in the Holocene and during the last glacial period have been linked to periods of more intense Southern Westerlies. Consequently these unconformities might mark the initiation of periods of more intense Westerlies during the last glacial period.

The seismic stratigraphy of Lac d'Armor has one very remarkable feature: the formation of sediment drift deposits during the deposition of the youngest seismic unit. Such a construction indicates the presence of strong bottom currents. A likely creator of such currents is wind. Currently the force of the Southern Westerly wind in Kerguelen should not be underestimated. The sudden onset of these sediment drifts argues for a sudden strengthening of the Southern Westerlies somewhere in the Holocene. Again an absolutely dated time frame is missing for this seismic records, so only estimates can be made for its timing.

Sediment cores were collected in two lakes in Chile: one in Lago Villarrica (39°S) and one in Laguna Parrillar (53°S). The 14m sediment core of Lago Villarrica only spans

the Holocene (sediment core bottom age of ca. 9500 cal a BP). The 7 m sediment core of Laguna Parrillar spans a much longer period of time (sediment core bottom age of ca. 44000 cal a BP). The analysis of the sediment cores was particularly useful in determining the timing of variations of the Southern Westerlies' wind strength and position.

The 44000 year long sediment record of Laguna Parrillar revealed drastic changes in the Southern Westerly wind's intensity. From 44000 cal a BP until ca. 12500 cal a BP the lake environment and lake level was mostly controlled by the thickness of its glacial dam, since the main outlet was blocked by the Magellan Strait glacier. When the Magellan Strait glacier receded the lake level would have been lower. As glacier advances are largely controlled by Westerly wind intensity, a retreat of the glacier dam reflected a decrease in the Southern Westerly wind strength. Another important factor affecting the lake sedimentation is the duration of the ice cover of the lake. During cold periods, probably associated with strong Westerlies, the lake was covered by ice the entire year. In times of weaker Southern Westerlies there might have been ice-free lake water periods. After 12500 cal a BP the sedimentation in the lake basin became controlled by the wind, the Southern Westerly wind. A first sign of Holocene Westerly wind strengthening appears around 7800 cal a BP, when wind strength appears to decrease again. The most obvious strengthening of the Southern Westerlies occurred at ca. 4000 cal a BP.

A sediment record of Lago Villarrica disclosed information about Holocene changes in the strength and position of the Southern Westerlies. During the Early Holocene the Southern Westerlies' strength was weakened and/or the Westerlies had shifted more poleward. Around 6000 cal a BP the Southern Westerlies' influence increased in the area, but the largest intensification occurred around 4000 cal a BP.

In Lago Villarrica also an El Niño Southern Oscillation signal was detected. ENSO currently creates large interannual variations in the climate of north and central Chile. The Lago Villarrica lake record, however, indicates that an ENSO influence might have been present in the Early Holocene.

All of these records show changes in the intensity of the Southern Hemisphere Westerlies. When absolute ages are available these changes seem to be rather synchronous at both 39°S and 53°S, therefore not really indicating clear shifts of the Southern Westerlies. There is, however, a slight asynchronous behaviour during the last 1000 years, a period during which the influence of the El Niño Southern Oscillation is stronger South Central Chile.

Samenvatting

Het klimaat varieert continu doorheen de tijd. Onafhankelijk van de reikwijdte van de invloed van menselijke activiteiten op het globale klimaatsysteem, zal het klimaat blijven variëren in de toekomst. Dit is onbetwistbaar; alleen de aard van de verandering, de toekomstige variabiliteit en de mate waarin de gevolgen van menselijke activeiten het klimaat zullen beïnvloeden of misschien zelfs zullen domineren zijn twijfelachtig.

Recent is de mensheid meer en meer ontvankelijk geworden voor het fenomeen klimaatverandering, aangezien extreme klimaatmanifestaties ons dwingen om het begrip 'normaal' te heroverwegen. In het verleden gebruikte men enkele decennia van meteorologische observaties om de draagwijdte van klimaatcondities op een welbepaalde plaats te kunnen evalueren. Deze methode veronderstelt echter dat het klimaat stabiel is en dat deze basis gebruikt kan worden als veilige richtlijn voor toekomstvoorspellingen. Indien het klimaat echter verandert, is deze benadering echter incorrect.

Paleoklimaatwerk is het enige betrouwbare werktuig om klimaatcondities uit het verleden te reconstrueren en om te kunnen evalueren hoe snel natuurlijke systemen kunnen veranderen.

De focus van de meerderheid van dit werk richt zich op het einde van de laatste ijstijd. Dit is voornamelijk, omdat de opwarming van de aarde op het einde van de laatste ijstijd vergelijkbaar is of zelfs van een grotere magnitude dan de door de mens geïnduceerde klimaatveranderingen verwacht voor de toekomst, zij het dan aan een veel tragere snelheid.

Klimaat omvat de statistiek van temperatuur, vochtigheid, atmosferische druk, wind, regen en andere meteorologische metingen in een bepaalde regio gedurende een lange periode. Variaties en veranderingen van deze parameters worden georkestreerd door veranderingen in de zonnestraling en de vijf geïnterrelateerde klimaatcomponenten: atmosfeer, hydrosfeer, cryosfeer, biosfeer en geosfeer. De menselijke kennis van deze vijf componenten en van de manier waarop ze elkaar beïnvloeden blijkt even 'gevoelig voor verandering' als het klimaat zelf. En hoewel paleoklimaatonderzoek al wordt uitgevoerd gedurende verschillende decennia, toch blijkt onze kennis onvoldoende om patronen van veranderingen over grote regio's van de aarde te kunnen begrijpen: in het bijzonder de veranderingen in het zuidelijk halfrond.

Een belangrijke klimaatcomponent van het zuidelijk halfrond zijn de zuidelijke westenwinden. Deze dominante wind in de zuidelijke middelste breedtegraden (30-60°S) van de aardatmosfeer blazen van west naar oost tussen het hoge drukgebied van de subtropen en het lage drukgebied nabij Antarctica. Dit windsysteem vertoont behoorlijk wat variatie van seizoen tot seizoen en van jaar tot jaar.

Tot en met de vroege jaren '90 werden de westenwinden niet als belangrijk beschouwd in het globale klimaatsysteem. Op dit moment veronderstelt men echter dat de zuidelijke westenwinden, samen met de Antarctische circumpolaire stroming, de zuidelijke warmteflux en de concentratie aan atmosferische koolstofdioxide reguleren, en tevens in staat zijn om klimaatsignalen, zoals El Niño Southern Oscillation (ENSO), snel te kunnen doorgeven. Veranderingen in de intensiteit van de

zuidelijke westenwinden doorheen de tijd zullen dergelijke klimaatsignalen versterken of reduceren.

Deze thesis onderzoekt veranderingen van het klimaat in het verleden in het zuidelijk halfrond, meerbepaald in de middenste breedtegraden, door gebruik te maken van meersedimenten. Aangezien meren veel kleinere waterreservoirs vormen dan oceanen, zullen ze sneller reageren op een externe verandering zoals een klimaatverandering. De reactie van een meersysteem op een dergelijke verandering zal zijn sporen achterlaten in het sediment dat accumuleert op de bodem van het meer. Er wordt grote nadruk gelegd op het beter begrijpen van het gedrag van de zuidelijke westenwinden gedurende de laatste 45000 jaar van de aardgeschiedenis.

Twee verschillende technieken werden geselecteerd om deze sedimenten te bestuderen. Eerst werd er een seismische inspectie uitgevoerd. Deze techniek creëert een acoustisch beeld van de totale meeropvulling. Dit laat een quasi drie-dimensionele reconstructie toe van de sedimentopvulling in het meerbekken. De resolutie van deze techniek is echter nogal laag (1000 jaar lange variaties). Bijgevolg kunnen korte termijn variaties niet gedetecteerd worden. Om deze beperking te omzeilen, kunnen er ook sedimentkernen genomen worden. Een sedimentkern kan echter niet dezelfde lange tijdsperiode overbruggen als een seismische studie, noch laat het een drie-dimensionele reconstructie toe, maar het laat wel toe klimaatvariaties op een veel kortere tijdsschaal te ontdekken (100 tot 10 jaar lange variaties). Wanneer beide technieken gecombineerd worden kan de klimaatgeschiedenis van een regio in elk aspect ontleed worden.

De seismische stratigrafie van vijf verschillende meren werd in detail bestudeerd: vier meren in het Chileense merendistrict (Lago Villarrica, Lago Calafquén, Lago Panguipulli and Lago Riñihue op 39-40°S) en één meer in de Kerguelen archipelago (Lac d'Armor op 49°S). In het algemeen, toonde de hoge resolutie seismische reflectie studie de volledige opvulling van het meerbekken. Bijgevolg kon er een goede reconstructie gemaakt worden van de evolutie van de verschillende meerbekkens.

De hoge resolutie seismische reflectieprofielen van de vier meren in het Chileense merendistrict vertonen vier belangrijke seismische onconformiteiten in elk meerbekken. Deze vier onconformiteiten werden waarschijnlijk gecreëerd door gletsjeractiviteit. De aanwezigheid van deze onconformiteiten wijst erop dat de gletsjers in deze meerbekkens minder krachtig en ver reikten gedurende de laatste voor- en achteruit schrijdingen van de ijsmassa dan tijdens de creatie van de oudste onconformiteit. Deze informatie kan als een aanwijzing beschouwd worden dat de klimaatcondities in de middelste breedtegraden van het zuidelijk halfrond verschilden van die van het noordelijke halfrond waar de gletsjervooruitschrijdingen net het verste reikten tijdens de laatste ijstijd. Aangezien er geen absolute dateringen voor handen zijn voor deze vier onconformiteiten, is het moeilijk om een tijdsaanduiding te creëren voor deze gebeurtenissen. Vooruitschrijdingen van de gletsjers in de zuidelijke Andes gedurende de laatste 100 jaar, in het Holoceen en tijdens de laatste ijstijd worden gelinkt aan periodes van intensere zuidelijke westenwinden. Bijgevolg markeren deze onconformiteiten waarschijnlijk periodes van sterkere westenwinden tijdens de laatste ijstijd.

De seismische stratigrafie van Lac d'Armor vertoont een bijzonder kenmerk: de vorming van een sedimentdriftafzetting tijdens de afzetting van de jongste seismische eenheid. Deze drift wijst op de aanwezigheid van sterke bodemstromingen. Dergelijke stromingen worden vaak gegenereerd door wind. Op dit moment valt de kracht van de zuidelijke westenwinden op het archipelago niet te

onderschatten . De plotse opbouw van de driftafzetting wijst op het plots versterken van de zuidelijke westenwinden gedurende het Holoceen. Opnieuw ontbreken er echter absolute dateringen, waardoor er slechts een ruwe schatting van het tijdstip kan gemaakt worden.

Er werden sedimentkernen genomen in twee meren in Chili: één kern in Lago Villarrica (39°S) en één kern in Laguna Parrillar (53°S). De 14 m lange sedimentkern van Lago Villarrica omvat enkel het Holoceen (het sediment onderaan de kern heeft een ouderdom van ca. 9500 cal a BP). De 7 m lange sedimentkern van Laguna Parrillar beslaat een veel langere periode (het sediment onderaan de kern heeft een ouderdom van ca 45000 cal a BP). De analyse van de sedimentkernen was vooral belangrijk voor het bepalen van het tijdstip van de variaties van de positie en intensiteit van de zuidelijke westenwinden.

De 45000 jaar oude sedimentkern van Laguna Parrillar toont aan dat er drastische veranderingen optraden in de intensiteit van de zuidelijke westenwinden. Van 45000 cal a BP tot 12500 cal a BP werd de uitstromende rivier van het meer geblokkeerd door een glestjerdam, de Magellaanse gletsjer. Zolang de blokkade aanwezig was, kon er geen water uit het meer stromen; van zodra deze gletsjer achteruitschreed was dit echter wel mogelijk. Aangezien het gedrag van de gletsjers in de zuidelijke Andes sterk afhankelijk zijn van de intensiteit van de zuidelijke westenwinden, bijgevolg wijst een achteruitschrijding van de gletsjer op een afname van de sterkte van deze winden. Een andere belangrijke factor in deze periode is de duur van de ijsbedekking van het meer. Gedurende koude periodes, die waarschijnlijk gelinkt kunnen worden aan sterke westenwinden, was het meer het ganse jaar bevroren. Gedurende periodes dat de kracht van de westenwinden afnam, was het meer waarschijnlijk af en toe ijsvrij. Na 12500 cal a BP werd de sedimentatie van het meer vooral gecontroleerd door de kracht van de zuidelijke westenwind en de daarmee geassocieerde golfwerking en stromingen. Een eerste aanwijzing van een toename in de intensiteit van de westenwinden in het Holoceen vond plaats omstreeks 7800 cal a BP; kort hierna nam deze intensiteit echter weer af. De meest opvallende intensiteitstoename vond plaats omstreeks 4000 cal a BP; nadien werd er geen duidelijke afname meer geregistreerd.

De Holocene sedimentkern van Lago Villarrica geeft informatie vrij over de veranderingen in de kracht en positie van de zuidelijke westenwinden gedurende de laatste 10000 jaar. Tijdens het Vroeg Holoceen waren de zuidelijke westenwinden zwakker en/of bevonden ze zich in een meer polaire locatie. Omstreeks 6000 cal a BP nam de invloed van de zuidelijke westenwinden echter toe, met een nog sterkere toename rond 4000 cal a BP.

Het sediment in Lago Villarrica vervat ook een El Niño Southern Oscillation signaal. ENSO veroorzaakt op dit moment grote variaties in het klimaat van noord en centraal Chili van jaar tot jaar. De sedimentkern van Lago Villarrica geeft echter aan dat er misschien ook een ENSO invloed was in het Vroeg Holoceen.

Al deze verschillende records geven aan dat er wijzingen optraden in de intensiteit van de zuidelijke westenwinden doorheen de tijd. Uit de records die absoluut gedateerd werden, blijkt dat deze veranderingen tamelijk synchroon verliepen zowel op 39°S als op 53°S. Bijgevolg is het niet helemaal duidelijk of de positie van de zuidelijke westenwinden verandert of enkel de intensiteit van het windsysteem. Er is echter een asynchroon gedrag in de intensiteit van de westenwinden de laatste 1000 jaar. Een mogelijke verklaring hiervoor is de grote ENSO invloed op het klimaat van zuid centraal Chili. De ENSO invloed is namelijk veel minder van belang voor de regio van zuidelijke Chili.

I. Preface

Kenneth Boulding (1973):
"... whereas all experiences are of the past, all decisions are about the future ... it is the great task of human knowledge to bridge this gap and find those patterns in the past which can be projected into the future as realistic images ..."

We live in unusual times. Greenhouse gas concentrations are increasing rapidly and are now much higher than they have been for the last 420000 years (Petit et al., 1999). Global average temperatures exceed anything seen in the last thousand years (Mann et al., 1999). The evidence is now overwhelming that such changes are a consequence of human activities, but these are superimposed on underlying natural variations. How can we distinguish the human from the natural impacts? The search for this answer will only be successful when we have developed insight into the full range of natural variability of the climate system. That range is illustrated by events of the past and it is only by unravelling those events that we will be able to predict the future, and our place in it.

Climate has varied continuously on all timescales. Irrespective of the extent to which human activities lead to changes in the global climate system, it will continue to vary in the future. This is unquestioned; doubts surround only the nature of change and future variability and the degree to which the consequences of human activities will influence or perhaps even dominate it.

In many parts of the world the public has become highly aware of the issues concerning climate change in recent years as individual extreme events have forced a reappraisal of what is meant by 'normal'. In the past, it was common for a few decades of meteorological observations to be taken as indicative of the likely range of conditions which would be experienced at a certain place. But all this inherently assumed a stable climate, one for which a baseline established on data from the past could be relied upon to provide safe guidance for the future. If the climate is changing, such an approach is fundamentally flawed.

Change is an inherent characteristic of climate. Globally, the 1990s was the warmest decade of the twentieth century, and 1998 the warmest year of the instrumental record (Mann et al., 1998). Yet this is the century considered to be 'normal' for the purpose of designing structures and for environmental management and protection generally. Clearly, what is normal may turn out to be very abnormal when a longer time perspective is employed. This implies a need for establishing the range of climate conditions existing in the past.

Palaeoclimate work is the only reliable tool to reconstruct climate conditions in the past and to evaluate how fast natural systems can change.

The focus for much of this work has centred on the termination of the last ice age. The primary reason for this is that the warming associated with this termination is of similar or even larger magnitude than the human-induced climate modification expected under future greenhouse-gas scenarios (Watson et al., 2001) although the rate of change was much slower.

'Rate of change' is one of the critical pieces of the jigsaw that palaeoclimate studies can provide. The risk of abrupt climate change is recognised as very important and inherently difficult for future climate change prediction (Watson et al., 2001). Human systems are quite adaptable to change so long as it is gradual and predictable. The same systems may collapse under even moderate change scenarios if the rate of change is too great.

Climate encompasses the statistics of temperature, humidity, atmospheric pressure, wind, rainfall, atmospheric particle count and other meteorological elemental measurements in a given region over long periods of time. Variations and changes in these parameters are orchestrated by changes in solar radiation and the five interrelated climate components: atmosphere, hydrosphere, cryosphere, biosphere and geosphere. Regardless of man's efforts to understand these five components and how they affect each

other, the comprehension of this system is as sensitive to change as current climate. Even though many decades of palaeoenvironmental research have gone by, we still do not have adequate understanding of the patterns of change over huge swatches of the globe's surface, and, in particular, the Southern Hemisphere.

Being relatively small bodies of water in comparison with the oceans, lakes can respond relatively quickly to an external forcing variable such as climate. The response of the lake system to such change will leave traces in the sediment which accumulates on the bottom of the lake.

This thesis investigates past climate change in southern part of the world, and more particularly the mid-latitudes of the Southern Hemisphere. These latitudes are wedged in between two major climate drivers: the Antarctic system and the Tropics. The region itself is lashed by the Southern Westerly winds. Until the early 1990s, the Southern Westerlies were generally not regarded as a particularly important component of the global climate system. Currently this wind system exhibits considerable variability on intra- and interannual time scales in both its intensity and its geographic position. These changes in strenght and position of the Southern Westerlies were most likely even larger in the past when considering centennial or millenial time scales, especially at times when climate changed drastically (e.g. the end of the last ice age). The main focus of this research is to better understand the behaviour of this Southern Westerly wind system during the last 45000 years of the Earth's history. To investigate the Southern Westerlies, sediments of three different lakes in the mid-latitudes of the Southern Hemisphere were selected: two lakes in southern Chile (at 39°S and 53°S) and one lake in the Kerguelen Archipelago (49°S). The timing of variations of the Southern Westerlies' wind strength and position were determined using the lakes' deposits, because these climatic changes highly affected the studied lake systems.

In Lago Villarrica also an El Niño Southern Oscillation (ENSO) signal was detected. ENSO currently creates large interannual variations in the climate of north and central Chile. The Lago Villarrica lake record, however, indicates that an ENSO influence might have been present in the Early Holocene. In general the Westerly wind signal of the Lago Villarrica and Laguna Parrillar record are rather synchronous, however, during the last 1000 years, when the ENSO influence has been noted to be stronger, the lakes react differently. This might indicate that ENSO influences the behaviour of the Westerlies in ENSO dominated regions.

References

Boulding, K., 1973. Foreword. In: F. Polak (Editor), *The images of the future*. Elsevier, Amsterdam, The Netherlands, pp. 319.

Mann, M.E., Bradley, R.S. and Hughes, M.K., 1998. Global-scale temperature patterns and climate forcing over the past six centuries. *Nature*, **392**: 779-787.

Mann, M.E., Bradley, R.S. and Hughes, M.K., 1999. Northern Hemisphere temperatures during the past millenium: Inferences, uncertainties, and limitations. *Geophysical Research Letters*, **26**(6): 759-762.

Petit, J.R., Jouzel, J., Raynaud, D., Barkov, N.I., Barnola, J.M., Basile, I., Bender, M., Chappellaz, J., Davis, M., Delaygue, G., Delmotte, M., Kotlyakov, V.M., Legrand, M., Lipenkov, V.Y., Lorius, C., Pepin, L., Ritz, C., Saltzman, E. and Stievenard, M., 1999. Climate and atmospheric history of the past 420,000 years from the Vostok ice core, Antarctica. *Nature*, **399**(6735): 429-436.

Watson, R.T., Albritton, D.L., Barker, T., Bashmakov, I.A., Canziani, O., Christ, R., Cubasch, U., Davidson, O., Gitay, H., Griggs, D., Halsnaes, K., Houghton, J., House, J., Kundzewicz, Z., Lal, M., Leary, N., Magadza, C., McCarthy, J.J., Mitchell, J.F.B., Moreira, J.R., Munasinghe, M., Noble, I., Pachauri, R., Pittock, B., Prather, M., Richels, R.G., Robinson, J.B., Sathaye, J., Schneider, S., Scholes, R., Stocker, T., Sundararaman, N., Swart, R., Taniguchi, T. and Zhou, D., 2001. *Climate Change 2001: Synthesis Report, IPCC*. Cambridge University Press, Cambridge.

II. (Palaeo)Climatology and its Challenges

As they sailed up the River Nile, the ancient Greeks noticed that it became warmer. Being logical in their search for explanation, they assumed that the Earth must slope towards the sun. The word 'climate' traces its roots from this now discredited deduction, being derived from a Greek word meaning 'slope' (O'Hare et al., 2005). Climate is a broad composite of the average condition of a region, measured by its temperature, amount of rainfall or snowfall, snow and ice cover, wind direction and strength as well as other factors. Climate specifically applies to longer-term changes (years and longer) in contrast to the shorter fluctuations that last, hours, days or weeks and are referred to as weather (Ruddiman, 2008). This study tackles a small piece of the puzzle to understand patterns and causes of past climate change – i.e., palaeoclimatology. Natural archives recovered out of lake sediments in southern Chile and in the Kerguelen Archipelago located in the mid-latitudes of the Southern Hemisphere are used, since this is a rather data-deprived part of the globe in the realm of past climate studies.

II.1. Why Lakes?

Lakes, by definition, are enclosed bodies of standing water surrounded by land. Most lakes are surrounded by watersheds that are large relative to the lake's area, and they are environments of relatively rapid sediment accumulation in comparison with most oceans or many other terrestrial settings. A high degree of depositional continuity at varying timescales is a hallmark feature of most lakes.

Being relatively small bodies of water in comparison with the ocean, lakes can respond relatively quickly to an external forcing variable (Scholz, 2001). The rapidity of this response varies both within a lake, for example from nearshore to offshore environments, and between lakes.

All lakes are subject to a variety of extrinsic and intrinsic forcing variables that regulate the subsequent history of the lake, such as climate, watershed bedrock composition, tectonic and volcanic activity, vegetation and aquatic biota, and human activities (Cohen, 2003) (Figure II-1). All of these variables are highly interactive.

Palaeolimnologists study lake deposits because they provide archives of the lake's history and of local and regional changes in these extrinsic and intrinsic forcings, which are both highly resolved in time and of long duration.

Palaeolimnological records are contained in three types of archives. The first is the lake water itself. A second more durable form of archive is the geomorphology of the lake basin. However, perhaps the most important archive of change is contained in the accumulated sediments as these provide the most durable archives since they can persist long after the lake itself or the geomorphology are obliterated. Archives are not complete or completely accurate depictions of the lake's history. They have been filtered in ways that are both beneficial and detrimental to reconstruction of this history (Cohen, 2003).

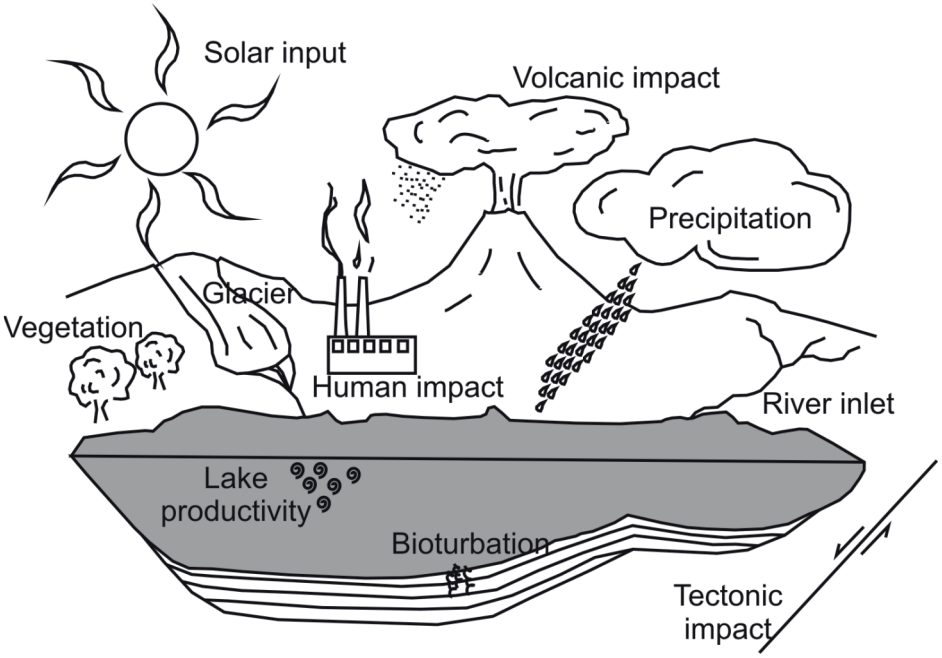

Figure II-1: A simple model of the important factors controlling lake sedimentation (modified after Cohen, 2003)

On short time scales, palaeolimnological archives interface with or extend the ecological monitoring of lakes for management purposes and allow the timing and rates of human impacts to be determined. On longer timescales, palaeolimnology can be used to provide extremely detailed records of the climatic, tectonic and biotic evolution of the Earth's surface. While oceanic records are most of the time continuous and span a large time frame, mostly reflecting a response to more global climatic patterns, lakes are especially good recorders of regional or local climate change. Changing climate systems affect the continents often more drastically and are more locally constricted. Lakes are useful, as they provide the few continuous archives, which can record local and regional changes relevant to past and present human activity and distribution.

II.2. Why the Mid-Latitudes of the Southern Hemisphere?

In the early decades of palaeoclimatic research, Quaternary climate reconstructions mainly focused on the Northern Hemisphere. At millennial time-scales, this was justified by the recognition of the dominant role of the North Atlantic region in modulating climate change (Kershaw and Chappellaz, 2007). There is, however, an

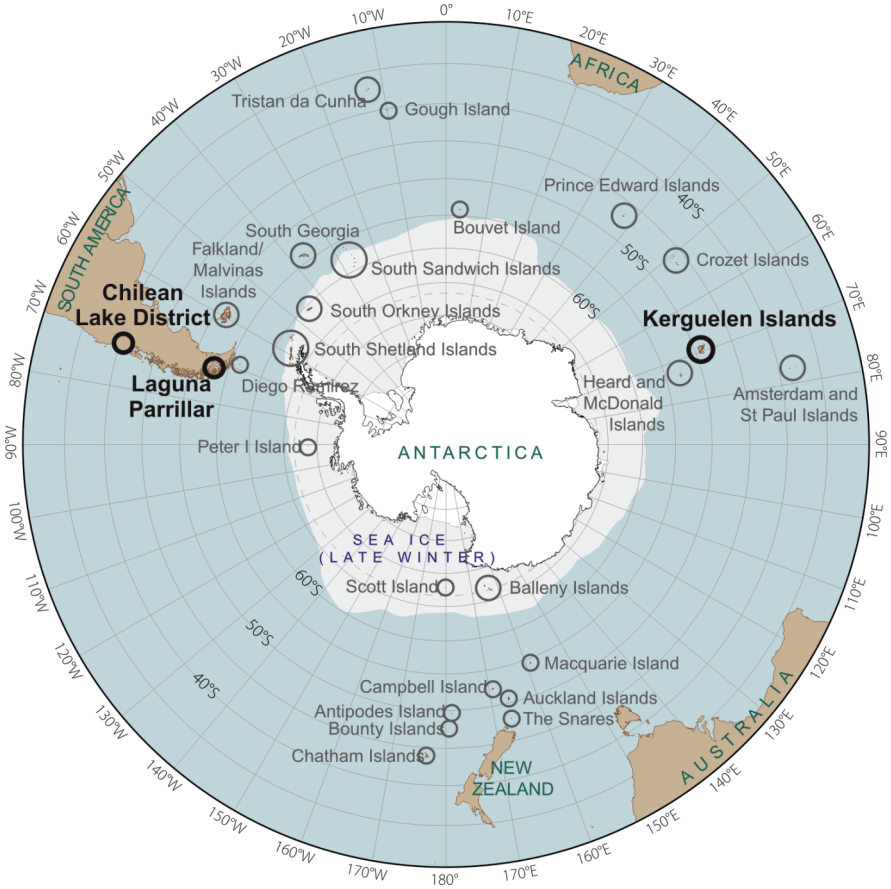

Figure II-2: Continental landmasses and islands in the Southern Hemisphere between 30°S and 90°S. The locations of the study sites studied in this work are in black.

increasing realisation that a global synthesis is needed in order to refine climate change models and it is acknowledged that southern and low-latitude climate mechanisms have a much greater impact on palaeoclimate than previously thought. An ever increasing amount of Antarctic past and present day climate records has enabled comparisons between Arctic and Antarctic climate modes through time, and has enabled the development of models, which have indicated that, during the Last Deglaciation, rapid climate oscillations in the Northern Hemisphere might have been triggered by gradual changes in the Southern Hemisphere high latitudes, through a bipolar seesaw mechanism (Knorr and Lohmann, 2003; Weaver et al., 2003; Wolff et al., 2009). Similarly, the tropics have been recognized as playing a larger role in global climate modulation than previously thought (Beaufort et al., 2001; Cane and Evans, 2000; Gasse, 2000).

The Southern Hemisphere has dominantly more water than land masses compared to the Northern Hemisphere (Figure II-2). Therefore, changes in oceanic systems have a larger influence on this part of the Earth. Due to the absence of large continents, large weather systems (e.g. Southern Westerly Winds (SWW), or Southern Westerlies) are not deflected or perturbed by the continents, contrary to what is more the case in the Northern Hemisphere.
The mid-latitudes of the Southern Hemisphere (30°S-60°S) are wedged in between two major climate change drivers: the Antarctic system is isolated from the rest of the Earth by the Antarctic Circumpolar Current (ACC) and the tropics with its dynamic Intertropical Convergence Zone (ITCZ). In between, the study area of the thesis, the region itself is lashed by the howling SWW, of which the core is centered at around 50°S. Since it is still not clear what drives and/or propagates global climate and climate change: the Arctic, the Antarctic or the Tropics; and what the importance of the SWW is, this region is thought to be the key to understanding which of these players orchestrates climate in this area (Ackert et al., 2008).

Southern South America and the Sub-Antarctic Islands, like the Kerguelen Archipelago, are the only land present in the mid-latitudes of the Southern Hemisphere (Figure II-2). Hence they are the only areas where continental records of past climate change can be obtained. These regions have also experienced very dramatic changes from being covered by large glaciers and ice sheets during glacial times, to becoming almost completely ice free mountains during interglacial periods of the last ca. 2.5 Ma.

II.3. Modern Climate Systems in the Southern Hemisphere

The Earth's climate is driven by the general circulation system of the atmosphere and its interactions with heat sources and sinks on its surface, its oceanic water masses, land masses and its polar ice caps. The circulation is driven by both vertical and horizontal (especially latitudinal) imbalances in the distribution of heat over the surface of the Earth (Martens and Rotmans, 1999). A set of continuously moving wind systems and both high and low pressure cells blanket the Earth at relatively low elevations, driven by the combination of unequal heat distribution on the Earth's surface and the Coriolis effects of the Earth's rotation.

II.3.1. The Southern Westerly Wind Belt

The wind belts encircling the planet are organised into three cells: the Hadley Cell (0°-30°N/S), the Ferrel Cell (30°N/S-60°N/S), and the Polar Cell (60°N/S-90°N/S). The atmospheric boundary between the Ferrel and Polar cell is known as the Polar Front. In winter this front shifts equatorward. The mid-

latitudes of the Southern Hemisphere are influenced by the Ferrel Cell and the SWW system found beneath this cell. The SWW are of primary importance in regulating the regional climate and climate change due to their influence on deep-ocean circulation and changes in atmospheric CO_2 (Rojas et al., 2009). South of 40°S, low-level westerly flow, the Southern Westerlies, prevails year round over the oceans and the continent of South America, although its influence is a little bit weaker here (Garreaud et al., 2009). The belt of the Southern Westerlies is largely symmetric over the Southern Hemisphere, due to the absence of significant land masses to the south of 35°S, and has a rather modest annual cycle (Figure II-3). In particular, the Southern Westerlies are strongest during austral summer, peaking between 45° and 55°S. During the austral winter, the jet stream moves into subtropical latitudes (its axis is at about 30°S) and the low-level Southern Westerlies expand equatorward but weaken, particularly at ~50°S (Garreaud et al., 2009). During the austral summer the northern margin of the Southern Westerly belt contracts (Hodgson and Sime, 2010). Through this seasonal cycle, the main locus of precipitation largely follows the mean zonal wind maximum (Moy et al., 2009). In general,

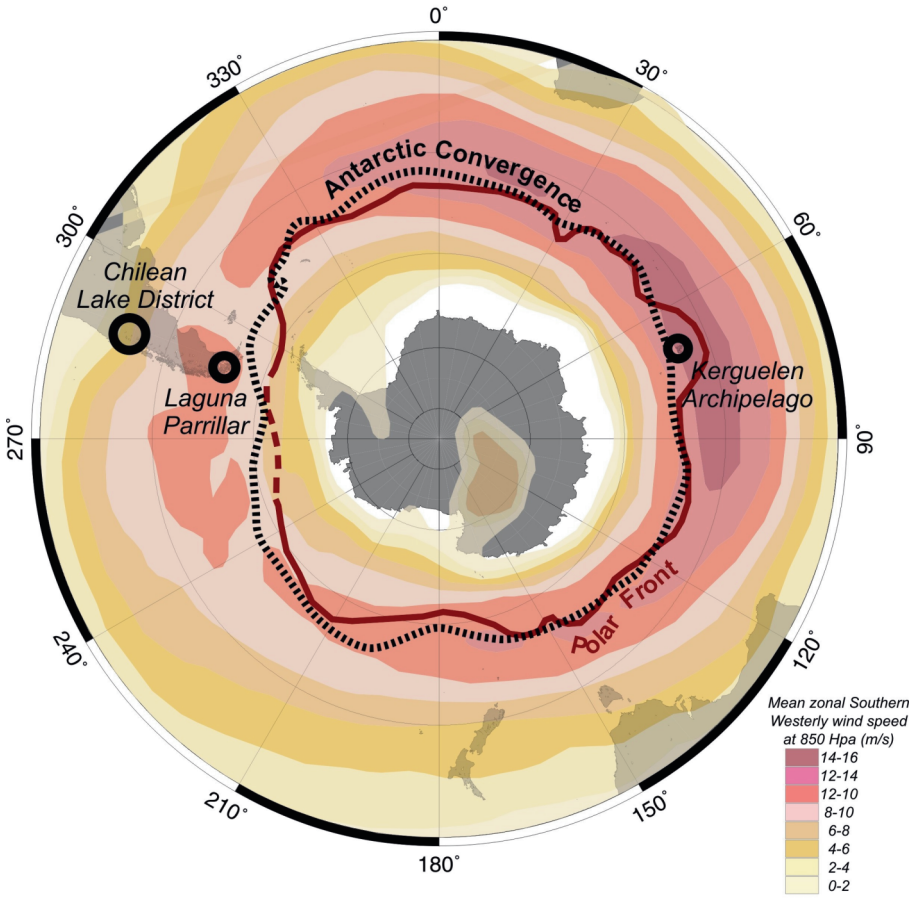

Figure II-3: Location of the Antarctic Convergence (dashed black line) (Barker and Thomas, 2004), the Polar Front (full red line) (Belkin and Gordon, 1996) and the mean zonal Southern Westerly winds at 850 HPa during the period 1961-1990 with contour interval of 2m/s (Kalnay et al., 1996; Shulmeister et al., 2004). The study regions are accentuated with a black circle.

precipitation exhibits an overall positive correlation with zonal wind speeds. In southern Patagonia, however, precipitation is more evenly distributed throughout the year with a small maximum during the austral autumn. In contrast, precipitation in northern Patagonia is more seasonal with higher amounts during the winter when the subtropical high and the jet are located farther to the north (Moy et al., 2009). In South America, the presence of the Andes Cordillera creates also a marked zonal asymmetry with very wet conditions to the west of the Cordillera (Chile) due to the large amounts of moisture supplied by the Southern Westerlies and very dry conditions to the east (Argentina) (Cerveny, 1998).

II.3.2. The Antarctic Circumpolar Current

The Southern Westerlies are strongly associated with the Antarctic Circumpolar Current (ACC). The ACC is the most important current in the Southern Ocean, and the only current that flows completely around the globe. Its eastward flow is driven by the Southern Westerlies (Barker and Thomas, 2004). The main 'axis' of the ACC is located at the Antarctic Convergence, which forms the boundary between the cold Antarctic waters and the relatively warmer Sub-Antarctic waters. The Antarctic Convergence is the oceanographic manifestation of the atmospheric boundary known as the Polar Front. The Kerguelen Archipelago lies approximately on this convergence (Figure II-3).

II.3.3. The Antarctic and El Niño Southern Oscillation

The Southern Westerlies and the linked ACC are influenced both by Antarctic and tropical oscillations, since they are 'physically' connected with the polar and tropical circulation cells and because they are linked with the upper tropospheric polar jet. The most notable of these processes are the Antarctic Oscillation (AAO) and the El Niño Southern Oscillation (ENSO). Both of these large-scale ocean-atmosphere processes play a role in altering not only temperatures at seasonal to inter-annual timescales, but also precipitation amount and distribution through changes in the strength and latitudinal position of the Southern Westerlies (Garreaud et al., 2009).

The AAO is the leading pattern of tropospheric circulation variability south of 20°S. It is characterized by pressure anomalies of one sign centered in the Antarctic and anomalies of the opposite sign on a circumglobal band at about 40–50°S (Thompson et al., 2000). The positive phase of the AAO is associated with increased surface pressure and geopotential heights over the mid-latitudes and a strengthening and poleward shift of the Southern Westerlies. Opposite conditions prevail during the negative phase. There is a large response of the surface air temperature to the south of 40°S, such that warming is associated with the positive phase of the AAO (Thompson et al., 2000). Large-scale warming is largest in austral summer. Over the last 30 years, a strengthening of atmospheric circulation in the high southern latitudes is evident in direct instrumental observations (Marshall, 2003) and wind fields derived from reanalysis from data sets (Thompson and Wallace, 2000), reflecting a trend towards the positive mode or phase of the AAO. The AAO shows also a strong connection to ENSO events (Grimm and Ambrizzi, 2009).

ENSO is a coupled ocean-atmosphere phenomenon rooted in the tropical Pacific, characterized by irregular fluctuations between its warm (El Niño) and cold (La Niña) phases with a periodicity ranging from 2 to 7 years. During an El Niño event, rainfall shifts from the western Pacific towards the Americas (Karoly, 1989; Rasmusson and Wallace, 1983). Although it might not be as obvious as in Central Chile, El Niño-Southern Oscillation (ENSO) mechanism may have had significant

effects also in the higher latitudes (Cane, 2005).

The overall pattern is that El Niño episodes (a positive Multivariate ENSO Index or MEI or a negative Southern Isolation Index or SOI) are associated with above-normal precipitation and cold air anomalies during spring between 30-38°S in Chile and a rainfall deficit and warmer surface temperatures in austral summer between 38°-41°S in Chile (Montecinos and Aceituno, 2003; Montecinos et al., 2000). Opposite rainfall and temperatures are observed during La Niña episodes. There is a positive correlation between rainfall and wind strength for the 38-41°S Chilean region. This implies weaker Southern Westerlies during an El Niño event and stronger Southern Westerlies during a La Niña event (Montecinos and Aceituno, 2003).

II.4. Holocene and Late Pleistocene Climate Change

Global climate has fluctuated throughout the entire Earth's history. The occurrence of repeated warm and cold episodes can be tracked through all geological eras (Figure II-4). But why do scientist focus so much on Quaternary climate change, if the Quaternary only spans 2 million years of the total 5 billion years of the Earth's history?

What makes the Quaternary so distinctive is the combination of high amplitude and high frequency climatic oscillations, coupled with the intensity of the colder periods. Relatively swift changes between very different climate regimes have given rise to a rich, but complex record of landforms, sediments and biological remains (Lowe and Walker, 1997). In the Quaternary continents and oceans had reached their current positions. Orbital-scale changes have dominantly been driving climate in this period. Orbital-scale changes have occurred throughout the entire record,

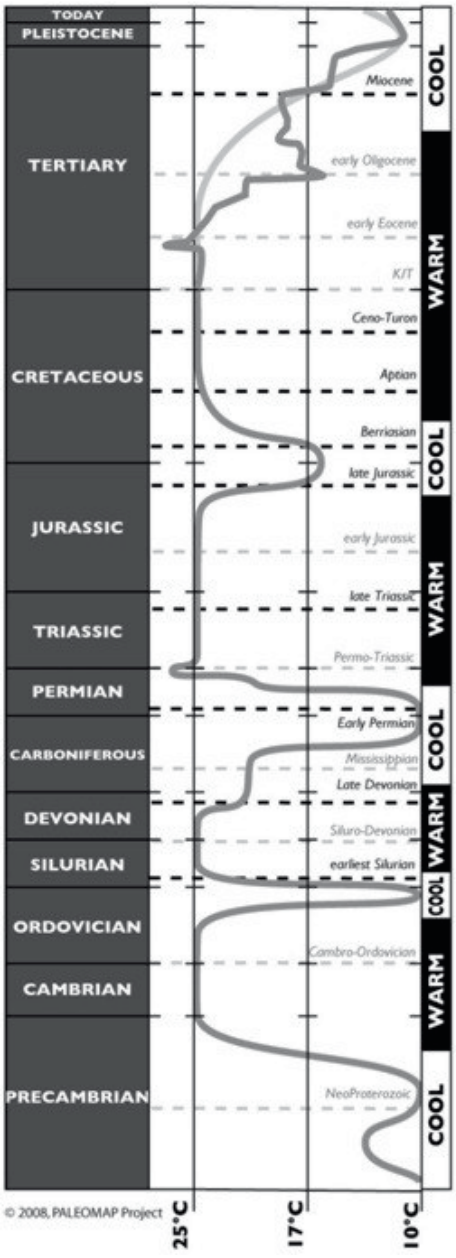

Figure II-4: Variation of the global temperature throughout the Earth's history (from PALEOMAP, 2008)

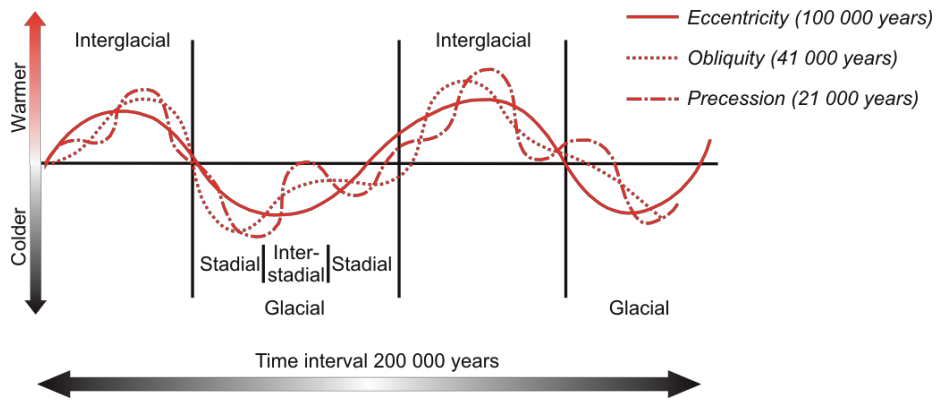

Figure II-5: Possible combined effect of the orbital cycles on the glacial-interglacial temperatures (from O'Hare et al., 2005)

but rarely were its effects so drastic and rapid (Figure II-5 and Figure II-6).

The lake records discussed in this work span the period of the Late Pleistocene and Holocene, i.e. the last ca. 50 000 years, representing the last Glacial, cold phase, a swift transition into a warm period, also called Termination (Broecker and van Donk, 1970), and the current Interglacial, warm phase. Past changes in the strength and latitudinal position of the ACC and the Southern Westerlies are thought to play a major role in global climate changes via their impact on atmospheric CO_2 across a variety of time-scales ranging from decadal to orbital scale (Anderson et al., 2009; Hodgson and Sime, 2010; Toggweiler et al., 2006). Model simulations suggest that the glacial expansion of circum-Antarctic sea-ice has had a much stronger influence than Northern Hemisphere sea-ice, possibly because of its far greater areal extent (Chiang et al., 2003; Chiang and Bitz, 2005). Antarctic sea-ice expansion reinforces the Southern Hemisphere oceanic and atmospheric frontal zones to move equatorward (Stuut et al., 2004; Stuut and Lamy, 2004).

II.4.1. The Interhemispheric See-Saw

In general, Quaternary Glacial-Interglacial cycles are considered to be induced by the Earth's orbital variations: eccentricity, obliquity and precession. These three orbital parameters can act positively together to increase the amount of insolation received by the Earth to produce a warm, Interglacial phase. At other times the amount of received insolation is reduced, generating a cold, Glacial phase and sometimes these factors might act and counteract to produce local warming, or an interstadial, or local cooling resulting in a stadial (O'Hare et al., 2005) (Figure II-5).

On a millennial time-scale, however, there seems to be a semi-regular, out-of-phase relationship between climate variability between Antarctic and Greenland ice core records. This phenomenon is called the bipolar see-saw (Blunier and Brook, 2001; Broecker, 1998). On average Antarctic climate change leads that of Greenland by 1000 to 2500 years (Blunier et al., 1998). Warming into an Interstadial or Interglacial is often more slow and gradual in Antarctica, while this happens more rapidly and abruptly in the Northern Hemisphere (Blunier and Brook, 2001). Cold, Northern Dansgaard-Oeschger (D-O) events are preceded by Antarctic warmings (Blunier and Brook, 2001). Overall, during the gradual warming of Antarctic

Interstadials, Arctic temperatures remained cold or cooling (Figure II-6). The most widely suspected culprit is the 'conveyor' circulation in the Atlantic Ocean (Broecker, 1998; Stocker, 1998). A switch-off of the Atlantic circulation causes about 300 years later a rise in the atmospheric CO_2 levels (Ahn and Brook, 2008) as the deep ocean warms and releases CO_2 owing to decreased stratification of the southern ocean (Toggweiler, 1999) or decreased Antarctic sea ice (Stephens and Keeling, 2000). This decreased stratification of the southern ocean, therefore implying an increase in upwelling of CO_2 enriched Antarctic bottom waters, has also been linked the last couple of years to the position and strength of the Southern Westerlies. A modelling study suggests that during cold periods the Southern Westerlies shift equatorward (Toggweiler et al., 2006). Consequently the core of the Southern Westerlies is no longer aligned with the main axis of the ACC, reducing Southern Ocean upwelling. Each time northern sea ice expanded during D-O events and the Atlantic Meridional Overturning Circulation (AMOC) slowed down, the ITCZ was pushed towards the Southern Hemisphere, effectively pushing the Southern Westerly belt poleward (Anderson et al., 2009; Lamy et al., 2007; Timmermann et al., 2005), aligning it with the ACC, and reinforcing southern ocean upwelling (Barker et al., 2009). Such a southward shift has also been associated with an increase in Southern Westerly wind strength (Rind et al., 2001). This later hypothesis stresses again the importance of understanding and reconstructing the behaviour of the Southern Westerlies. But what about the southern mid-latitudes, do they follow the southern or northern beat? Most oceanic records tend to be synchronous with Antarctic climate change records (Calvo et al., 2007; Kaiser, 2005; Lamy et al., 2004; Pahnke and Zahn, 2005). Terrestrial records, on the other hand, often contradict each other. Denton et al. (1999a) and Moreno et al. (2001) state that the Northern Hemisperhic signal dominates climate change in the

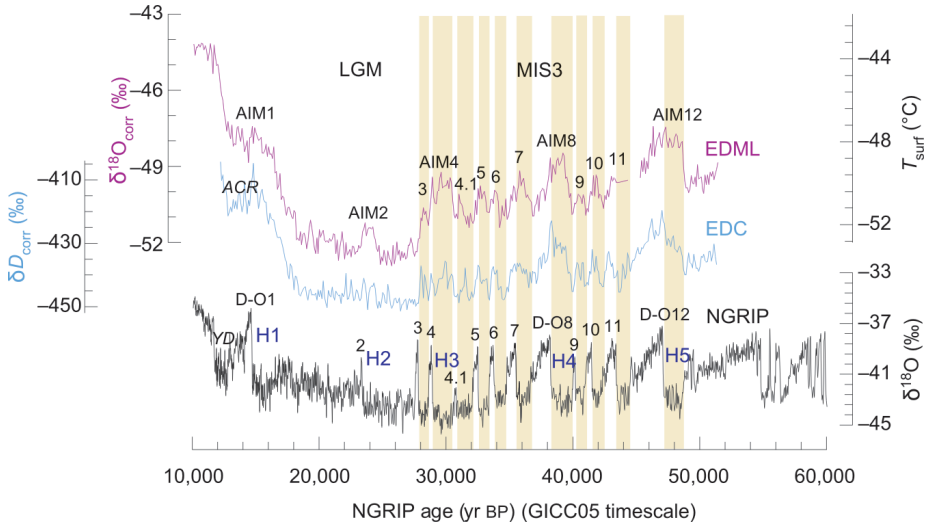

Figure II-6: The Bipolar See-Saw: Methane synchronised isotope curves of the ice core records of Greenland (NGRIP)(Andersen et al., 2006; Rasmussen et al., 2006) and Antarctica (EDML: EPICA Dronning Maud Land and EDC: EPICA Dome C) (Barbante et al., 2006; Stenni et al., 2003) revealing that each Antarctic warming corresponds to a stadial in Greenland (yellow bars) (after Barbante et al., 2006). The moments of massive iceberg discharges in the North Atlantic, the so-called Heinrich events (H1-H5), are also indicated (Bond and Lotti, 1995).

southern mid-latitudes on both orbital and millennial timescales. Sugden et al. (2005) prefers to call it a blend of a northern (orbital) and southern (millennial) signal, while Schaefer et al. (2006; 2009) and Shulmeister et al. (2006) argue that Southern Hemisphere warming pre-dates the northern warming pulse, not only in Antarctica, but also in the mid-latitudes and that Holocene glacier fluctuations are not synchronous with it either. These conflicting results not only exist on at glacial-interglacial scales, but also on smaller scales. Whether a Deglaciation Climate Reversal is present during the transition from the last Glacial to the current Interglacial period or even absent is still debated (Barrows et al., 2007; Bennett et al., 2000; Glasser et al., 2004; Haberle and Bennett, 2004; Hoganson and Ashworth, 1992; Kaplan et al., 2010; Massaferro et al., 2005; Singer et al., 1998). Whether this cold reversal is synchronous with the northern Younger Dryas (YD) – 12890-11650 cal a BP (Stuiver et al., 1995) – (Heusser and Streeter, 1980; Ivy-Ochs et al., 1999; Massaferro and Brooks, 2002; Moreno, 1997; Moreno et al., 1999), the southern Antarctic Cold Reversal (ACR) – 14000-12500 cal a BP (Jouzel et al., 2001) – (Lamy et al., 2004; McCulloch et al., 2005a; Moreno et al., 2009; Turney et al., 2007; Vandergoes et al., 2008) as it has been observed in some regions in the Southern Hemisphere outside Antarctica, or whether that the cooling occurred after the onset of the ACR, but before the onset of the YD remains controversial (in South America some authors refer to this reversal as the Huelmo-Mascardi Cold Reversal, HMCR) (Bertrand et al., 2008; Hajdas et al., 2003; Hellstrom et al., 1998; Massaferro et al., 2009; Newnham and Lowe, 2000; Williams et al., 2005).
In the Chilean Lake District and New Zealand, this cold reversal is influenced by both the southern ACR and northern YD signal. In Southern South America (south of 50°S) the cold reversal is generally synchronous with the ACR. In Central Patagonia, despite being at the same latitude as New Zealand's Southern Island, such a cold reversal has not been identified.

II.4.2. The Last Glacial Maximum

At the Last Glacial Maximum (LGM), southern mid-latitudinal climate had the following characteristics. Firstly the Southern Westerlies had probably shifted northwards, as implied from wetter climatic conditions traced in pollen records (Heusser, 1989), marine records (Lamy et al., 2001; Lamy et al., 2004; Stuut and Lamy, 2004), glacial records (Lowell et al., 1995), and modelling studies (Hulton et al., 2002; Rojas et al., 2009; Wainer et al., 2005; Wyrwoll et al., 2000). In general, climate was cold and humid on the western side of the Andes south of 33°S (Hoganson and Ashworth, 1992; Lamy et al., 2004; Massaferro et al., 2009; McCulloch and Davies, 2001; Moreno, 1997; Moreno et al., 1999; Sugden et al., 2005). Secondly, north of this region, climate was more arid (Lamy et al., 1998; Lamy et al., 1999; Lamy et al., 2000) and to the east of the Andes climate was more arid as well (Gilli et al., 2005; Haberzettl et al., 2009). Thirdly, mean summer temperatures were probably about 5-6°C below present values (Hulton et al., 2002; Lowell et al., 1995; Sugden et al., 2002).

During the LGM the southern part of the South American continent (38-56°S) was covered by the Patagonian Ice Sheet, the largest ice sheet in the Southern Hemisphere excluding the Antarctic Ice Sheets. The landform record indicates that the Patagonian Ice Sheet consisted of many outlet glaciers and local cirques and independent ice domes. The western part of this ice sheet extended beyond the current shorelines south of 41°S (Glasser et al., 2008; Hulton et al., 2002; McCulloch et al., 2000) (Figure II-7). Most of these glaciers, especially the glaciers located on the western side of the Andes, were warm-based (Glasser et al., 2008).

Information on the former ice cover of Sub-Antarctic islands like Kerguelen is more speculative and poorly

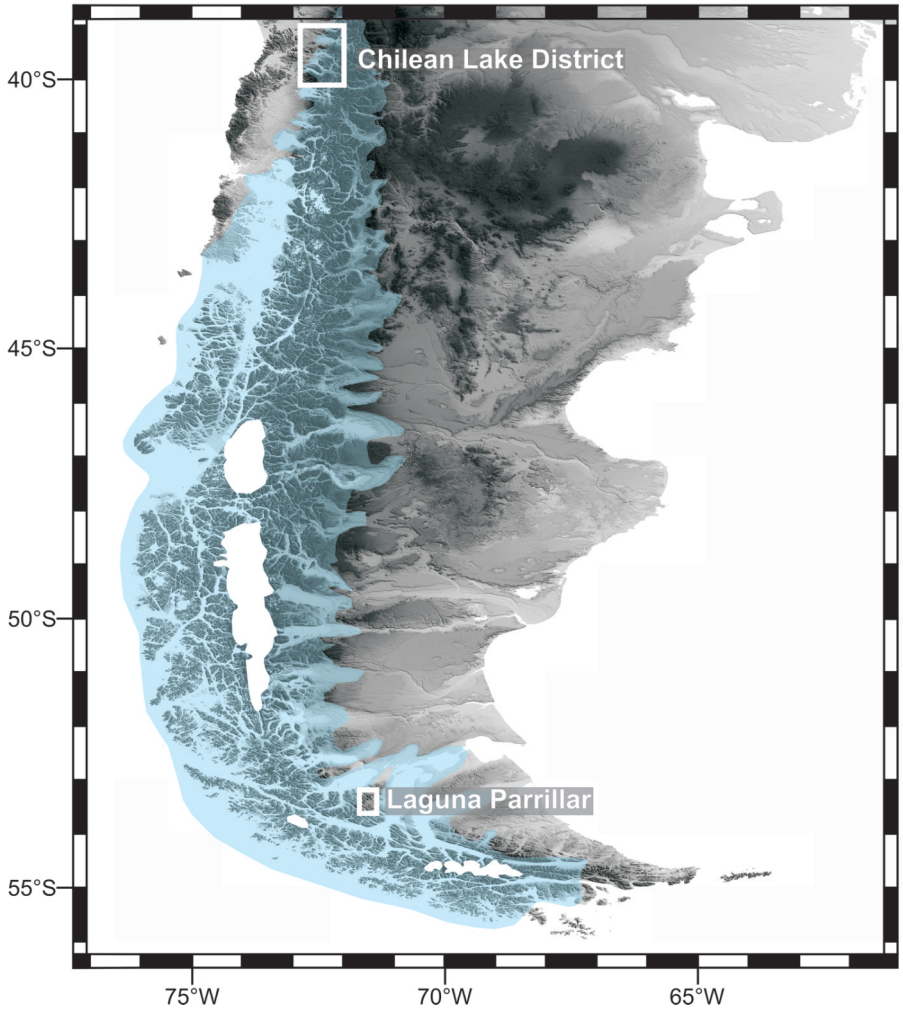

Figure II-7: Location of the current Patagonian Ice Sheets (in white) and glacier reconstruction of the Patagonian Ice Sheet during the LGM (in blue) (glacial limits after McCulloch et al., 2000) and the location of the two study areas in Chile.

constrained (Hall, 2004).

Antarctic ice cores provide a record of dust flux variability to Antarctica, which is thought to reflect changes in atmospheric circulation and environmental conditions in dust source areas (Delmonte et al., 2008; Diekmann et al., 2000; Lambert et al., 2008; Mahowald et al., 1999; Petit et al., 1999; Winckler et al., 2008). Isotopic tracers suggest that South America, more specifically Patagonia, is the dominant source of the dust (Basile et al., 1997; Delmonte et al., 2008; Delmonte et al., 2004; Gaiero et al., 2007). The mechanism behind the variable dust deposition remains unclear (Lambert et al., 2008). Four main drivers have been proposed: 1) increase in the vigour of atmospheric circulation (Sugden et al., 2009); 2) reduced hydrological cycle and vegetation cover in the source areas; 3) lowered sea-level exposing the continental shelfs; 4) reduced glacial atmospheric washout during transport

prolongs the atmospheric lifetime of mineral dust aerosol (Lambert et al., 2008). The attribution of dust peaks to sea-level lowering and the exposure of the South American continental shelf is problematic, however, because the dust decline occurs before sea level rose significantly at the end of the last glacial cycle (Sugden et al., 2009). In general, it is assumed that temporal changes in the strength of the Patagonian mineral dust source are the main factor (Fischer et al., 2007). Such changes might be modulated by Patagonian glacier snouts dumping their sediment on easily mobilised outwash plains or by terminating directly into pro-glacial lakes (Kaiser and Lamy, 2010; Sugden et al., 2009).

II.4.3. The Last Termination

From a synthesis of key proxy records, McCulloch et al. (2000) concluded that there was a sudden rise in temperature that initiated deglaciation of the Patagonian Ice Sheet sychronously over 16° of latitude at 17500–17150 cal a BP. There was a second step of warming in the Chilean Lake District at 15650–15350 cal a BP, which saw temperatures rise to close to modern values. A third warming step, particularly clear in southern Chile, occurred ca 11400 cal a BP. Following the initial warming, there was a lagged response in precipitation as the Southern Westerlies, after a delay of ca. 1600 years, migrated from their northern glacial location to their present latitude, which was attained by 14300 cal a BP (McCulloch et al., 2000). Modelling results also indicate that deglaciation happened very rapidly. In just 2000 years, the Patagonian Ice Sheet was reduced by 80% (Hulton et al., 2002).

II.4.4. The Deglaciation Climate Reversal (DCR)

The timing and manifestation of the DCR event is inconsistent between the different records in South America. Continental records in the Lake District and in Chiloé have been interpreted as cooling (Ariztegui et al., 1997; Denton et al., 1999b; Hajdas et al., 2003; Heusser and Streeter, 1980; Massaferro et al., 2009; Moreno et al., 2001; Moreno and Leon, 2003), whereas the alkenone and radiolarian based record of a marine record reveal a clear warming (Lamy and Kaiser, 2009). There are many records which do not record this cooling and often records that do contradict each other as to whether this period was drier (Massaferro et al., 2009) or more humid (Hajdas et al., 2003; Moreno and Leon, 2003). In addition, many pollen records mention fire disturbance (Hajdas et al., 2003; McCulloch and Davies, 2001; Moreno, 2004; Moreno and Leon, 2003), which may not necessarily imply cooling, and some records even mention warming (Markgraf et al., 2007; White et al., 1994). Glacier fluctuation studies suggest glacial readvances (Sugden et al., 2005) (46-55°S). A cooling would imply a slight northward movement of atmospheric and oceanographic systems in the southeast Pacific (Lamy and Kaiser, 2009). Around 12600 cal a BP the Northern and Southern Patagonian Ice Sheet completely separated (Turner et al., 2005).

II.4.5. The Holocene

Globally, the geographic pattern of Holocene climate fluctuations remains uncertain. Although generally weaker in amplitude than the dramatic shifts of the last glacial cycle, Holocene climate variations have been larger and more frequent than commonly recognised. Changes in insolation related both to the Earth's orbital variations and solar variability played a central role in the global scale changes in climate of the last 11500 cal a BP (Mayewski et al., 2004). Since Holocene climatic fluctuations are less drastic, they are often overlooked and sometimes contradictory.

Maximum warm conditions prevailed during the early Holocene according to alkenone sea surface temperatures of marine records (Kaiser 2005; Kaiser et al., 2005; Kaiser et al., 2008). Pollen records show drier (Abarzua et al., 2004;

Moreno, 2004; Moreno and Leon, 2003) or wetter conditions (Heusser and Streeter, 1980) during this period. This was most likely related to an intensification of the Southern Westerlies (Mayewski et al., 2004).

During the middle Holocene drier conditions existed (Abarzua et al., 2004; Mayewski et al., 2004; Moreno, 2004; Moreno and Leon, 2003) as the Southern Westerly belt shifted poleward (Gilli et al., 2005; Haberzettl et al., 2007; Lamy et al., 1999; Wagner et al., 2007). Modelling studies (Clement et al., 1999; Clement et al., 2000) and palaeorecords (Moy et al., 2002) suggest a more La Niña-like state of ENSO in this period. Around 3000 years ago modern ENSO variability was established (Sandweiss et al., 2001). During the last 2000-1000 years the strength of the ENSO variability has increased even more (Cane, 2005).

Two very well studied climatic periods are the Little Ice Age (LIA) from 1400 to 1800 AD and the Medieval Climatic Anomaly (MCA) from 950-1250 AD. The LIA was a period of colder temperatures in Europe. A prominent forcing factor possibly explaining the lower temperatures during the LIA in the Northern Hemisphere relates to changes in solar activity (Meyer and Wagner, 2009). A secondary forcing factor relates to an increase in volcanic activity (Bradley, 1985). A third theory deals with changes in ocean circulation. Lund et al. (2006) assumed that the Gulfstream was around 15-25% weaker during the LIA, because the Southern Westerly belt was probably located in a more northerly position during the austral summer (Meyer and Wagner, 2009). This would have resulted in more precipitation in northern and less in southern South Aermica. The opposite should be true for the MCA. However, proxy records show more precipitation in both northern and southern Patagonia during the LIA and less during the MCA (Bertrand et al., 2005; Boës and Fagel, 2008; Haberzettl et al., 2005; Huber and Markgraf, 2003; Lamy et al., 2001; Lamy et al., 2002; Mayr et al., 2005; Mohtadi et al., 2008; Moy et al., 2008). Another conundrum is why the record of Lago Guanaco (Moy et al., 2008) was in anti-phase (Moy et al., 2009) with the records of Lago Potrok Aike (Haberzettl et al., 2005) and Laguna Azul (Mayr et al., 2005). When Lago Guanaco recorded a dry climate, Lago Potrok Aike and Laguna Azul should have recorded a humid climate, but all records however are humid or dry simultaneously.

Similarly, the MCA is characterized by relatively warm conditions in the Northern Hemisphere, whereas regions in the Southern Hemisphere exhibit a cooling trend (Haberzettl et al., 2005; Mann et al., 2009).

II.5. Study Regions

II.5.1. Southern Chile

Southernmost South America is an important location for examining the timing and nature of climate change. The region of Patagonia including Tierra del Fuego spans ca. 15°of latitude and is the southernmost continuous landmass outside of Antarctica. Southern Chile is a key site to understand past climate variations, because it is located on the windward side of the Andes and at the northern limit of the influence of the Southern Westerlies.

Two major ice masses (the North and South Patagonian Icefields) and numerous snow- and ice-capped volcanoes and mountain icefields currently exist in this region.
The Southern Andes (33-56°S) are the result of the convergence between the oceanic Nazca plate, the oceanic Antarctic plate and the continental South American plate (DeMets et al., 1994; Lavenu and Cembrano, 1999). These three plates join around 46°S in a triple junction. Notwithstanding constant subduction all along the western edge of the South American

plate, active volcanism occurs only in four separate regions in the entire Andean Cordillera: the Northern (NVZ) (5°N-2°S), Central (CVZ) (14-27°S), Southern (SVZ) (33-46°S) and Austral Volcanic Zone (AVZ) (49-55°S) (Stern, 2004) (Figure II-15). Active volcanism is linked to the subduction angle, which has to be in between 25 and 30° to create magma (Stauder, 1973).

II.5.1.1. Chilean Lake District

Three main physiogeographic features characterize the Chilean Lake District (38-42°S): the Coastal Range, the Chilean Longitudinal Valley and the Andes. The Coastal Range with elevations generally below 500 m is dominated by primarily - Palaeozoic - low-grade metamorphic rocks (Thornburgh and Kulm, 1987). The Central Valley is filled with up to 4000 m thick alluvial sediments of Oligocene/Miocene to Quaternary age. The Andes reaches only elevations of 2000 m or less south of 37°S (Lomnitz, 1962) with a number of higher outlying peaks to the east (e.g. Cerro Tronador, 3554 m a.s.l.) and isolated volcanoes (e.g. Volcan Osorno, 2652 m a.s.l. and Volcan Villarrica 2847 m a.s.l.). The primary folding phase of the main cordillera began during the lower to upper Cretaceous and was followed by uplift during the upper Miocene/lower Pliocene (Paskoff, 1976). The lower Andes mainly consist of iron-poor plutonic basement rocks, while the high Andes are dominated by iron-rich basaltic to andesitic volcanics resulting from Pliocene to recent volcanic activity (Thornburgh and Kulm, 1987).

The continuity of the Central Valley is interrupted near the study area by the Loncoche Horst (39°3'-40°S), formed by the same metamorphic rocks making up the Coastal Range (Figure II-8).

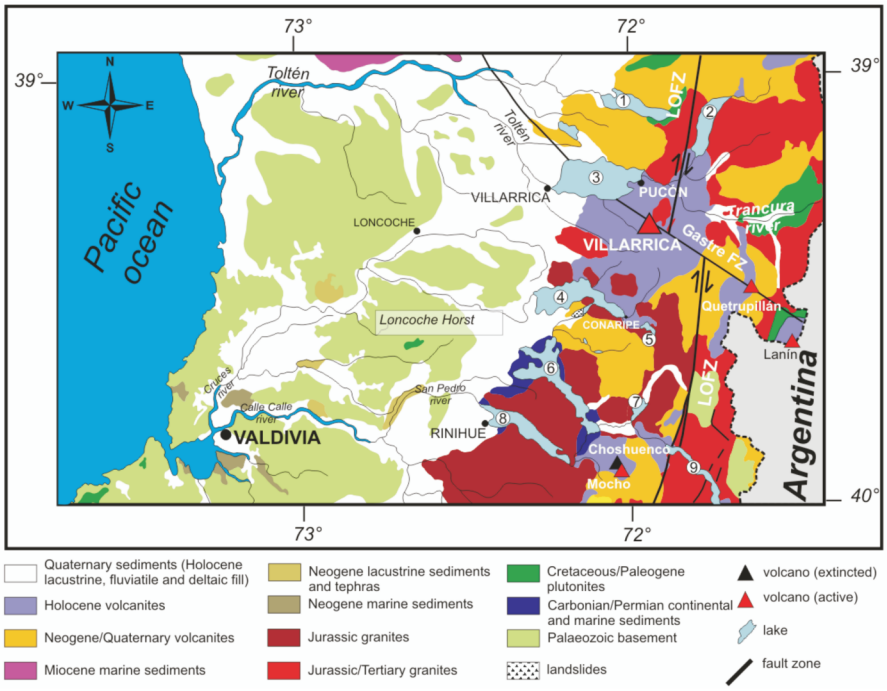

Figure II-8: Geological map and tectonic lineaments of the northern Chilean Lake District with the most important volcanoes and lakes. 1: Lago Colico; 2: Lago Caburgua; 3: Lago Villarrica; 4: Lago Calafquén; 5: Lago Pellaifa; 6: Lago Panguipulli; 7: Lago Neltume; 8; Lago Riñihue; 9: Lago Pirehueico (from Volland, 2006)

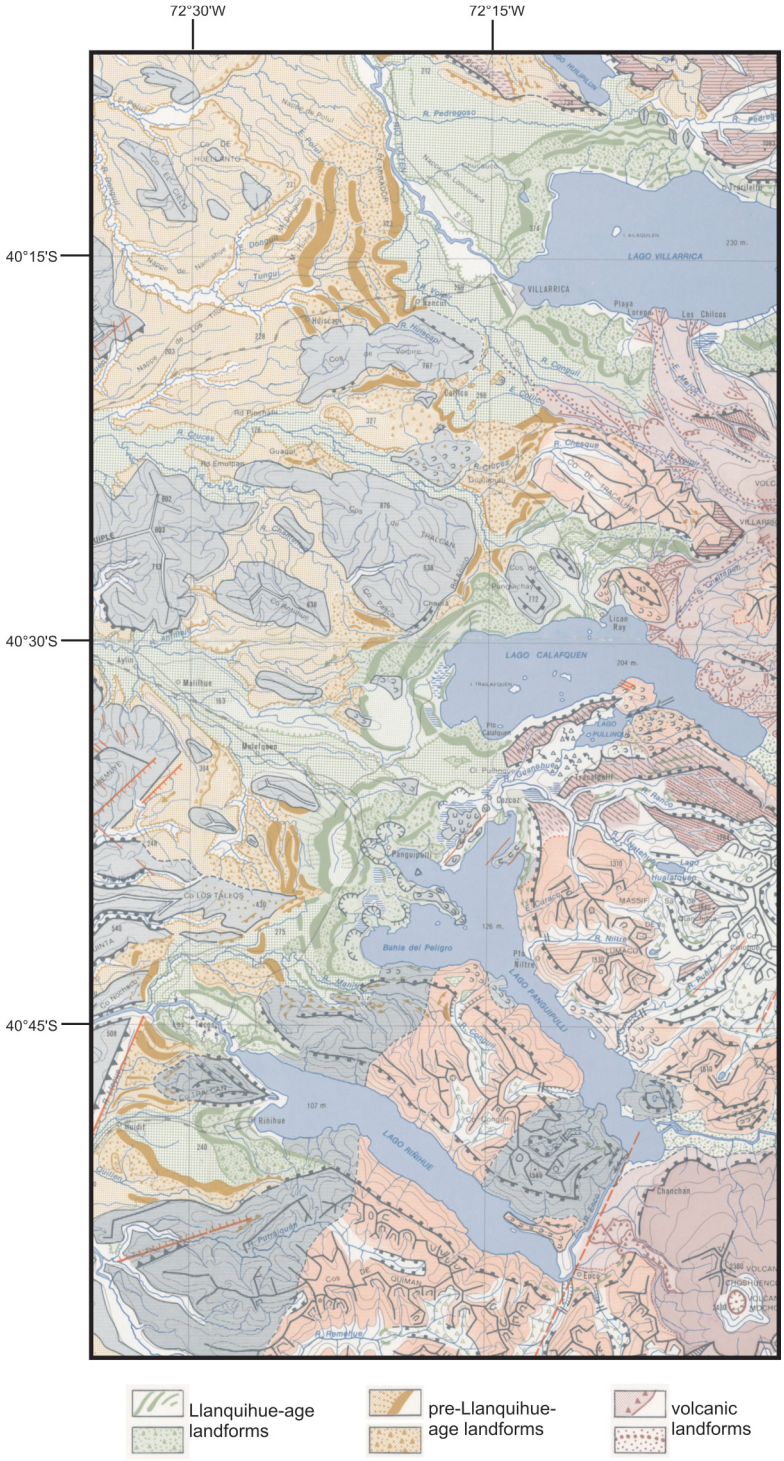

Figure II-9: Geomorphological map of the northern Chilean Lake District: 1:250 000 (from Laugenie, 1982)

In the Chilean Lake District, large piedmont glaciers developed during glacial periods on the western side of the Andes and the maximum positions of these outlet glaciers are, in general, marked by arcuate terminal moraines (Glasser et al., 2008). The glaciers eroded deep basins as they emerged from the Andean mountain front and their terminal moraines now impound the lakes that give their name to the Chilean Lake District. Remnants of glacial landforms formed during at least four first-order glacial periods can be found in the Chilean Lake District (Clayton et al., 1997; Laugenie, 1982; Mercer, 1976a; Porter, 1981). The innermost moraines around the lakes were formed during the last glaciations, also called the Llanquihue glaciation (75000-14000 cal a BP) (Clapperton, 1993) (Figure II-9). Dating of the terminal moraines around Lago Llanquihue demonstrated that there have been at least three to four, but possibly as many as six, readvances during the last glacial episode alone (Denton et al., 1999b; Lowell et al., 1995; Mercer, 1976b; Porter, 1981). The expansion of glaciers into the Chilean lake basins occurred during an interval of known global cooling, but it has also been suggested that the advance was driven largely by a northwards migration of the Polar Front, which resulted in a substantial increase in precipitation in the Lake District (Heusser, 1989; Hulton et al., 1994; Lamy et al., 2004). All Chilean Lake District glacial geomorphological studies indicate the glaciers still completely covering the lake basins by ca. 18000 cal a BP (Bentley, 1997; Denton et al., 1999b; Lowell et al., 1995). The lacustrine record of Lago Puyehue indicates, however, a completely ice-free lake existed by that time (Sterken et al., 2008) and the Puyehue glacier must have retreated much earlier out of the lake basin (Charlet et al., 2008; Heirman et al., in press). Most studies have generalised the timing of glacial advances and retreats for the entire region although datations of moraines in the Chilean Lake District are mostly limited to Lago Llanquihue and Seno de Reloncaví and there are no ages for moraines north of Lago Puyehue. The discrepancy between the lacustrine record of Lago Puyehue and the geomorphological records mean that the timing of climatic events in the Chilean Lake District remains open to discussion.

The present-day climate in the Chilean Lake District is humid-temperate with an average mean annual precipitation of ca. 2000 mm/a, which can increase up to 5000 mm/a with increasing altitude. Mean annual air temperature is 6-9°C. This style of precipitation and temperature is responsible for the development of the dense and temperate 'Valdivian' rainforest present throughout the entire region.

The Chilean Lake District is located in the Southern Volcanic Zone (SVZ). A prominent tectonic feature in this zone is the Liquiñe-Ofqui Fault Zone, a dextral strike-slip lineament, which controls the location of some of the larger stratovolcanoes and of the small monogenetic Holocene minor eruptive centres (Stern, 2004). Historically this volcanic zone is the most active zone in Chile. Lahars, lava flows and ashfalls have been the main volcanic hazards and during Late-Pleistocene and Holocene. Pyroclastic flows, surges and debris avalanches have occurred (Stern et al., 2007).This region is not only volcanically, but also seismologically very active. The large thrust earthquakes, responsible for most of the damage recorded in history, are located along the coast from 18°S to 46°S (the triple-junction) (Barrientos, 2007; Lomnitz, 2004). The largest ever historical earthquake was the 22nd of May 1960 Valdivia earthquake (Mw: 9.5). Return periods for events of Mw: 8 are of the order of 80 to 130 years for any given region in Chile (Barrientos, 2007). Megathrust earthquakes seem to have much longer return periods, with a mean recurrence interval of 220-440 years (Moernaut, 2010).

The main study area focuses on Lago Villarrica and the three largest lakes of the Siete Lagos (Lago Calafquén, Lago Panguipulli and Lago Riñihue). The Siete Lagos is an interlinked hydrological system of 8 lakes. Lago Pellaifa drains into Lago Calafquén, which drains through Lago Pullinque into Lago Panguipulli, which also receives the outflowing water of Lago Lacar (Argentina), Lago Pireheuico and Lago Neltume. All these lakes drain into Lago Riñihue whose outflow is connected to the Pacific Ocean. All these lakes are oligotrophic, monomictic, and temperate lakes with winter mixing and summer stratification (Campos et al., 1981; Campos et al., 1987; Campos et al., 1983). Lake water temperatures vary between 9.5-10°C for the entire water column in winter to ca. 22°C of the surface water in summer (Campos et al., 1981; Campos et al., 1987; Campos et al., 1983). In summer, the thermocline is generally located at a depth of 25 to 30 m (Campos et al., 1981; Campos et al., 1987; Campos et al., 1983). The total hardness of the lake water can be considered soft for all lakes (Campos et al., 1981; Campos et al., 1987; Campos et al., 1983). The lake level of these lakes varies seasonally with a lower lake level in summer and a higher lake level in autumn and winter. Maxima in phytoplankton biomass production occur in spring and summer. The species that contribute most to the biomass are mostly diatom species. These species also remain present in the phytoplankton throughout the year and can be considered periannual (Campos et al., 1987; Campos et al., 1983).

II.5.1.1.1. Lago Villarrica

Lago Villarrica (39°15'S; 72°02'W; 214 m a.s.l.) is a large, elliptic, glacigenic lake of 21 km by 9 km with a maximum depth of 167 m (Campos et al., 1983). Lago Villarrica's catchment area has a surface of about 2650 km² and comprises Volcán Villarrica (2847 m a.s.l.), Volcán Quetrupillán (2360 m a.s.l.) and Volcán Sollipulli (2282 m a.s.l.).

Morphologically, Lago Villarrica consists of a single, deep central basin (up to 167 m depth), and a shallower area with more morphological variability in the SW part of the lake (Figure II-10). Lago Villarrica is shallower than the lakes of the Siete Lagos, probably because, during glacial times, the glacier snout opened out in a much wider valley, allowing it to expand laterally instead of being pushed forward in the narrow pre-mountain-range valleys which is the case in the Siete Lagos (Laugenie, 1982). small island (Isla Allaquillén), that forms part of the grano-dioritic basement, is partly buried by the Licán Ignimbrite (Volland, 2006). This island marks the transition from a central, shallower platform to the deep basin. The western part of Lago Villarrica is morphologically protected from laharic inflows by the presence of the moraine ridges. Its main tributary is the Río Trancura, the course and extended alluvial plain of which have been strongly influenced by lava flows and lahars from Volcán Villarrica. Río Toltén, which cross-cuts the moraine ridges, constitutes the outflow of the lake towards the Pacific Ocean (Figure II-10). During deglaciation and/or in the Early Holocene Lago Villarrica's lake level was probably higher as can be deduced from the presence of palaeolake terraces found around the lake (Laugenie, 1982).

II.5.1.1.2. Lago Calafquén

Lago Calafquén (39°31'S; 72°11'W; 204 m a.s.l.) is a large, elongate, glacigenic lake, 24 km long by 2 to 6 km wide, and has a maximum depth of 212 m (Volland et al., 2007). Lago Calafquén is the largest lake of the hydrologically interlinked system of three overdeepened glacial lake basins (Lagos Calafquén, Panguipulli and Riñihue).The present day outlet is located at the narrow gorge of Hueninca, which provides fluvial connection with Lago Pullinque (200 m a.s.l.), a small and shallow (up to 25 m deep) landslide-dammed lake (Laugenie, 1982). The major inflowing river (Río Pellaifa) is located in the eastern extremity of Lago Calafquén and drains Lago Pellaifa and a mountainous area more to the north

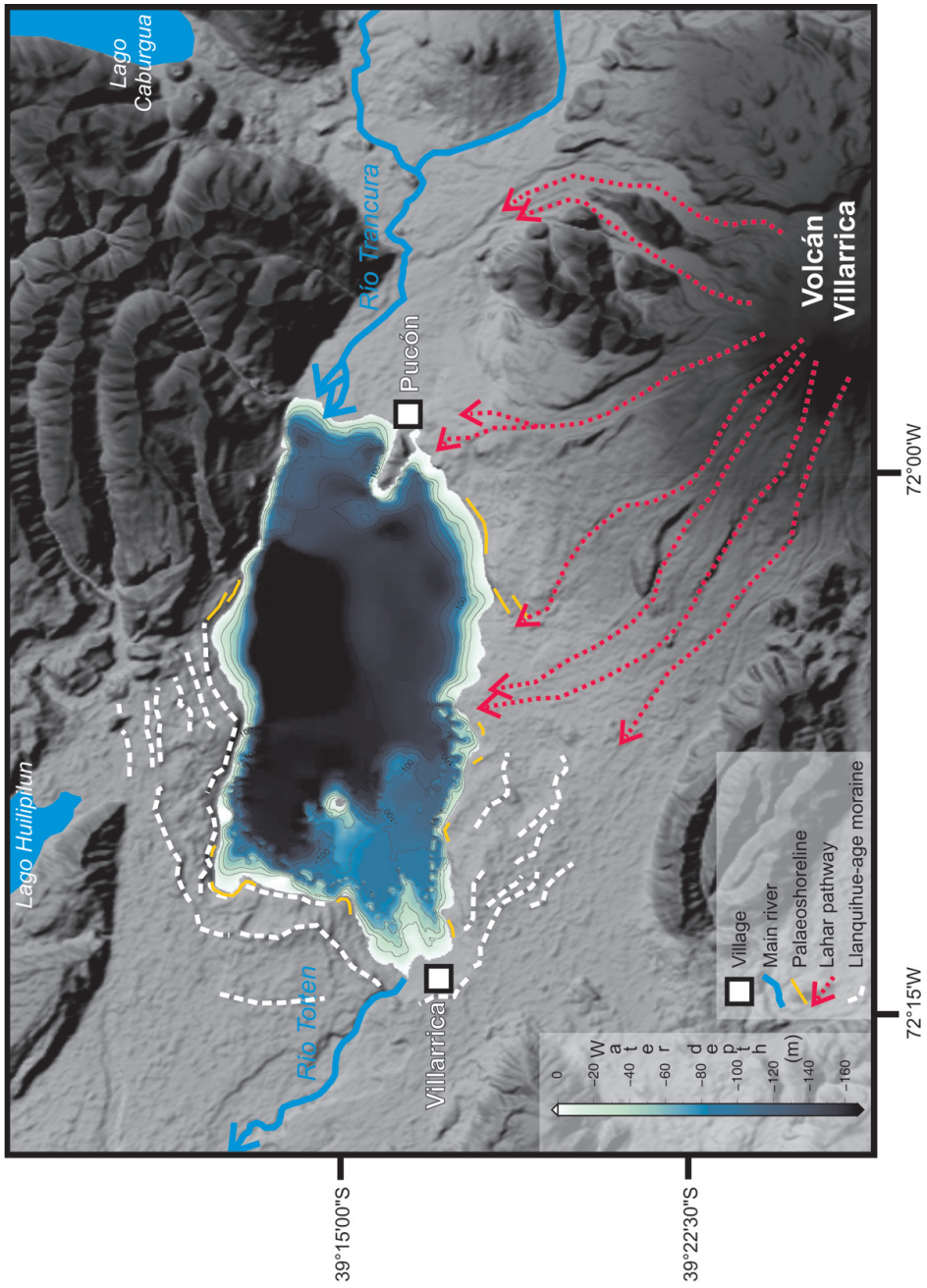

Figure II-10: Bathymetric map of Lago Villarrica (combination of the bathymetric map of Campos et al., 1983 and SHOA and seismic data). Location of the main geomorphological features in the area (adapted from Clayton et al., 1997; Laugenie, 1982)

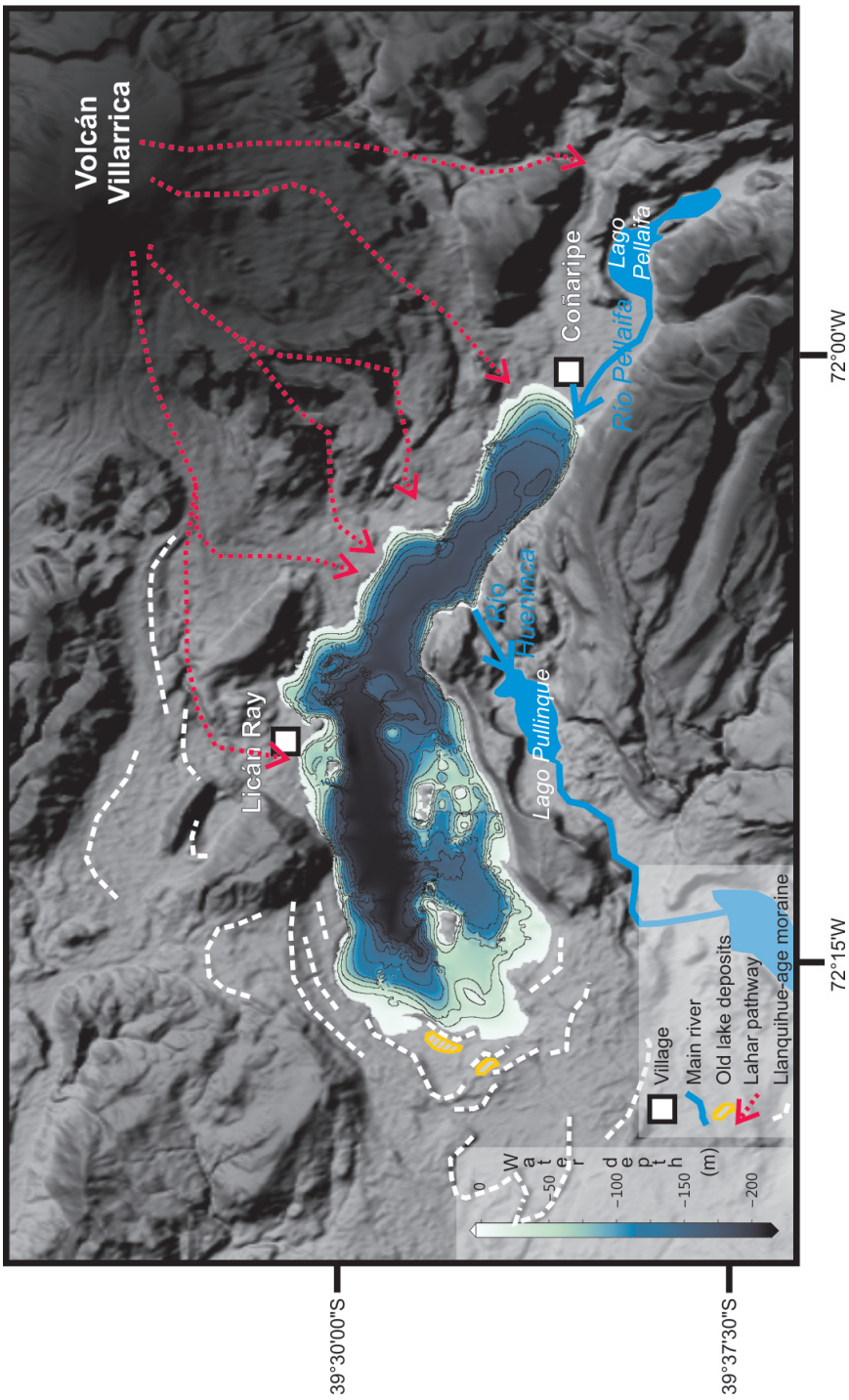

Figure II-11: Bathymetric map of Lago Calafquén (combination of the bathymetric map of Volland et al., 2007 and seismic data). Location of the main geomorphological features in the area (adapted from Laugenie, 1982)

of it. Volcán Villarrica borders the area to the north-east of the lake. Numerous destructive lahars were produced on its flanks during historical times, known to have damaged the towns of Licán Ray and Coñaripe. Rivers on these flanks (e.g. Río Chaillupén) are periodically waterbearing and deliver substantial amounts of coarse sediments to the lake system (Volland et al., 2007) (Figure II-11). Some parts of the western inner moraine belt around Lake Calafquén are submerged as the result of a major Holocene lake-level rise (Laugenie, 1982).

Morphologically, Lake Calafquén consists of a narrow, elongate and deep basin in the east and a wider area in the west with greater morphological complexity. This western part consists of a flat-bottomed deep basin (210 m deep), a SW sub-basin (150 m deep) and a SW elevated platform (65 m deep). Two small E-W oriented valleys are located east of the SW basin (Figure II-11). These areas are separated and bounded by prominent topographic highs, including those that form several islands in the middle of the lake. Differential glacial erosion between different rock types is probably the main cause of the present day morphological variability (Moernaut, 2010).

II.5.1.1.3. Lago Panguipulli

Lago Panguipulli (39°43'S; 72°12' W; 131 m a.s.l.) is a large, elongate, glacigenic lake, 24 km long by 3 to 10 km wide, with a maximum depth of 268 m

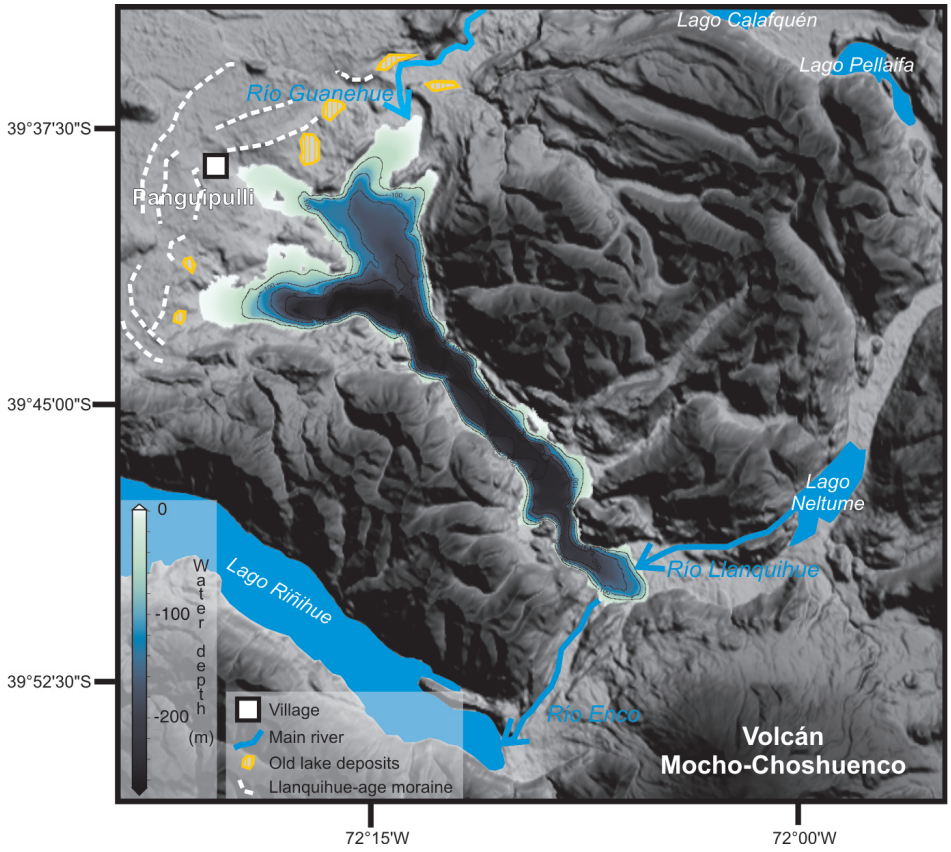

Figure II-12: Bathymetric map of Lago Panguipulli (combination of the bathymetry of Campos et al., 1981 and seismic data). Location of the main geomorphological features in the area (adapted from Laugenie, 1982)

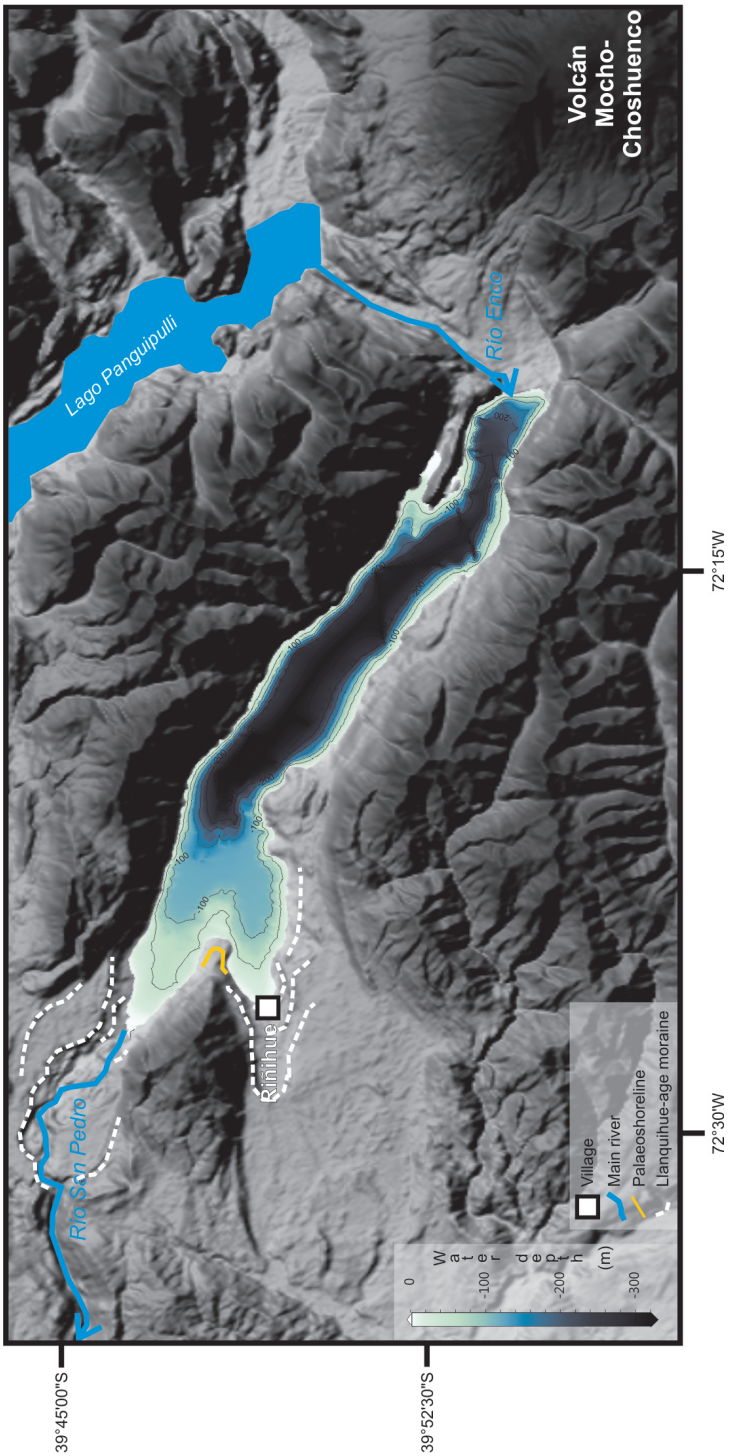

Figure II-13: Bathymetric map of Lago Riñihue. (combatination of the bathymetry of Campos et al., 1987 and seismic data). Location of the main geomorphological features in the area (adapted from Laugenie, 1982)

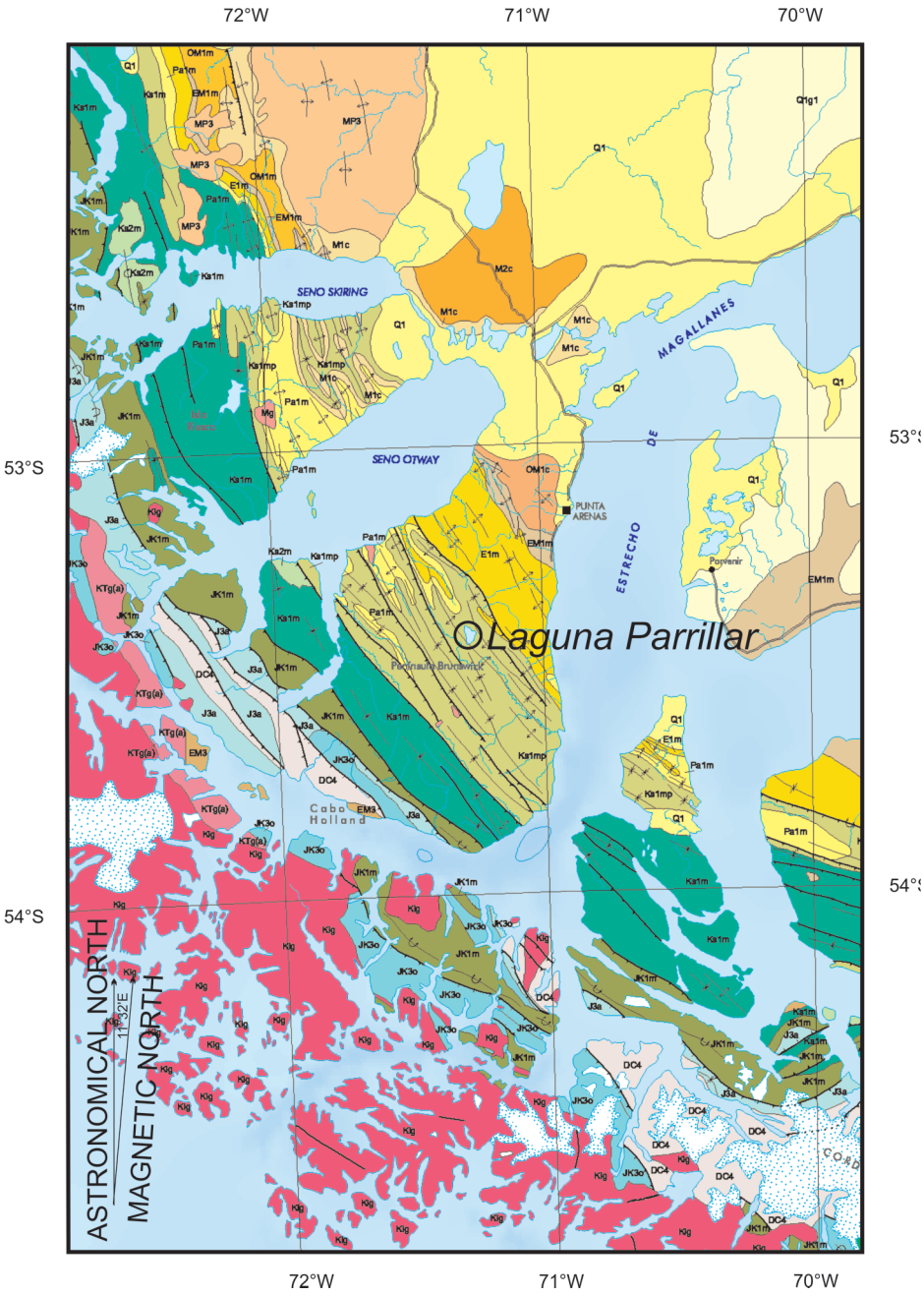

Figure II-14: Geological map of southern Patagonia (adapted from SERNAGEOMIN, 2003)

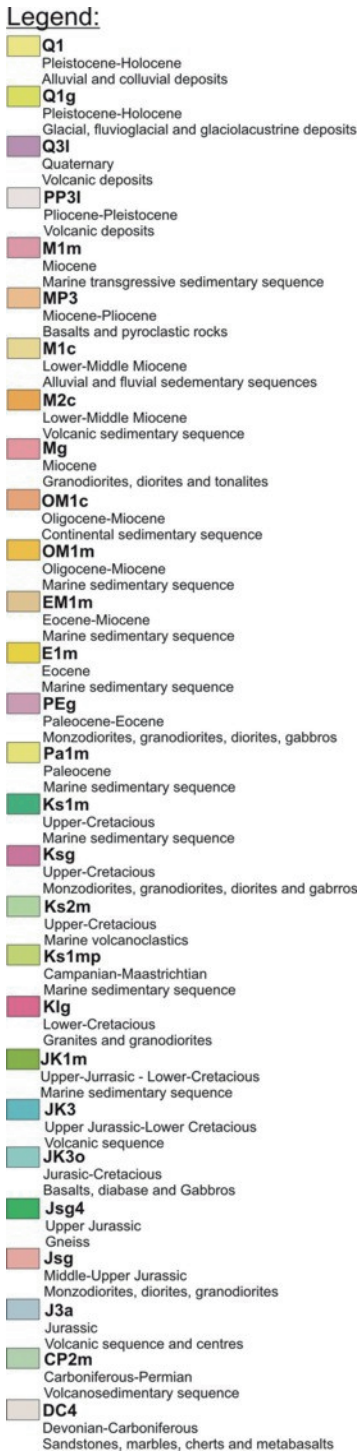

(Campos et al., 1981). In the western part, the lake outline shows four lobes ("fingers") with associated successions of moraine ridges. Río Huanehue and Río Llanquihue constitute the major inflowing rivers. Río Guanehue drains an area to the north, which encompasses Lago Pullinque, Lago Calafquén and Lago Pellaifa, while Río Llanquihue drains an eastern area, which encompasses Lago Neltume, Lago Pirihueico and Lago Lacar (Argentina). Río Enco forms the outflow of the lake and runs through the Enco Gorge towards Lago Riñihue (Figure II-12).

Morphologically, Lago Panguipulli consists of a narrow, elongated and deep basin that extends into the SW lobe, and a major sub-basin in the northwest part of the lake. A local bathymetric map of this NW sub-basin shows that it is characterized by a complex step-like morphology, with platforms around 120 m and 180 m depth, and that it connects with the deep basin trough a narrow subaqueous gorge (Figure II-12). The fjord-like deep basin was excavated in the Plutonic Unit of Panguipulli (140-130 Ma) while the complex western part of the lake was excavated in the Middle to Upper Triassic Panguipulli Formation (Rodríguez et al., 1999).

II.5.1.1.4. Lago Riñihue

Lago Riñihue (39°49'S; 72°20'W; 107 m a.s.l.) is a large, elongate, glacigenic lake, 28 km long by 3 to 4 km wide, with a maximum depth of 323 m (Campos et al., 1987). Its present day outlet (Río San Pedro) drains the entire Siete Lagos hydrografic network. The main tributary (Río Enco) is located in the eastern extremity of Lago Riñihue and drains Lago Panguipulli. Volcán Mocho-Choshuenco borders the SE extremity of the lake (Figure II-13) and its volcanic products (pyroclastic and laharic deposits, lava flows: Rodríguez et al., 1999) have episodically obstructed the Río Enco passage, which influenced the lake level evolution of Lago Riñihue and Lago Panguipulli.

Morphologically, Lago Riñihue consists of a narrow and elongated deep basin (up to 323 m deep), and two sub-basins (~120 m deep) in the western part. These sub-basins are separated by an E-W oriented ridge (Figure II-13). This westwards opening and shallowing of the lake basin spatially correlates with the geological boundary between the Futrono-Riñihue Batholite in the east and the Trafun Metamorphic Complex in the west (Rodríguez et al., 1999).

II.5.1.2. Southern Patagonia

Geomorphologically, southern Patagonia can be divided from west to east into the Coastal Range and pre-Andean mountain chain consisting of many small islands, the Andean Mountain Chain consisting of larger islands, fjords and canals, the trans-Andean range of islands, peninsulas and fjords and finally the Patagonian steppe or pampas (Endlicher and Santana, 1988).

Mean annual precipitation values are very high in the pre-Andes and Andes (up to 5000 mm/a), but this quickly reduces to 1500 m/a over a distance of only a few kilometres while going east (Endlicher and Santana, 1988). Further east the amount is reduced further to values of ca. 429.8 m/a in the area of Punta Arenas, the main city in this part of Chile, located at the western edge of pampas (Santana, 1984).
The mean annual temperature in Punta Arenas is 6.5°C (Endlicher and Santana, 1988). The wind blows dominantly from the west with a mean annual wind speed of 4.6 m/s, with maxima of 7 to 8 m/s in spring and summer and minimum values of 4 to 5 m/s in winter. Wind speed rarely drops below 3.2 m/s (Endlicher and Santana, 1988).

The southernmost and pre-Andean and Andean mountains consist of Mesozoic plutonic rocks with some volcanics at its eastern edge. The geology of trans-Andes, including the Brunswick Peninsula, consists mostly of Late-Jurassic, Cretaceous to Eocene marine deposits consisting of (glauconite-rich) argillites and sandstones. The pampas are developed in Quaternary-age glacial deposits (Dollenz, 1983; SERNAGEOMIN, 2003) (Figure II-14).

The Antarctic plate subducts at a much slower rate (2 cm/a) under the South American plate than the Nazca plate (7.8 cm/a) further to the north (DeMets et al., 1994). The slow convergence rate and the type of subduction are probably the main reasons for the relative lack of seismicity on the western margin of South America south of the triple junction (Barrientos, 2007).

The Austral Volcanic Zone (AVZ) only includes six volcanic centres, five stratovolcanoes: Lautaro (49°S), Viedma (49.4°S), Aguillera (50.2°S), Reclus (51°S) and Monte Burney (52.3°S) and one dome complex: Cook Island (54.9°S) (Figure II-15). Lautaro is the only centre with a documented historic eruption, which occurred in 1959 (Martinic, 1988). Tephra records indicate that each of the five stratovolcanoes has had Holocene explosive activity (Kilian et al., 2003; Stern, 2008). The presence of only six volcanic centres with relatively few geochemically distinctive, explosive eruptions allows the construction of a tephrochronological framework for this region (Stern, 2008).

The largest and best-developed moraine complexes are those developed in the areas occupied by former outlet glacier in Seno Skyring, Seno Otway, Estrecho Magallenes and Bahía Inútil. The location and behaviour of these glaciers appears to be strongly topographically controlled, with former outlet glaciers repeatedly occupying the low-lying topographic depressions and receding up-valley from their maximum positions (Glasser et al., 2008). The LGM in this area is reasonably well established at 25000-23000 cal a BP for a terminal moraine in the Magellan Strait (McCulloch et al., 2005b) and 20000-18000 cal a BP in Bahía Inútil (Bentley et al., 2005; Kaplan et al., 2007; McCulloch et al., 2005b).

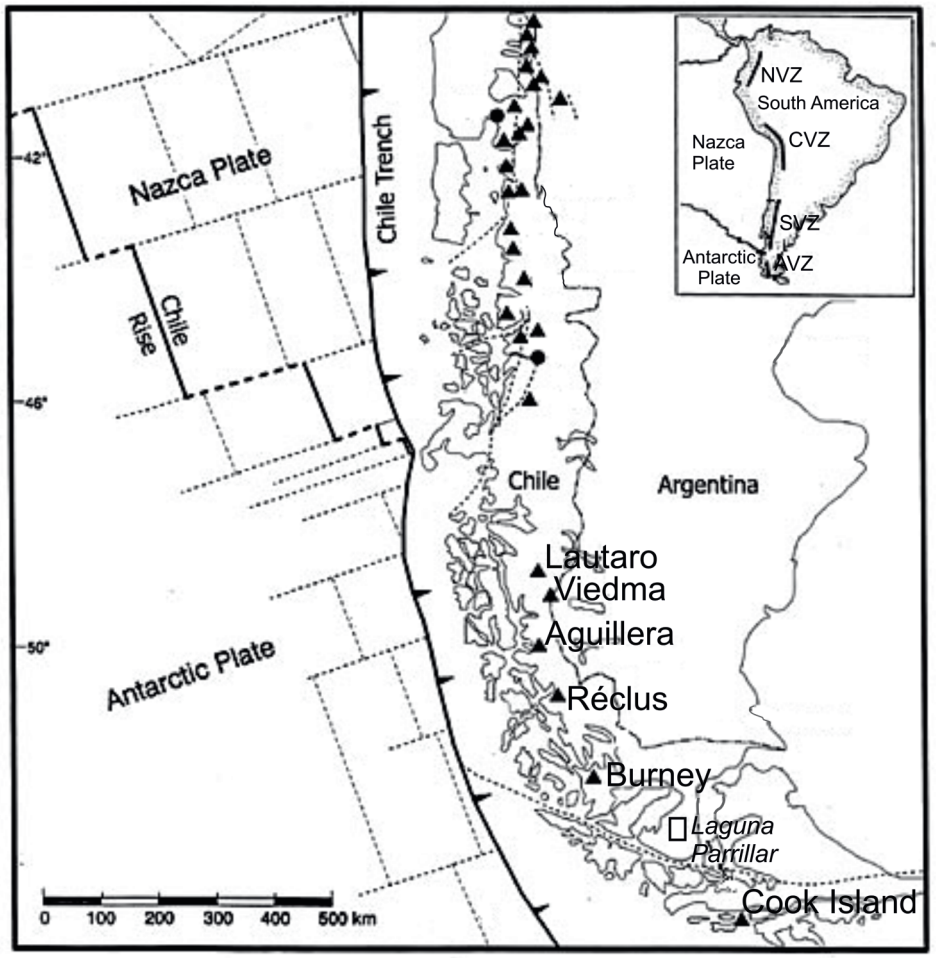

Figure II-5: The volcanoes of the Southern (SVZ) and Austral Volcanic Zone (AVZ) (adapted from Naranjo and Stern, 2004).

II.5.1.2.1. Laguna Parrillar

Laguna Parrillar is a large body of fresh water located in the middle of the Brunswick Peninsula in the fjord region of Southern Patagonia. The lake is located within the limits of Reserva Forestal 'El Parrillar', a national park. The park was created on the 22nd of April 1977 and encompasses an area of 20814 ha. Laguna Parrillar is located at ca. 294 m a.s.l. in a round depression surrounded by moorlands and mountain chains covered with Nothofagus forest (Dollenz, 1983) (Figure II-16). The area receives more rain than Punta Arenas and is partially protected from the dominant Southern Westerly winds. There are two important rivers that enter the lake in the north and the northeast and there is one outlet in the southern corner of the lake (Figure II-16). Due to its location at the interior of the Brunswick Peninsula temperatures can be lower than Punta Arenas and daily thermic oscillations can be large (Dollenz, 1983).

The geology in the area of the national park consists of gray stratified argillites and gray argillites with calcium concretions, glauconite-rich argillites and glauconite-rich sandstones of Late-

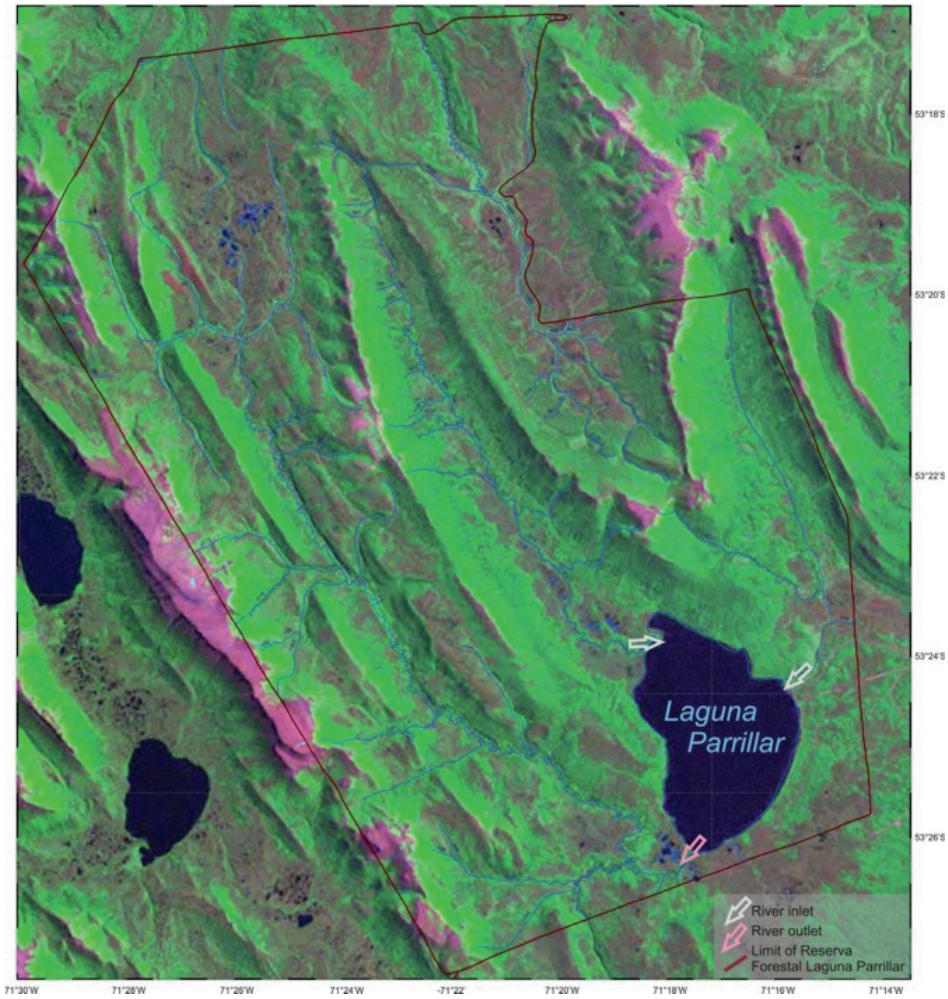

Figure II-16: Laguna Parrillar, its rivers and its catchment (false colour Landsat picture). The colours of the Landsat picture give an idea about the vegetation, with beige-gray colours indicating moorland, green Nothofagus forest and pink exposed bedrock.

Cretaceous to Eocene age (Dollenz, 1983).

Laguna Parrillar is located outside the LGM moraine limits (Bentley et al., 2005; Clapperton et al., 1995; Glasser et al., 2008; McCulloch and Bentley, 1998; McCulloch et al., 2005a) in what Bentley et al. (2005) classified as a pre-last-glaciation weathering zone based on morphology, weathering, soil cover and colour on satellite image.. LGM ice-sheet reconstructions (Glasser et al., 2008; McCulloch et al., 2000; Sugden et al., 2009) and ice-sheet modeling (Hulton et al., 2002) do not demonstrate the presence of ice on the elevated (294 m a.s.l.) and exposed, inland position of the lake. Therefore, Laguna Parrillar could have remained ice free during the LGM and a high-resolution, pre-LGM sedimentary record is potentially preserved in the lake deposits (Figure II-17).

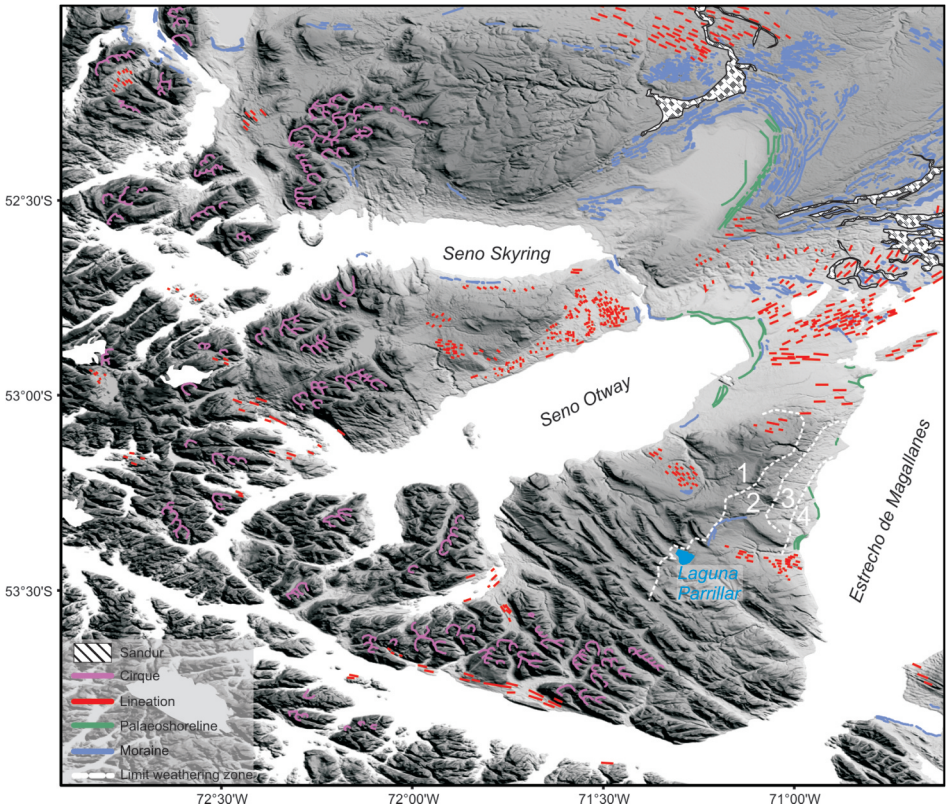

Figure II-17: Glacial landforms present in the Brunswick Peninsula and its surroundings (adapted from Glasser et al., 2008). The white numbers indicate Bentley et al.'s (2005) weathering zones. The deposits of the last glaciations belong to zone 3 and 4. Weathering zone 1 and 2 are much older.

II.5.2. Kerguelen Archipelago

Iles Kerguelen is a sub-Antarctic archipelago consisting of one major island (Grande Terre), several minor ones, about 300 islets and rocks, and outliers. It is partly volcanic with a total area of 7215 km² and a peak elevation of 1850 m (Grand Ross). Grand Ross is also the youngest volcanic edifice. The archipelago is the emerged part of a Large Igneous Province (LIP), the Kerguelen Plateau. It was formed by giant basalt eruptions ca. 40 Ma. Since then, hot spot-type volcanism remained due to the persistence of a mantle plume. This resulted in the formation of several volcanic massifs (Figure II-18). The youngest published eruption is linked to the Dome Carva Volcano Complex located on the Rallier-du-Baty Peninsula and happened about 28000 years ago (Gagnevin et al., 2003). Arnaud et al. (2009) found on the other hand evidence for much more recent eruptions (875-895 AD) of the Mount Vulcain Volcano also located on the Rallier-du-Baty Peninsula in the form of an ash layer in Lac d'Armor (Figure II-18).

The main island features high mountains and plateaus with deep lakes formed by glacier erosion. The coast is characterised by deeply incised fjords. The Cook glacier covering 10% of the island is a remnant of the LGM ice sheet. Due to the absence of any major landmasses in the region, the climate in Kerguelen is dominated by oceanic processes. The islands are located on

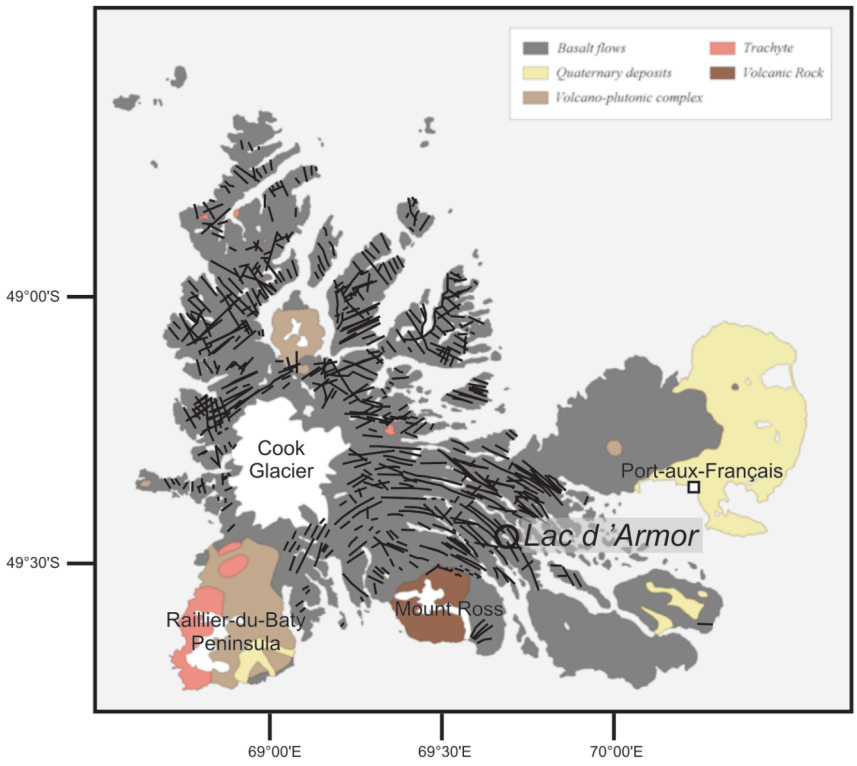

Figure II-18: Geological map of the Kerguelen archipelago (adapted from Giret, 1980; Nougier, 1970a; Nougier, 1970b). The black lines represent faults.

the Antarctic Convergence (Barker and Thomas, 2004) and in the core of the Southern Westerlies (Kalnay et al., 1996; Shulmeister et al., 2004). The Polar Front is situated just north of Kerguelen (Belkin and Gordon, 1996). The climate is in general cold (a mean annual temperature of 4.5°C), windy (100 km/h winds in all months), heavily clouded and rainy (more than 3200mm/a on the west coast, less than 800 mm/a on the east coast) (Frenot et al., 1997b). Consequently, the major oceanic currents – the ACC (Barker and Thomas, 2004; Gersonde et al., 2005) – and atmospheric circulation – the dominating Southern Westerlies (Shulmeister et al., 2004; Wyrwoll et al., 2000) – control climatic conditions (Figure II-3).

Currently the ocean around the islands is ice free, but during the LGM Antarctic sea ice might have reached as far north as this location (Gersonde et al., 2005; Gersonde and Zielinski, 2000). The extent of the Kerguelen island ice cover during the LGM is heavily debated (Hall, 1990). Some authors claim that the LGM ice extent was very limited and that the fjords and glacial valleys are the result of earlier glacial events (Bellair, 1965; Nougier, 1972). Hall (1984) suggested they are LGM in age. The lack of tills in some areas (Bellair, 1965) and the absence of isostatic rebound (Bellair, 1965; Testut et al., 2006) argues for the case of incomplete ice cover. There may have been major centres of ice growth in the higher areas to the west with a number of locations of only cirque glacier growth (Hall, 2004). A key component in the consideration of Grand Terre is the localised changes to

topography induced by volcanic and tectonic history throughout the Quaternary and the influences that this may have had on both glaciation and preservation of earlier glacial imprints (Hall, 2004).

While the Kerguelen Plateau has been the focus of several palaeoclimate-orientated oceanographic studies (e.g. Dezileau et al., 2003; Villa and Persico, 2006; Whitehead and McMinn, 2002), the island itself and its many lakes remained hitherto largely unexplored. Previous land-based, palaeoclimatic studies are confined to peat bogs (e.g. Bellair, 1970; Frenot et al., 1997a; Frenot et al., 1993; Frenot et al., 1997b; Young and Schofield, 1973), the lake records remained unexplored.

II.5.2.1. Lac d'Armor

Lac d'Armor, 3.5 km long and on average 0.5 km wide, was selected for this study, because of its location with respect to the main glacier on the island and its accessibility. The lake is located southwest of Port-Aux-Français, the only village on the island and of the Golfe du Morbihan. A shallow sill of only a few meters high and a couple of hundred meters wide, separates the lake from the Fjord Henri Bossière. Lac d'Armor has two major inlets, one in the northwest (Rivière du Nord) and one in the south (Rivière du Diable) and one minor, nameless, inlet in the north. The southern river connects four lakes (Lac Parcival, Lac Lancelot, Lac d'Enfer and Lac d'Argoat) and several small ponds with Lac d'Armor, which is the final connection of this fresh water system with the ocean (Figure II-19).

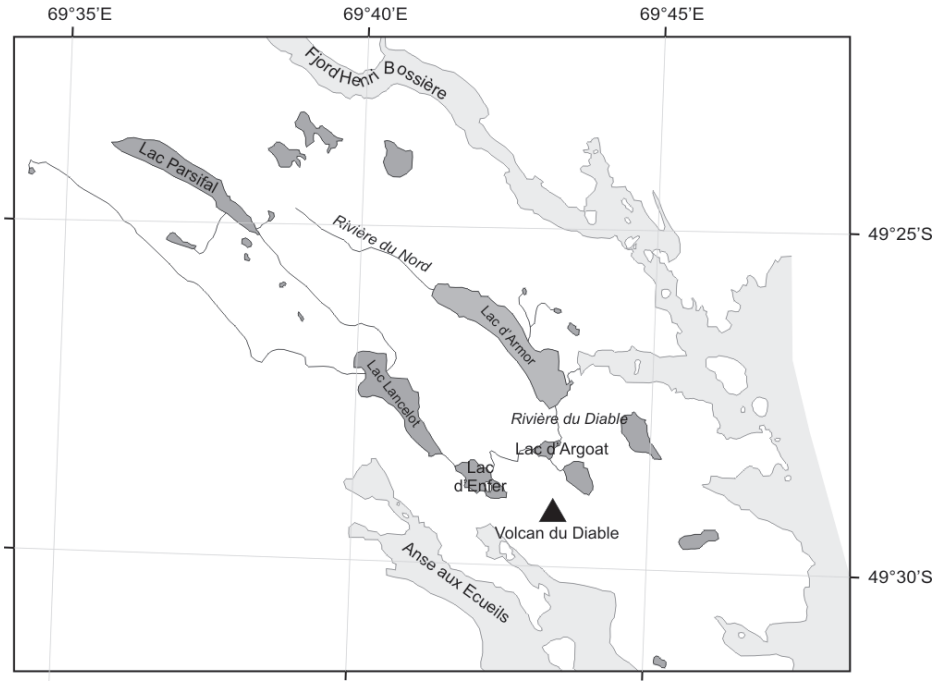

Figure II-19: Lac d'Armor and its catchment

References

Abarzua, A.M., Villagran, C. and Moreno, P.I., 2004. Deglacial and postglacial climate history in east-central Isla Grande de Chiloe, southern Chile (43 degrees S). *Quaternary Research*, **62**(1): 49-59.

Ackert, P.J., Becker, R.A., Singer, B.S., Kurz, M.D., Caffee, M.W. and Mickelson, D.M., 2008. Patagonian glacier response during the Late-Glacial-Holocene transition. *Science*, **321**: 392-395.

Ahn, J. and Brook, E.J., 2008. Atmospheric CO2 and climate on millennial time scales during the last glacial period. *Science*, **322**: 83-85.

Andersen, K.K., Svensson, A., Johnsen, S.J., Rasmussen, S.O., Bigler, M., Rothlisberger, R., Ruth, U., Siggaard-Andersen, M.L., Steffensen, J.P., Dahl-Jensen, D., Vinther, B.M. and Clausen, H.B., 2006. The Greenland Ice Core Chronology 2005, 15-42 ka. Part 1: constructing the time scale. *Quaternary Science Reviews*, **25**(23-24): 3246-3257.

Anderson, R.F., Ali, S., Bradtmiller, L.I., Nielsen, S.H.H., Fleisher, M.Q., Anderson, B.E. and Burckle, L.H., 2009. Wind-driven upwelling in the southern ocean and the deglacial rise in atmospheric CO2. *Science*, **323**: 1443-1448.

Ariztegui, D., Bianchi, M.M., Masaferro, J., Lafargue, E. and Niessen, F., 1997. Interhemispheric synchrony of late-glacial climatic instability as recorded in proglacial Lake Mascardi, Argentina. *Journal of Quaternary Science*, **12**(4): 333-338.

Arnaud, F., Révillon, S., Poulenard, J., Fanget, B., Boone, D. and Heirman, K., 2009. First reconstruction of last millennium flooding activity on Kerguelen archipelago (50°S, subantarctic Indian Ocean) from Lake Armor sediment: implications for southern hemisphere cyclonic circulation changes, *Conference abstract for EGU*, Vienna, Austria.

Barbante, C., Barnola, J.-M., Becagli, S., Beer, J., Bigler, M., Boutron, C., Blunier, T., Castellano, E., Cattani, O., Chappellaz, J., Dahl-Jensen, D., Debret, M., Delmonte, B., Dick, D., Falourd, S., Faria, S., Federer, U., Fischer, H., Freitag, J., Frenzel, A., Fritzsche, D., Fundel, F., Gabrielli, P., Gaspari, V., Gersonde, R., Graf, W., Grigoriev, D., Hamann, I., Hansson, M., Hoffmann, G., Hutterli, M.A., Huybrechts, P., Isaksson, E., Johnsen, S., Jouzel, J., Kaczmarska, M., Karlin, T., Kaufmann, P., Kipfstuhl, S., Kohno, M., Lambert, F., Lambrecht, A., Lambrecht, A., Landais, A., Lawer, G., Leuenberger, M., Littot, G., Loulergue, L., Lüthi, D., Maggi, V., Marino, F., Masson-Delmotte, V., Meyer, H., Miller, H., Mulvaney, R., Narcisi, B., Oerlemans, J., Oerter, H., Parrenin, F., Petit, J.-R., Raisbeck, G., Raynaud, D., Röthlisberger, R., Ruth, U., Rybak, O., Severi, M., Schmitt, J., Schwander, J., Siegenthaler, U., Siggaard-Andersen, M.-L., Spahni, R., Steffensen, J.P., Stenni, B., Stocker, T.F., Tison, J.-L., Traversi, R., Udisti, R., Valero-Delgado, F., Broeke, M.R.v.d., Wal, R.S.W.v.d., Wagenbach, D., Wegner, A., Weiler, K., Wilhelms, F., Winther, J.-G. and Wolff, E., 2006. One-to-one coupling of glacial climate variability in Greenland and Antarctica. *Nature*, **444**(7116): 195-198.

Barker, P.F. and Thomas, E., 2004. Origin, signature and palaeoclimatic influence of the Antarctic Circumpolar Current. *Earth-Science Reviews*, **66**(1-2): 143-162.

Barker, S., Diz, P., Vautravers, M.J., Pike, J., Knorr, G., Hall, I.R. and Broecker, W.S., 2009. Interhemispheric Atlantic seesaw response during the last deglaciation. *Nature*, **457**: 1097-1103.

Barrientos, S.E., 2007. Earthquakes in Chile. In: T. Moreno and W. Gibbons (Editors), *The Geology of Chile*. The Geological Society of London, London, pp. 263-287.

Barrows, T.T., Lehman, S.J., Fifield, L.K. and De Deckker, P., 2007. Absence of cooling in New Zealand and the adjacent ocean during the Younger Dryas chronozone. *Science*, **318**: 86-89.

Basile, I., Grousset, F.E., Revel, M., Petit, J.R., Biscaye, P.E. and Barkov, N.I., 1997. Patagonian origin of glacial dust deposited in East Antarctica (Vostok and Dome C) during glacial stages 2, 4 and 6. *Earth and Planetary Science letters*, **146**(3-4): 573-589.

Beaufort, L., de Garidel-Thoron, T., Mix, A.C. and Pisias, N.G., 2001. ENSO-like forcing on oceanic primary production during the Late Pleistocene. *Science*, **293**: 2440-2444.

Belkin, I.M. and Gordon, A.L., 1996. Southern Ocean fronts from the Greenwich meridian to Tasmania. *Journal of Geophysical Research-Oceans*, **101**(C2): 3675-3696.

Bellair, N., 1970. Palynologie d'une troubière de Pointe-Denis. *Bulletin de l'Association française pour l'étude du Quairtaire*, **22**(1): 49-51.

Bellair, P., 1965. Un example de glaciation aberrante, les Iles Kerguelen. *Comité National Français des Recherches Antarctiques*, **11**: 1-27.

Bennett, K.D., Haberle, S.G. and Lumley, S.H., 2000. The last glacial-Holocene Transition in Southern Chile. *Science*, **290**: 325-328.

Bentley, M.J., 1997. Relative and radiocarbon chronology of two former glaciers in the Chilean Lake District. *Journal of Quaternary Science*, **12**: 25-33.

Bentley, M.J., Sugden, D.E., Hulton, N.R.J. and McCulloch, R.D., 2005. The landforms and pattern of deglaciation in the Strait of Magellan and Bahia Inu'til, southernmost South America. *Geografiska Annaler Series a-Physical Geography*, **87A**(2): 313-333.

Bertrand, S., Charlet, F., Charlier, B., Renson, V. and Fagel, N., 2008. Climate variability of Southern Chile since the Last Glacial Maximum: a continuous sedimentological record from Lago Puyehue (40°S). *Journal of Paleolimnology*, **39**: 179-195.

Blunier, T. and Brook, E.J., 2001. Timing of millennial-scale climate change in Antarctica and Greenland during the last glacial period. *Science*, **291**(5501): 109-112.

Blunier, T., Chappellaz, J., Schwander, J., Dällenbach, A., Stauffer, B., Stocker, T.F., Raynaud, D., J.Jouzel, Clausen, H.B., Hammer, C.U. and Johnsen, S.J., 1998. Asynchrony of Antarctic and Greenland climate change during the last glacial period. *Nature*, **394**: 739-744.

Boës, X. and Fagel, N., 2008. Relationship between southern Chilean varved lake sediments, precipitation and ENSO for the last 600 years. *Journal of Paleolimnology*, **39**(2): 237-252.

Bond, G.C. and Lotti, R., 1995. Iceberg Discharges into the North-Atlantic on Millennial Time Scales During the Last Glaciation. *Science*, **267**(5200): 1005-1010.

Bradley, R.S., 1985. *Quaternary paleoclimatology. Methods of paleoclimate reconstruction*. Allen & Unwin, London, 472 pp.

Broecker, W.S., 1998. Paleocean Circulation during the Last Deglaciation: A Bipolar Seesaw? *Paleoceanography*, **13**(2): 119-121.

Broecker, W.S. and van Donk, J., 1970. Insolation changes, ice volumes, and the O18 record in deep-sea cores. *Review of Geophysics and Space Physics*, **8**(1): 169-198.

Calvo, E., Pelejero, C., De Deckker, P. and Logan, G.A., 2007. Antarctic deglacial pattern in a 30 kyr record of sea surface temperature offshore South Australia. *Geophysical Research Letters*, **34**(13): L13707.

Campos, H., Arenas, J., Steffen, W. and Agüero, G., 1981. Morphometrical, physical and chemical limnology of lake Panguipulli (Valdivia, Chile). *Neues Jahrbuch für Geologie und Paläontologie, Monatshefte*, **10**: 603-625.

Campos, H., Steffen, W., Agüero, G., Parra, O. and Zúñiga, L., 1987. Limnology of lake Riñihue. *Limnologica*, **18**(2): 339-357.

Campos, H., Steffen, W., Román, C., Zúñiga, L. and Agüero, G., 1983. Limnological

studies in Lake Villarrica: Morphometric, physical, chemical, planktonical factors and primary productivity. *Archiv für Hydrobiologie Supplement*, **65**(4): 371-406.

Cane, M.A., 2005. The evolution of El Nino, past and future. *Earth and Planetary Science Letters*, **230**(3-4): 227-240.

Cane, M.A. and Evans, M., 2000. Climate variability - Do the tropics rule? *Science*, **290**(5494): 1107-1108.

Cerveny, R.S., 1998. Present climates of South America. In: J.E. Hobbs, J.A. Lindesay and H.A. Bridgman (Editors), *Climates of the southern continents: Present, past and future*. John Wiley & Sons, Chichester, pp. 107-135.

Charlet, F., Chapron, E., De Batist, M., Pino, M. and Urrutia, R., 2008. Seismic stratigraphy of Lago Puyehue (Chilean Lake District): new views on its deglacial and Holocene evolution. *Journal of Paleolimnology*, **39**: 163-177.

Chiang, J.C.H., Biasutti, M. and Battisti, D.S., 2003. Sensitivity of the Atlantic Intertropical Convergence Zone to Last Glacial Maximum boundary conditions. *Paleoceanography*, **18**(4): 18.

Chiang, J.C.H. and Bitz, C.M., 2005. Influence of high latitude ice cover on the marine Intertropical Convergence Zone. *Climate Dynamics*, **25**(5): 477-496.

Clapperton, C., 1993. *Quaternary geology and geomorphology of South America*. Elsevier, Amsterdam, The Netherlands, 779 pp.

Clapperton, C.M., Sugden, D.E., Kaufman, D.S. and McCulloch, R.D., 1995. The Last Glaciation in Central Magellan-Strait, Southernmost Chile. *Quaternary Research*, **44**(2): 133-148.

Clayton, J.D., Clapperton, C.M. and Antinao Rojas, J.L., 1997. Las glaciaciones Pleistocenas en la cuenca del lago Villarrica, Andes del sur, *Congresso Geológico Chileno*, Antafagosta, Chile.

Clement, A.C., Seager, R. and Cane, M.A., 1999. Orbital controls on the El Niño/Southern Oscillation and the tropical climate. *Paleoceanography*, **14**(4): 441-456.

Clement, A.C., Seager, R. and Cane, M.A., 2000. Suppression of El Niño during the mid-Holocene by changes in the Earth's orbit. *Paleoceanography*, **15**(6): 731-737.

Cohen, A.S., 2003. *Paleolimnology - The History and Evolution of Lake Systems*. Oxford University Press, Oxford, 500 pp.

Delmonte, B., Andersson, P.S., Hansson, M., Schöberg, H., Petit, J.R., Basile-Doelsch, I. and Maggi, V., 2008. Aeolian dust in East Antarctica (EPICA-Dome C and Vostok): Provenance during glacial ages over the last 800 kyr. *Geophysical Research Letters*, **35**(7): L07703.

Delmonte, B., Basile-Doelsch, I., Petit, J.R., Maggi, V., Revel-Rolland, M., Michard, A., Jagoutz, E. and Grousset, F., 2004. Comparing the Epica and Vostok dust records during the last 220,000 years: stratigraphical correlation and provenance in glacial periods. *Earth-Science Reviews*, **66**(1-2): 63-87.

DeMets, C., Gordon, R.G., Argus, D.F. and Stein, S., 1994. Effect of recent revisions to the geomagnetic reversal time scale on estimates of current plate motions. *Geophysical Research Letters*, **21**(20): 2191-2194.

Denton, G.H., Heusser, C.J., Lowell, T.V., Moreno, P.I., Andersen, B.G., Heusser, L.E., Schlüchter, C. and Marchant, D.R., 1999a. Interhemispheric linkage of paleoclimate during the last glaciation. *Geografiska Annaler*, **81A**(2): 107-153.

Denton, G.H., Lowell, T.V., Heusser, C.J., Schlüchter, C., Andersen, B.G., Heusser, L.E., Moreno, P.I. and Marchant, D.R., 1999b. Geomorphology, stratigraphy, and radiocarbon chronology of Llanquihue drift in the area of the southern Lake District, Seno Reloncaví, and Isla Grande de Chiloé, Chile. *Geografiska Annaler*, **81A**(2): 167-229.

Dezileau, L., Reyss, J.L. and Lemoine, F., 2003. Late Quaternary changes in biogenic opal fluxes in the southern Indian Ocean. *Marine Geology*, **202**(3-4): 143-158.

Diekmann, B., Kuhn, G., Rachold, V., Abelmann, A., Brathauer, U., Fütterer, D.K., Gersonde, R. and Grobe, H., 2000. Terrigenous sediment supply in the Scotia Sea (Southern Ocean): response to Late Quaternary ice dynamics in Patagonia and on the Antarctic Peninsula. *Palaeogeography, Palaeoclimatology, Palaeoecology*, **162**(3-4): 357-387.

Dollenz, O.A., 1983. Fitosociologia de la Reserva Forestal "El Parrillar", Peninsula de Brunswick, Magallanes. *Anales del Instituto de la Patagonia*, **14**: 109-118.

Endlicher, W. and Santana, A., 1988. El clima del sur de la Patagonia y sus aspectos ecologicos. Un siglo de mediciones climatologicas en Punta Arenas. *Anales del Instituto de la Patagonia*, **18**: 57-86.

Fischer, H., Fundel, F., Ruth, U., Twarloh, B., Wegner, A., Udisti, R., Becagli, S., Castellano, E., Morganti, A., Severi, M., Wolff, E., Littot, G., Röthlisberger, R., Mulvaney, R., Hutterli, M.A., Kaufmann, P., Federer, U., Lambert, F., Bigler, M., Hansson, M., Jonsell, U., de Angelis, M., Boutron, C., Siggaard-Andersen, M.-L., Steffensen, J.P., Barbante, C., Gaspari, V., Gabrielli, P. and Wagenbach, D., 2007. Reconstruction of millennial changes in dust emission, transport and regional sea ice coverage using the deep EPICA ice cores from the Atlantic and Indian Ocean sector of Antarctica. *Earth and Planetary Science Letters*, **260**(1-2): 340-354.

Frenot, Y., Gloaguen, J.-C., Van De Vijver, B. and Beyens, L., 1997a. Datation de quelques sediments tourbeux holocenes et oscillations glaciaires aux iles Kerguelen. *Comptes Rendus de l'Academie des Sciences - Series III - Sciences de la Vie*, **320**(7): 567-573.

Frenot, Y., Gloaguen, J.C., Picot, G., Bougere, J. and Benjamin, D., 1993. Azorella-Selago Hook - Used to Estimate Glacier Fluctuations and Climatic History in the Kerguelen Islands over the Last 2 Centuries. *Oecologia*, **95**(1): 140-144.

Frenot, Y., Gloaguen, J.C. and Trehen, P., 1997b. Climate change in Kerguelen Islands and colonization of recently deglaciated areas by Poa kerguelensis and P. annua. In: B. Battaglia, J. Valencia and D.W.H. Walton (Editors), *Antarctic communities: species, structures and survival.* Cambridge University Press, Cambridge, pp. 358-366.

Gagnevin, D., Ethien, R., Bonin, B., Moine, B., Feraud, G., Gerbe, M.C., Cottin, J.Y., Michon, G., Tourpin, S. and Mamias, G., 2003. Open-system processes in the genesis of silica-oversaturated alkaline rocks of the Rallier-du-Baty Peninsula, Kerguelen Archipelago (Indian Ocean). *Journal of Volcanology and Geothermal Research*, **123**(3-4): 267-300.

Gaiero, D.M., Brunet, F., Probst, J.-L. and Depetris, P.J., 2007. A uniform isotopic and chemical signature of dust exported from Patagonia: Rock sources and occurrence in southern environments. *Chemical Geology*, **238**(1-2): 107-120.

Garreaud, R.D., Vuille, M., Compagnucci, R. and Marengo, J., 2009. Present-day South American climate. *Palaeogeography, Palaeoclimatology, Palaeoecology*, **281**(3-4): 180-195.

Gasse, F., 2000. Hydrological changes in the African tropics since the Last Glacial Maximum. *Quaternary Science Reviews*, **19**(1-5): 189-211.

Gersonde, R., Crosta, X., Abelmann, A. and Armand, L., 2005. Sea-surface temperature and sea ice distribution of the Southern Ocean at the EPILOG Last Glacial Maximum--a circum-Antarctic view based on siliceous microfossil records. *Quaternary Science Reviews*, **24**(7-9): 869-896.

Gersonde, R. and Zielinski, U., 2000. The reconstruction of late Quaternary Antarctic sea-ice distribution - the use of diatoms as a proxy for sea-ice. *Palaeogeography Palaeoclimatology Palaeoecology*, **162**(3-4): 263-286.

Gilli, A., Anselmetti, F.S., Ariztegui, D., Beres, M., McKenzie, J.A. and Markgraf, V., 2005. Seismic stratigraphy, buried beach ridges and contourite drifts: the Late Quaternary history of the closed Lago Cardiel basin, Argentina (49 degrees S). *Sedimentology*, **52**(1): 1-23.

Giret, A., 1980. Carte géologique au 1/50.000 de la péninsule Rallier du Baty. *Comité National Français des Recherches Antarctiques*, **45**.

Glasser, N.F., Harrison, S., Winchester, V. and Aniya, M., 2004. Late Pleistocene and Holocene palaeoclimate and glacier fluctuations in Patagonia. *Global and Planetary Change*, **43**: 79-101.

Glasser, N.F., Jansson, K.N., Harrison, S. and Kleman, J., 2008. The glacial geomorphology and Pleistocene history of South America between 38°S and 56°S. *Quaternary Science Reviews*, **27**(3-4): 365-390.

Grimm, A.M. and Ambrizzi, T., 2009. Teleconnections into South America from the tropics and extratropics on interannual and intraseasonal timescales. In: F. Vimeux, F. Sylvestre and M. Khodri (Editors), *Past climate variability in South America and surrounding regions, Developments in Paleoenvironmental Research 14*. Springer, Dordrecht, The Netherlands, pp. 159-191.

Haberle, S.G. and Bennett, K.D., 2004. Postglacial formation and dynamics of North Patagonian Rainforest in the Chonos Archipelago, southern Chile. *Quaternary Science Reviews*, **23**(23-24): 2433-2452.

Haberzettl, T., Anselmetti, F.S., Bowen, S.W., Frey, M., Mayr, C., Zolitschka, B., Ariztegui, D., Mauz, B., Ohlendorf, C., Kastner, S., Lücke, A., Schäbitz, F. and Wille, M., 2009. Late Pleistocene dust deposition in the Patagonian steppe - extending and refining the paleoenvironmental and tephrochronological record from Laguna Potrok Aike back to 55 ka. *Quaternary Science Reviews*, **28**: 2927-2939.

Haberzettl, T., Corbella, H., Fey, M., Janssen, S., Lücke, A., Mayr, C., Ohlendorf, C., Schäbitz, F., Schleser, G.H., Wille, M., Wulf, S. and Zolitschka, B., 2007. Lateglacial and Holocene wet-dry cycles in southern Patagonia: chronology, sedimentology and geochemistry of a lacustrine record from Laguna Potrok Aike, Argentina. *The Holocene*, **17**: 297-310.

Haberzettl, T., Fey, M., Lucke, A., Maidana, N., Mayr, C., Ohlendorf, C., Schabitz, F., Schleser, G.H., Wille, M. and Zolitschka, B., 2005. Climatically induced lake level changes during the last two millennia as reflected in sediments of Laguna Potrok Aike, southern Patagonia (Santa Cruz, Argentina). *Journal of Paleolimnology*, **33**(3): 283-302.

Hajdas, I., Bonani, G., Moreno, P.I. and Ariztegui, D., 2003. Precise radiocarbon dating of late-glacial cooling in mid-latitude South America. *Quaternary Research*, **59**(1): 70-78.

Hall, K., 1984. Evidence in favour of an extensive ice cover on sub-antarctic kerguelen island during the last glacial. *Palaeogeography Palaeoclimatology Palaeoecology*, **47**: 225-232.

Hall, K., 1990. Quaternary glaciations in the Southern Ocean: Sector 0° Long.- 180° Long. *Quaternary Science Reviews*, **9**: 217-228.

Hall, K., 2004. Quaternary glaciation of the Sub-Antarctic Islands. In: J. Ehlers and P. Gibbard (Editors), *Quaternary Glaciations Extent and Chronology - Part III: South America, Asia, Africa, Australasia, Antarctica* Elsevier, Amsterdam, The Netherlands, pp. 339-345.

Heirman, K., De Batist, M., Charlet, F., Moernaut, J., Chapron, E., Brümmer, R., Pino, M. and Urrutia, R., in press. Detailed seismic stratigraphy of Lago Puyehue: implications for the mode and timing of glacier retreat in the Chilean Lake District. *Journal of Quaternary Science*.

Hellstrom, J., McCulloch, M. and Stone, J., 1998. A detailed 31,000-year record of climate and vegetation change, from the isotope geochemistry of two New Zealand speleothems. *Quaternary Research*, **50**(2): 167-178.

Heusser, C. and Streeter, S.S., 1980. A temperature and precipitation record of the past 16,000 years in Southern Chile. *Science*, **210**(4476): 1345-1347.

Heusser, C.J., 1989. Southern westerlies during the last glacial maximum. *Quaternary Research*, **31**: 423-425.

Hodgson, D.A. and Sime, L.C., 2010. Southern Westerlies and CO2. *Nature Geoscience*, **3**: 666-667.

Hoganson, J.W. and Ashworth, A.C., 1992. Fossil beetle evidence for climatic change 18,000-10,000 years B.P. in South-Central Chile. *Quaternary Research*, **37**: 101-116.

Huber, U.M. and Markgraf, V., 2003. European impact on fire regimes and vegetation dynamics at the steppe-forest ecotone of southern Patagonia. *The Holocene*, **13**(4): 567-579.

Hulton, N., Sugden, D., Payne, A. and Clapperton, C., 1994. Glacier modelling and the climate of Patagonia during the Last Glacial Maximum. *Quaternary Research*, **42**: 1-19.

Hulton, N.R.J., Purves, R.S., McCulloch, R.D., Sugden, D.E. and Bentley, M.J., 2002. The last glacial maximum and deglaciation in southern South America. *Quaternary Science Reviews*, **21**: 233-241.

Ivy-Ochs, S., Schluchter, C., Kubik, P.W. and Denton, G.H., 1999. Moraine exposure dates imply synchronous Younger Dryas glacier advances in the European Alps and in the Southern Alps of New Zealand. *Geografiska Annaler Series a-Physical Geography*, **81A**(2): 313-323.

Jouzel, J., Masson, V., Cattani, O., Falourd, S., Stievenard, M., Stenni, B., Longinelli, A., Johnsen, S.J., Steffensen, J.P., Petit, J.-R., Schwander, J., Souchez, R. and Barkov, N.I., 2001. A new 27 ky high resolution East Antarctic climate record. *Geophysical Research Letters*, **28**: 3199-3202.

Kaiser, J., 2005. *Sea-surface temperature variability in the Southeast Pacific during the Last Glacial-Interglacial cycle and relationships to paleoenvironmental changes in Central and Southern Chile*. PhD Thesis, Universität Bremen, Bremen, 138 pp.

Kaiser, J. and Lamy, F., 2010. Links between Patagonian Ice Sheet fluctuations and Antarctic dust variability during the last glacial period (MIS 4-2). *Quaternary Science Reviews*, **29**(11-12): 1464-1471.

Kaiser, J., Lamy, F. and Hebbeln, D., 2005. A 70-kyr sea surface temperature record off southern Chile (Ocean Drilling Program Site 1233). *Paleoceanography*, **20**(4): PA4009.

Kaiser, J., Schefuss, E., Lamy, F., Mohtadi, M. and Hebbeln, D., 2008. Glacial to Holocene changes in sea surface temperature and coastal vegetation in north central Chile: high versus low latitude forcing. *Quaternary Science Reviews*, **27**: 2064-2075.

Kalnay, E., Kanamitsu, M., Kistler, R., Collins, W., Deaven, D., Gandin, L., Iredell, M., Saha, S., White, G., Woollen, J., Zhu, Y., Leetmaa, A., Reynolds, R., Chelliah, M., Ebisuzaki, W., Higgins, W., Janowiak, J., Mo, K.C., Ropelewski, C., Wang, J., Jenne, R. and Joseph, D., 1996. The NCEP/NCAR 40-Year Reanalysis Project. *Bulletin of the American Meteorological Society*, **77**(3): 437-471.

Kaplan, M.R., Coronato, A., Hulton, N.R.J., Rabassa, J.O., Kubik, P.W. and Freeman, S.P.H.T., 2007. Cosmogenic nuclide measurements in southernmost South America and implications for landscape change. *Geomorphology*, **87**: 284-301.

Kaplan, M.R., Schaefer, J.M., Denton, G.H., Barrell, D.J.A., Chinn, T.J.H., Putnam, A.E., Andersen, B.G., Finkel, R.W., Schwartz, R. and Doughty, A.M., 2010. Glacier retreat in New Zealand during the Younger Dryas stadial. *Nature*, **467**: 194-197.

Karoly, D.J., 1989. Southern Hemisphere Circulation Features Associated with El Niño-Southern Oscillation Events. *Journal of Climate*, **2**(11): 1239-1252.

Kershaw, P. and Chappellaz, J., 2007. Editorial: Developments in Southern Hemisphere paleoclimate research. *Pages News*, **15**(2): 2-2.

Kilian, R., Hohner, M., Biester, H., Wallrabe-Adams, H.J. and Stern, C.R., 2003. Holocene peat and lake sediment tephra record from the southernmost

Chilean Andes (53-55 degrees S). *Revista geológica de Chile*, **30**(1): 23-37.
Knorr, G. and Lohmann, G., 2003. Southern Ocean origin for the resumption of Atlantic thermohaline circulation during deglaciation. *Nature*, **424**(6948): 532-536.
Lambert, F., Delmonte, B., Petit, J.R., Bigler, M., Kaufmann, P.R., Hutterli, M.A., Stocker, T.F., Ruth, U., Steffensen, J.P. and Maggi, V., 2008. Dust-climate couplings over the past 800,000 years from the EPICA Dome C ice core. *Nature*, **452**(7187): 616-619.
Lamy, F., Hebbeln, D., Röhl, U. and Wefer, G., 2001. Holocene rainfall variability in southern Chile: a marine record of latitudinal shifts of the Southern Westerlies. *Earth and Planetary Science Letters*, **185**: 369-382.
Lamy, F., Hebbeln, D. and Wefer, G., 1998. Late quaternary precessional cycles of terrigenous sediment input off the Norte Chico, Chile (27.5 degrees S) and palaeoclimatic implications. *Palaeogeography Palaeoclimatology Palaeoecology*, **141**(3-4): 233-251.
Lamy, F., Hebbeln, D. and Wefer, G., 1999. High-resolution marine record of climatic change in mid-latitude Chile during the last 28,000 years based on terrigenous sediment parameters. *Quaternary Research*, **51**: 83-93.
Lamy, F. and Kaiser, J., 2009. Glacial to Holocene paleoceanographic and continental paleoclimate reconstructions based on ODP Site 1233/GeoB 3313 off southern Chile. In: F. Vimeux, F. Sylvestre and M. Khodri (Editors), *Past climate variability in South America and surrounding regions, Developments in Paleoenvironmental Research 14*. Springer, Dordrecht, The Netherlands, pp. 129-156.
Lamy, F., Kaiser, J., Arz, H.W., Hebbeln, D., Ninnemann, U., Timm, O., Timmermann, A. and Toggweiler, J.R., 2007. Modulation of the bipolar seesaw in the Southeast Pacific during Termination I. *Earth and Planetary Science Letters*, **259**: 400-413.
Lamy, F., Kaiser, J., Ninnemann, U., Hebbeln, D., Arz, H.W. and Stoner, J., 2004. Antartic timing of surface water changes off Chile and Patagonian Ice Sheet response. *Science*, **304**: 1959-1962.
Lamy, F., Klump, J., Hebbeln, D. and Wefer, G., 2000. Late Quaternary rapid climate change in northern Chile. *Terra Nova*, 12(1): 8-13.
Lamy, F., Ruhlemann, C., Hebbeln, D. and Wefer, G., 2002. High- and low-latitude climate control on the position of the southern Peru-Chile Current during the Holocene. *Paleoceanography*, **17**(2): 1028.
Laugenie, C., 1982. *La région des lacs, Chili méridional*, Université de Bordeaux III, Bordeaux, France, 822 pp.
Lavenu, A. and Cembrano, J., 1999. Compressional- and transpressional-stress pattern for Pliocene and Quaternary brittle deformation in fore arc and intra-arc zones (Andes of Central and Southern Chile). *Journal of Structural Geology*, **21**: 1669-1691.
Lomnitz, C., 1962. On Andean structure. *Journal of Geophysical Research*, **67**(1): 351-363.
Lomnitz, C., 2004. Major earthquakes of Chile: a historical survey, 1535-1960. *Seismological Research Letters*, **75**: 368-378.
Lowe, J.J. and Walker, M.J.C., 1997. *Reconstructing Quaternary environments (2nd ed)*. Pearson Prentice Hall, 446 pp.
Lowell, T.V., Heusser, C.J., Andersen, B.G., Moreno, P.I., Hauser, A., Heusser, L.E., Schluchter, C., Marchant, D.R. and Denton, G.H., 1995. Interhemispheric Correlation of Late Pleistocene Glacial Events. *Science*, **269**(5230): 1541-1549.
Lund, C., Lynch-Stieglitz, J. and Curry, W.B., 2006. Gulf Stream weakened in 'Little Ice Age'. *Nature*, **444**: 601-604.
Mahowald, N., Kohfeld, K., Hansson, M., Balkanski, Y., Harrison, S.P., Prentice, I.C.,

Schulz, M. and Rodhe, H., 1999. Dust sources and deposition during the last glacial maximum and current climate: A comparison of model results with paleodata from ice cores and marine sediments. *Journal of Geophysical Research*, **104**(D13): 15895-15916.

Mann, M.E., Zhang, Z., Rutherford, S., Bradley, R.S., Hughes, M.K., Shindell, D., Ammann, C., Faluvegi, G. and Ni, F., 2009. Global signatures and dynamical origins of the Little Ice Age and Medieval Climate Anomaly. *Science*, **326**: 1256-1260.

Markgraf, V., Whitlock, C. and Haberle, S., 2007. Vegetation and fire history during the last 18,000 cal yr B.P. in Southern Patagonia: Mallín Pollux, Coyhaique, Province Aisén (45°41'30"S, 71°50'30"W, 640m elevation). *Palaeogeography Palaeoclimatology Palaeoecology*, **254**: 492-507.

Marshall, G.J., 2003. Trends in the Southern Annular Mode from Observations and Reanalyses. *Journal of Climate*, **16**: 4134-4143.

Martens, P. and Rotmans, J., 1999. *Climate Change: An Integrated Perspective*. Kluwer Academic, Dordrecht, the Netherlands.

Martinic, M., 1988. Actividad volcanic historica en la region de Magallanes. *Revista geológica de Chile*, **15**: 181-186.

Massaferro, J. and Brooks, S.J., 2002. Response of chironomids to Late Quaternary environmental change in the Taitao Peninsula, southern Chile. *Journal of Quaternary Science*, **17** (2): 101-111.

Massaferro, J., Brooks, S.J. and Haberle, S.G., 2005. The dynamics of chironomid assemblages and vegetation during the Late Quaternary at Laguna Facil, Chonos Archipelago, southern Chile. *Quaternary Science Reviews*, **24**(23-24): 2510-2522.

Massaferro, J.I., Moreno, P.I., Denton, G.H., Vandergoes, M. and Dieffenbacher-Krall, A., 2009. Chironomid and pollen evidence for climate fluctuations during the Last Glacial Termination in NW Patagonia. *Quaternary Science Reviews*, **28**: 517-525.

Mayewski, P.A., Rohling, E.E., Stager, J.C., Karlen, W., Maasch, K.A., Meeker, L.D., Meyerson, E.A., Gasse, F., van Kreveld, S., Holmgren, K., Lee-Thorp, J., Rosqvist, G., Rack, F., Staubwasser, M., Schneider, R.R. and Steig, E.J., 2004. Holocene climate variability. *Quaternary Research*, **62**(3): 243-255.

Mayr, C., Fey, M., Haberzettl, T., Janssen, S., Lucke, A., Maidana, N.I., Ohlendorf, C., Schabitz, F., Schleser, G.H., Struck, U., Wille, M. and Zolitschka, B., 2005. Palaeoenvironmental changes in southern Patagonia during the last millennium recorded in lake sediments from Laguna Azul (Argentina). *Palaeogeography Palaeoclimatology Palaeoecology*, **228**(3-4): 203-227.

McCulloch, R.D. and Bentley, M.J., 1998. Late glacial ice advances in the Strait of Magellan, southern Chile. *Quaternary Science Reviews*, **17**(8): 775-787.

McCulloch, R.D., Bentley, M.J., Purves, R.S., Hulton, N.R.J., Sugden, D.E. and Clapperton, C.M., 2000. Climatic inferences from glacial and paleaoecological evidence at the last glacial termination, southern South America. *Journal of Quaternary Science*, **15**(4): 409-417.

McCulloch, R.D., Bentley, M.J., Tipping, R.M. and Clapperton, C.M., 2005a. Evidence for late-glacial ice dammed lakes in the central Strait of Magellan and Bahia Inutil, southernmost South America. *Geografiska Annaler Series a-Physical Geography*, **87A**(2): 335-362.

McCulloch, R.D. and Davies, S.J., 2001. Late-glacial and Holocene palaeoenvironmental change in the central Strait of Magellan, southern Patagonia. *Palaeogeography Palaeoclimatology Palaeoecology*, **173**(3-4): 143-173.

McCulloch, R.D., Fogwill, C.J., Sugden, D.E., Bentley, M.J. and Kubik, P.W., 2005b. Chronology of the last glaciation in central Strait of Magellan and Bahia Inutil, southernmost South America. *Geografiska Annaler Series a-Physical*

Geography, **87A**(2): 289-312.
Mercer, J.H., 1976a. Glacial history of southernmost South America. *Quaternary Research*, **6**: 125-166.
Mercer, J.H., 1976b. The last glaciation in Chile: a radiocarbon-dated chronology, *Primer Congresso Geologico Chileno*, Santiago, Chile, pp. D55-D68.
Meyer, I. and Wagner, S., 2009. The Little Ice Age in southern South America: Proxy and model based evidence. In: F. Vimeux, F. Sylvestre and M. Khodri (Editors), *Past climate variability in South America and surrounding regions, Development in Paleoenvironmental Research 14.* Springer, Dordrecht, The Netherlands, pp. 395-412.
Moernaut, J., 2010. *Sublacustrine landslide processes and their paleoseismological significance: Revealing the recurrence rate of giant earthquakes in South-Central Chile*. PhD Thesis, Ghent University, Ghent, 274 pp.
Mohtadi, M., Rossel, P., Lange, C.B., Pantoja, S., Böning, P., Repeta, D.J., Grunwald, M., Lamy, F., Hebbeln, D. and Brumsack, H.-J., 2008. Deglacial pattern of circulation and marine productivity in the upwelling region off central-south Chile. *Earth and Planetary Science Letters*, **272**(1-2): 221-230.
Montecinos, A. and Aceituno, P., 2003. Seasonality of the ENSO-Related Rainfall Variability in Central Chile and Associated Circulation Anomalies. *Journal of Climate*, **16**(2): 281-296.
Montecinos, A., Díaz, A. and Aceituno, P., 2000. Seasonal Diagnostic and Predictability of Rainfall in Subtropical South America Based on Tropical Pacific SST. *Journal of Climate*, **13**(4): 746-758.
Moreno, P.I., 1997. Vegetation and climate near Lago Llanquihue in the Chilean Lake District between 20200 and 9500 C-14 yr BP. *Journal of Quaternary Science*, **12**(6): 485-500.
Moreno, P.I., 2004. Millennial-scale climate variability in northwest Patagonia over the last 15000 yr. *Journal of Quaternary Science*, **19**(1): 35-47.
Moreno, P.I., François, J.P., Villa-Martínez, R.P. and Moy, C.M., 2009. Millennial-scale variability in Southern Hemisphere westerly wind activity over the last 5000 years in SW Patagonia. *Quaternary Science Reviews*, **28**(1-2): 25-38.
Moreno, P.I., Jacobson, G.L., Lowell, T.V. and Denton, G.H., 2001. Interhemispheric climate links revealed by a late-glacial cooling episode in southern Chile. *Nature*, **409**(6822): 804-808.
Moreno, P.I. and Leon, A.L., 2003. Abrupt vegetation changes during the last glacial to Holocene transition in mid-latitude South America. Journal of Quaternary *Science*, **18**(8): 787-800.
Moreno, P.I., Lowell, T.V., Jacobson, G.L. and Denton, G.H., 1999. Abrupt vegetation and climate changes during the last glacial maximum and last termination in the Chilean Lake District: A case study from Canal de la Puntilla (41 degrees s). *Geografiska Annaler Series a-Physical Geography*, **81A**(2): 285-311.
Moy, C.M., Dunbar, R.B., Moreno, P.I., Francois, J.-P., Villa-Martínez, R., Mucciarone, D.M., Guilderson, T.P. and Garreaud, R.D., 2008. Isotopic evidence for hydrologic change related to the westerlies in SW Patagonia, Chile, during the last millenium. *Quaternary Science Reviews*, **27**: 1335-1349.
Moy, C.M., Moreno, P.I., Dunbar, R., Kaplan, M.R., Francois, J.-P., Villalba, R. and Haberzettl, T., 2009. Climate change in Southern South America during the last two millenia. In: F. Vimeux, F. Sylvestre and M. Khodri (Editors), *Past climate variability in South America and surrounding regions, Developments in Paleoenvironmental Research 14*. Springer, Dordrecht, The Netherlands, pp. 353-393.
Moy, C.M., Seltzer, G.O., Rodbell, D.T. and Anderson, D.M., 2002. Variability of El Niño/Southern Oscillation activity at millennial timescales during the Holocene epoch. *Nature*, **420**: 162-165.

Naranjo, J.A. and Stern, C., 2004. Holocene tephrochronology of the southernmost part (42°30'-45°S) of the Andean Southern Volcanic Zone. *Revista geológica de Chile*, **31**(2): 225-240.

Newnham, R.M. and Lowe, D.J., 2000. Fine-resolution pollen record of late-glacial climate reversal from New Zealand. *Geology*, **28**(8): 759-762.

Nougier, J., 1970a. Carte géologique de reconnaissance au 1/200.000. *Comité National Français des Recherches Antarctiques*, **27**(2): 256.

Nougier, J., 1970b. Contribution à l'étude géologique et géomorphologique des îles Kerguelen. *Comité National Français des Recherches Antarctiques*, **27**(1): 440.

Nougier, J., 1972. Aspects de morpho-tectonique glaciaire aux Iles Kerguelen. Revue de Géographie Physique et de Géologie Dynamique (2), 14(5): 499-506.

O'Hare, G., Sweeney, J. and Wilby, R., 2005. *Weather, Climate and Climate Change - Human Perspectives*. Pearson Prentice Hall, Harlow, England.

Pahnke, K. and Zahn, R., 2005. Southern hemisphere water mass conversion linked with North Atlantic climate variability. *Science*, **307**(5716): 1741-1746.

PALEOMAP, 2008. *PALEOMAP project*: http://www.scotese.com.

Paskoff, R.P., 1976. Quaternary of Chile: The state of research. *Quaternary Research*, **8**: 2-31.

Petit, J.R., Jouzel, J., Raynaud, D., Barkov, N.I., Barnola, J.M., Basile, I., Bender, M., Chappellaz, J., Davis, M., Delaygue, G., Delmotte, M., Kotlyakov, V.M., Legrand, M., Lipenkov, V.Y., Lorius, C., Pepin, L., Ritz, C., Saltzman, E. and Stievenard, M., 1999. Climate and atmospheric history of the past 420,000 years from the Vostok ice core, Antarctica. *Nature*, **399**(6735): 429-436.

Porter, S.C., 1981. Pleistocene glaciation in the southern Lake District of Chile. *Quaternary Research*, **16**: 263-292.

Rasmussen, S.O., Andersen, K.K., Svensson, A.M., Steffensen, J.P., Vinther, B.M., Clausen, H.B., Siggaard-Andersen, M.L., Johnsen, S.J., Larsen, L.B., Dahl-Jensen, D., Bigler, M., Rothlisberger, R., Fischer, H., Goto-Azuma, K., Hansson, M.E. and Ruth, U., 2006. A new Greenland ice core chronology for the last glacial termination. *Journal of Geophysical Research-Atmospheres*, **111**(D6): D06102.

Rasmusson, E.M. and Wallace, J.M., 1983. Meteorological Aspects of the El Niño/Southern Oscillation. *Science*, **222**(4629): 1195-1202.

Rind, D., Russell, G., Schmidt, G., Sheth, S., Collins, D., deMenocal, P. and Teller, J., 2001. Effects of glacial meltwater in the GISS coupled atmospheric-ocean model. 2. A bipolar seesaw in Atlantic Deep Water production. *Journal of Geophysical Research*, **106**(D21): 27355-27365.

Rodríguez, C., Pérez, Y., Moreno, H., Clayton, J., Antinao, J.L., Duhart, P. and Martin, M., 1999. *Area de Panguipulli-Riñihue, Région de los Lagos*. Servicio Nacional de Geología y Minería, Mapas Geológicos 10, escala 1:100 000, Santiago.

Rojas, M., Moreno, P., Kageyama, M., Crucifix, M., Hewitt, C., Abe-Ouchi, A., Ohgaito, R., Brady, E.C. and Hope, P., 2009. The Southern Westerlies during the last glacial maximum in PMIP2 simulations. *Climate Dynamics*, **32**: 525-548.

Ruddiman, W.F., 2008. *Earth's Climate: Past and Future (2nd edition)*. W.H. Freeman and Company, New York.

Sandweiss, D.H., Maasch, K.A., Burger, R.L., Richardson, J.B., Rollins, H.B. and Clement, A., 2001. Variation in Holocene El Nino frequencies: Climate records and cultural consequences in ancient Peru. *Geology*, **29**(7): 603-606.

Santana, A.A., 1984. Variacion de las precipitaciones de 97 años en Punta Arenas como indice de posibles cambios climaticos. *Anales del Instituto de la Patagonia*, **15**: 51-60.

Schaefer, J.M., Denton, G.H., Barrell, D.J.A., Ivy-Ochs, S., Kubik, P.W., Andersen, B.G., Phillips, F.M., Lowell, T.V. and Schlüchter, C., 2006. Near-synchronous interhemispheric termination of the last glacial maximum in Mid-Latitudes.

Science, **312**: 1510-1513.
Schaefer, J.M., Denton, G.H., Kaplan, M.R., Putnam, A.E., Finkel, R.C., Barrell, D.J.A., Andersen, B.G., Schwartz, R., Mackintosh, A., Chinn, T.J.H. and Schlüchter, C., 2009. High-frequency Holocene glacier fluctuations in New Zealand differ from the northern signature. *Science*, **324**: 622-625.
Scholz, C.A., 2001. Applications of seismic sequence stratigraphy in lacustrine basins. In: W.M. Last and J.P. Smol (Editors), *Tracking Environmental Change Using Lake Sediments. Volume 1: Basin Analysis, Coring and Chronological Techniques.* Kluwer Academic Publishers, Dordrecht, The Netherlands, pp. 7-22.
SERNAGEOMIN, 2003. *Mapa Geológico de Chile: versión digital*. Servicio Nacional de Geología y Minería, Publicación Geológica Digital, No. 4, Santiago.
Shulmeister, J., Goodwin, I., Renwick, J., Harle, K., Armand, L., McGlone, M.S., Cook, E., Dodson, J., Hesse, P.P., Mayewski, P. and Curran, M., 2004. The Southern Hemisphere westerlies in the Australasian sector over the last glacial cycle: a synthesis. *Quaternary International*, **118-19**: 23-53.
Shulmeister, J., Rodbell, D.T., Gagan, M.K. and Seltzer, G.O., 2006. Interhemispheric linkages in climate change: paleo-perspectives for future climate change. *Climate of the Past*, **2**: 167-185.
Singer, C., Shulmeister, J. and McLea, B., 1998. Evidence against a significant Younger Dryas cooling event in New Zealand. *Science*, **281**(5378): 812-814.
Stauder, W., 1973. Mechanism and spatial distribution of Chilean earthquakes with relation to subduction of the oceanic plate. *Journal of Geophysical Research*, **78**(23): 5033-5061.
Stenni, B., Jouzel, J., Masson-Delmotte, V., Röthlisberger, R., Castellano, E., Cattani, O., Falourd, S., Johnsen, S.J., Longinelli, A., Sachs, J.P., Selmo, E., Souchez, R., Steffensen, J.P. and Udisti, R., 2003. A late-glacial high-resolution site and source temperature record derived from the EPICA Dome C isotope records (East Antarctica). *Earth and Planetary Science Letters*, **217**(1-2): 183-195.
Stephens, B.B. and Keeling, R.F., 2000. The influence of Antarctic sea ice on glacial-interglacial CO 2 variations. *Nature*, **404**(6774): 171-174.
Sterken, M., Verleyen, E., Sabbe, K., Terryn, G., Charlet, F., Bertrand, S., Boës, X., Fagel, N., Batist, M.D. and Vyverman, W., 2008. Late Quaternary climatic changes in southern Chile, as recorded in a diatom sequence of Lago Puyehue (40°40' S). *Journal of Paleolimnology*, **39**: 219-235.
Stern, C., 2008. Holocene tephrochronology record of large explosive eruptions in the southernmost Patagonian Andes. *Bulletin of Volcanology*, **70**(4): 435-454.
Stern, C.R., 2004. Active Andean volcanism: its geologic and tectonic setting. *Revista geológica de Chile*, **31**(2): 161-206.
Stern, C.R., Moreno, H., López-Escobar, L., Clavero, J.E., Lara, L.E., Naranjo, J.A., Parada, M.A. and Skewes, M.A., 2007. Chilean Volcanoes. In: T. Moreno and W. Gibbons (Editors), *The Geology of Chile*. The Geological Society of London, London, pp. 147-178.
Stocker, T.F., 1998. The Seesaw Effect. *Science*, **282**(5386): 61-62.
Stuiver, M., Grootes, P.M. and Braziunas, T.F., 1995. The GISP2 delta O-18 climate record of the past 16,500 years and the role of the sun, ocean, and volcanoes. *Quaternary Research*, **44**(3): 341-354.
Stuut, J.-B.W., Crosta, X., van der Borg, K. and Schneider, R., 2004. Relationship between Antarctic sea ice and southwest African climate during the late Quaternary. *Geology*, **32**(10): 909-912.
Stuut, J.B.W. and Lamy, F., 2004. Climate variability at the southern boundaries of the Namib (Southwestern Africa) and Atacama (northern Chile) coastal deserts during the last 120,000 yr. *Quaternary Research*, **62**(3): 301-309.
Sugden, D.E., Bentley, M.J., Fogwill, C.J., Hulton, N.R.J., McCulloch, R.D. and

Purves, R.S., 2005. Late-glacial glacier events in southernmost South America: A blend of 'northern'and 'southern' hemispheric climatic signals? *Geografiska Annaler Series a-Physical Geography*, **87A**(2): 273-288.

Sugden, D.E., Hulton, N.R.J. and Purves, R.S., 2002. Modelling the inception of the Patagonian icesheet. *Quaternary International*, **95**-6: 55-64.

Sugden, D.E., McCulloch, R.D., Bory, A.J.-M. and Hein, A.S., 2009. Influence of Patagonian glaciers on Antarctic dust deposition during the last glacial period. *Nature Geoscience*, **2**: 281-285.

Testut, L., Wöppelmann, G., Simon, B. and Téchiné, P., 2006. The sea level at Port-aux-Français, Kerguelen Island, from 1949 to the present. *Ocean Dynamics*, **56**(5/6): 464-472.

Thompson, D.W.J. and Wallace, J.M., 2000. Annular modes in the extratropical circulation. Part I: Month-to-month variability. *Journal of Climate*, **13**(5): 1000-1016.

Thompson, D.W.J., Wallace, J.M. and Hegerl, G.C., 2000. Annular modes in the extratropical circulation. Part II: Trends. *Journal of Climate*, **13**(5): 1018-1036.

Thornburgh, T. and Kulm, L.D., 1987. Sedimentation in the Chilean Trench: petrofacies and provenance. *Journal of Sedimentary Petrology*, **57**: 55-74.

Timmermann, A., Krebs, U., Justino, F., Goosse, H. and Ivanochko, T., 2005. Mechanisms for millenial-scale global synchronization during the last glacial period. *Paleoceanography*, **20**: PA4008.

Toggweiler, J.R., 1999. Variation of Atmospheric CO2 by Ventilation of the Ocean's Deepest Water. *Paleoceanography*, **14**(5): 571-588.

Toggweiler, J.R., Russell, J.L. and Carson, S.R., 2006. Midlatitude westerlies, atmospheric CO2, and climate change during the ice ages. *Paleoceanography*, **21**(2): PA2005.

Turner, K.J., Fogwill, C.J., McCulloch, R.D. and Sugden, D.E., 2005. Deglaciation of the eastern flank of the North Patagonian Icefield and associated continental-scale lake diversions. *Geografiska Annaler Series a-Physical Geography*, **87A**(2): 363-374.

Turney, C.S.M., Roberts, R.G., de Jonge, N., Prior, C., Wilmshurst, J.M., McGlone, M.S. and Cooper, J., 2007. Redating the advance of the New Zealand Franz Josef Glacier during the Last Termination: evidence for asynchronous climate change. *Quaternary Science Reviews*, **26**: 3037-3042.

Vandergoes, M.J., Dieffenbacher-Krall, A.C., Newnham, R.M., Denton, G.H. and Blaauw, M., 2008. Cooling and changing seasonality in the Southern Alps, New Zealand during the Antarctic Cold Reversal. *Quaternary Science Reviews*, **27**(5-6): 589-601.

Villa, G. and Persico, D., 2006. Late Oligocene climatic changes: Evidence from calcareous nannofossils at Kerguelen Plateau Site 748 (Southern ocean). *Palaeogeography Palaeoclimatology Palaeoecology*, **231**(1-2): 110-119.

Volland, S., 2006. *Sediment dynamics in Lago Calafquén and Lago Villarica (Northern Patagonia - Chile): A baseline study on sedimentological processes and considerations in assessing palaeoenvironmental change*, Technischen Universität München, München, 341 pp.

Volland, S., Sturm, M., Lukas, S., Pino, M. and Müller, J., 2007. Geomorphological and sedimentological evolution of a lake basin under strong volcano-tectonic influence: Lake Calafquén (South Central Chile). *Quaternary International*, **161**(1): 32-45.

Wagner, S., Widmann, M., Jones, J., Haberzettl, T., Lücke, A., Mayr, C., Ohlendorf, C., Schäbitz, F. and Zolitschka, B., 2007. Transient simulations, empirical reconstructions and forcing mechanisms for the Mid-holocene hydrological climate in southern Patagonia. *Climate Dynamics*, **29**(4): 333-355.

Wainer, I., Clauzet, G., Ledru, M.-P., Brady, E. and Otto-Bliesner, B., 2005. Last Glacial Maximum in South America: Paleoclimate proxies and model results.

Geophysical Research Letters, **32**(8): L08702.
Weaver, A.J., Saenko, O.A., Clark, P.U. and Mitrovica, J.X., 2003. Meltwater pulse 1A from Antarctica as a trigger of the bolling-allerod warm interval. *Science*, **299**(5613): 1709-1713.
White, J.W.C., Ciais, P., Figge, R.A., Kenny, R. and Markgraf, V., 1994. A high-resolution record of atmospheric CO2 content from carbon isotopes in peat. *Nature*, **367**(6459): 153-156.
Whitehead, J.M. and McMinn, A., 2002. Kerguelen Plateau Quaternary-late Pliocene palaeoenvironments: from diatom, silicoflagellate and sedimentological data. *Palaeogeography Palaeoclimatology Palaeoecology*, **186**(3-4): 335-368.
Williams, P.W., King, D.N.T., Zhao, J.X. and Collerson, K.D., 2005. Late Pleistocene to Holocene composite speleothem 18O and 13C chronologies from South Island, New Zealand--did a global Younger Dryas really exist? *Earth and Planetary Science Letters*, **230**(3-4): 301-317.
Winckler, G., Anderson, R.F., Fleisher, M.Q., McGee, D. and Mahowald, N., 2008. Covariant Glacial-Interglacial Dust Fluxes in the Equatorial Pacific and Antarctica. *Science*, **320**(5872): 93-96.
Wolff, E.W., Fischer, H. and Röthlisberger, R., 2009. Glacial terminations as southern warmings without northern control. *Nature Geoscience*, **2**: 206-209.
Wyrwoll, K.-H., Dong, B. and Valdes, P., 2000. On the position of southern hemisphere westerlies at the Last Glacial Maximum: an outline of AGCM simulation results and evaluation of their implications. *Quaternary Science Reviews*, **19**: 881-898.
Young, S.B. and Schofield, E.K., 1973. Pollen evidence for Late Quaternary climate changes on Kerguelen Islands. *Nature*, **245**: 311-312.

III. Methodology

The analysis of sediment is one of the most powerful means available of reconstructing the environmental history of the Quaternary period. Proxies are preserved physical characteristics of the past that enable us to reconstruct the environmental conditions that prevailed during that part of the Earth's history represented by the available sediment record. Studies of past environments begin by understanding the types of proxy applicable to the available material and the methods used in their analysis. One must be aware of the difficulties associated with each method used and the assumptions each method entails.

III.1 Basin analysis

Lake basin physiography is often compressed relative to ocean basins. Sedimentary-facies variations may be abrupt both laterally and vertically, but, like their marine counterparts, lacustrine studies can provide high-resolution sediment records. In lakes, the environmental control is often much more amplified than in the oceanic sediments (Scholz, 2001). High-resolution reflection seismic surveying is a very powerful technique for lake-basin studies as it allows a non-destructive and non-invasive, quasi three-dimensional exploration of the whole sedimentary infill. Many glacigenic lakes contain up to hundreds of metres of sediment in their basin, often deposited in a rather short time span: i.e. from deglaciation to present (Charlet et al., 2008; Eyles and Mullins, 1997; Van Rensbergen et al., 1999; Van Rensbergen et al., 1998). Consequently the majority of sediment-core studies literally just scrape the surface of the story buried in the lake basin. A large-scale basin exploration is these days also considered as a requisite first step applied prior to sample collection or core site selection.

III.1.1. Seismic Acquisition

III.1.1.1. Chilean Lake District

The Renard Centre of Marine Geology (RCMG) has collected a large amount of high-resolution reflection seismic data in the Chilean Lake District over the last decade. Reconnaissance surveys were conducted on the lakes to get a general overview of the general infill. This happened on Lago Villarrica in 2002 (Figure III-1), on Lago Panguipulli in 2005 (Figure III-3) and on Lago Riñihue (Figure III-4) and Lago Calafquén in 2007 (Figure III-2). Based on these results Lago Villarrica was then explored in further detail in 2007 (Figure III-1).

During every survey the small research vessel, Huala II, from the Universidad Austral de Chile was used to tow the equipment through the lake water. Navigation and positioning of the equipment was done with a SIMRAD GPS. The acoustic source is a "Centipede" multi-electrode sparker (300 J, main-frequency: 800-2000 Hz) to which energy was provided by a CSP-500 power supply (Applied Acoustics) which was connected to a generator. For fresh-water applications, this source is put inside a plastic bag filled with salt water in order to create the required conductive environment (6 buckets containing 3 kg of salt in total). A SIG single-channel streamer was used for the detection of the seismic reflections. It was towed as near as possible to the water surface to insure a high-resolution response. This streamer has an active length of 2.7 m, and consists of 10 hydrophones with 0.3 m spacing. The detected signal is pre-amplified in the streamer. The positioning data and seismic signals were recorded digitally with an ELICS Delph-2 system, after analogue bandpass filtering to remove noise with frequencies lower than 200 Hz and higher than 2300 Hz.

Overall, the seismic resolution is in the range of 50-75 cm (Rayleigh criterion). The penetration of the acoustic signal varies significantly within a single lake basin. In the western part of the lakes, the geophysical penetration is mostly excellent and the entire sediment infill is imaged, but the geophysical imaging is often very poor in the eastern parts of the lake basins, where penetration is limited due to gas blanking.

III.1.1.2. Laguna Parrillar

An exploratory seismic survey was conducted in Laguna Parrillar. To rapidly determine a suitable coring location. The deepest part of the lake basin was investigated with an Innomar Parametric Echo Sounding System SES 96 mounted on the platform also used for coring. To determine the sound velocity of the lake water, Conductivity-Temperature-Depth sensor (CTD) measurements were undertaken.

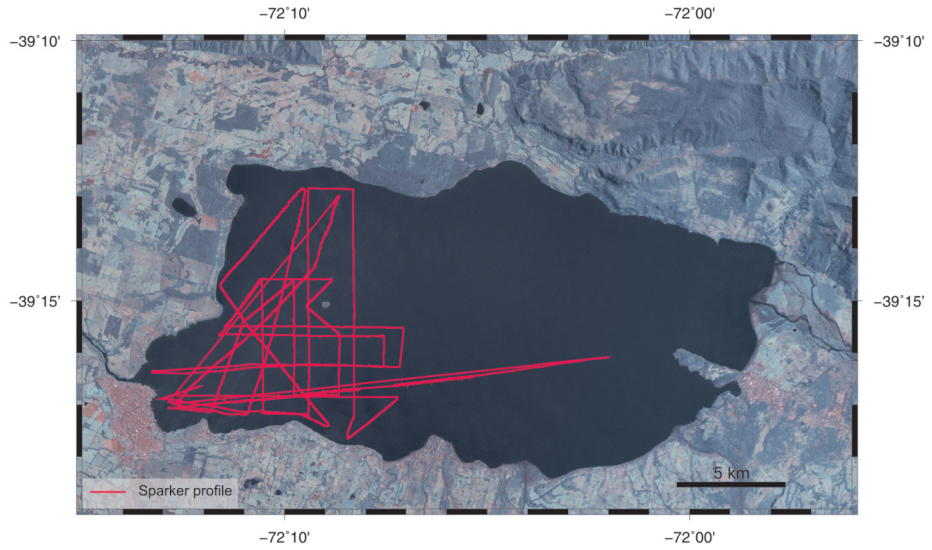

Figure III-1: Seismic survey lines on Lago Villarrica

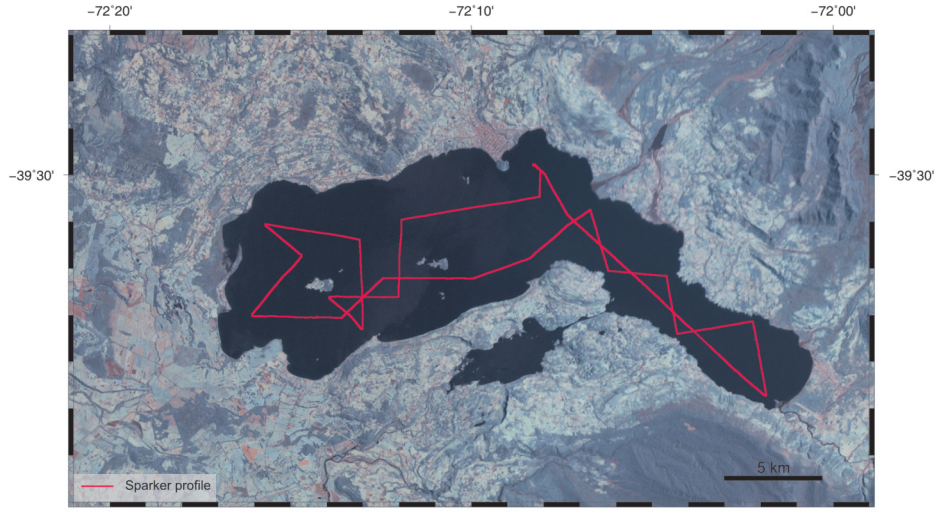

Figure III-2: Seismic survey lines on Lago Calafquén

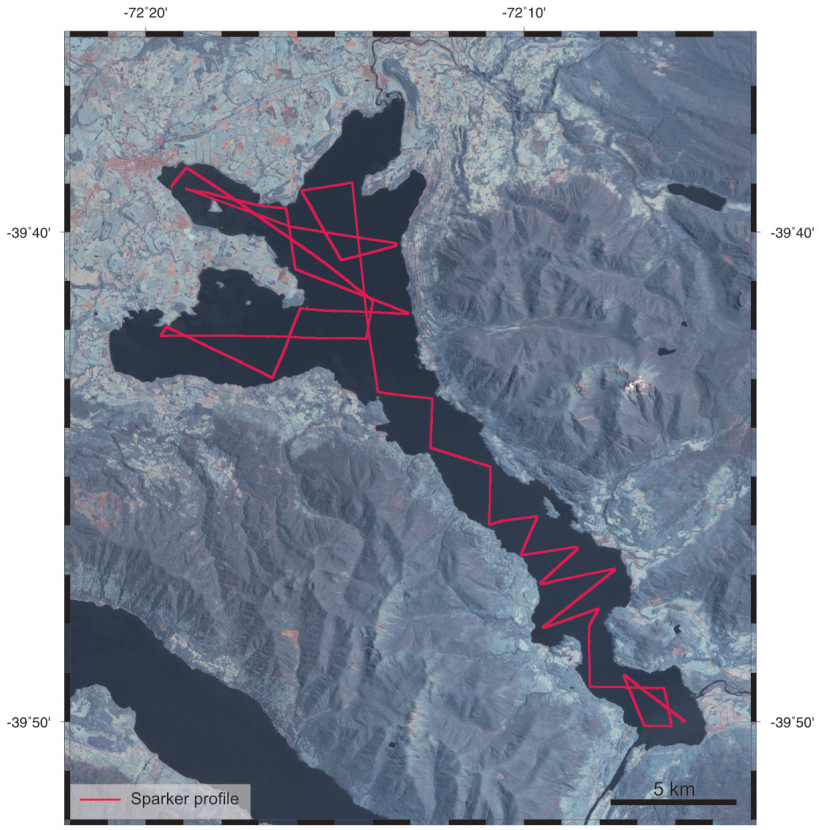

Figure III-3: Seismic survey lines on Lago Panguipulli

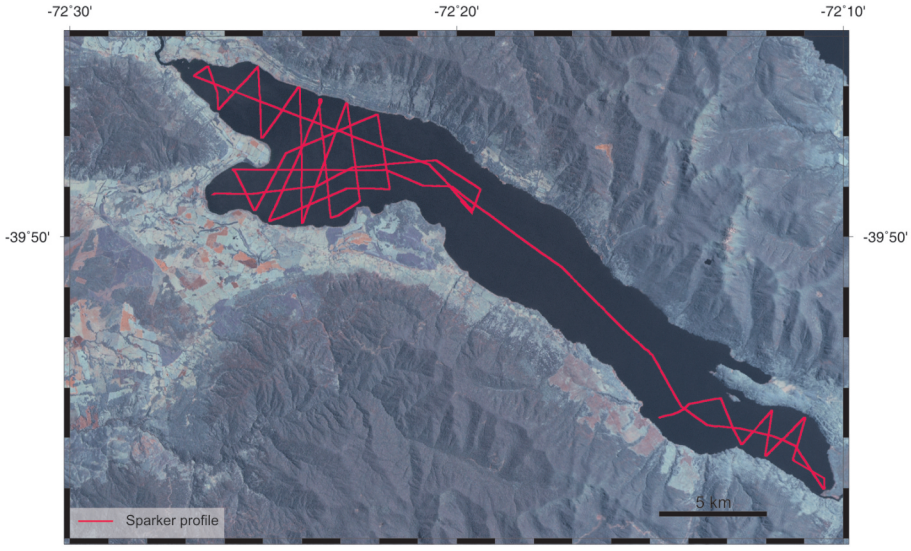

Figure III-4: Seismic survey lines on Lago Riñihue

III.1.1.3. Kerguelen Archipelago

During the field campaign of November-December 2006, carried out in collaboration with the Université de Savoie and IPEV, Lac d'Armor was selected for high-resolution reflection seismic surveying (Figure III-5). Lac d'Armor turned out to be better suited in terms of wind direction, glacial context and accessibility than other targeted lakes in Val Studer in the Kerguelen Archipelago. The lake was surveyed with a C-Boom seismic source (with a dominant frequency of ca. 1700 Hz). A SIG single-channel streamer was used for the detection of the seismic reflections, towed as near as possible to the water surface to insure a high-resolution response. This streamer has an active length of 2.7 m, and consists of 10 hydrophones with 0.3 m spacing. The detected signal was pre-amplified in the streamer. Navigation was undertaken by GPS. During the expedition a ROCKLAND band pass filter was used at 200 Hz high-pass and 60 KHz low-pass. The filtered signal was recorded in the ELICS Delph-2 system on an ACME portable computer.

Although the seismic resolution of the C-Boom system should be theoretically higher than the one from the sparker system (20cm), this is not the case for the Lac d'Armor data due to the high amount of noise that was recorded at the same time. Consequently, the data was processed after the expedition on the Promax seismic processing system at RCMG, where a frequency band-pass filter of 500-4000 Hz was applied.

III.1.2. Seismic-Stratigraphic Analysis

Seismic-stratigraphic interpretation was performed using the Kingdom Suite 7.5 program. Using the classical seismic interpretation criteria of Mitchum et al. (1977) a seismic-stratigraphic framework was constructed to divide the reflections present in the profiles in different seismic units, each representing their own seismic facies. In the whole lake (or sometimes even in areas within one lake) seismic units could be mapped in 3 dimensions if the

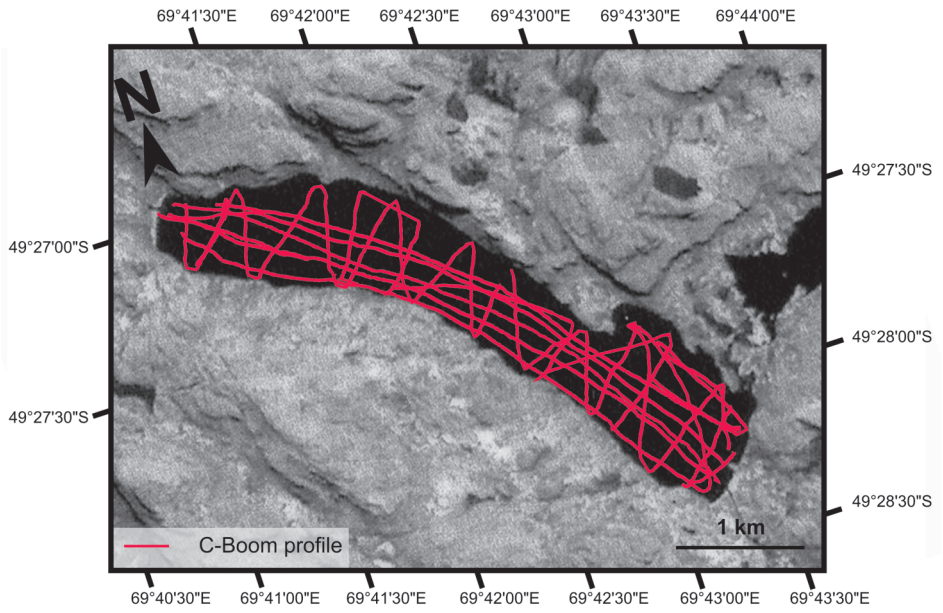

Figure III-5: Seismic survey lines on Lac d'Armor

network of seismic profiles collected was dense enough and if gas blanking did not prevent mapping of the units. Grids and maps were created with Golden Software Surfer 9, Global Mapper v8.3 and GMT v4.2, using the interpreted horizon picks exported from Kingdom Suite 7.5.

For the bathymetry, time-to-depth conversion was done using a mean acoustic velocity of 1500 m/s in the water column. For the sedimentary infill, time-to-depth conversion was done using a velocity of 1750 m/s. This velocity is used as an average (Eyles and Mullins, 1997), based on seismic velocity studies carried out in several glacial lakes, showing that velocities in such environments generally vary between 1500 m/s in the uppermost deposits and 2100 m/s deeper in the sedimentary sequence (Finckh et al., 1984).

The seismic-stratigraphic data was used to determine the optimal location to take a long sediment core to study the upper 7 to 14 m of Lago Villarrica and Laguna Parrillar in higher detail.

III.2. Core Analysis

After a large-scale, basin-wide study, one or more suitable locations for core collection were selected in the lake. A sediment core generally allows the study of the top 10 to 20 m of a lacustrine sequence. Multi-proxy sedimentological, biological and geochemical analytical techniques were applied to each of the cores collected.

III.2.1. Core Acquisition

Collecting a sediment core is, in many ways, the most critical part of the palaeolimnological process, as any errors or problems encountered during core collection can rarely be corrected "after-the-fact" (Glew et al., 2001). The success of the entire project, and all the subsequent, time-consuming analyses, depends on this first step: the recovery of a good sediment core.

Gravity cores only sample the top 20 to 100 cm of the lake sediment, but they contribute greatly in understanding the current sedimentation patterns in different areas of the lake basin. This creates the opportunity to assess the influence of different factors (e.g. rivers) controlling sediment deposition and can help in determining the most suitable location for a longer sediment core. The collection of a piston core is more elaborate, but allows the study of the lake sedimentation over much longer time periods.

The sediment cores investigated in this study were taken in Lago Villarrica and Laguna Parrillar. The short cores in both lakes were collected with a UWITEC gravity coring system deployed from an inflatable zodiac. Depending of the type of sediment this corer can penetrate up to 1 m after a controlled fall of about 5 to 7 m (wind conditions permitting). Depending on the purpose of the core collection, the sediment filled gravity core liners were sealed, wrapped and transported to Ghent University untouched. Some gravity cores from Laguna Parrillar (PSC-1 to 5) (Figure III-7 and Table III-1) were sliced at 1 cm intervals and bagged before shipping. In Lago Villarrica only the top 5 cm of several gravity cores were kept, bagged and sent frozen to Ghent University (Figure III-6 and Table III-1).

Long sediment cores were collected in two phases. During the first phase most of the Lago Villarrica core (VILL) was obtained during the austral summer of 2007 with the UWITEC piston coring system and platform of the British Antarctic Survey. During the second phase, April and May 2009, a similar UWITEC system was used, but this time in collaboration with Trier University (Figure III-6 and Table III-1). In 2009, a long sediment core was collected from Laguna Parrillar (Figure III-7 and Table III-1) and the missing section of the long core of Lago Villarrica recovered.

Both UWITEC systems consist of a

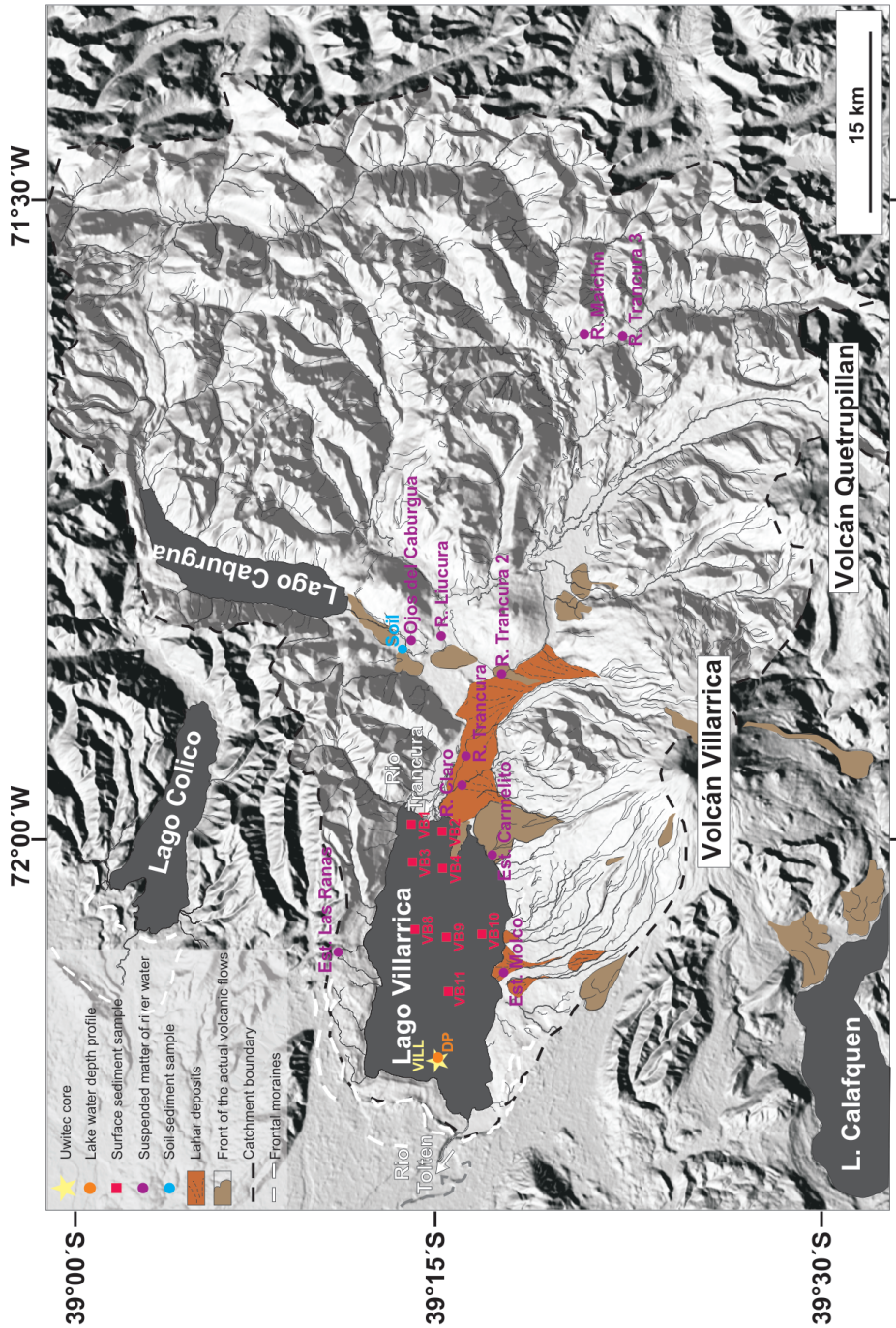

Figure III-6: Locations of the long core, surface sediment samples, soil sample and river and lake water samples taken in Lago Villarrica and its catchment

Table III-1: Location and specification of the different samples taken in the area in and around Lago Villarrica and Laguna Parrillar. PC = piston core, GC = gravity core, FRW = filtered river water sample, FLW = filtered lake water sample, LC = Livingstone core, SS = surface sediment sample, DP = depth profile with filtered lake water samples taken at the surface and at -5, -10, -15, -20, -25, -30, -40, -60 and -80 m.

Region	Sample type	Sample name	Date	Latitude (°S)	Longitude (°W)	Remark
Villarrica	PC	VILL	12/2007 and 05/2009	39.25662	72.17222	14 m
Villarrica	GC	VILLSC03	17/05/09	39.25662	72.17222	SS
Villarrica	GC	VB1	19/05/09	39.23977	71.97878	SS
Villarrica	GC	VB2	19/05/09	39.25949	71.98469	SS
Villarrica	GC	VB3	19/05/09	39.24115	72.00886	SS
Villarrica	GC	VB4	19/05/09	39.2599	72.01488	SS
Villarrica	GC	VB8	19/05/09	39.24248	72.06458	SS
Villarrica	GC	VB9	19/05/09	39.26225	72.07181	SS
Villarrica	GC	VB10	19/05/09	39.28431	72.06923	SS
Villarrica	GC	VB11	19/05/09	39.26327	72.11601	SS
Villarrica	Soil	Caburgua Rd.	21/05/09	39.24084	71.82978	
Villarrica	FRW	E. Molco	16/05/09	39.30011	72.10183	
Villarrica	FRW	E. Carmelito	16/05/09	39.29194	72.00477	
Villarrica	FRW	R. Claro	21/05/09	39.27259	71.94528	
Villarrica	FRW	R. Trancura	21/05/09	39.2732	71.92302	
Villarrica	FRW	R. Liucura	21/05/09	39.26106	71.82647	
Villarrica	FRW	O. Caburgua	21/05/09	39.23855	71.83493	
Villarrica	FRW	R. Trancura 2	21/05/09	39.27987	71.86242	
Villarrica	FRW	R. Maichín	21/05/09	39.34387	71.5738	
Villarrica	FRW	R. Trancura 3	21/05/09	39.37369	71.57919	
Villarrica	FRW	R. Las Ranas	22/05/09	39.19498	72.08231	
Villarrica	FLW	Depth profile	17/05/09	39.25664	72.17123	DP
Parrillar	GC	PSC1	06/12/07	53.41182	71.28645	sliced
Parrillar	GC	PSC2	10/12/07	53.40936	71.29236	sliced
Parrillar	GC	PSC3	10/12/07	53.40528	71.27547	sliced
Parrillar	GC	PSC4	10/12/07	53.40546	71.27878	sliced
Parrillar	GC	PSC5	10/12/07	53.40761	71.28108	sliced
Parrillar	PC	PAR1	01/04/09	53.41097	71.28594	7 m
Parrillar	LC	PAR-1A-liv	14/02/07	53.40578	71.27767	0.5 m

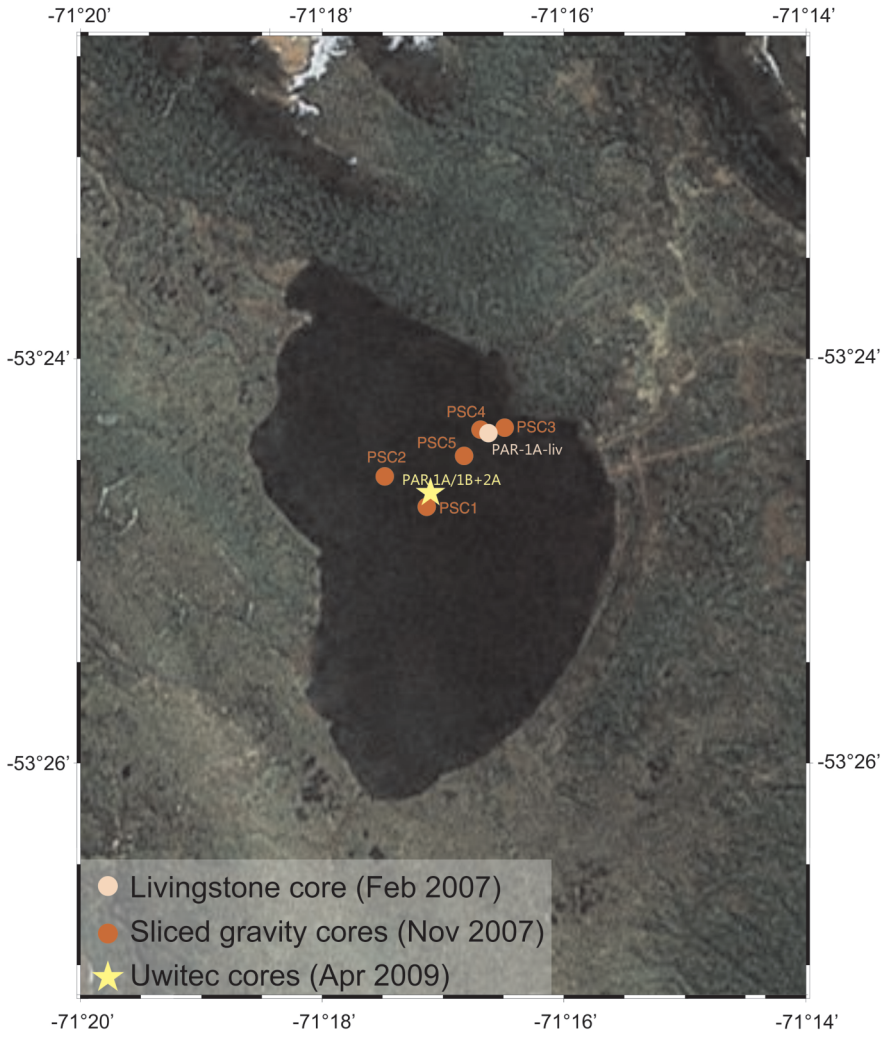

Figure III-7: Locations of the cores taken in Laguna Parrillar

platform that is kept above the coring site with four anchors. A plastic liner with a diameter of 60 mm is inserted in the metal core barrel. Depending on the system this barrel has a length of 2 m (British Antarctic Survey) or 5 m (Trier University). Two drives had to be collected at every site for every section, the second drive overlapping the first drive by 1 m. Using this technique a 14 m long composite core profile, consisting of fourteen 2 m and one 5 m long sections, was collected in Lago Villarrica. Similary, a 7 m long core, consisting of two 5 m long sections, was extracted from Laguna Parrillar. A gravity core was also collected at both sides to obtain an undisturbed sediment-water interface, because the piston coring system always tends to disturb the upper 10 to 15 cm of the lake sediment due to its unconsolidated nature.

One 50 cm long livingstone core (PAR-1A-liv) was collected from the margin of Laguna Parrillar with the equipment of the British Antarctic Survey during the austral summer of 2007 (Figure III-7 and Table III-1).

III.2.2. Multi-Sensor Core Logging (GEOTEK)

Geophysical core logging is the first step in sediment core analysis. This technique allows a rapid, quasi-continuous, non-destructive analysis of the physical sediment properties. One of the most common geophysical core scanners is the GEOTEK multi-sensor core logger (MSCL), which measures gamma-ray attenuation bulk density, magnetic susceptibility and P-wave velocity of the sediment at the same time in discrete steps of 1 mm up to several cms.

Magnetic susceptibility (MS) is the degree of magnetization of a material in response to an external magnetic field. Changes in MS are due to variations in the concentration and/or the composition of the magnetic minerals, grain size and the overall density of sediment retained in whole core analysis. Gamma density is used to estimate the bulk density of sediments and serves as an indicator for porosity and lithological changes. P-wave velocity reflects variations in the lithology, porosity and density of the bulk sediment. The gamma-ray bulk density data and the magnetic susceptibility data are especially useful for the construction of composite core profiles, detection of tephras and major lithological/sedimentological changes.

The GEOTEK logger of the Limnogeology laboratory at ETH Zürich was used to measure the gamma-ray attenuation bulk density, magnetic susceptibility (using a loop sensor) and P-wave velocity of the sediment of all closed sediment cores in discrete steps of 0.5 cm. Reliable P-wave velocity data was not obtained, mostly likely due to gas present in the sediment or due to the formation of air gaps between the sediment and the core liner (Gunn and Best, 1998). All measurements were performed on whole cores. The advantage of the whole-core magnetic susceptibility loop sensor is its higher signal to noise ratio. This configuration is better for sediments with low magnetic susceptibility (Gunn and Best, 1998). The loop sensor, however, gives a much lower resolution reading than a magnetic point sensor as it averages the magnetic reading over a distance of 28 cm (Gunn and Best, 1998).

III.2.3. High-Resolution Magnetic Susceptibility

The magnetic susceptibility of the sediments was remeasured after opening, this time directly on the exposed surface of one of the core halves. The resolution of these measurements is higher since the sensor receives 50 % of its signal from the upper 3 mm of sediment with a maximum diameter of influence of 2 cm (Gunn and Best, 1998). Consequently the point MS measurements reveal much finer variations in magnetic susceptibility. The higher resolution of the MS measurments allows a more precise core-to-core correlation, but gives also more detailed information on the terrigeneous (allochtonous) yield of the catchment area. Magnetic susceptibility can be regarded as a proxy for minerogenic contribution to the sediment, since iron-bearing minerals are common in many rock types and their weathering products (Zolitschka et al., 2001). Variations in magnetic susceptibility therefore reflect changes in weathering and transport rate resulting from various environmental triggers. Also the detection of very thin tephra laminae, which were sometimes not correctly observed during the original core description, is possible.

A Bartington MS2E point sensor from the Royal Observatory of Belgium or from the Department of Soil Management (UGent) was used. Every 2.5 mm was measured by moving the magnetic sensor by hand and an instrument drift correction was performed every 20 readings.

III.2.4. Macroscopic Core Description

The foundation for any detailed sediment core investigation should be a detailed description of the range of sediment facies present in the core. Careful examination of the exposed core surface has already the potential to uncover important changes in the lake environment and its catchment.

After the geophysical core logging the sediment cores were split in half. Subsequently the surfaces of each halve were cleaned with a small glass slide to obtain a smooth and clear surface. Cores taken in the austral summer of 2007 were opened, sampled and described at the Université de Liège - while all other cores were opened, sampled and described at Ghent University.

Each core was described in high detail, paying particular attention to changes in sediment colour, texture and structures present. Sediment colour was determined using a Munsell Color Scale. When observing the sediment texture a qualitative description of the grain size and sorting was made. The sediment structures were classified as either coring-induced structures (e.g. downward curving of the laminae), or natural structures (e.g. laminae thickness). Tephra deposits were studied in detail.

III.2.5. Smear slide Analysis

A smear slide is a thin layer of unconsolidated sediment embedded on a glass slide for petrographic microscopic examination. Smear slides are a powerful method for rapidly evaluating tiny quantities of sediment (mineralogy, provenance, form, size) as the basis for sediment classification. Tephras and ash falls are also easily identified with this technique. Smear slides should be taken at regular intervals, not only where "special" features are present. Smear slides can also be useful to detect minor changes in the sediment, which are not so clear when describing the core macroscopically.

First, laminae were selected where smear slides were to be taken. This could be a lamina different from the main sediment body or a lamina which seemed to represent the main characteristics of the main sediment body. A glass slide was labelled for each interval and a small amount of the sediment extracted with a tooth pick and placed on a glass slide with a drop of distilled water. The tooth pick was used to smear this sediment as thinly and evenly as possible over the slide. Next the slide was placed on a hot plate until the water completely evaporated. Then a few drops of Canada Balsam were added to the sediment on the slide and this mixture covered with a slide cover. The slides were left to dry for a couple of days before examination under a petrographic microscope. This method is also useful for determinating the clay-silt-sand ratio, i.e., the ratio of terrigeneous versus aquatic material, the amount of microfossils, the main minerals.

III.2.6. High-Resolution Photo Analysis

Representative images of split sediment cores document geological records, serve as visual aids for multimedia, and provide samples for image analysis. Also the appearance of the sediment is digitised without disturbing the sediment core. It is possible to enhance desired structures with a number of applications (Cooper, 1997). The human brain is excellent at detecting and recognising patterns and spatial relationships, but very poor at estimating quantitative information from images (Saarinen and Petterson, 2001).

All sediment cores were photographed at 5 cm intervals with a CANON EOS 450D camera and stitched together in CorelPhoto X4. The cores from the 2007 expedition were taken with bulbs with a rather yellow light. All other cores were photographed in a specially designed

light box where neon light illumination with a colour resembling natural light was used and where this light was equally distributed. This time every 15 cm of the core was photographed and these 15 cm segments were stitched together in Corel Photo Paint X4.

III.2.7. X-Ray Fluorescence Scanning (XRF)

X-ray fluorescence is a semi-quantitative, non-destructive method which provides high-resolution records of chemical-elemental composition on split sediment cores (Jansen et al., 1998; Richter et al., 2006). An X-ray is emitted and ejects an electron from an inner shell of an atom. The resulting vacancy is subsequently filled by an electron falling back from an outer shell, and the energy between both shells is emitted as electromagnetic radiation. The wavelength of the emitted radiation is characteristic for each element and the amplitudes of peaks in the XRF spectrum are proportional to the concentration of corresponding elements in the analysed sample (Jenkins and De Vries, 1970).

Prior to scanning the sediment cores, the surface of the sediment is carefully flattened and irregularities from core slicing are removed. Subsequently, the sediment surface is covered with a thin (4 µm) Ultralene film in order to further diminish the surface roughness, and to prevent drying of the core or contamination of the prism unit during core logging (Richter et al., 2006). XRF scanning data is semi-quantitative, recording the relative downcore variations of the elemental composition of the sediment (Richter et al., 2006). When the sediment contains medium to coarse sand-sized particles effects of sample inhomogeneity and surface roughness are pronounced and the measured data is often not so reliable (Richter et al., 2006). Elemental ratios or log-ratios are recommended to express the downcore variations to circumvent this issue and overcome spurious patterns created by variations in water and organic material (Weltje and Tjallingii, 2008).

The major chemical element composition was analysed using an AVAATECH XRF core scanner. For the majority of the Villarrica cores we used the scanner at the MARUM institute in Bremen for VILLSC02, VILL2FG and all the Parrillar cores we used the scanner at the Royal Netherlands Institute for Sea Research (Royal NIOZ). The same protocol and apparatus settings were used at both laboratories. Element intensities were recorded in three runs with a resolution of 1 cm for the sediment cores of Lago Villarrica. Only the two first runs were used for the Laguna Parrillar cores, this time at a resolution of 1 mm. In a first run, element intensities were measured for the elements ranging from Al to Co using a computer controlled forced air cooled Oxford 50 Watt X-ray source operating 10 kV. In a second run the element intensities for the elements ranging from Zn to Zr were determined with the X-ray source operating at 30 kV. In a third run the element intensities of the elements Ba, Rb and U were measured with an X-ray source operating at 50 kV.

III.2.8. Water Content Analysis

The water content of sediment is often related to major sedimentological changes within in the core. It also influences the results of the MSCL and XRF core scanner measurements (Weber et al., 1997; Weltje and Tjallingii, 2008).

Immediately after opening the sediment cores, to prevent a minimum of water loss through the drying of the sediment halves, one half of the sediment was sampled every cm and its water content was estimated using Equation III-1. The analysis of the water content of the sediment was done on the Lago Villarrica sediment by extracting a third of a half core sediment slice every cm and weighing it before and after a 24 h drying period in a oven at 105°C. For Laguna Parrillar a

full half core slice of the sediment was extracted every cm, and its mass was measured before and after freeze-drying the for 48 h.

$$WC=\left(\frac{WW-DW}{WW}\right)*100$$

(*Equation III-1*)

WC = water content (%)
WW = weight wet sediment (g)
DW = weight dry sediment (g)

III.2.9. Loss-On-Ignition (LOI)

Loss-on-ignition (LOI) is a cheap, simple and widely applied method used to estimate the organic and carbonate content of sediments. The method is based on the linear relations between LOI values and organic and inorganic content (Dean, 1974; Heiri et al., 2001; Santisteban et al., 2004), and is used widely in palaeolimnological studies, because fluctuations in carbon content often correlate to biological changes, which, in turn can relate to changes in catchment processes and, sometimes, local or regional climate. In a first reaction organic matter is oxidised to carbon dioxide at a temperature of 550°C (LOI_{550}). In a second reaction at 950°C (LOI_{950}) carbonates evolve into carbon dioxide. The sample's weight loss is directly correlated to the amount of organic matter and carbonate present in the sediment (Dean, 1974).

The Heiri et al. (2001) method was used to determine the percentage of organic matter and carbonate present in all the samples from Lago Villarrica and on a few test samples from Laguna Parrillar. In addition, the core top samples of several Lago Villarrica gravity cores were analysed (Figure III-6 and Table III-1). After drying the sediment for 24 h at 105°C, the sample was ground to ensure a homogeneous fine powder. One gram of sediment was extracted after homogenisation, since LOI_{550} can be influenced by the sample weight (Heiri et al., 2001). Subsequently the samples were heated at 550°C for 4 h in a muffle furnace. The weight loss was measured and they were heated again for 2 h at 950°C after which the samples were reweighted.

LOI_{550} is calculated using Equation III-2. LOI_{950} is calculated using Equation III-3. The weight loss by LOI at 950 °C multiplied by 1.36 should theoretically equal the weight of the carbonate in the original sample (Bengtsson and Enell, 1986).

$$LOI_{550}=\left(\frac{DW_{105}-DW_{550}}{DW_{105}}\right)*100$$

(Equation III-2)

$$LOI_{950}=\left(\frac{DW_{550}-DW_{950}}{DW_{550}}\right)*100$$

(Equation III-3)

LOI_{550} = LOI at 550°C (%)
LOI_{950} = LOI at 950°C (%)
DW_{105} = weight dry sediment after oven-drying for 24h at 105°C (g)
DW_{550} = weight dry sediment after combustion for 4h at 550°C (g)
DW_{950} = weight dry sediment after combustion for 2h at 950°C (g)

III.2.10. Total Organic Carbon (TOC), Total Nitrogen (TN) and Carbon and Nitrogen Isotopes

Organic matter content of lake sediments provides a variety of indicators that can be used to reconstruct palaeoenvironments of lakes and their watersheds. It constitutes a minor but important fraction of lake sediments and it provides information that is influenced by both natural and human-induced changes in local and regional ecosystems (Meyers, 1997; Meyers and Lallier-Vergés, 1999; Meyers and Teranes, 2001). Total organic carbon (TOC) concentrations are influenced by both the initial production of biomass and the subsequent degree of degradation, so they integrate the different origins of organic matter, delivery routes, depositional processes and amount of preservation (Meyers

and Lallier-Vergés, 1999; Meyers and Teranes, 2001). The origin of sedimentary organic matter from aquatic as opposed to land sources can be distinguished by the characteristic C/N ratio compositions of algae and vascular plants (Meyers and Lallier-Vergés, 1999; Meyers and Teranes, 2001). The carbon isotopic composition of organic matter in lake sediments is important in assessing organic matter sources, for reconstructing past productivity rates and for identifying changes in the availability of nutrients in surface water (Meyers and Teranes, 2001). The nitrogen isotopic composition of sediment organic matter is useful in identifying changes in the past availability of nitrogen to aquatic producers (Meyers and Teranes, 2001). The dynamics of biogeochemical nitrogen cycling are more complicated than those of carbon, thereby making interpretations of $\partial^{15}N$ records more difficult (Talbot, 2001).

Samples of both lakes were analysed for their carbon and nitrogen content as well as for the isotopic composition of these two elements. In Lago Villarrica, a resolution of 1 sample every 10 cm was used. In Laguna Parrillar a more irregular sampling strategy was applied: one sample every 4 cm was taken in the uppermost 88 cm, one sample every 2 cm from a depth of 88 to 196 cm and one sample every 30 cm from 196 to 695 cm. These sampling intervals were chosen based on a preliminary age model, to make sure their would be an even spacing in time of the analysed samples. The core top samples of several Lago Villarrica gravity cores and one soil sample were measured (Figure III-6 and Table III-1). All samples were freeze-dried, ground and homogenized using an agate mortar. From each of these powdered sediment samples, 10 to 50 mg (based on the results of LOI_{550} results) was transferred to a cleaned silver cup. Depending on the size of the sample 30 to 50 µl milli-Q was added into the silver cup. Together with the milli-Q, 50 µl of HCl (5%) was added in order to remove any possibly present carbonates following the in situ acidification method of Verardo et al. (1990) (using HCl instead of H_2SO_3). Subsequently the filled silver cups were dried overnight in an oven at 50°C. After drying, the cups were closed with tweezers.

Total organic carbon (TOC), total nitrogen (TN) and carbon and nitrogen isotopic measurements were carried out at the Free University of Brussels (VUB) in collaboration with Dr. Eddy Keppens. Bulk samples were analysed with a Thermo-Elektron Corp. Delta V isotope ratio mass spectrometer in continuous flow mode on-line connected to a Thermo-Finnigan Interscience "Flash" EA 1112 series Element Analyser via a Finnigan Conflo III interface. Diatomic nitrogen and carbon dioxide for mass spectrometric analysis were generated by O_2 flash combustion at 980°C, chromatographically separated, purified and carried to the mass spectrometer by a He flow. The isotopic compositions of nitrogen and carbon were measured sequentially together with N_2 and CO_2 reference working gasses, calculated with the fixed ∂-values of these reference gasses ($\partial^{15}N$: ~6.621 ‰ and $\partial^{13}C$: ~36.376 ‰) and calibrated with the inter-laboratory standards IAEA-N1 (ammonium sulphate, $\partial^{15}N$: +0.43 ‰ +/- 0.04 ‰) (Boehlke and Coplen, 1995) and IAEA-CH 6 (sucrose, $\partial^{13}C$: -10.449 ‰ +/- 0.030 ‰) (Coplen et al., 2006a; Coplen et al., 2006b). TN and TOC contents were calculated by comparing the areas of respective peaks (of N_2 and CO_2) with those of the certified reference material acetanilide (C_8H_9ON), taking into account its C- and N-content (C: 71.09 %, N: 10.36 %) and the weight of analysed reference material. All inter-laboratory standards and certified reference material, wrapped in clean silver cups as well as blank silver cups were measured repeatedly, i.e. between each set of 6 to 7 samples. Both the certified reference material acetanilide and the inter-laboratory standards IAEA-N1 were analyzed in suites of 5 aliquots of increasing weights between 0.05 to 1

mg, such as to cover the range of expected TN and TOC contents of the samples and to be able to assess the nitrogen isotopic composition of the blank, while considering the blank's carbon isotopic composition negligible. The sample representativeness and the measurement precision was determined by remeasuring 31% of the samples. The error on the $\partial^{13}C$ measurements is 0.56 ‰. The errors on the TN and TOC are 0.005 % and 0.046 % respectively.

III.2.11. Particle Size Analysis (PSA)

Grain size is the most fundamental property of sediment particles, affecting their entrainment, transport and deposition. Particle size analysis (PSA) therefore provides important clues to the sediment provenance, transport history and depositional conditions (e.g., Folk and Ward, 1957).

The Lago Villarrica sediment was measured every 2 cm (without any removal of organic matter, biogenic silica or carbonates). This decision was made to allow the comparison of the PSA data of Lago Villarrica with the PSA data of Lago Puyehue (Bertrand et al., 2008), since the samples were also untreated in this study. About 0.5 cm^3 of sediment was added to a 0.05 % calgon (sodium hexamethaphosphate) solution to facilitate disaggregation and dispersion of the sediment particles.

Samples from Laguna Parrillar were treated before analysis, both organic matter and carbonates were removed. The samples were not treated for the removal of biogenic silica, since the smear-slide analysis showed ignorable presence of this substance. Samples were selected at different resolutions at different intervals: from 0 to 88 cm one sample every 4 cm, from 88 to 196 cm one sample every 2 cm and from 196 to 695 one sample every 8 cm. The Laguna Parrillar sampling intervals were chosen based on a preliminary age model, to make sure their would be an even spacing in time of the analysed samples. To remove all organic material ca. 1 g of freeze-dried sediment, 25 ml of distilled water and 10 ml of H_2O_2 (33%) were mixed in a 250 ml glass beaker and this mixture was boiled on a hot plate until the reaction of the organic matter with the H_2O_2 had stopped. Subsequently the mixture in the beaker was diluted to total amount of 100 ml adding distilled water. To remove any carbonates 10 ml HCl (10%) was added, while heating the mixture to boiling point for 1 minute exactly. Then the beaker was filled up to the edge with more distilled water and the sediment was left overnight to settle. The next day the supernatant was removed and the treated sediment was passed on to a 50 ml centrifuge tube. The sediment was washed with distilled water using the following technique: filling the centrifuge tubes containing the sediment with distilled water, spinning the tubes for 5 minutes at 4000 rpm in a centrifuge, removing the supernatant and repeating this process two more times. After rinsing the sediment 25 ml of a 0.2 % calgon solution was added to facilitate disaggregation and dispersion of the sediment particles.

Prior to all PSA measurements, all sediments were continuously shaken for at least 12 h to make sure that the calgon-sediment solution was completely disaggregated and dispersed. The particle-size distributions of the sediment of both lake cores were measured on a Malvern Mastersizer 2000 laser granulometer (size range: 0.02 to 2000 µm) with Autosampler and Hydro G dispersion unit at the National Oceanography Centre Southampton (NOCS). For every sample the distributions of three consecutive PSA runs were checked for consistency and the appropriate distributions were averaged to create the final size distribution. The same measurement settings were used for both Lago Villarrica and Laguna Parrillar with the only exception that no sonification was used with the Lago Villarrica sediment to make sure no diatom frustules or glass shards were broken, therefore

changing their particle size. A pre-measurement sonification of 40 % was used during 15 seconds on the Laguna Parrillar samples, this was necessary to break up the clay particles.

An assessment of the sample representativeness and the measurement precision of the instrument, based on replicate and repetitive measurements of 5 % of the samples, indicates an average PSA mode error of 2.91 % and an average correlation (R_2) between replicate/repetitive and original measurements of 0.99.
Standard statistical parameters (modal size, sorting and kurtosis) of the PSA distributions were calculated according to Folk and Ward (1957) as implemented in the GRADISTAT software (Blott and Pye, 2001).

III.2.12. Biomarkers (TEX_{86}/BIT)

In order to understand global climate patterns and processes, we must be able to quantify past continental temperature variability. The $\delta^{18}O$ values of microfossils are commonly used to reconstruct palaeotemperature, as these values seem to depend of the water temperature in which the organism was growing at that time. In lacustrine palaeoclimate investigations this approach has been applied to ostracods (von Grafenstein et al., 1999) or diatoms (Hu and Shemesh, 2003). Lipids present in the membranes of certain organisms are also known to vary with growth temperatures (Schouten et al., 2002). One of the best examples of such lipids are the isoprenoid glycerol dialkyl glycerol tetraethers (GDGTs) which can contain up to eight cyclopentane rings (DeRosa and Gambacorta, 1988). These ether linked GDGT produced by Archaea typically contain 0 to 4 cyclopentane moieties with two glycerol head groups (Powers et al., 2010) (Figure III-8). Culture studies have shown that there is a strong relationship between the average number of cyclopentane rings in the isoprenoid GDGTs and the growth temperature of the Archaea (Uda et al. 2001). Based on these GDGT membrane lipids, the TEX_{86} sea surface temperature (SST) proxy has recently been developed (Schouten et al., 2002). TEX_{86} is a palaeothermometer index based on the composition of temperature sensitive membrane lipids of the picoplankton Crenarchaeota. Another GDGT based proxy is the branched vs. isoprenoid tetraether (BIT) index. The branched GDGTs (Figure III-8) are thought to be produced by anaerobic terrestrial bacteria (Weijers et al., 2006; Weijers et al., 2009). The BIT index is therefore a proxy for the relative fluvial input of terrestrial organic matter, mostly soil derived material, in the marine environment (Hopmans et al., 2004). The presence of the isoprenoid and branched GDGTs has been reported in lake sediments (Blaga et al., 2009; Powers et al., 2010; Powers et al., 2004).

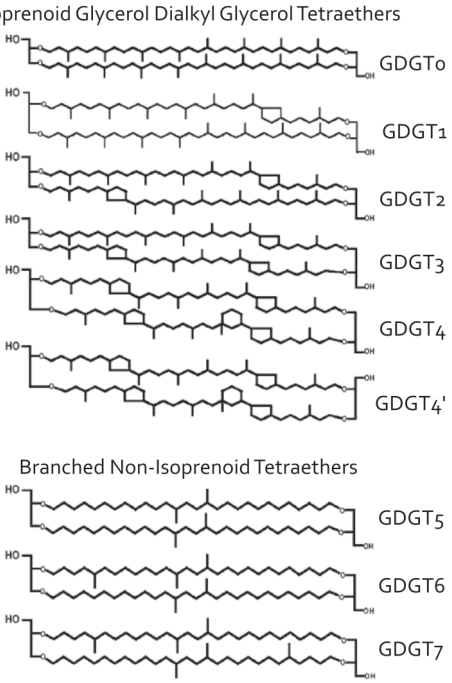

Figure III-8: The glycerol dialkyl glycerol tetraether (GDGT) structures and their numbers (after Blaga et al., 2009) as they are used in the TEX86 and BIT calculations. GDGT 4' is a stereoisomer of GDGT 4.

TEX_{86} values are determined using Equation III-4 (Schouten et al., 2002).

$$TEX_{86}=\frac{GDGT2+GDGT3+GDGT4'}{GDGT1+GDGT2+GDGT3+GDGT4'}$$

(Equation III-4)

The distribution pattern has been shown to be primarily dependent on growth temperature (Wuchter et al., 2004). Using the TEX_{86} value a number of calibration equations can used to calculate the lake water surface temperature.

The BIT index is calculated using Equation III-5 (Hopmans et al., 2004).

$$BIT=\frac{GDGT5+GDGT6+GDGT7}{GDGT4+GDGT5+GDGT6+GDGT7}$$

(Equation III-5)

The BIT index ranges in value from close to 0, indicating predominantly aquatic organic matter to 1, indicating mostly soil derived organic matter. The distribution of soil-derived GDGT membrane lipids which are measured to determine the BIT index can be used in palaeoenvironmental studies to estimate past mean annual air temperature (MAAT) and soil pH (Weijers et al., 2007). Recent studies have shown, however, that the source of soil-derived GDGTs in lake sediments is ambiguous, it is not clear whether only temperature and pH in the catchment are the driving factors (Blaga et al., 2010; Tierney and Russell, 2009; Tierney et al., 2010).

The following analyses were performed at NIOZ, the Netherlands in collaboration with Dr. Jaap Sinninghe Damsté. Forty-five sediment samples of the VILL core of Lago Villarrica in the top 840 cm were measured for TEX_{86} and BIT. Several surface sediment samples, one soil sample and the suspended matter of river and lake water of Lago Villarrica and its catchment were also measured for the same parameters (Figure III-6 and Table III-1). After freeze-drying and, where necessary, homogenization with a mortar and pestle, lipids were extracted from ca. 1 g of dry sediment. Sediments were extracted using an Accelerated Solvent Extractor (DIONEX ASE 200). A mixture of DCM/methanol (9:1; v/v) was flushed through at a temperature of 120°C and a pressure of 7.6*106 Pa, three times, with 5 minute intervals between flushings. Extracts were concentrated by rotary evaporation, and after drying over a Na_2SO_4 column using DCM as an eluent, they were separated by column chromatography for analyses. By using an activated Al_2O_3 column, the apolar and polar fractions were obtained with hexane:DCM 9:1 (v/v) and DCM:MeOH 1:1 (v/v), respectively, as an eluent. The polar fraction was dried under a nitrogen flow, dissolved in hexane:isopropanol 99:1 by sonication, and prior to injection, filtered through a 0.45 µm PTFE filter. GDGTs were measured (injection volume 10 µl) using HPLC/atmospheric pressure positive-ion chemical ionization (APCI)/MS according to Schouten et al. (2007). To enable detection of low concentrations of GDGTs, a modification in the scanning procedure was made, as the single ion monitoring (SIM) mode was used to increase sensitivity and reproducibility (m/z 1302, 1300, 1298, 1296, 1292, 1050, 1036 and 1022 for the different GDGT isomers)(Schouten et al., 2007). Samples used for TEX_{86} analyses were used also for BIT index analyses (Hopmans et al., 2004). After analyzing the mass chromatograms, peaks that were at least one order of magnitude greater than the background noise were integrated and used for TEX_{86} and BIT calculation. TEX_{86} values were determined according to Equation III-4. Temperature estimates were obtained using the lake calibration (Equation III-6) by Blaga et al. (2009):

$$TEX_{86}=0.018*ALST+0.019$$

(Equation III-6)

ALST = annual lake surface temperature

This equation gave the same temperature for the mean annual lake

surface temperature as the temperature obtained of Lago Villarrica by Campos et al. (1983). BIT index values were calculated using Equation III-5.

III.2.13. Relative Palaeointensity (RPI)

Due to the high natural variability of the Earth's geomagnetic field, palaeomagnetic variations in sediment cores can be a powerful tool for establishing high-resolution chronologies. The Earth's magnetic field is a vector and can be completely characterised by three elements at any point in time and space. The first element is declination (D), the angle of deviation in the horizontal plane between the geographic north and the magnetic north. The second element is inclination (I), the dip angle of the magnetic vector below the horizontal plane. The final element is the magnitude of the field or the geomagnetic intensity (F). The earth's main magnetic field shows three types of spatial and temporal variations on timescales that are useful for dating and correlation purposes in studies of lake sediment (King and Peck, 2001). These three types of variation are geomagnetic secular variations (SV), excursions, and reversals and they are defined by both the amplitude of the change in field direction, the intensity and the duration of the change and the type of instability (Jacobs, 1994). The changing character of the Earth's magnetic field has both a directional component, and also changes in intensity. Obtaining the magnetic intensity is a bit more complex, since it is not possible to directly measure this intensity, therefore normalizations have to be calculated (Tauxe, 1993). Fluctuations of the geomagnetic field during the Holocene are rather poorly known. Marine sedimentary records often lack resolution in the Holocene due to low sedimentation rates, and, in many cases, the Holocene part of the record is missing due to difficulties in adequately recovering the uppermost sediments using piston coring techniques. Lakes or specific marine environments (e.g., estuaries, continental shelves), on the other hand, can have sufficiently high sedimentation rates suitable for obtaining high-quality Holocene records of the geomagnetic field.

In addition to both D and I, the relative palaeointensity record can be used, as a regional correlation tool. To be suitable for palaeointensity correlation the sediment must meet rigorous criteria (Banerjee and Mellema, 1974; King et al., 1982b; Levi and Banerjee, 1976; Tauxe, 1993). Relative palaeointensity variations of sediments can be determined by normalising the natural remanent magnetisation (NRM) of the deposits for down-core changes in the concentration of remanence carrying grains (Channell et al., 1997; King et al., 1982a; Levi and Banerjee, 1976; Tauxe, 1993).

The dipolar fluctuations of the field modulate the production of cosmogenic isotopes in the high atmosphere. The question is to know at which time scale these fluctuations are present. Recent paleointensity studies suggest that geomagnetic field intensity influences cosmogenic production on millennial to sub-millennial timescales (Snowball and Sandgren, 2002; St-Onge et al., 2003). In contrast, a stack of well-dated paleointensity records from Fennoscandia does not support this conclusion, as sub-millennial changes in the individual RPI records are not represented in the stacked data (Snowball et al., 2007). This demonstrates the need for an increased RPI database covering the Holocene period in order to understand the temporal and spatial variations of past geomagnetic field strength and establish the time scale at which geomagnetic field intensity and cosmogenic isotope flux are linked (Sarnthein et al., 2002; Snowball and Muscheler, 2007).

First the sediment was tested for its dominant type of magnetic minerals

and their shape. To obtain reliable palaeomagnetic measurements it is preferable to have mostly (titano)magnetite, a low coercivity mineral (Tauxe, 1998). The magnetic minerals were separated from the rest of the dried sediment with a magnet and then studied under a binocular microsope. Subsequently one half of the split sediment core sections was continuously sampled using U-channels (plastic containers with a 2x2 cm cross-section, with a clip-on lid constituting one of the sides) (Weeks et al., 1993). Magnetic properties were measured by Dr Catherine Kissel and Camille Wandres at the Laboratoire des Sciences du Climat et de l'Environnement (LSCE) at Gif-sur-Yvette. The magnetic properties of these U-channels were measured at 2 cm intervals using a small access 2G 755 SRM magnetometer equipped with high resolution DC squids and housed in a mu-metal shielded room. Due to the finite width (~4.5 cm) of the magnetometer response function (Guyodo et al., 2002; Weeks et al., 1993), each 2 cm interval measurement is not independent. First the low field susceptibility (*k*) was measured using a Bartington. Natural remanent magnetization (NRM) was determined after demagnetization at peak fields using 10 steps at a translation speed of 4 cm s-1 (Brachfeld et al., 2004) (10 mT, 15 mT, 20 mT, 25 mT, 30 mT, 35 mT, 40 mT, 50 mT, 60 mT and 80 mT). At each step, the intensity, declination and inclination were measured. Component magnetization directions were computed by principle component analysis (Kirschvink, 1980) incorporating all demagnetization steps. The anhysterestic remanent magnetization (ARM) was acquired directly in a 100 mT alternating field (AF) and in a 0.05 mT bias field at a 1 cm/s translation speed (Brachfeld et al., 2004) and this value was multiplied by two to obtain the k_{ARM}. k_{ARM} is the so-called susceptibility of ARM. k_{ARM} has been demagnetized using the same steps as NRM. The isothermal remanent magnetization (IRM) was acquired along the axis of the U-channel. The saturated IRM was acquired stepwise (6 steps at 50, 100, 200, 300, 500, 1000 mT) along the axis of the u-channel and then demagnetized using the same 10 steps as for ARM and NRM. After the final acquisition at 1T, a reverse field of 0.3 T was applied and the magnetization was measured to obtain the S-ratio (Equation III-7).

$$\text{S-ratio} = \frac{IRM_{(-0.3T)}}{IRM_{(1T)}}$$

(Equation III-7)

III.2.14. Geochemical Analysis of Volcanic Glass Shards

Volcanic ash (tephra) forms a regional chronostratigraphic marker that can be used to correlate simultaneous events at different sites. The occurrence of a known tephra in a lake core or stratigraphic section is often treated as the equivalent of a radiocarbon date (Beierle and Bond, 2002; Blockley et al., 2005).

Laguna Parrillar is located in the Andean Austral Volcanic Zone (AVZ), the southern most active volcanic segment in the Andes. Regionally widespread tephras are present in southern Patagonia (Kilian et al., 2003; Stern, 2008). Auer (1974) recognised that tephra layers in Tierra del Fuego could be used as effective isochrons for correlation between different deposits in the region. More recent studies (Haberle and Lumley, 1998; Kilian et al., 2003; Stern, 2008) have proven that the geochemical composition of the volcanic ash deposits of five Holocene, large-volume eruptions is sufficiently unique to use them as chronostratigraphic markers in the region.

The glass shards of two tephras present in two cores of Laguna Parrillar (PAR1 and PAR-1A-liv) (Figure III-7 and Table III-1) were analysed for their geochemical composition. This analysis was done by Dr. Stephen Roberts of the British Antarctic Survey. The samples were

prepared by wet sieving (through 250-63 µm, 125-63 µm and 10-63 µm meshes), and, where necessary, by removing organic residues by floatation (in densities of 2 or 2.45 g/cm^3) for an electron probe micro-analyser (EPMA). The oven-dried (40°C overnight) 63-250 µm and 63-125 µm fractions were mounted onto frosted glass slides using Epo-Tek 301 epoxy resin. Sections were lapped on a Logitech LP50 for ~30 min using calcined aluminium oxide (15 micron) abrasive powder mixed with water to obtain 165 µm thick samples. Sections were cleaned using detergent (Teepol), placed in an ultrasonic bath for about 2 min, and dried with industrial mentholated spirit and a hair dryer. Cleaned sections were then polished on a Buehler Metaserv polishing machine using Texmet 1000 polishing cloth, using a 'single-stage' polishing technique (i.e. one 25 min cycle using aluminium oxide polishing powder mixed with water, followed by a 1 min cycle of polishing using Buehler Mastermet colloidal silica on a Buehler Chemomet polishing cloth). After this process, insufficient grains were exposed on the 165 µm thick surface. Therefore, samples were ground by hand to a thickness of mostly 50 µm where the maximum number of shards were exposed on the surface. Samples were then polished using 6, 3, 1 µm diamond paste and carbon coated. All the samples were analysed at the School of Geosciences, University of Edinburgh, using a Cameca SX100 electron probe analyser. The instrument was operated at 15 kV and with a beam diameter of 5 µm, with analysis of Na, Mg, Al, Si, K and Ca at 2 nA and F, P, S, Cl, Ti, Mn and Fe at 80 nA (Hayward, in review). For all elements, the Kα X-ray line was measured and the counting time on peak was 20s and on background positions 10s, except for F (50s+40s), Mn (60s+50s) and Fe (50s+40s). Calibration used natural jadeite (Na), wollastonite (Si, Ca), apatite (P), barite (S), orthoclase (K) and synthetic glass (BIR1g, Al), spinel (Mg), MnRb fluoride (F), halite (Cl), rutile (Ti), fayalite (Fe) and pure metallic Mn. Beam current was determined by the insertion of a Faraday cup into the path of the beam. Analyses were made from a single point in the thickest part of each shard. In general one analysis per shard was undertaken to avoid the effects of beam induced element mobilisation from closely adjacent locations. Between 10 and 30 shards were analysed, as recommended by Hunt and Hill (1993). Sodium and Potassium were measured during the first counting period to minimise the possibility of beam-induced mobilisation. Calibration to volcanic glass standards (USGS fused basaltic standard BHV02g and the Lipari Obsidian) was performed at the start and end of each day. Counter dead time was corrected for a ZAF correction applied to account for the effects of atomic number (Z), absorption (A) and fluorescence (F) (Sweatman and Long, 1969) via Cameca's PeakSight software v4.2 using the X-Phi data processing algorithm.

III.2.15. X-Ray Diffractometry (XRD)

X-ray diffractometry (XRD) is one of the most important and widely used methods for mineralogical assessment of lake sediments. This analysis can be performed on the bulk inorganic assemblage of the deposit (i.e., bulk mineralogy), on a specific group of minerals (e.g., carbonate minerals) or on a specific grain size fraction (e.g., clay mineralogy). One disadvantage of this technique is that it is only applicable to crystalline material. Lake sediments sometimes contain amorphous inorganic matter (e.g. glass tephra shards, clays derived from weathering of volcanic deposits like allophane) which cannot be evaluated by XRD. Minerals however are fundamental components of sediment. From a genetic perspective there are three types: 1) authigenic minerals that originate within the water column, 2) detrital minerals that are brought in the lake via surface streams, shoreline erosion, sheet flood, mass movement or aeolian activity, 3) diagenetic minerals derived from post-depositional

alteriation of bottom sediment (Last, 2001). In both lakes, in this study, the detrital component is the most important. These minerals reflect the interaction of several factors: 1) tectonic and weathering conditions within the watershed, 2) sediment provenance, 3) transport processes. Thus, changes in the detrital component can be used to deduce variations in drainage basin size and morphology and fluctuations in the climatic regime of the area.

XRD measurements were performed at Université de Liège by Dr. Nathalie Fagel. In Lago Villarrica the bulk mineralogy of 43 samples, taken at random intervals in the core, was measured. In Laguna Parrillar samples were selected at different resolutions at different intervals: from 0 to 196 cm one sample every 2 cm and from 196 to 695 one sample every 30 cm. These levels were analysed for both bulk and clay mineralogy.

Bulk mineralogy was achieved by X-ray diffraction (XRD) on a Bruker D8-Advance diffractometer with CuKα radiations. Bulk samples were powdered to 250 µm using an agate mortar. An aliquot was separated and mounted as unoriented powder by the back-side method (Brindley and Brown, 1980). The powder was scanned by XRD between 2° and 45° 2θ. The data were analysed in a semi-quantitative way following Cook et al. (1975). The intensity of the primary peak of each mineral was measured and corrected by a multiplication factor. For amorphous material, a mean correction factor was obtained from diffraction results on mixtures of known quantities of amorphous material and quartz. Bertrand et al. (2005) calculated a mean correction factor of 75, applied to the maximum of the broad diffraction band at 3.7 Å. In general we can assume an error of ca. 5% has be taken in consideration (Cook et al., 1975).

For the clay mineralogy, the sediment was sieved at 63 µm. The clay (< 2 µm fraction) was concentrated from the 63 µm fraction after 50 minutes of sedimentation (Stokes's settling law). Oriented mounts were realised by the "glass-slide method" (Moore and Reynolds, 1989) and subsequently scanned on the diffractometer. Slides containing crystallised clays after air drying test (N) were also scanned after ethylene-glycol solvation during 24 h (EG) and after heating at 500°C during 4 h (500).

III.2.16. Grain Surface Textures

The shape of a grain shape, its roundness and angularity, is not only determined by its mineralogy, but also by the type of transport by different geological agents. The 'surface character', which is defined by microtextures, is also a good source environment indicator (Mahaney, 2002). The scanning electron microscope (SEM) is used to image sand grain surface topography to define source environments. The SEM is thus used to separate ancient depositional environments associated with wind, water, ice (glacial environments) and weathering-diagenesis (Krinsley and Doornkamp, 1973). Since sand grains are often transported more than once, separating modern from ancient microtextures depends strongly upon the original textural imprint (imprint energy), grain age, and all the diagenetic processes that operated over post-depositional time (Mahaney, 2002). By studying a group of grains in great detail, the effects of more than one stage of development can be separated.

Nine samples taken at levels with a large sand-sized fraction were selected in the sediment core of Laguna Parrillar. These samples were treated before analysis, both organic matter and carbonates were removed. The samples were not treated for the removal of biogenic silica, since the smearslide analysis showed ignorable presence of this substance. Samples were selected at different resolutions at different intervals: from 0 to 88 cm one sample every 4 cm, from 88 to 196 cm one sample every 2 cm and from 196 to 695

one sample every 8 cm. To remove all organic material ca. 1 g of freeze-dried sediment, 25 mL of distilled water and 10 mL of H_2O_2 (33%) were mixed in a 250 mL glass beaker and this mixture was boiled on a hot plate until the reaction of the organic matter with the H_2O_2 had stopped. Subsequently the mixture in the beaker was diluted to total amount of 100 mL adding distilled water. To remove any carbonates 10 mL HCl (10%) was added, while heating the mixture to boiling point for 1 minute exactly. Then the beaker was filled up to the edge with more distilled water and the sediment was left overnight to settle. The next day the supernatant was removed and the treated sediment was passed on to a 50 mL centrifuge tube. The sediment was washed with distilled water using the following technique: filling the centrifuge tubes containing the sediment with distilled water, spinning the tubes for 5 minutes at 4000 rpm in a centrifuge, removing the supernatant and repeating this process two more times. After rinsing the sediment was sieved through a 63 µm mesh. The fraction larger than 63 µm was subsequently ovendried for 24 h at 40°C. A small sub-sample of dried sediment was selected ad random and sprinkled lightly onto a piece of paper. Next the self-adhesive surface of a JEOL aluminium stub (10 mm diameter) was pushed onto the scattered sand grains. Sediment-loaded stubs were then sputter coated with gold, in preparation for scanning electron microscopic analysis. During SEM analysis first a general description of the sample was made, based on the roundness and angularity of the grains in general and how well sorted the sample is. Subsequently an amount of grains was studied and described separately in great detail. Dr. Mieke Thierens helped with the identification of the microtextures.

III.2.17. Pollen Analysis

Pollen grains are produced and dispersed as part of the plant reproductive process. Analysis of the pollen content of sediment samples is the principal technique available for determining vegetation response to past terrestrial environmental change. This change can have a climatic or antropogenic cause (Bennett and Willis, 2001).

The pollen analysis was carried out at the RCMG at Ghent University by Dr. Ana Maria Abarzua. She also counted the pollen slides and interpreted the results. 1.5 cm^3 volumetric subsamples were taken at 10, 20 or 30 cm intervals and were prepared using standard techniques (KOH deflocculation, HF digestion, and acetolysis) (Faegri and Iversen, 1989). The basic pollen sum included at least 300 pollen grains of trees, upland shrubs and herbs. Lycopodium tracer spores were added to each sample in order to calculate absolute pollen concentrations (grains cm^{-3}). Pollen data were analyzed and plotted using Tilia 2.0.b.4 (Grimm, 1991-1993) and Tilia Graph View version 2.0.2. (Grimm, 2004). The pollen sequence was divided into zones using stratigraphically constrained cluster analysis, CONISS (Constrained Incremental Sum of Squares) (Grimm, 1987). In each pollen slide charcoal particles were also counted and their concentration was calculated (particles cm^{-3}) in relation to the Lycopodium tracer.

III.2.18. Diatom Analysis

Diatoms (Bacillariophyta) are unicellular algae, living in wet habitats, ranging from freshwater to hypersaline lakes, to rivers and oceans, and in wet terrestrial habitats. Diatom analysis is a widely used technique in palaeolimnology, because of the good preservation of their silica cell walls, which permits easy identification to species level, and because they are known to respond well to different ecological and environmental changes (Battarbee et al., 2001).

The diatom analysis was performed at PAE at Ghent University by Evelien Van de Vyver and Margo Eekhaut. They counted the diatom slides and

Table III-2: Samples sent to the Poznan Radiocarbon Laboratory or to the NOSAMS facility

Lake	Sample name	Sample depth (cm)	Nature of sample	Laboratory
Lago Villarrica	VILL VSC1-0	0.5	bulk sample	Poznan
Lago Villarrica	*VILLSC02-68*	*68.5*	*wood fragment*	*NOSAMS*
Lago Villarrica	VILLSC02-68	68.5	bulk sample	NOSAMS
Lago Villarrica	VILL1-TEST-I-59	84.05	bulk sample	NOSAMS
Lago Villarrica	VILL TESTI-73	98.05	bulk sample	Poznan
Lago Villarrica	VILL1-TEST-II-49	156.8	bulk sample	NOSAMS
Lago Villarrica	VILL2B-I-102	279	bulk sample	NOSAMS
Lago Villarrica	VILL1C-I-105	390.45	bulk sample	NOSAMS
Lago Villarrica	VILL1C-II-56	448.7	bulk sample	NOSAMS
Lago Villarrica	VILL1D-I-66	616.6	bulk sample	NOSAMS
Lago Villarrica	VILL2D-II-57	770.25	bulk sample	NOSAMS
Lago Villarrica	VILL1E-I-12	779.4	bulk sample	NOSAMS
Lago Villarrica	*VILL 1EI-W*	*779.9*	*wood fragment*	*Poznan*
Lago Villarrica	VILL1E-II-32	890.9	bulk sample	NOSAMS
Lago Villarrica	VILL 1EII-93	951.9	bulk sample	Poznan
Lago Villarrica	VILL1F-I-89	1039.4	bulk sample	NOSAMS
Lago Villarrica	VILL1G-I-7	1196.45	bulk sample	NOSAMS
Lago Villarrica	VILL 1GII-93	1374.55	bulk sample	Poznan
Laguna Parrillar	PARSCI-0	0.5	bulk sample	NOSAMS
Laguna Parrillar	PARSCIII-21	21.5	bulk sample	NOSAMS
Laguna Parrillar	PAR1A-I-46	55	bulk sample	NOSAMS
Laguna Parrillar	PAR1A-I-65	74	bulk sample	NOSAMS
Laguna Parrillar	PAR1A-I-83	92	bulk sample	NOSAMS
Laguna Parrillar	PAR1A-II-29	130.2	bulk sample	NOSAMS
Laguna Parrillar	PAR1A-II-90	191.2	bulk sample	NOSAMS
Laguna Parrillar	PAR1A-III-94	290.3	bulk sample	NOSAMS
Laguna Parrillar	PAR1B-II-41	548.6	bulk sample	NOSAMS
Laguna Parrillar	PAR1B-III-bottom	694.6	bulk sample	NOSAMS

interpreted the results. The samples for this analysis were taken every 20 cm. They were oxidised using hydrogen peroxide (Renberg, 1990) and were spiked with polystyrene microspheres (concentration: 6.79 x 10^6 ml^{-1}) to allow for quantitative analysis (Battarbee and Kneen, 1982). Frustules were mounted in Naphrax® medium. Transects were scanned at a magnification of 10 x 100 x with an, Olympus BX 51 light microscope and a Zeiss Axioplan II light microscope. A minimum of 400 valves was counted per sample. Cluster analysis, constrained by sample depth, was performed on the relative diatom abundances using the program CONISS (Constrained Incremental Sum of Squares) (Grimm, 1987). Diatom data were analyzed and plotted using Tilia 2.0b4 (Grimm, 1991-1993) and Tilia Graph View 2.0.2 (Grimm, 2004).

III.2.19. AMS Radiocarbon Dating and Age Modelling

A good age control of the sediment core is necessary to allow comparisons and correlations on a local, regional and global scale. Radiocarbon dating (^{14}C) is one of the most widely used radiometric dating methods available. Lake sediments usually contain a certain amount of organic carbon in the form of terrestrial or aquatic plant and/or animal debris and are therefore suitable for radiocarbon dating. Because of the large variety of different deposits constituting lake sediment a large number of unknown factors will influence the resulting radiocarbon age, especially when it was obtained on bulk sediment (Björck and Wohlfarth, 2001). Lake-water composition, in particular the isotopic ratio of the dissolved carbon in the water, is sometimes also a limiting factor on the accuracy of the radiocarbon age (Olsson, 1991). It is therefore very important to know as much as possible about the depositional environment and the post-depositional processes, which may have affected the radiocarbon sample, when interpreting its results.

All radiocarbon dates were obtained by AMS (Accelerator Mass Spectrometry), most of them on the total organic content of bulk sediment samples since hardly any macrofossils or macro-remains were present. In Lago Villarrica two pieces of wood were found in the sediment. They were sent to a lab for radiocarbon dating together with a bulk sample of the same depth to determine which processes might have affected age results of the bulk samples (Table III-2). A surface sample was sent to determine how many years the radiocarbon age would differ from the present (age 0 or -60 cal a BP). A first series of samples was analysed at Poznan Radiocarbon laboratory in Poland (Czernik and Goslar, 2001). A second group was analysed at NOSAMS (National Ocean Sciences Accelerator Mass Spectrometry Facility) in Woods Hole USA (Table III-2).

Calibration of radiocarbon ages to calendar ages was performed using Oxcal v4.1 (Bronk Ramsey, 2009) using the ShCal04 southern hemisphere calibration curve (McCormac et al., 2004) for the Holocene and the IntCal04 calibration curve (Reimer et al., 2004) for the ages stretching beyond this time frame. Age models of these radiocarbon sequences were constructed using Blaauw's (2010) method. For both lakes alternative methods were used to determine whether or not the bulk radiocarbon samples suffer from contamination from old organic material washed in from the catchment. In both cases, this was tested using the tephras present in the cores and comparing the obtained ages for these volcanic ashes with ages of the same ashes in other locations in other core studies by colleagues or found in literature.

References

Auer, V., 1974. The isorhythmicity subsequent to the Fuego-Patagonian and Fennoscandian ocean transgressions of the latest glaciation. *Annales Academiae Scientiarum Fennicae III, Geologica-Geographica*, **115**: 1-188.

Banerjee, S.K. and Mellema, J.P., 1974. A new method for the determination of paleointensity from the A.R.M. properties of rocks. *Earth and Planetary Science Letters*, **23**(2): 177-184.

Battarbee, R.W., Jones, V.J., Flower, R.J., Cameron, N.G., Bennion, H., Carvalho, L. and Juggins, S., 2001. Diatoms. In: J.P. Smol, H.J.B. Birks and W.M. Last (Editors), *Tracking Environmental Change Using Lake Sediments. Volume 3: Terrestrial, Algal, and Siliceous Indicators.* Kluwer Academic Publishers, Dordrecht, the Netherlands, pp. 155-202.

Battarbee, R.W. and Kneen, M., 1982. The use of electronically counted microspheres in absolute diatom analysis. *Limnology and Oceanography*, **27**: 184-188.

Beierle, B. and Bond, J., 2002. Density-induced settling of tephra through organic lake sediments. *Journal of Paleolimnology*, **28**: 433-440.

Bengtsson, L. and Enell, M., 1986. Chemical analysis. In: B.E. Berglund (Editor), *Handbook of Holocene Palaeoecology and Palaeohydrology.* John Wiley & Sons Ldt., Chichester, pp. 423-451.

Bennett, K.D. and Willis, K.J., 2001. Pollen. In: J.P. Smol, H.J.B. Birks and W.M. Last (Editors), *Tracking Environmental Change Using Lake Sediments. Volume 3: Terrestrial, Algal and Siliceous Indicators.* Kluwer Academic Publishers, Dordrecht, The Netherlands, pp. 5-32.

Bertrand, S., Boes, X., Castiaux, J., Charlet, F., Urrutia, R., Espinoza, C., Lepoint, G., Charlier, B. and Fagel, N., 2005. Temporal evolution of sediment supply in Lago Puyehue (Southern Chile) during the last 600 yr and its climatic significance. *Quaternary Research*, **64**(2): 163-175.

Bertrand, S., Charlet, F., Charlier, B., Renson, V. and Fagel, N., 2008. Climate variability of Southern Chile since the Last Glacial Maximum: a continuous sedimentological record from Lago Puyehue (40°S). *Journal of Paleolimnology*, **39**: 179-195.

Björck, S. and Wohlfarth, B., 2001. 14C chronostratigraphic techniques in paleolimnology. In: W.M. Last and J.P. Smol (Editors), *Tracking Environmental Change Using Lake Sediments. Volume 1: Basin Analysis, Coring and Chronological Techniques.* Kluwer Academic Publishers, Dordrecht, The Netherlands, pp. 205-245.

Blaauw, M., 2010. Methods and code for `classical' age-modelling of radiocarbon sequences. *Quaternary Geochronology*, **5**(5): 512-518.

Blaga, C., Reichart, G.-J., Heiri, O. and Sinninghe Damsté, J., 2009. Tetraether membrane lipid distributions in water-column particulate matter and sediments: a study of 47 European lakes along a north–south transect. *Journal of Paleolimnology*, **41**(3): 523-540.

Blaga, C.I., Reichart, G.-J., Schouten, S., Lotter, A.F., Werne, J.P., Kosten, S., Mazzeo, N., Lacerot, G. and Sinninghe Damsté, J.S., 2010. Branched glycerol dialkyl glycerol tetraethers in lake sediments: Can they be used as temperature and pH proxies? *Organic Geochemistry*, **41**(11): 1225-1234.

Blockley, S.P.E., Pyne-O'Donnell, S.D.F., Lowe, J.J., Matthews, I.P., Stone, A., Pollard, A.M., Turney, C.S.M. and Molyneux, E.G., 2005. A new and less destructive laboratory procedure for the physical separation of distal glass tephra shards from sediments. *Quaternary Science Reviews*, **24**(16-17): 1952-1960.

Blott, S.J. and Pye, K., 2001. GRADISTAT: A grain size distribution and statistics package for the analysis of unconsolidated sediments. *Earth Surface Processes and Landforms*, **26**(11): 1237-1248.

Boehlke, J.K. and Coplen, T., 1995. Reference and intercomparison materials for stable isotopes of light elements. *International Atomic Energy Agency, Vienna, IAEA TECDOC*, **825**: 51-66.

Brachfeld, S.A., Kissel, C., Laj, C. and Mazaud, A., 2004. Behavior of u-channels during acquisition and demagnetization of remanence: implications for paleomagnetic and rock magnetic measurements. *Physics of the Earth and Planetary Interiors*, **145**(1-4): 1-8.

Brindley, G.W. and Brown, G., 1980. *Crystal structures of clay minerals and their x-ray identification.* Mineralogical Society Monograph, 5, London, 495 pp.

Bronk Ramsey, C., 2009. Bayesian analysis of radiocarbon dates. *Radiocarbon*, **51**(1): 337-360.

Campos, H., Steffen, W., Román, C., Zúñiga, L. and Agüero, G., 1983. Limnological studies in Lake Villarrica: Morphometric, physical, chemical, planktonical factors and primary productivity. *Archiv für Hydrobiologie Supplement*, **65**(4): 371-406.

Channell, J.E.T., Hodell, D.A. and Lehman, B., 1997. Relative geomagnetic paleointensity and d18O at ODP Site 983 (Gardar Drift, North Atlantic) since 350 ka. *Earth and Planetary Science Letters*, **153**: 103-118.

Charlet, F., Chapron, E., De Batist, M., Pino, M. and Urrutia, R., 2008. Seismic stratigraphy of Lago Puyehue (Chilean Lake District): new views on its deglacial and Holocene evolution. *Journal of Paleolimnology*, **39**: 163-177.

Cook, H.E., Johnson, P.D., Matti, J.C. and Zemmels, I., 1975. Methods of sample preparation and x-ray diffraction data analysis, x-ray mineralogy laboratory. In: A.G. Kaneps (Editor), *Initial reports of the DSDP*, Washington DC, pp. 997-1007.

Cooper, M.C., 1997. The use of digital image analysis in the study of laminated sediments. *Journal of Paleolimnology*, **19**(1): 33-40.

Coplen, T.B., Brand, W.A., Gehre, M., Groning, M., Meijer, H.A.J., Toman, B. and Verkouteren, R.M., 2006a. After two decades a second anchor for the VPDB d13C scale. *Rapid Communications in Mass Spectrometry.*

Coplen, T.B., Brand, W.A., Gehre, M., Groning, M., Meijer, H.A.J., Toman, B. and Verkouteren, R.M., 2006b. New guidelines for delta 13C measurements. *Analytical Chemistry*, **78**(7): 2439-2441.

Czernik, T. and Goslar, T., 2001. Preparation of graphite targets in the Gwilice radiocarbon laboratory for AMS 14C dating. *Radiocarbon*, **43**(2): 283-291.

Dean, W.E.J., 1974. Determination of carbonate and organic matter in calcareous sediments and sedimentary rocks by loss on ignition: comparison with other methods. *Journal of Sedimentary Petrology*, **44**(1): 242-248.

DeRosa, M. and Gambacorta, A., 1988. The lipids of archaeabacteria. *Progress in Lipid Research*, **27**: 153-175.

Eyles, N. and Mullins, H.T., 1997. Seismic-stratigraphy of Shuswap Lake, British Columbia, Canada. *Sedimentary Geology*, **109**: 283-303.

Faegri, K. and Iversen, J., 1989. *Textbook of pollen analysis.* John Wiley & Sons, London, United Kingdom, 327 pp.

Finckh, P., Kelts, K. and Lambert, A., 1984. Seismic stratigraphy and bedrock forms in perialpine lakes. *Geological Society of America Bulletin*, **95**: 1118-1128.

Folk, R.L. and Ward, W., 1957. Brazos river bar: A study in the significance of grain size parameters. *Journal of Sedimentary Petrology*, **27**: 3-26.

Glew, J.R., Smol, J.P. and Last, W.M., 2001. Sediment core collection and extrusion. In: W.M. Last and J.P. Smol (Editors), *Tracking Environmental Change Using Lake Sediments. Volume 1: Basin Analysis, Coring, and Chronological Techniques.* Kluwer Academic Publishers, Dordrecht, The Netherlands, pp. 73-105.

Grimm, E.C., 1987. CONISS: a FORTRAN 77 program for stratigraphically constrained cluster analysis by the method of incremental sum of squares.

Computer and Geosciences, **13**: 13-35.
Grimm, E.C., 1991-1993. *Tilia 2.0 Version b.4 and TiliaGraph.* Ilinois State Museum, Springfield, Ilinois.
Grimm, E.C., 2004. *TGView Version 2.0.2.* Illinois State Museum, Springfield, Ilinois.
Gunn, D.E. and Best, A.I., 1998. A new automated nondestructive system for high resolution multi-sensor core logging of open sediment cores. *Geo-Marine Letters*, **18**(1): 70-77.
Guyodo, Y., Channell, J.E.T. and Thomas, R.G., 2002. Deconvolution of u-channel paleomagnetic data near geomagnetic reversals and short events. *Geophysical Research Letters*, **29**(17): 1845.
Haberle, S.G. and Lumley, S.H., 1998. Age and origin of tephras recorded in postglacial lake sediments to the west of the southern Andes, 44°S to 47°S. *Journal of Volcanology and Geothermal Research*, **84**(3-4): 239-256.
Hayward, C.L., in review. High spatial resolution electron probe microanalysis of tephras and melt inclusions without beam-induced chemical modification. *The Holocene*.
Heiri, O., Lotter, A.F. and Lemcke, G., 2001. Loss on ignition as a method for estimating organic and carbonate content in sediments: reproducibility and comparability of results. *Journal of Paleolimnology*, **25**(1): 101-110.
Hopmans, E.C., Weijers, J.W.H., Schefuß, E., Herfort, L., Sinninghe Damsté, J.S. and Schouten, S., 2004. A novel proxy for terrestrial organic matter in sediments based on branched and isoprenoid tetraether lipids. *Earth and Planetary Science Letters*, **224**(1-2): 107-116.
Hu, F.S. and Shemesh, A., 2003. A biogenic silica d18O record of climatic change during the last glacial-interglacial transition in southwestern Alaska. *Quaternary Research*, **59**: 379-385.
Hunt, J. and Hill, P.G., 1993. Tephra geochemistry: a discussion of some persistent analytical problems. *The Holocene*, **3**(3): 271-278.
Jacobs, J.A., 1994. *Reversals of the Earth's Magnetic Field*. Cambridge University Press, Cambridge, 346 pp.
Jansen, J.H.F., Van der Gaast, S.J., Koster, B. and Vaars, A.J., 1998. CORTEX, a shipboard XRF-scanner for element analyses in split sediment cores. Marine *Geology*, **151**(1-4): 143-153.
Jenkins, R. and De Vries, J.L., 1970. *Practical X-ray Spectrometry*. MacMillan, London.
Kilian, R., Hohner, M., Biester, H., Wallrabe-Adams, H.J. and Stern, C.R., 2003. Holocene peat and lake sediment tephra record from the southernmost Chilean Andes (53-55° S). *Revista geológica de Chile*, **30**(1): 23-37.
King, J., Banerjee, S.K., Marvin, J. and Özden, Ö., 1982a. A comparison of different magnetic methods for determining the relative grain size of magnetite in natural materials: some results from lake sediments. *Earth and Planetary Science Letters*, **59**(2): 404-419.
King, J. and Peck, J., 2001. Use of paleomagnetism in studies of lake sediments. In: W.M. Last and J.P. Smol (Editors), *Tracking Environmental Change Using Lake Sediments. Volume 1: Basin Analysis, Coring and Chronological Techniques.* Kluwer Academic Publishers, Dordrecht, The Netherlands, pp. 371-389.
King, J.W., Banerjee, S.K., Marvin, J. and Özdemir, Ö., 1982b. A comparison of different magnetic methods for determining the relative grain size of magnetite in natural materials: some results from lake sediments. *Earth and Planetary Science Letters*, **59:** 404-419.
Kirschvink, J.L., 1980. The least-squares line and plane and the analysis of paleomagnetic data. Geophysical Journal of the Royal Astronomical Society, **62**(3): 699-718.
Krinsley, D.H. and Doornkamp, J.C., 1973. *Atlas of quartz sand surface textures.* Cambridge University Press, Cambridge, 91 pp.
Last, W.M., 2001. Mineralogical analysis of lake sediments. In: W.M. Last and J.P.

Smol (Editors), *Tracking Environmental Change Using Lake Sediments. Volume 2: Physical and Geochemical Methods.* Kluwer Academic Publishers, Dordrecht, The Netherlands, pp. 143-187.

Levi, S. and Banerjee, S.K., 1976. On the possibility of obtaining relative paleointensities from lake sediments. *Earth and Planetary Science Letters*, **29**: 219-226.

Mahaney, W.C., 2002. *Atlas of sand grain surface textures and applications*. Oxford University Press, Oxford, England, 237 pp.

McCormac, F.G., Hogg, A.G., Blackwell, P.G., Buck, C.E., Higham, T.F.G. and Reimer, P.J., 2004. SHCal04 Southern Hemisphere calibration, 0-11.0 cal kyr BP. *Radiocarbon*, **46**(3): 1087-1092.

Meyers, P.A., 1997. Organic geochemical proxies of paleoceanographic, paleolimnologic, and paleoclimatic processes. *Organic Geochemistry*, **27**(5-6): 213-250.

Meyers, P.A. and Lallier-Vergés, E., 1999. Lacustrine Sedimentary Organic Matter Records of Late Quaternary Paleoclimates. *Journal of Paleolimnology*, **21**(3): 345-372.

Meyers, P.A. and Teranes, J.L., 2001. Sediment organic matter. In: W.M. Last and J.P. Smol (Editors), *Tracking environmental change using lake sediments. Volume 2: Physical and geochemical methods.* Kluwer Academic Publishers, Dordrecht, The Netherlands, pp. 239-269.

Mitchum, R.M.J., Vai, P.R. and Sangree, J.B., 1977. Stratigraphic interpretation of seismic reflection patterns in depositional sequences In: C.E. Payton (Editor), *Seismic stratigraphy applications to the hydrocarbon exploration.* American Association of Petroleum Geologist, Tulsa Oklahoma, pp. 117-133.

Moore, D.M. and Reynolds, R.C.J., 1989. *X-ray diffraction and the identification and analysis of clay minerals*. Oxford University Press, Oxford, 332 pp.

Olsson, I., 1991. Accuracy and precision in sediment chronology. *Hydrobiologia*, **214**: 25-34.

Powers, L., Werne, J.P., Vanderwoude, A.J., Sinninghe Damsté, J.S., Hopmans, E.C. and Schouten, S., 2010. Applicability and calibration of the TEX86 paleothermometer in lakes. *Organic Geochemistry*, **41**(4): 404-413.

Powers, L.A., Werne, J.P., Johnson, T.C., Hopmans, E.C., Damsté, J.S.S. and Schouten, S., 2004. Crenarchaeotal membrane lipids in lake sediments: a new paleotemperature proxy for continental paleoclimate reconstruction. *Geology*, **32**: 613-616.

Reimer, P.J., Baillie, M.G.L., Bard, E., Bayliss, A., Beck, J.W., Bertrand, C.J.H., Blackwell, P.G., Buck, C.E., Burr, G.S., Cutler, K.B., Damon, P.E., Edwards, R.L., Fairbanks, R.G., Friedrich, M., Guilderson, T.P., Hogg, A.G., Hughen, K.A., Kromer, B., McCormac, G., Manning, S., Ramsey, C.B., Reimer, R.W., Remmele, S., Southon, J.R., Stuiver, M., Talamo, S., Taylor, F.W., van der Plicht, J. and Weyhenmeyer, C.E., 2004. IntCal04 terrestrial radiocarbon age calibration, 0-26 cal kyr BP. *Radiocarbon*, **46**(3): 1029-1058.

Renberg, I., 1990. A procedure for preparing large sets of diatom slides from sediment cores. *Journal of Paleolimnology*, **4**: 87-90.

Richter, T.O., Van Der Gaast, S., Koster, B., Vaars, A., Gieles, R., De Stigter, H.C., De Haas, H. and Van Weering, R.C.E., 2006. The Avaatech XRF Core Scanner: technical description and applications to NE Atlantic sediments. In: R.G. Rothwell (Editor), *New Techniques in Sediment Core Analysis.* Geological Society Special Publications, London, pp. 39-50.

Saarinen, T. and Petterson, G., 2001. Image analysis techniques. In: W.M. Last and J.P. Smol (Editors), *Tracking Environmental Change Using Lake Sediments. Volume 2: Physical and Geochemical methods.* Kluwer Academic Publishers, Dordrecht, The Netherlands, pp. 23-39.

Santisteban, J.I., Mediavilla, R., López-Pamo, E., Dabrio, C.J., Zapata, M.B.R.,

García, M.J.G., Castaño, S. and Martínez-Alfaro, P.E., 2004. Loss on ignition: a qualitative or quantitative method for organic matter and carbonate mineral content in sediments? *Journal of Paleolimnology*, **32**(3): 287-299.

Sarnthein, M., Kennett, J.P., Allen, J.R.M., Beer, J., Grootes, P., Laj, C., McManus, J. and Ramesh, R., 2002. Decadal-to-millennial-scale climate variability--chronology and mechanisms: summary and recommendations. *Quaternary Science Reviews*, **21**(10): 1121-1128.

Scholz, C.A., 2001. Applications of seismic sequence stratigraphy in lacustrine basins. In: W.M. Last and J.P. Smol (Editors), *Tracking Environmental Change Using Lake Sediments. Volume 1: Basin Analysis, Coring and Chronological Techniques.* Kluwer Academic Publishers, Dordrecht, The Netherlands, pp. 7-22.

Schouten, S., Hopmans, E.C., Schefuß, E. and Sinninghe Damsté, J.S., 2002. Distributional variations in marine crenarchaeotal membrane lipids: a new tool for reconstructing ancient sea water temperatures? *Earth and Planetary Science Letters*, **204**(1-2): 265-274.

Schouten, S., Huguet, C., Hopmans, E.C. and Sinninghe Damsté, J.S., 2007. Improved analytical methodology of the TEX86 paleothermometry by high performance liquid chromatography /atmospheric pressure chemical ionization-mass spectrometry. *Analytical Chemistry*, **79**: 2940-2944.

Snowball, I. and Muscheler, R., 2007. Palaeomagnetic intensity data: an Achilles heel of solar activity reconstructions. *The Holocene*, **17**(21): 851-859.

Snowball, I. and Sandgren, P., 2002. Geomagnetic field variations in northern Sweden during the Holocene quantified from varved lake sediments and their implications for cosmogenic nuclide production rates. *The Holocene*, **12**(5): 517-530.

Snowball, I., Zillén, L., Ojala, A., Saarinen, T. and Sandgren, P., 2007. FENNOSTACK and FENNORPIS: Varve dated Holocene palaeomagnetic secular variation and relative palaeointensity stacks for Fennoscandia. *Earth and Planetary Science Letters*, **255**(1-2): 106-116.

St-Onge, G., Stoner, J.S. and Hillaire-Marcel, C., 2003. Holocene paleomagnetic records from the St. Lawrence Estuary, eastern Canada: centennial- to millennial-scale geomagnetic modulation of cosmogenic isotopes. *Earth and Planetary Science Letters*, **209**(1-2): 113-130.

Stern, C., 2008. Holocene tephrochronology record of large explosive eruptions in the southernmost Patagonian Andes. *Bulletin of Volcanology*, **70**(4): 435-454.

Sweatman, T.R. and Long, J.V.P., 1969. Quantitative electron-probe microanalysis of rock-forming minerals. *Journal of Petrology*, **10**(2): 332-379.

Talbot, M.R., 2001. Nitrogen isotopes in palaeolimnology. In: W.M. Last and J.P. Smol (Editors), *Tracking environmental change using lake sediments. Volume 2: Physical and geochemical methods.* Kluwer Academic Publishers, Dordrecht, The Netherlands, pp. 401-439.

Tauxe, L., 1993. Sedimentary Records of Relative Paleointensity of the Geomagnetic-Field - Theory and Practice. *Reviews of Geophysics*, **31**(3): 319-354.

Tauxe, L., 1998. *Paleomagnetic principles and practice*. Kluwer Academic Publishers, Dordrecht, 299 pp.

Tierney, J.E. and Russell, J.M., 2009. Distributions of branched GDGTs in a tropical lake system: Implications for lacustrine application of the MBT/CBT paleoproxy. *Organic Geochemistry*, **40**(9): 1032-1036.

Tierney, J.E., Russell, J.M., Eggermont, H., Hopmans, E.C., Verschuren, D. and Sinninghe Damsté, J.S., 2010. Environmental controls on branched tetraether lipid distributions in tropical East African lake sediments. *Geochimica Et Cosmochimica Acta*, **74**(17): 4902-4918.

Uda, I., Sugai, I., Itoh, I.H., and Itoh, T., 2001. Variation on molecular species of polar lipids from Thermoplasma acidophilum depends on growth temperature.

Lipids, **35**: 103–105.
Van Rensbergen, P., De Batist, M., Beck, C. and Chapron, E., 1999. High-resolution seismic stratigraphy of glacial to interglacial fill of a deep glaciogenic lake: Lake Le Bourget, Northwestern Alps, France. ***S**edimentary Geology*, **128**: 99-129.
Van Rensbergen, P., De Batist, M. and Manalt, F., 1998. High-resolution seismic stratigraphy of late Quaternary fill of Lake Annecy (northwestern Alps): evolution from glacial to interglacial sedimentary processes. *Sedimentary Geology*, **117**: 71-96.
Verardo, D.J., Froelich, P.N. and McIntyre, A., 1990. Determination of organic carbon and nitrogen in marine sediments using the Carlo Erba NA-1500 Analyzer. *Deep-Sea Research*, **37**(1): 157-165.
von Grafenstein, U., Erlenkeuser, H., Brauer, A., Jouzel, J. and Johnsen, S.J., 1999. A mid-European decadal isotope-climate record from 15,500 to 5000 years BP. *Science*, **284**(5420): 1654-1657.
Weber, M.E., Niessen, F., Kuhn, G. and Wiedicke, M., 1997. Calibration and application of marine sedimentary physical properties using a multi-sensor core logger. *Marine Geology*, **136**: 151-172.
Weeks, R., Laj, C., Endignoux, L., Fuller, M., Roberts, A., Manganne, R., Blanchard, E. and Goree, W., 1993. Improvements in long-core measurement techniques: applications in palaeomagnetism and palaeoceanography. *Geophysical Journal International*, **114**: 651-662.
Weijers, J.W.H., Panoto, E., van Bleijswijk, J., Schouten, S., Balk, M., Stams, A.J.M., Rijpstra, W.I.C. and Sinninghe Damsté, J.S., 2009. Constraints on the biological source(s) of the orphan branched tetraether membrane lipids. *Geomicrobiology Journal*, **26**: 402–414.
Weijers, J.W.H., Schouten, S., Spaargaren, O.C. and Sinninghe Damsté, J.S., 2006. Occurrence and distribution of tetraether membrane lipids in soils: Implications for the use of the TEX86 proxy and the BIT index. *Organic Geochemistry*, **37**: 1680–1693.
Weijers, J.W.H., Schouten, S., van den Donker, J.C., Hopmans, E.C. and Sinninghe Damsté, J.S., 2007. Environmental controls on bacterial tetraether membrane lipid distribution in soils. *Geochimica Et Cosmochimica Acta*, **71**(3): 703-713.
Weltje, G.J. and Tjallingii, R., 2008. Calibration of XRF core scanners for quantitative geochemical logging of sediment cores: Theory and application. *Earth and Planetary Science Letters*, **274**: 423-438.
Wuchter, C., Schouten, S., Coolen, M.J.L. and Sinninghe Damsté, J.S., 2004. Temperature-dependent variation in the distribution of tetraether membrane lipids of marine Crenarchaeota: implications for TEX86 paleothermometry. *Paleoceanography*, **19**: PA4028.
Zolitschka, B., Mingram, J., van der Gaast, S., Jansen, F.J.H. and Naumann, R., 2001. Sediment logging techniques. In: W.M. Last and J.P. Smol (Editors), *Tracking Environmental Change Using Lake Sediments. Volume 1: Basin Analysis, Coring, and Chronological Techniques.* Kluwer Academic Publishers, Dordrecht, The Netherlands, pp. 137-153.

IV. Low-resolution Climate Variability through Space and Time

Variability is the law of life. One of the variables that is having the most impact on the environment now, in the past and in the future is climate. Understanding climate has proven to be challenging. Taking a step back in order not to get lost in many, tiny details, observing climate variability on a low-resolution time scale might add towards a better understanding of the climate system.

High-resolution reflection seismic surveying is a very powerful technique for lake-basin studies as it allows a non-destructive and non-invasive, quasi three-dimensional exploration of the whole sedimentary infill. It usually allows an understanding of the lake-basin evolution on much larger time-scales and with a large spatial coverage than what can be achieved by sediment-core studies. The basin evolution of four lakes in the Chilean Lake District and of Lac d'Armor, a lake in the Kerguelen Archipelago, are discussed in this chapter by using bathymetric and reflection-seismic techniques. With these techniques changes in the physical stratigraphy of the sediment infill can be determined. Such changes point toward changes in how the sediment accumulated in the lake, thus changes in the limnology, terrigeneous influx, dispersion, ... Most of these accumulation changes are controlled by climate. Consequently climate variability on a millenial or larger time scale can be reconstructed for these regions, while assessing at the same time the influences of these climatic changes on the complete lake system.

IV.1. The Chilean Lake District

IV.1.1. Glacigenic-Lake Seismic Stratigraphy

Seismic surveys of glacigenic lakes over the last decades have shown a striking resemblance in seismic stratigraphy in different lakes in diverse parts of the world. Their infill generally represents the same succession of seismic facies and thus of depositional processes. There is a strong similarity between the European (Alpine) (Girardclos et al., 2003; Girardclos et al., 2005; Van Rensbergen et al., 1999; Van Rensbergen et al., 1998) and North American lakes (Eyles et al., 2000; Eyles and Mullins, 1997; Lazorek et al., 2006; Mullins and Halfman, 2001) in the uppermost units, which were deposited during the Holocene and the very last phases of the last deglaciation, but this similarity is less clear for the basal units, which represent the glacial and ice-contact deposits. In virtually all of these lake basins the glaciers removed all previously deposited sediment during their maximum extension, causing the resulting infill to be not older than the Last Glacial Maximum. Therefore only two major unconformities are present in these basins: one between the acoustic basement and the glacial/ice-contact sediments and one between the latter unit and the overlying glaciolacustrine deposits (Figure IV-1).

The glacigenic lakes in the Chilean Lake District (39-42°S) seem to differ from this general model. Analysis of reflection seismic data from several glacigenic lakes in the Lake District illustrates that the Chilean lakes comprise more erosional unconformities than their Northern-Hemisphere counterparts. Above these unconformities the 'classic', Alpine post-deglaciation units are present as has been observed in Lago Puyehue by Charlet et al. (2008) and Heirman et al. (in press) and in Lago Villarrica by Lahousse (2008).

IV.1.2. Chilean Lake District Unconformity Sequence

Striking in the seismic stratigraphy of Lago Villarrica, Calafquén, Panguipulli and Riñihue is the existence of a sequence of erosional unconformities (more than two) in the western, shallower lake-basin lobes (Figure IV-2, Figure IV-3, Figure IV-4, Figure IV-5 and

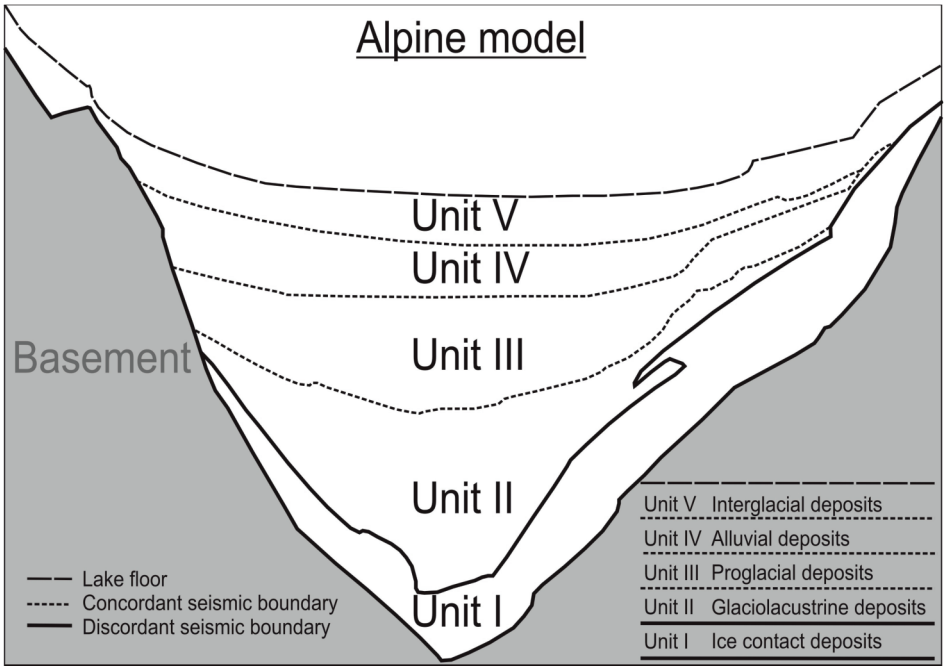

Figure IV-1: Model for the infill of European Alpine lakes (after Van Rensbergen et al., 1998)

Figure IV-6). These unconformities - sometimes exhibiting erosional relief of over 50 m - separate units that are acoustically sub-horizontally stratified, sometimes with an acoustically more chaotic unit in between them. Remarkably these lower stratified units are virtually undisturbed, except for some acoustic anomalies that can be interpreted as fluid-escape structures; no faulting or folding is observed.

Due to gas blanking, the seismic penetration is limited in the eastern and central parts of all lake basins, therefore preventing the study of the presence of this sequence of unconformities in those parts of the lakes. Fortunately, the western lake lobes have a good seismic penetration and reveal parallel running stories.

The unconformities only appear in specific parts of the lakes and have been imaged on only a couple of the seismic profiles. The lack of densely spaced survey lines, prevents the creation of a reliable grid and to properly map the extent and morphology of these unconformities.

The deepest unconformity (UC1) forms the boundary between the acoustic basement and the lake infill. In all the four lakes this acoustic basement exhibits a very irregular morphology. Above this boundary there is sometimes a facies of very chaotic seismic reflections. In Lago Calafquén and Lago Villarrica there is a
facies of parallel, horizontal reflections, which seem to be rather continuous (Stratified 1) (Figure IV-2 and Figure IV-4). This stratified facies is always covered by another group of chaotic seismic reflections. In Lago Riñihue only this chaotic facies is present, but the stratified facies is missing. Both unconformities, UC1 and UC2, are present in Lago Riñihue (Figure IV-6). In Lago Panguipulli the second unconformity (UC2) is absent (Figure IV-5).

The second unconformity (UC2), which

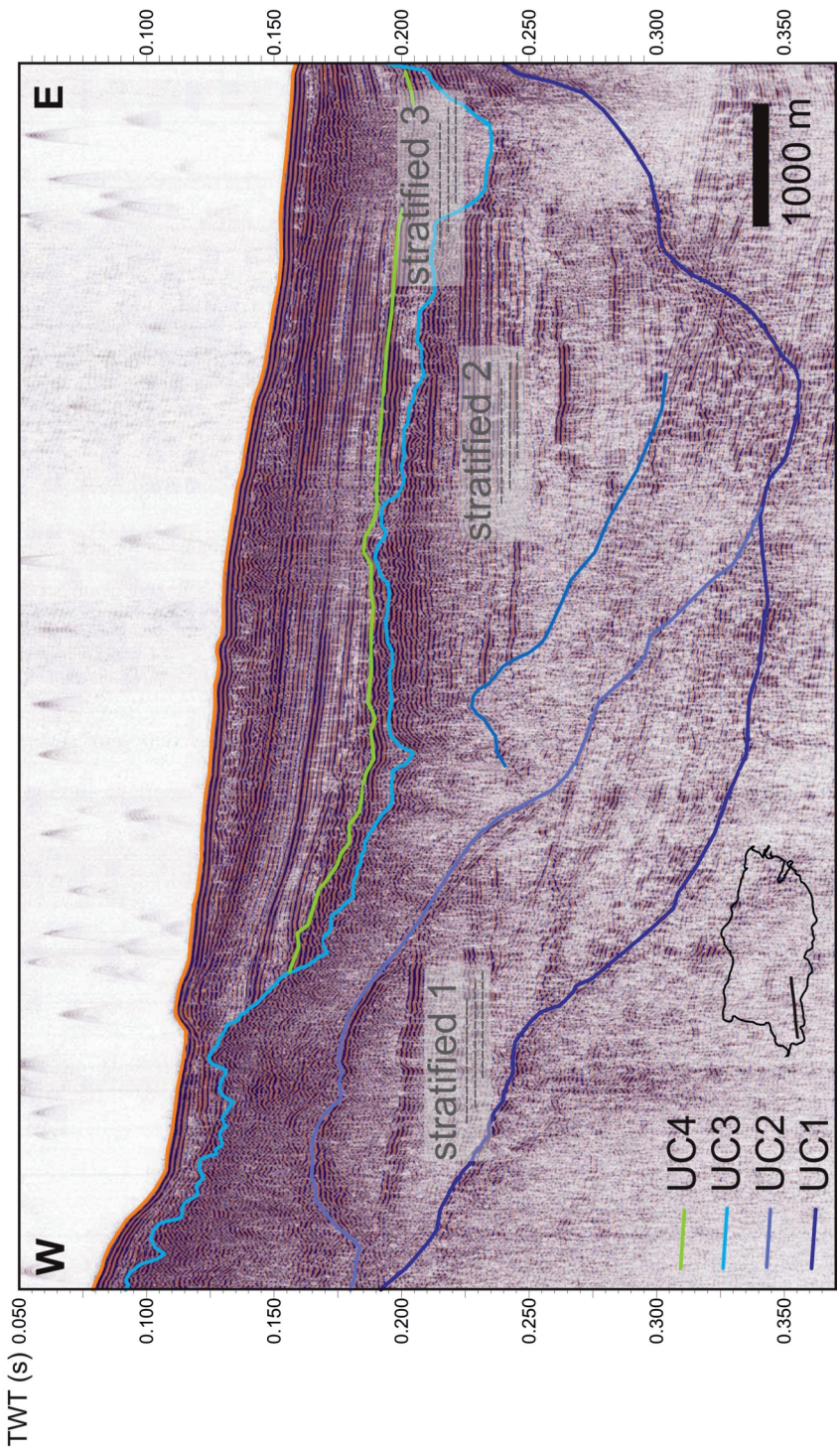

Figure IV-2: Seismic profile of Lago Villarrica

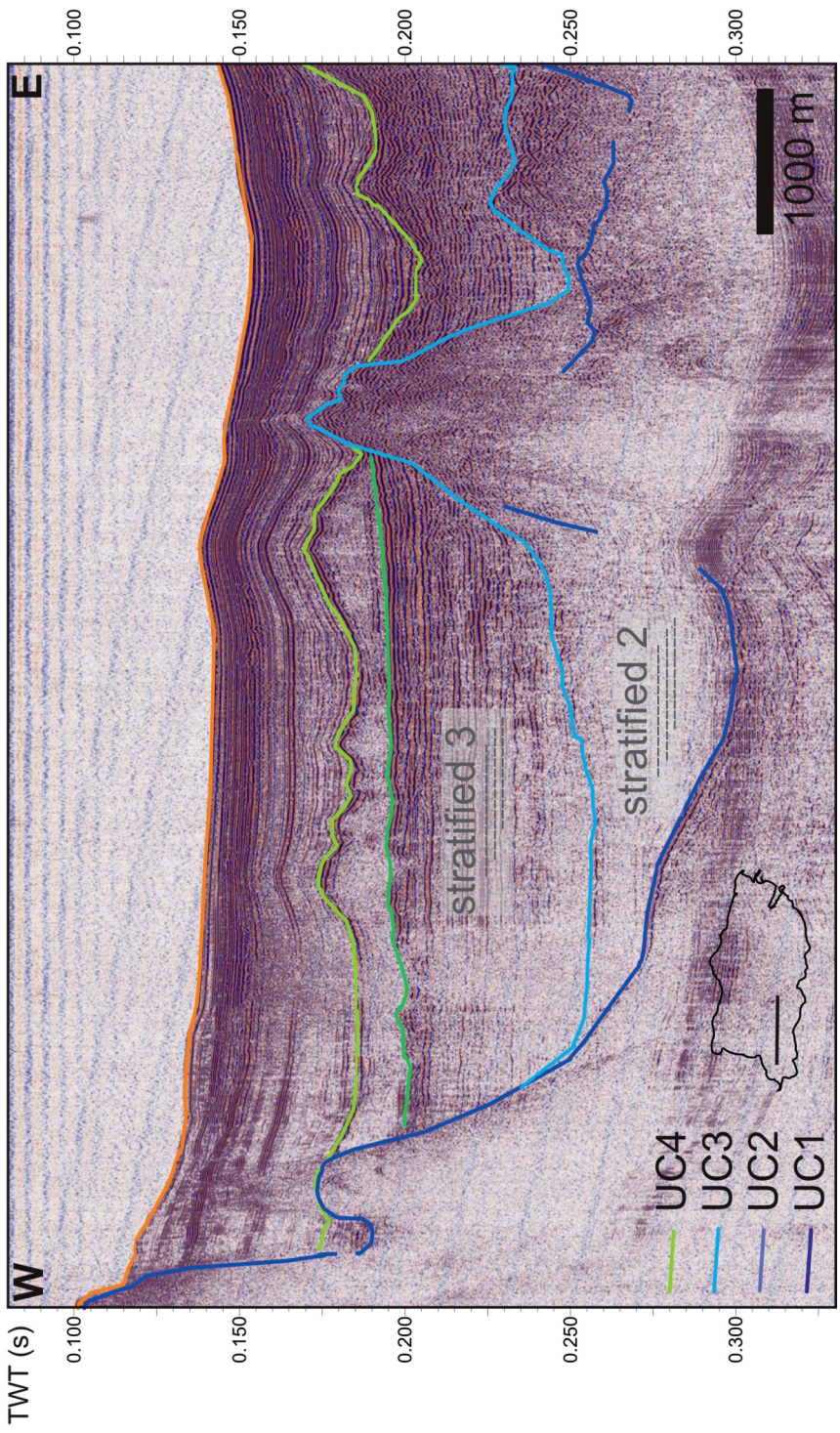

Figure IV-3: Seismic profile of Lago Villarrica

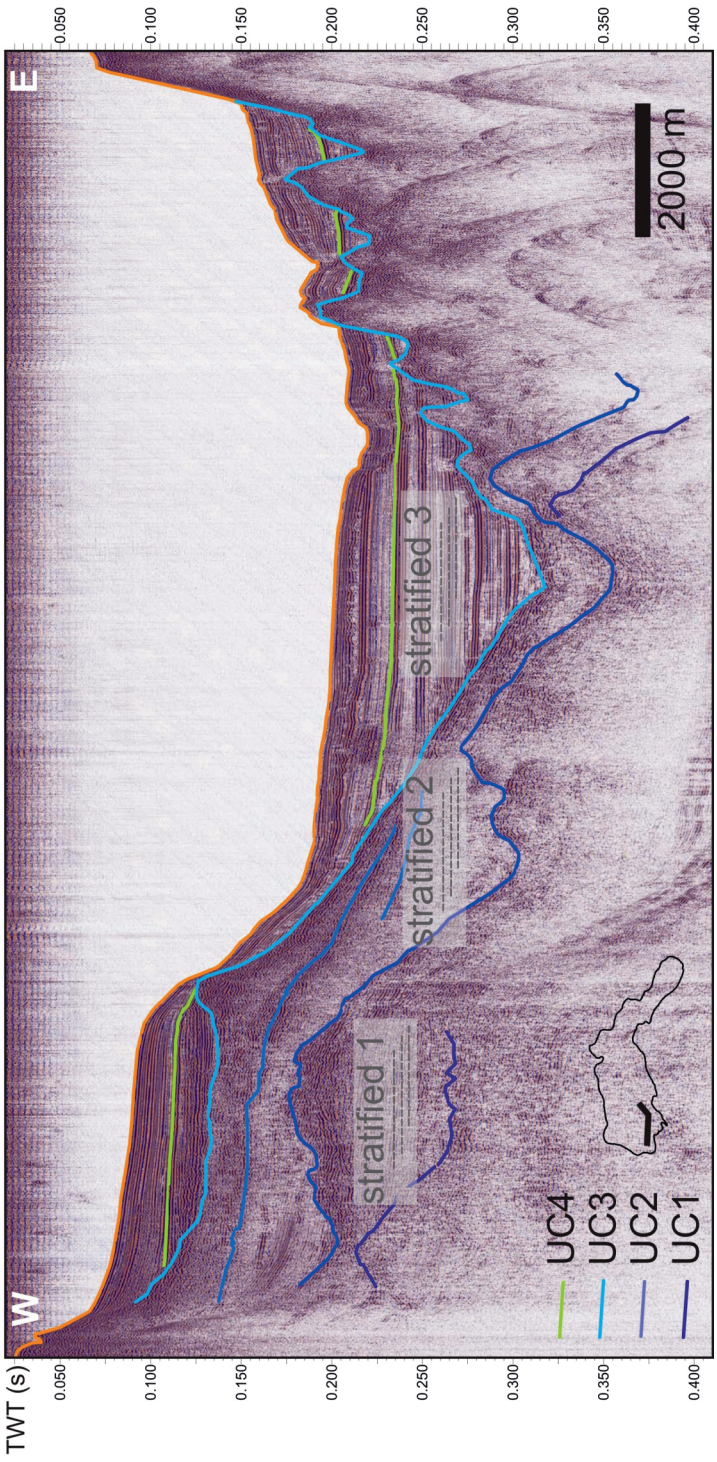

Figure IV-4: Seismic profile of Lago Calafquén

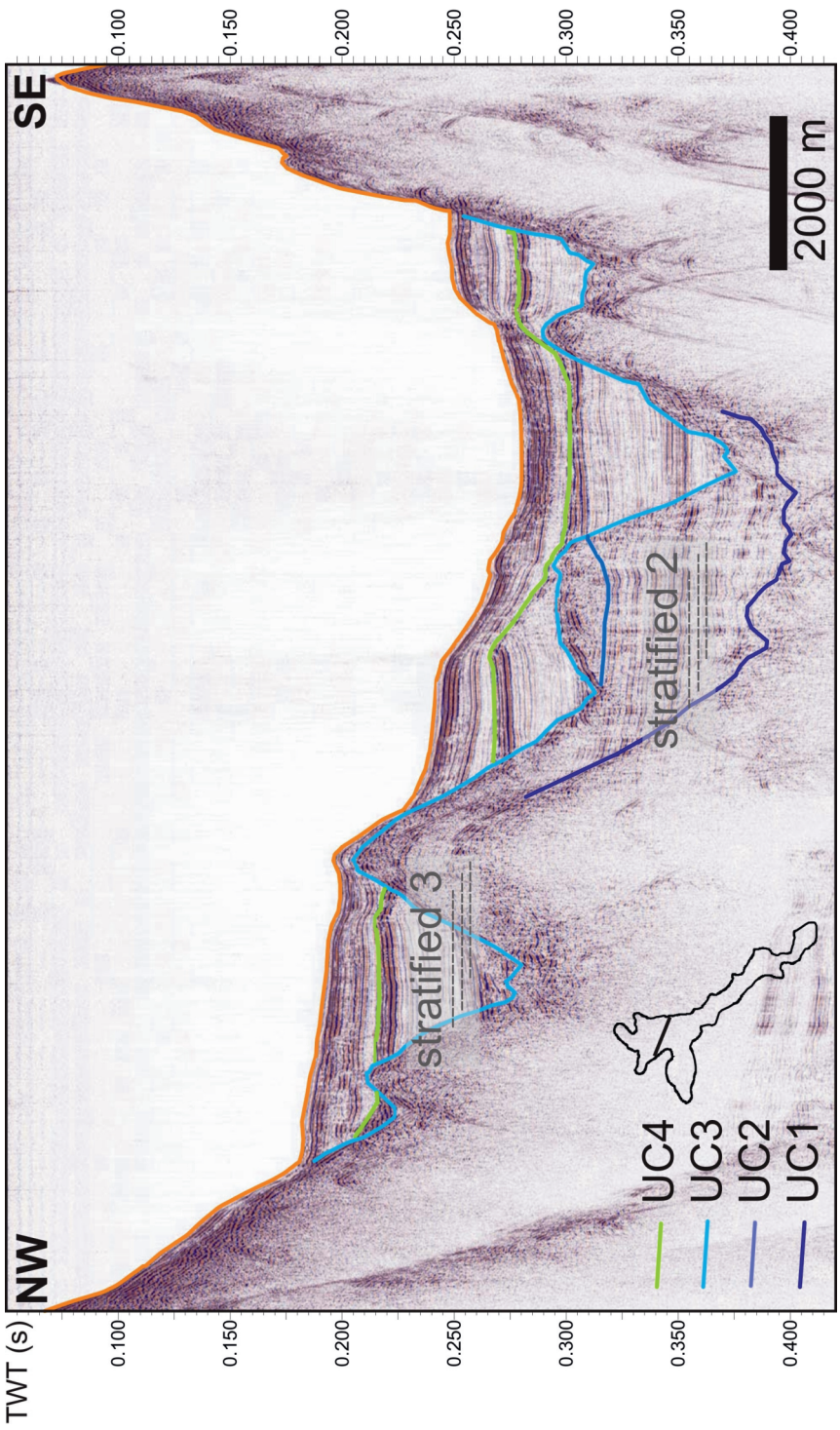

Figure IV-5: Seismic profile of Lago Panguipulli

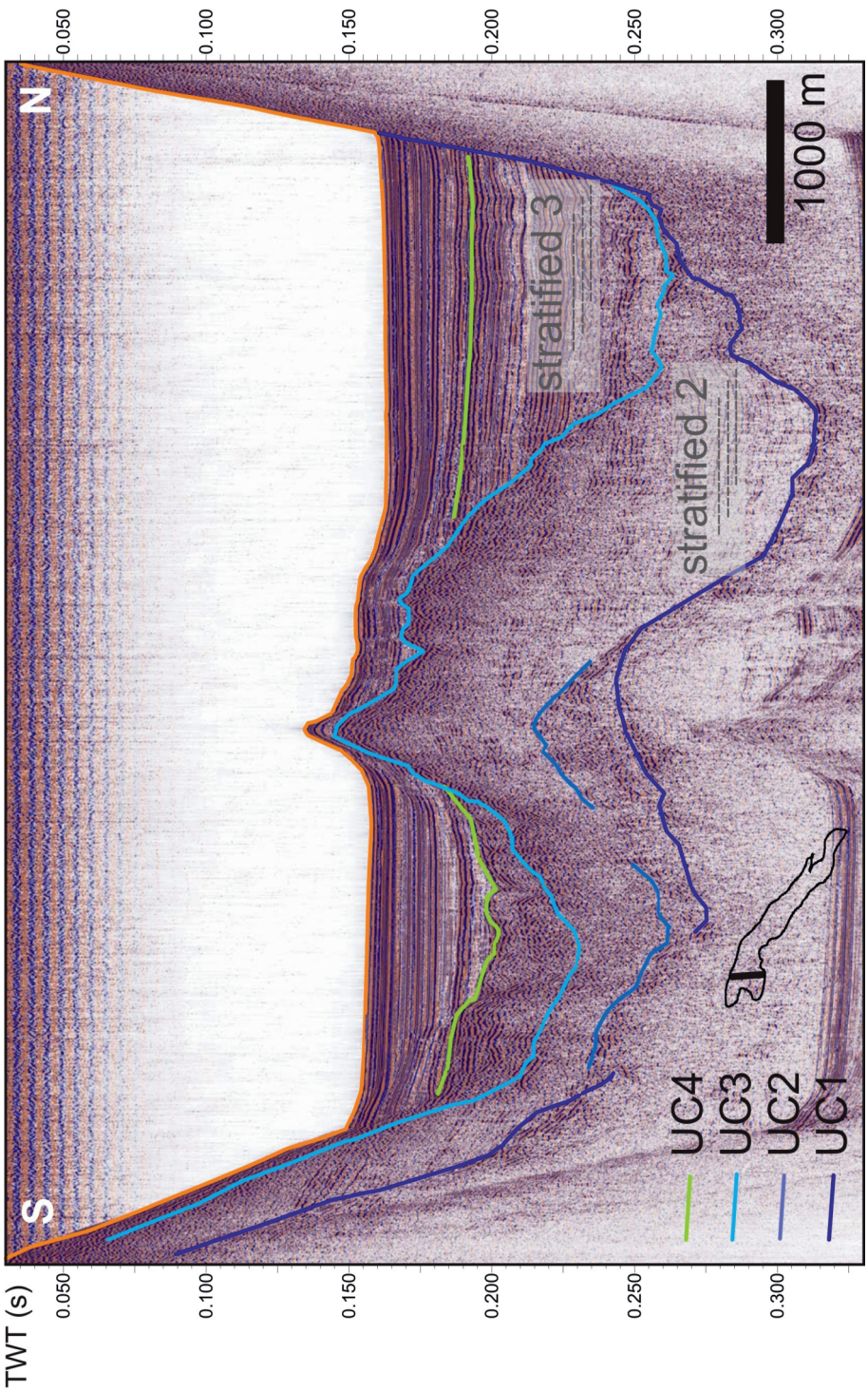

Figure IV-6: Seismic profile of Lago Riñihue

forms the boundary between this first stratified deposit and the one above also has a very irregular morphology. Again, there is a high density of chaotic reflections, and this chaotic facies is the most obvious between UC2 and UC3. All lakes, however, exhibit horizontally stratified reflections (Stratified 2) between these boundaries as well (Figure IV-2, Figure IV-3, Figure IV-4, Figure IV-5 and Figure IV-6).

The third unconformity (UC3) has an irregular morphology too. Just below this unconformity there is always the presence of chaotic reflections. Above UC3, however, the reflections are mostly parallel and continuous (Stratified 3) (Figure IV-3, Figure IV-4 and Figure IV-5), except for one area in Lago Riñihue (Figure IV-6) and Lago Villarrica (Figure IV-2). These reflections of this third stratified unit are all strong and continuous. The last unconformity (UC4), which forms the top boundary of the third stratified facies, has a rather smooth morphology (Figure IV-3, Figure IV-4 and Figure IV-5). The surface of the unconformity is almost parallel to the lake floor. The only exceptions to this, is in the areas where the chaotic reflections are present (Figure IV-3 and Figure IV-6).

IV.1.3. Origin of these Unconformities

The geology and geomorphology in the Chilean Lake District is the result of the combined action of three major processes: tectonics, volcanism and glacier activity. Although a volcanic origin of these sediments cannot totally be excluded considering the geodynamic setting of the region, the observed extensive, high-relief erosional surfaces are - however - most likely created by glacial erosion. Their presence in the seismic stratigraphy therefore suggests that the lake-basin infill has recorded multiple periods of glacier advance and retreat.

Although the glaciological and/or climatological process behind this glacier behaviour is unclear, we postulate that these stratified facies probably represent lacustrine deposits. These sediments either accumulated in a proglacial lake, far enough from the glacier snout not to be internally affected by it, or during a period of complete glacial retreat. The most important indication, however, is that with each advance the glacier had less erosional force and probably less time to be erosive, since less sediment was excavated and more stratified deposits were just overridden. The decreasing erosional force can also be deduced from the morphology of the unconformities. UC1 and UC2 exhibit a strong and very irregular morphology, clearly indicating an advancing glacier with a high erosion potential. UC4, on the other hand, is almost parallel to the modern lake floor. During the creation of this last unconformity, the glacier must have been almost unable to erode the sediment it advanced over.

IV.1.4. Palaeoclimatic Implications

The stratified facies inbetween the unconformities probably represent deposits from a previous interstadial period or a period of glacier retreat during the Last Glaciation. No interglacial-age deposits have been observed and documented near the lakes (Laugenie 1982). All geomorphological studies in the area indicate that the previous glaciation was more extensive than the last one, because the moraines of the previous glaciation in the Lake District are located further to the west (Andersen et al., 1999; Bentley, 1996; Clayton et al., 1997; Laugenie, 1982; Porter, 1981) (Figure II-9). A more extensive glaciation, like the penultimate glactiation in the Chilean Lake District, probably produced a glacier with a large erosional force, which would have been able to remove all previously deposited sediments from the lake basins. The glacier extent was also likely to have been more long-lasting, giving the glacier enough time to remove all

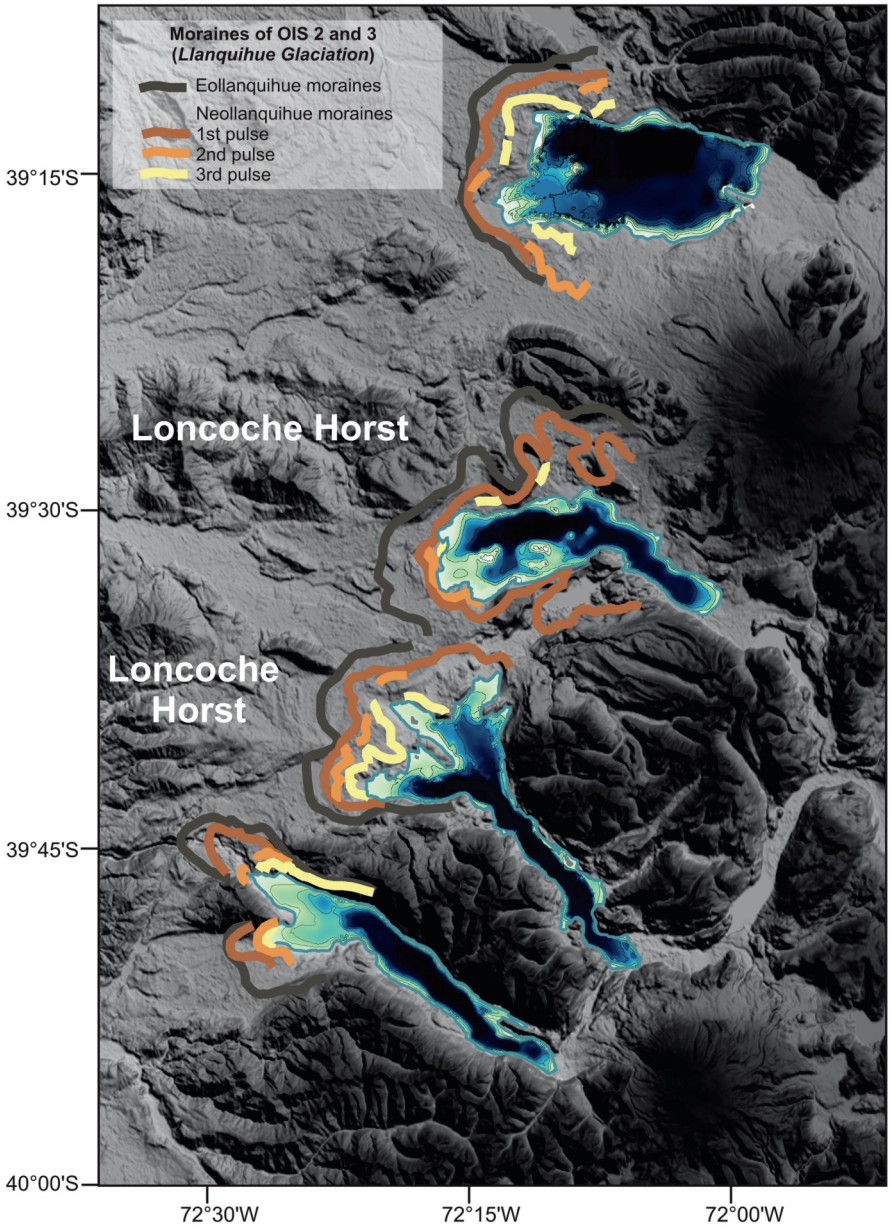

Figure IV-7: Location of the Oxygen Isotope Stage 2 and 3 moraines around the western shores of Lago Villarrica, Lago Calafquén, Lago Panguipulli and Lago Riñihue (after Laugenie, 1982) and the bathymetries of those lakes. For a detailed image of the bathymetries see Figure II-10, Figure II-11, Figure II-12 and Figure II-13

previously accumulated sediment. Preservation of interstadial lacustrine deposits is rarely reported in literature, but not uncommon in Chile (Laugenie, 1982). The presence of these sediments in almost all of the surveyed lakes indicates a similar depositional environment and mechanism of interaction between glacier and lacustrine environment in a still poorly understood South American glacial climate.

The region of the Siete Lagos (Lago Calafquén, Lago Panguipulli and Lago Riñihue) differs from the other lakes in the Chilean Lake District, since it is squeezed in between the Cordillera de Los Andes and the horst (Loncoche horst) and graben structures of the locally more easterly expanded Cordillera de La Costa. The absence of the large plains of the central valley prevented the glacier lobes from free expansion and constrained them to previously eroded glacial and fluvial valleys. Consequently, it is logical to expect the (de)glacial evolution of the Siete Lagos to be unusual. The presence of similar features in Lago Villarrica points towards a more regional explanation or presence of common factors, indicating a similar depositional environment and mechanism of interaction between glacier and lacustrine environment.

According to Laugenie (1982) this part of the Lake District experienced two important phases of glacier advance during the Last Glaciation (OIS 2 and 3): the Eollanquihue and Neollanquihue glaciation. The latter comprised at least three different pulses, which can be derived from the observation of three moraine ridges present around the western coasts of the lakes (Figure IV-7). These Neollanquihue moraines are thin, parallel ridges accompanied by less outwash deposits than the large Eollanquihue ridge (Laugenie, 1982). These thinner moraines might indicate a glacier with less erosional and motional force, but also a glacier, which had less time to develop a large moraine ridge like the Eollanquihue moraines. Consequently, we could argue that UC1 was created during the Eollanquihue advance and that UC2, UC3 and UC4 were created during the three pulses of the Neollanquihue advances.

These four lakes all experienced higher lake levels, which is indicated by the preservation of lake terraces and lacustrine deposits around the current lake edges (Laugenie, 1982). It is unclear whether these were deposited under proglacial or interstadial circumstances. Did these higher lake levels destabilise the glaciers more rapidly, causing them to lose contact with the lake bottom and start retreating? Even calving processes can cause a glacier to retreat. Climate is considered to be the dominant control mechanism on calving behaviour (Aniya et al., 1997), but calving dynamics can sometimes reverse the trend expected from climatic control (Warren and Aniya, 1999). If the onset of calving creates a proglacial lake, the glacier retreat can even accelerate (Warren and Aniya, 1999; Warren and Kirkbride, 2003). The lake geometry, especially in a deep basin, increases also the sensitivity of a glacier to calving losses and deep water may even delay ice advance (Cutler et al., 2001). Especially the lakes of the Siete Lagos are very deep in their eastern parts. Since so many factors affect calving behaviour, it is difficult to separate the climatic influence from local glacier behaviour. Such unstable glacier behaviour has been documented in another Chilean lake, Lago Puyehue (Charlet et al., 2008; Heirman et al., in press), south of these lakes and still located in the Chilean Lake District. Here, the construction of a large moraine in the lake itself prevented the glacier from readvancing (Heirman et al., in press). These four different lakes exhibit proof of similar glacier behaviour, indicating a common driver behind the glaciers' motion, this most likely is a climatic driver. Given the fact that the four lakes are located in slighly different geomorphological context, the most likely driver is climate.

Work by and Denton et al (Denton et al., 1999) in the Chilean Lake District indicates that the Eollanquihue moraines must be older than 50000 cal a BP. All the Neollanquihue moraines were formed later during several pulses, each new advance probably less extensive than the previous. The most important advance were at ca. 32400 cal a BP, ca. 29300 cal a BP, minimum two advances between 23000 and 26000 cal a BP and a last advance between 15000 and 16500 cal a BP (Denton et al., 1999; Lowell et al., 1995).

Not only in the Chilean Lake District was the pre-LGM ice sheet more expanded. This is also the case in Southern Patagonia (Kaplan et al., 2005; Kaplan et al., 2008; McCulloch et al., 2005), New Zealand (Shulmeister et al., 2010; Williams et al., 2009) and Australia (Barrows et al., 2001; Barrows et al., 2002). In general in the Southern Hemisphere mid-latitudes the LGM advance is not the major last advance in the latter part of the last glaciation (Shulmeister et al., 2006).

The advance around 30000-35000 cal a BP recorded in South America (Denton et al., 1999; Kaplan et al., 2005; Lowell et al., 1995), New Zealand (Vandergoes et al., 2005) and Australia (Barrows et al., 2001) could be a direct response to a Southern Hemispere insolation minimum at that time (Vandergoes et al., 2005). But not only temperature affects the temperate glaciers of the southern mid-latitudes. Precipitation is another important factor.

Last century advances (retreats) of glaciers in the Southern Alps and southern Andes are associated with stronger (weaker) Southern Westerlies (Fitzharris et al., 2007). Shulmeister (1999) and Shulmeister et al. (2004) suggested that Milankovitch forcing may play a role in Southern Hemisphere mid-latitude glacial advances through forcing of the Southern Hemisphere Westerly circulation. This predicts glacial events at Southern Hemisphere precessional maxima (i.e. 23 ka, 48 ka, 72 ka, 96 ka) (Shulmeister et al., 2010).

Using this information we can hypothesise that UC1 was created during the Eollanquihue advance, which has a minimum age of 50000 cal a BP. The three Neollanquihue advances UC,2, UC3 and UC4 were probably formed at the Southern Hemisphere insolation minimum (30000-35000 cal a BP), a period of Westerly intensification (23000 cal a BP) and maybe at the global LGM (16500-17500 cal a BP). This last advance can be considered debatable. The diatom record of Lago Puyehue indicates that this lake was completely ice free by ca. 18000 cal a BP (Sterken et al., 2008). A detailed study of the seismic stratigraphy of this lake estimates that the glacier had left the lake basin already somewhere between 24000 and 23000 cal a BP (Charlet et al., 2008; Heirman et al., in press). Nonetheless, a geomorphological study of the glacially associated features (e.g. moraines) around this same lake, estimates the lake to have only been ice free by 14100 cal a BP (Bentley, 1996; Bentley, 1997). The reasons behind these age discrepancy remain unresolved.

So, although a sudden temperature change is recorded around 17500-17150 cal a BP in the Chilean Lake District (Bertrand et al., 2008; McCulloch et al., 2000), moisture supply is also an important factor influencing glacier growth or decline. Temperature and changes in the intensity of the Southern Westerlies might not fluctuate synchronously.

IV.2. Lac d'Armor (Kerguelen Archipelago)

Morphologically, Lac d'Armor is an example of a fjord-like or perialpine lake (Cohen 2003).

IV.2.1. Bathymetry

Before this study the depths of the lakes on this archipelago were unknown. By combining the information obtained by seismic exploration and echosounding a bathymetry was constructed for Lac d'Armor.

Lac d'Armor has a rather complex bathymetry and structure, with two sub-basins: a southern sub-basin with a maximum water depth of 50 m and a northern sub-basin with a maximum water depth of 98 m (Figure IV-8). They are separated by a shallow sill, which culminates at about 20 m below the lake surface (Figure IV-8). This sill also compromises a small perched, sediment-filled sub-basin (Figure IV-9).

Remarkably the lake is much deeper than the nearby fjord Henri Bossière (Figure II-19), which has a depth of about 15 to 20 m (SHOM 1978).

IV.2.2. Seismic Stratigraphy

The sedimentary infill comprises a series of sedimentary units with distinctly different acoustic character and distribution. As the signal penetrates the complete sedimentary infill, it is possible to use the succession of infilling units to reconstruct the evolution of the dominant sedimentary processes in the lake through time since the last glacier retreated from the lake basin. The total infill is about 60 ms thick (ca. 50 m) in both the northern and southern basin and the thickest sedimentary sequence is located in the central part of both basins.

In general, four units, each with a distinct seismic facies, can be discerned in the lake basin infill. The acoustic basement shows no acoustic

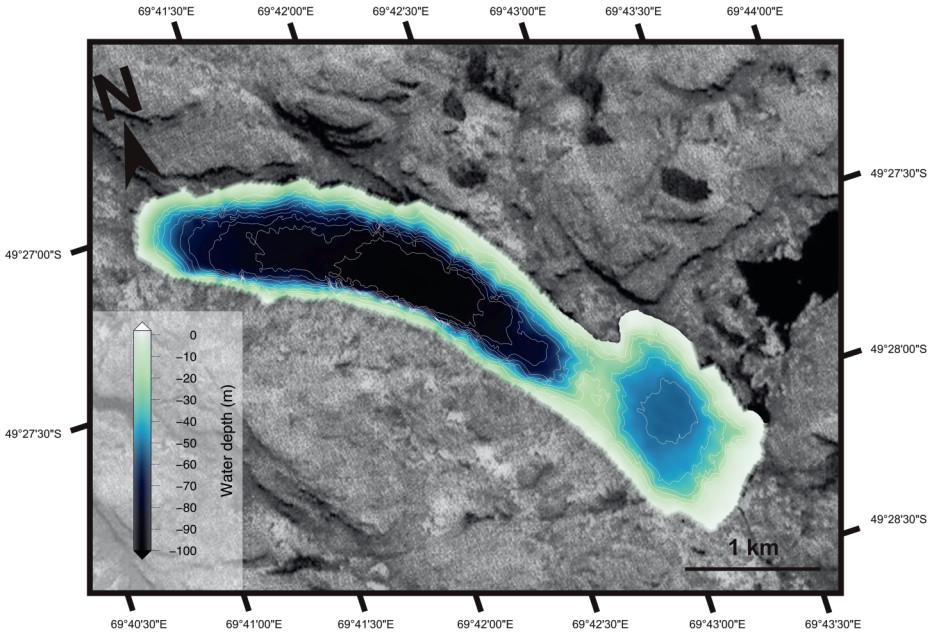

Figure IV-8: Bathymetry of Lac d'Armor based on the seismic profiles and single-beam echosounding data. (Contour lines are drawn every 10 m)

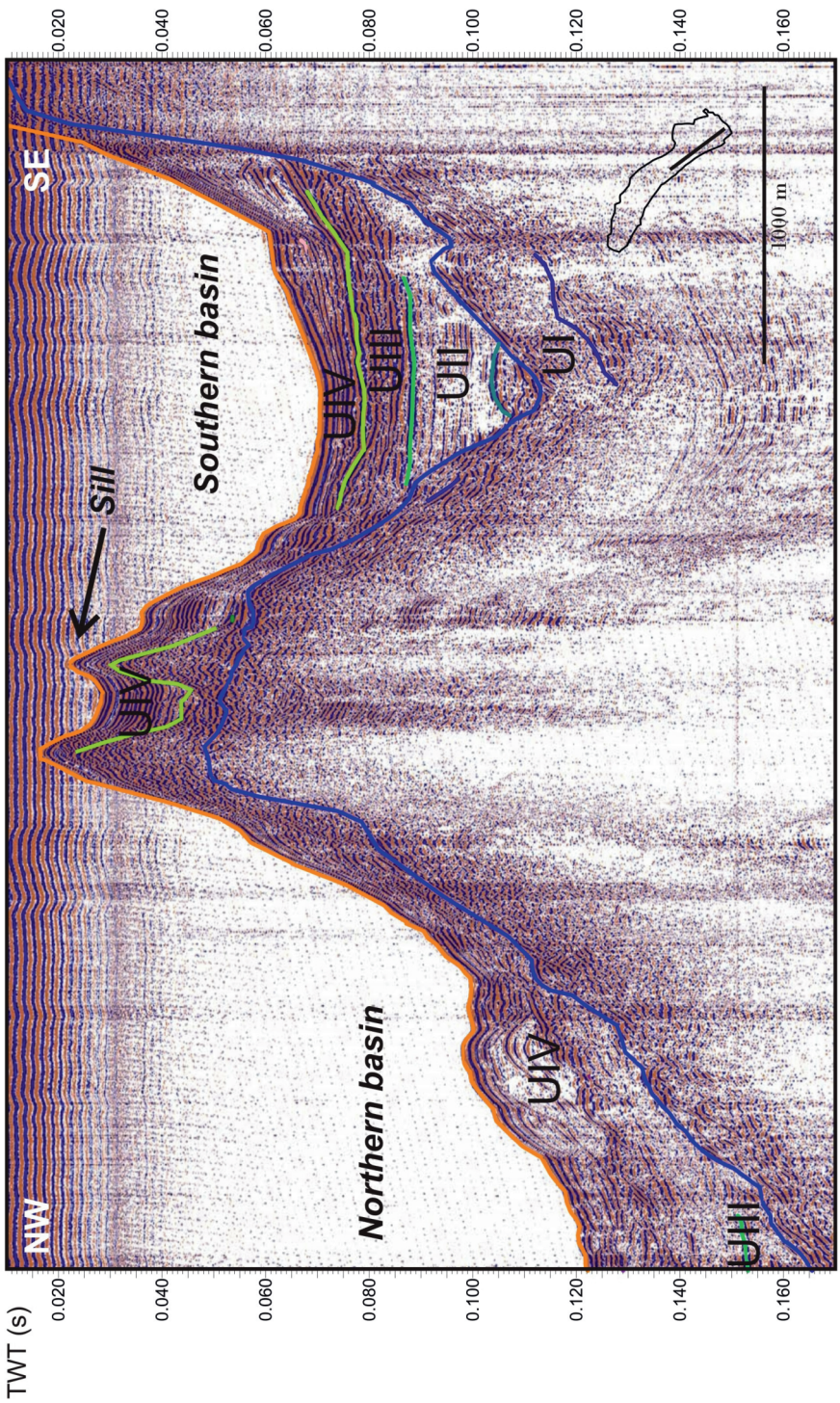

Figure IV-9: Seismic profile of Lac d'Armor showing the sill, which separates the northern and southern basin and the little basin on top of the sill

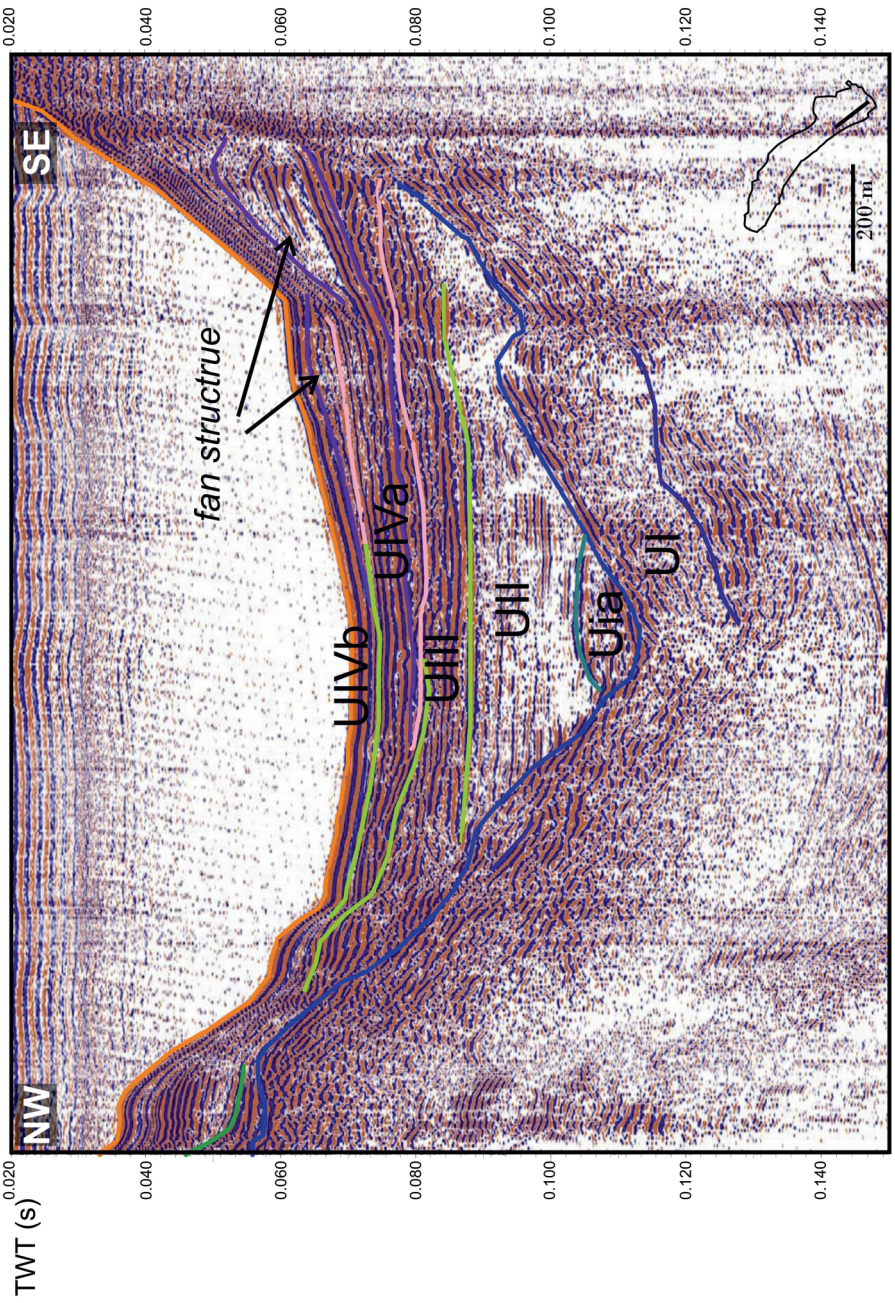

Figure IV-10: Seismic profile of Lac d'Armor of the southern basin

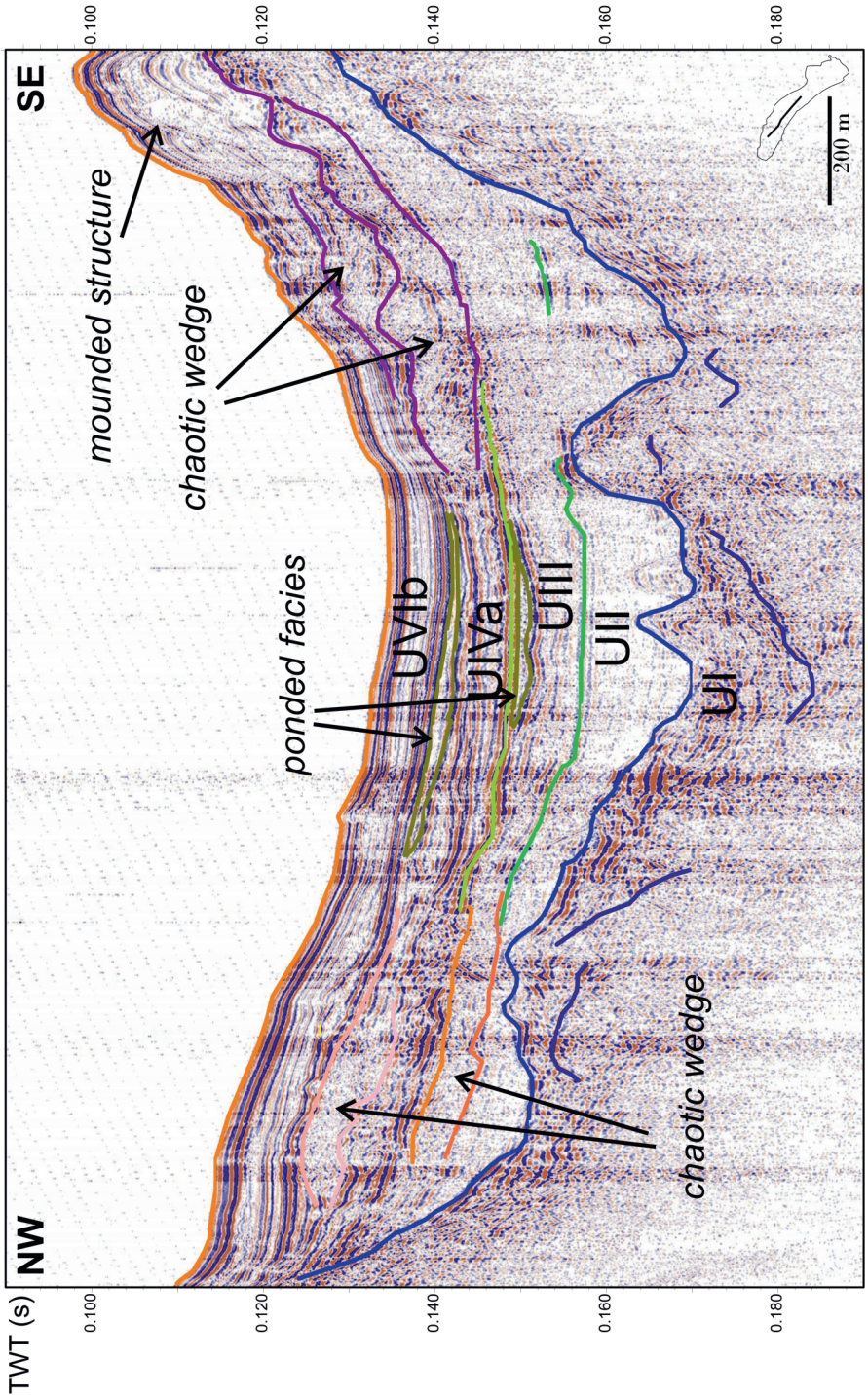

Figure IV-11: Seismic profile of Lac d'Armor of the northern basin

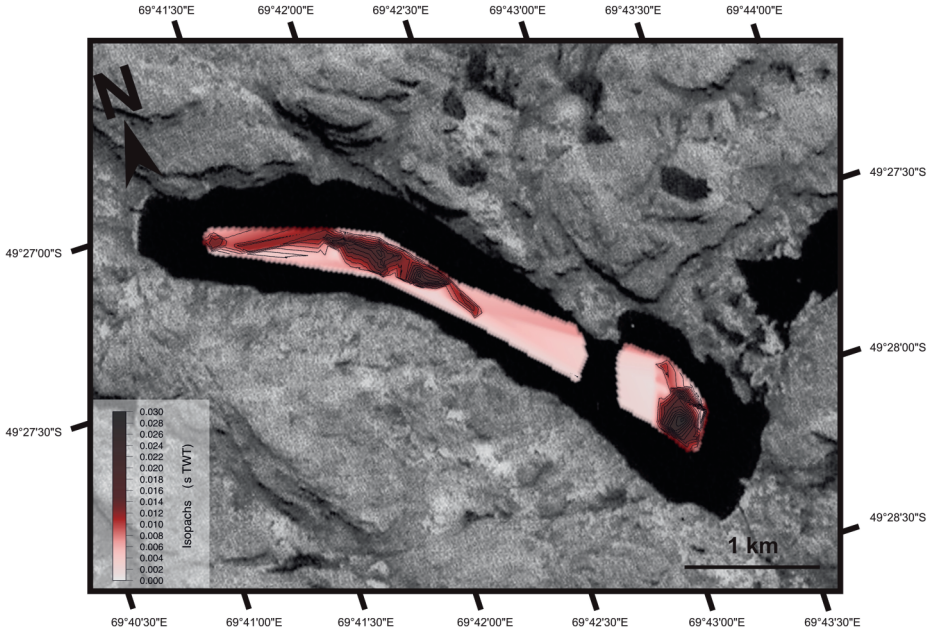

Figure IV-12: Isopach map illustrating the thickness variation of UII in Lac d'Armor

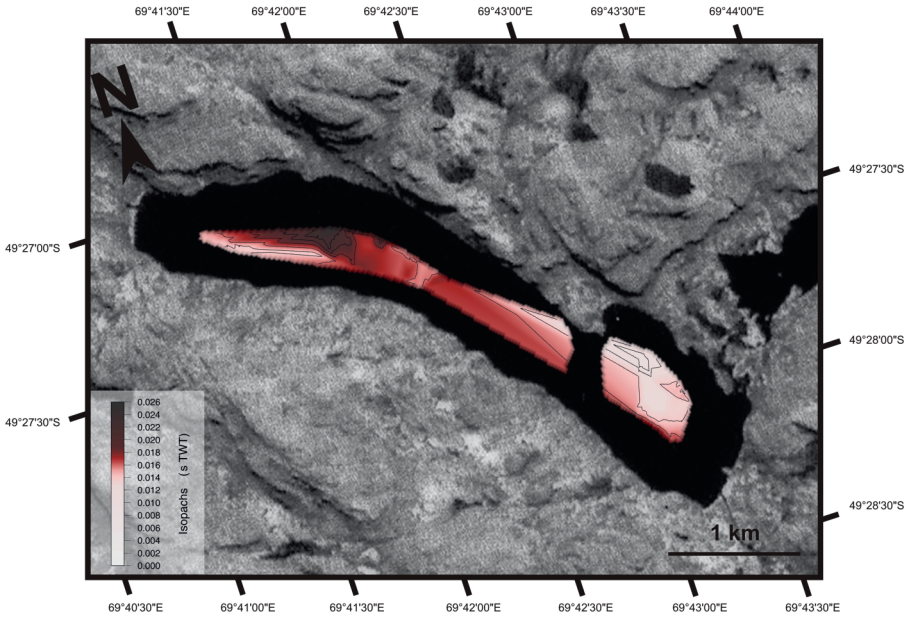

Figure IV-13: Isopach map illustrating the thickness variation of UIII in Lac d'Armor

stratification or internal structures and is excluded from this discussion.

IV.2.2.1. Unit I

The bottom Unit I directly overlies the acoustic basement and is characterized by a chaotic facies with discontinuous reflections (Figure IV-10 and Figure IV-11). The reflections have highly variable amplitudes, ranging from very low, locally producing an almost transparent facies to very high. Unit I is separated from the acoustic basement and from the overlying Unit II by unconformities, the upper unconformity having a strongly undulating morphology and producing a very high-amplitude reflection. The bottom boundary, however, is mostly invisible and was therefore not mapped throughout the lake basin. The lack of this continuous bottom boundary prevented the construction of an isopach map of the thickness of Unit I. In general, this unit is thicker in the deepest parts of the current basin. Here this unit is about 10 ms thick (ca. 8,5 m).

In the southern sub-basin, a sub-unit (Ia) lying on top of Unit I can be distinguished (Figure IV-10). This sub-unit is only present in the deepest part of the southern basin. Both units are separated by an unconformity associated with a high reflection amplitude. The top boundary of Unit Ia is also an unconformity, which is associated with a low-amplitude reflection. Amplitudes of sub-unit Ia's internal reflections are in general higher amplitude than those of UIa, but they lack continuity as well.

IV.2.2.2. Unit II

The overlying Unit II consists of a facies with slightly undulating, low-amplitude reflections. It is a unit with some (sub)-parallel reflections, which are sometimes discontinuous. The seismic facies contains much lower reflection amplitudes than in Unit I or is almost transparent (Figure IV-10 and Figure IV-11). This unit only occurs in the deepest parts of both sub-basins and smoothes the initial U-shaped morphology of the lake basin. The unit is thickest in the southern corner of the southern sub-basin and along the northeastern edge of the northern sub-basin (Figure IV-12). In those areas the unit is about 30 ms (ca. 25 m) thick.

IV.2.2.3. Unit III

The depocentre of Unit III is no longer focused in the deepest parts of the basin. This unit mostly consists of sub-parallel high-amplitude reflections (Figure IV-10 and Figure IV-11). The boundary between Unit II and III is marked by a continuous, high amplitude reflection. The boundary between Unit III and IV is also continuous and marked by a high amplitude reflection. Unit III has generally a lower reflection amplitude in the northern sub-basin, than in the southern. Almost transparent wedges with a chaotic reflections are present inside this unit (Figure IV-11).

The unit is rather thin in the southern sub-basin (on average 4 ms or ca. 3.5 m). . In this sub-basin the unit is the thickest at the southern edge (8 ms or ca. 7 m) and it thins towards the north (Figure IV-13). In the northern sub-basin the unit is thickest at the northern edge (12 ms or ca. 10.5 m) and there is another thick depocentre in the south. The thickest northern depocentre thins towards the south, while the southern one thins towards the north (Figure IV-13).

IV.2.2.4. Unit IV

Unit IV is a unit consisting of strong, continuous reflections (Figure IV-10 and Figure IV-11). The boundary between Unit III and IV is marked by the onset of mounded structures located in the southern corner of each sub-basin. The acoustic layering of Unit IV is often disrupted by prograding features from the southern or northern shore, where the river inlets are located (Figure IV-10). These features have internally a more chaotic character, but there are some internal structure, mostly consisting of downlapping reflections. There is quite a sudden shift in how far

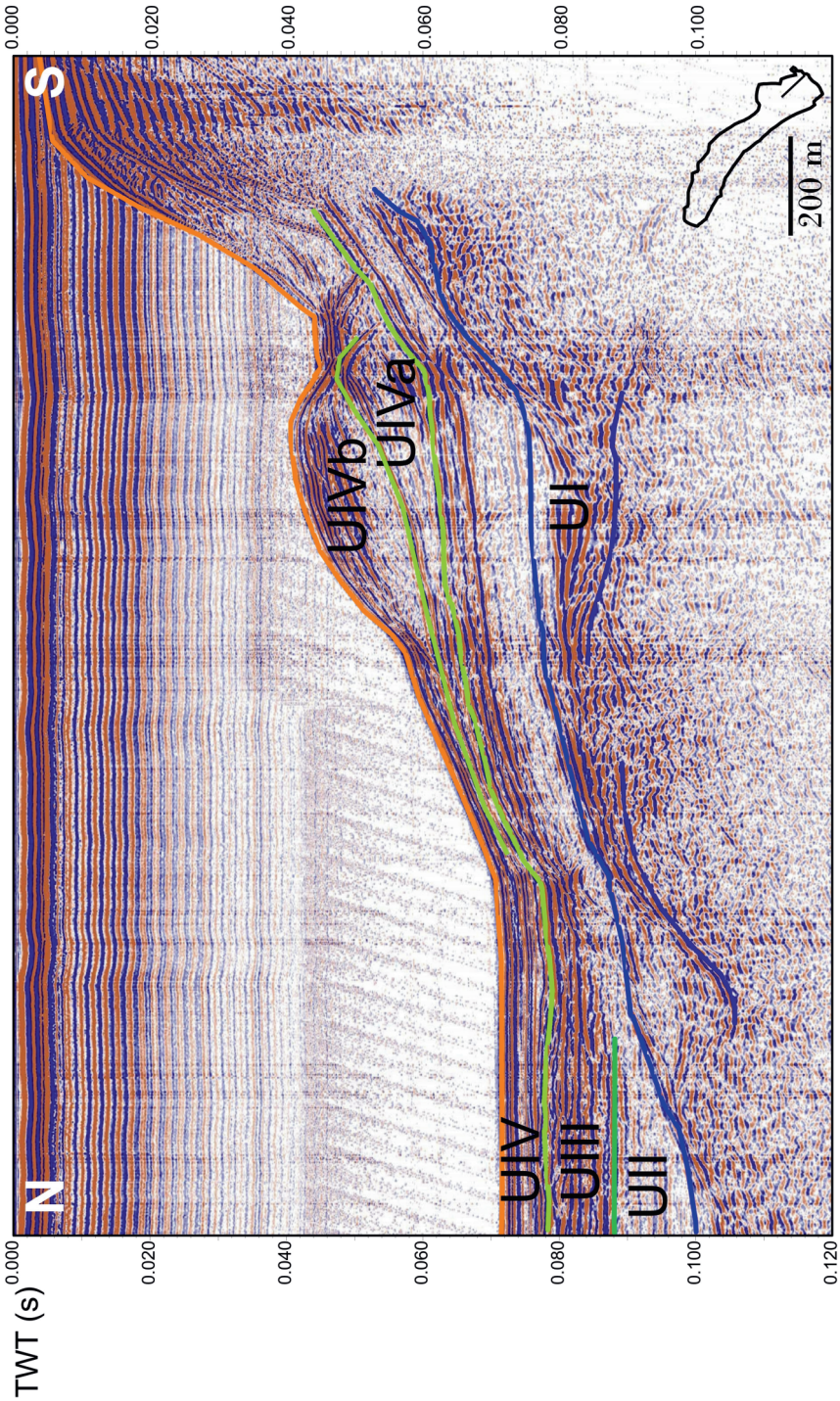

Figure IV-14: Seismic profile of Lac d'Armor showing the mounded structure in the southern basin

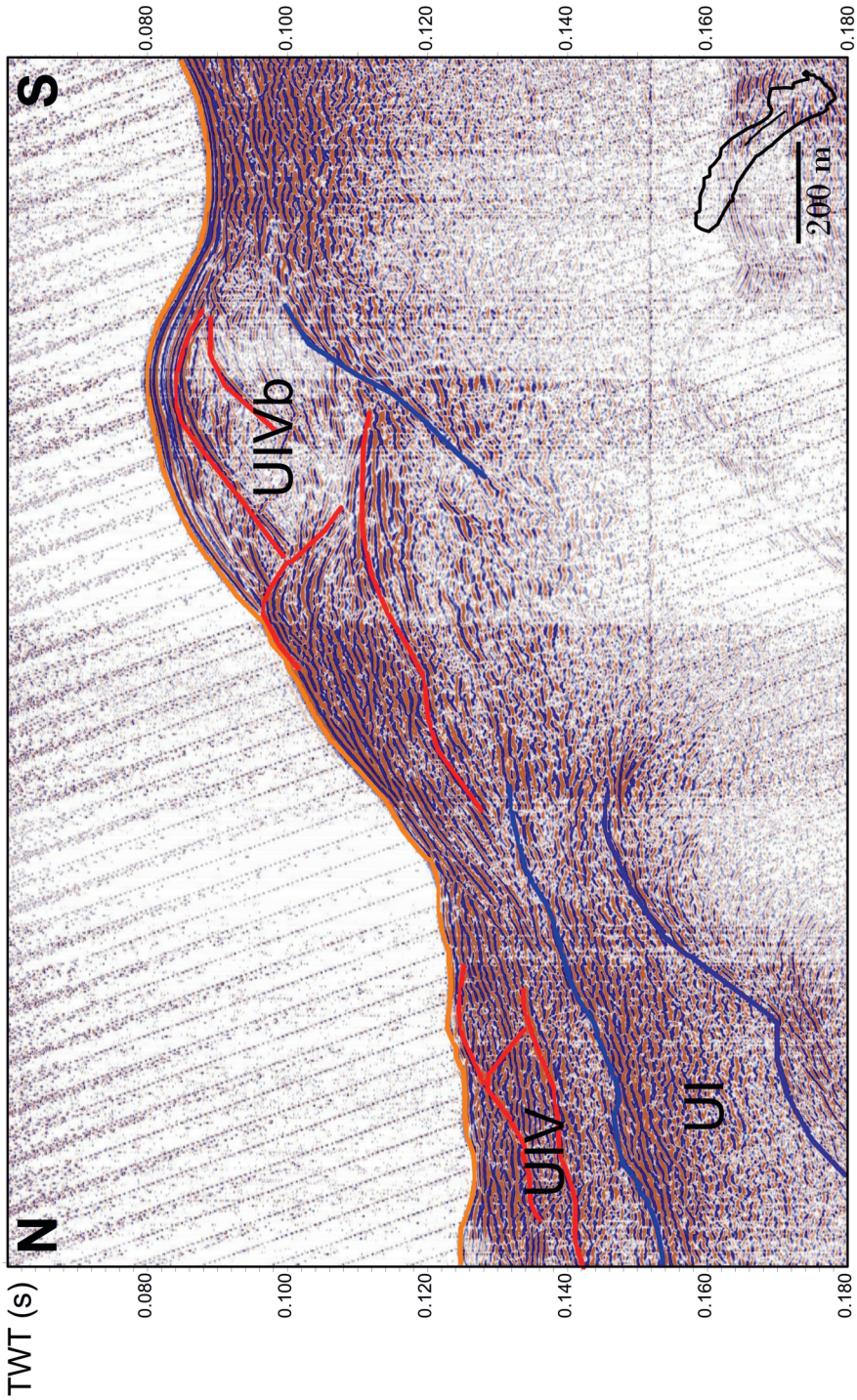

Figure IV-15: Seismic profile of Lac d'Armor showing the mounded structure in the northern basin

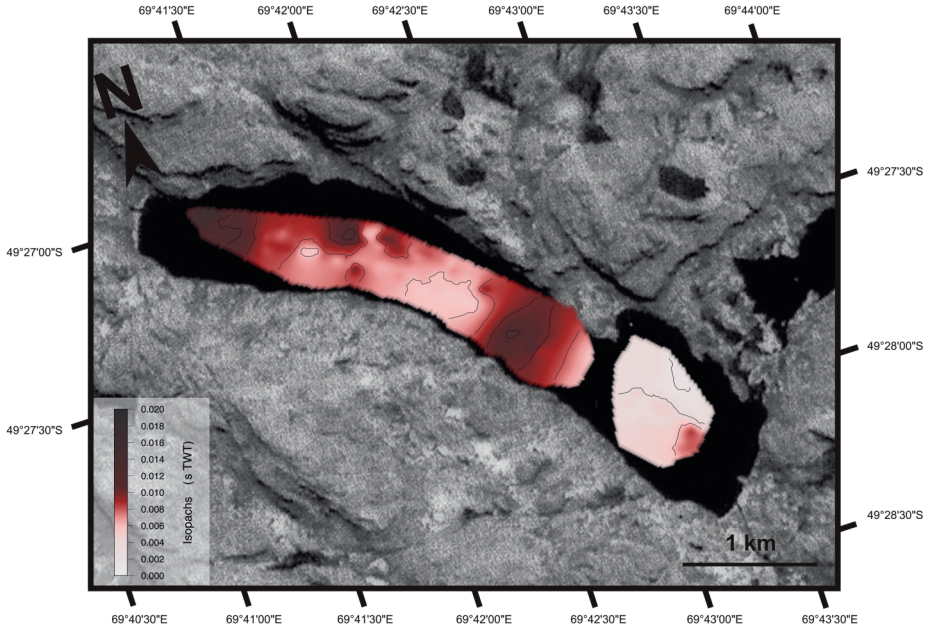

Figure IV-16: Isopach map illustrating the thickness variation of UIV in Lac d'Armor

these structures reach down into the basin. This shift marks the boundary between two sub-units (IVa and IVb). In UIVb the prograding features reach deeper into the lake basin. This boundary is also marked by a difference in the height of the mounded structures in the southern corners of the sub-basins (Figure IV-14 and Figure IV-15). In sub-unit IVa, they are not as high and steep as in UIVb. In sub-unit IVb, the slopes of these mounded structures get much steeper and the structures are higher.

In the lower part of Unit IV in the northern sub-basin there are also some chaotic wedges which thicken towards the sill and the northern shore. These wedges are most likely associated with thin ponded, transparent facies in the deepest parts of the northern sub-basin since they are located at the same stratigraphic level.

The unit is thickest at the southern edge of both sub-basins, this is the location of the mounded structures (Figure IV-16). In the southern basin the unit is 5 ms (ca. 4 m) thick, while it is up to 10 ms (ca. 8.5 m) in the northern sub-basin. In this latter sub-basin the unit is also thick close to the inlet of the Rivière du Nord and along the northern edge of the sub-basin.

Unit IV is also present in the small basin located on top of the sill, which separates the lake basin in two parts. Here the reflections of this unit are always continuous and never disrupted. This basin has a continuous draping infill, which is about 10 ms (ca. 8.5 m) thick.

IV.2.3. Interpretation: Seismic Units and Seismic Facies

IV.2.3.1. Acoustic Basement

The acoustic basement, lacking any internal structures, most likely represents the basaltic rock of the Large

Igneous Province, which forms the Kerguelen Plateau (Giret, 1980; Nougier, 1970a; Nougier, 1970b).

IV.2.3.2. Unit I

The bottom facies (Unit I) closely resembles the bottom facies described from many glacial lakes and fjords in Europe and North America (Eyles et al., 2000; Lønne and Syvitski, 1997; Syvitski and Lee, 1997; Van Rensbergen et al., 1999; Van Rensbergen et al., 1998) and which is generally interpreted as an ice-contact deposit. Unit Ib might be the relic of a meltwater tunnel.

IV.2.3.3. Unit II

Based on its stratigraphic position, low-amplitude facies and seismic similarities with other glacigenic lakes (Syvitski and Lee, 1997; Van Rensbergen et al., 1999; Van Rensbergen et al., 1998), this unit is interpreted to represent glaciolacustrine sediments deposited in a sub- or proglacial lake. A combination of density currents (underflows and turbidity currents) of meltwater caused the sediment to focus in the deepest parts of the basin (Eyles et al., 2000), hereby smoothing all previously created morphology on the lake floor.

IV.2.3.4. Unit III

During the deposition of Unit III the glacier had completely retreated from the Lac d'Armor basin. This unit is probably an outwash deposit created by sediment-loaded meltwater plumes (Seramur et al., 1997) entering the lake at the location of the current river inlets. In the southern basin the sediment-laden river water entering the lake was deflected to the southern edge of the lake. The opposite is true for the northern sub-basin.

The chaotic wedges in these units have the typical characteristics of sedimentary mass wasting deposits (Schnellmann et al., 2002). They might be the result of the collapse of oversteepened slopes. Oversteepened slopes are especially susceptible to earthquake-triggered failure (Moernaut pers. comm.). Very little is known about the seismicity in the Kerguelen area. The archipelago is located far away from tectonic plate boundaries, but earthquakes have been reported during the last century (USGS, 2007).

IV.2.3.5. Unit IV

The prograding structures at the river mouths indicate a higher input of terrigenous material by the rivers. The mounded depocentres resemble drift deposits and suggest the presence of strong bottom currents (Ceramicola et al., 2001; Gilli et al., 2005a; Gilli et al., 2005b). The increase in the height of these mounds from sub-unit IVa to IVb, might indicate an increase in the strength of the bottom currents. The river-derived sediments appear to have been concentrated in fan-like depocentres, as opposed to the more evenly distribution across the entire basin floor in Unit III.

The amplitude of all reflections are much lower than those in the glacigenic lakes in Chile (Charlet et al., 2008; Heirman et al., in press; Volland et al., 2007), and resemble the amplitudes encountered in lakes in the European Alps (Girardclos et al., 2005; Van Rensbergen et al., 1999; Van Rensbergen et al., 1998) and Canada (Eyles et al., 2000; Eyles and Mullins, 1997). In the Chilean lakes this sediment is almost entirely autochthonous, consisting predominantly of lacustrine algae (Bertrand et al., 2008), while the sediment of the lakes in the European Alps and in this lake still have an important terrestrial component (Arnaud et al., 2009).

The mass-wasting deposits in this unit, represented by the chaotic wedges, might be the result of the failure of oversteepened slopes. Some of them might be earthquake triggering, a mechanism to cause the failure of these oversteepened slopes (Moernaut pers. comm.). The ponded features associated to the mass-wasting deposits are most likely homogenites (Chapron et al., 1999), containing a homogeneous mixture of the material

that slumped down slope during a mass-wasting event.

IV.2.4. Environmental implications

The seismic stratigraphy of the sedimentary infill of Lac d'Armor depicts the evolution of the sedimentary environment in the lake basin during and after the last retreat from a glacier out of the basin. Very little is known about the timing of deglaciation in the Kerguelen Archipelago. A study by Frenot et al. (1997a) of a peat bog in the Plaine Ampère in front of the current Ampère glacier, which is an outlet glacier of the Cook glacier, is the only 'long', dated record available (Figure IV-17). Currently, Lac d'Armor is about 35 km away from the limit of the Cook glacier (Figure IV-17). The record of Frenot et al. (1997a) implies that the peat bog site was ice free between 10000 and 5000 cal a BP. Most likely, the glacier had left the Armor basin prior to 10000 cal a BP. A study of sea-ice expansion in the South Atlantic indicates the first retreat of the Antarctic sea ice around 18000-17000 cal a BP (Bianchi and Gersonde, 2004).

The extent of the Antarctic sea-ice is related to the position of the Polar Front (Gersonde et al., 2005), which currently lies almost on top of the Kerguelen Archipelago. A retreat of the sea ice and consequently of the Polar Front towards the south (Gersonde et al., 2005; Gersonde and Zielinski, 2000), would have initiated warming in the region of the Kerguelen Archipelago. Sometime between 18000 and 10000 cal a BP the Kerguelen ice sheet should have started to retreat. Initially, the retreating glacier was still present in the lake's catchment, resulting in the deposition of Unit II. After the glacier had retreated from the catchment, only rivers brought terrestrial material to the basin. During the deposition of Unit III, the river entering the lake water, dropping their load with the coarsest material closest to the inlet and the finer deeper in the basin. The amount of sediment brought by the rivers was probably rather limited compared to Unit IV. The fan structures of Unit IV indicate a higher

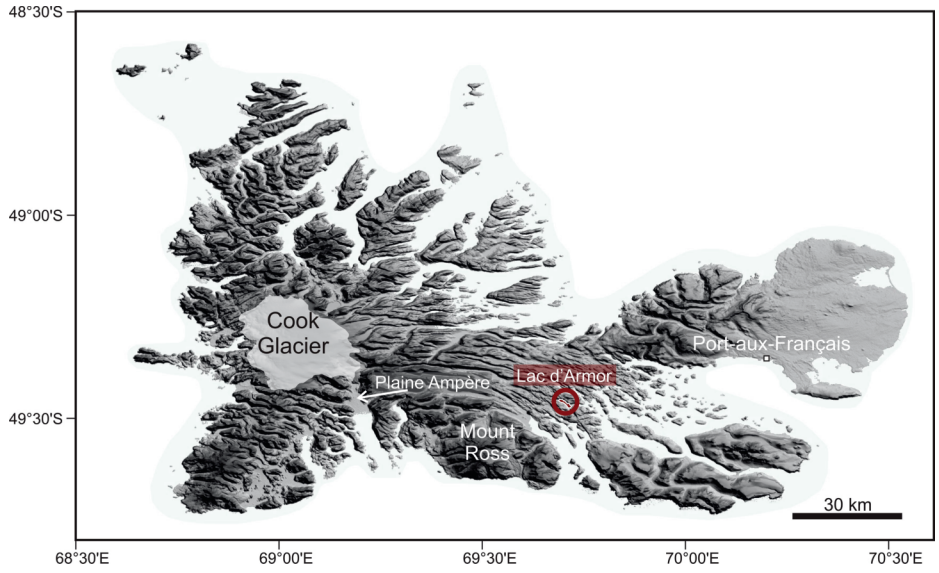

Figure IV-17: Location of Lac d'Armor in comparison to Plaine Ampère and the Cook Glacier

run-off and a larger supply of sediment in de Lac d'Armor basin.

The onset of the construction of the drift structures, indicates the formation of strong bottom currents. Currently the climate on the Kerguelen archipelago is dominated by the Southern Westerlies, and therefore very windy, with monthly averages of 100 km/h (Frenot et al. 1997b). Wind-induced waves have a great influence on sediment (re)distribution in lake systems, especially in shallow waters (Håkanson and Jansson, 1983). However, a large-scale steady state lake-circulation pattern due to a uniform wind stress, in this case the Southern Westerlies, generally also consists of a pair of counter-rotating gyres with downwind flow near the shores of the lake and upwind return flow in the deeper parts of the lake basin (Rao and Murty, 1970; Schwab and Beletsky, 2003). The pattern of these upwind return flow bottom currents is strongly controlled by bottom topography (Håkanson and Jansson, 1983). Consequently, it is not unlikely that these drift deposits are an indication of a strengthening of the Southern Westerlies. In Lago Cardiel, Argentina (49°S), the onset of Southern Westerly intensification has been dated at 6800 cal a BP (Gilli et al., 2005b) and in Laguna Potrok Aike (52°S) around 6000 cal a BP (Anselmetti et al., 2009). Since no age-depth model is available for the sedimentary infill of Lac d'Armor, we have to assume that the onset of the drift here was simultaneous with the onset of the formation of drift deposits in South American lakes. A strengthening of the Southern Westerlies would also imply an increase in precipitation, therefore explaining the higher run-off indicated by the development of the river-fan structures in Unit IV. The boundary between sub-unit IVa and IVb, might indicate that the Southern Westerlies' strength increased even more, leading to even stronger bottom currents and consequently higher and larger drift structures. Such a increase in strength has also been observed in Laguna Parrillar, southern South America (53°S) around 4000 cal a BP.

These wind-induced, strong bottom currents are responsible for the redistribution of the sediment brought in by the rivers. The sediment load from the Rivière du Diable seems to smaller than that of the Rivière du Nord (Figure II-19). This Rivière du Diable is also much shorter, than the Rivière du Nord. The Rivière du Diable connects Lac d'Armor with four other lakes. Most of the terrigenous material of the catchment of these lakes will already been deposited in one of these lake basins before it reaches the Rivière du Diable (Figure II-19).

References

Andersen, B.G., Denton, G.H. and Lowell, T.V., 1999. Glacial geomorphologic maps of Llanquihue drift in the area of the southern Lake District, Chile. *Geografiska Annaler*, **81A**(2): 155-166.

Aniya, M., Sato, H., Naruse, R., Skvarca, P. and Casassa, G., 1997. Recent glacier variations in the Southern Patagonian Icefield, South America. *Arctic and Alpine Research*, **29**(1-12).

Anselmetti, F.S. et al., 2009. Environmental history of southern Patagonia unravelled by the seismic stratigraphy of Laguna Potrok Aike. *Sedimentology*, **56**(4): 873-892.

Arnaud, F. et al., 2009. First reconstruction of last millennium flooding activity on Kerguelen archipelago (50°S, subantarctic Indian Ocean) from Lake Armor sediment: implications for southern hemisphere cyclonic circulation changes, *Conference abstract for EGU*, Vienna, Austria.

Barrows, T.T., Stone, J.O., Fifield, L.K. and Cresswell, R.G., 2001. Late Pleistocene glaciation of the Kosciusko Massif, Snowy Mountains, Australia. *Quaternary Research*, **55**: 179-189.

Barrows, T.T., Stone, J.O., Fifield, L.K. and Creswell, R.G., 2002. The timing of the Last Glacial maximum in Australia. *Quaternary Science Reviews*, **21**: 15-173.

Bentley, M., 1996. The role of lakes in moraine formation, Chilean Lake District. *Earth Surface Processes and Landforms*, **21**: 493-507.

Bentley, M.J., 1997. Relative and radiocarbon chronology of two former glaciers in the Chilean Lake District. *Journal of Quaternary Science*, **12**: 25-33.

Bertrand, S., Charlet, F., Charlier, B., Renson, V. and Fagel, N., 2008. Climate variability of Southern Chile since the Last Glacial Maximum: a continuous sedimentological record from Lago Puyehue (40°S). *Journal of Paleolimnology*, **39**: 179-195.

Bianchi, C. and Gersonde, R., 2004. Climate evolution at the last deglaciation: the role of the Southern Ocean. *Earth and Planetary Science Letters*, **228**(3-4): 407-424.

Ceramicola, S., Rebesco, M., De Batist, M. and Khlystov, O., 2001. Seismic evidence of small-scale lacustrine drifts in Lake Baikal (Russia). *Marine Geophysical Researches*, **22**(5-6): 445-464.

Chapron, E., Beck, C., Pourchet, M. and Deconinck, J.F., 1999. 1822 earthquake-triggered homogenite in Lake Le Bourget (NW Alps). *Terra Nova*, **11**: 86-92.

Charlet, F., Chapron, E., De Batist, M., Pino, M. and Urrutia, R., 2008. Seismic stratigraphy of Lago Puyehue (Chilean Lake District): new views on its deglacial and Holocene evolution. *Journal of Paleolimnology*, **39**: 163-177.

Clayton, J.D., Clapperton, C.M. and Antinao Rojas, J.L., 1997. Las glaciaciones Pleistocenas en la cuenca del lago Villarrica, Andes del sur, *Congresso Geológico Chileno*, Antafagosta, Chile.

Cutler, P.M., Mickelson, D.M., Colgan, P.M., MacAyeal, D.R. and Parizek, B.R., 2001. Influence of the Great Lakes on the dynamics of the southern Laurentide ice sheet: Numerical experiments. *Geology*, **29**(11): 1039-1042.

Denton, G.H. et al., 1999. Geomorphology, stratigraphy, and radiocarbon chronology of Llanquihue drift in the area of the southern Lake District, Seno Reloncaví, and Isla Grande de Chiloé, Chile. *Geografiska Annaler*, **81A**(2): 167-229.

Eyles, N., Boyce, J.I., Halfman, J.D. and Koseoglu, B., 2000. Seismic stratigraphy of Lake Waterton, a sediment-starved glaciated basin in the Rocky Mountains of Alberta, Canada and Montana, USA. *Sedimentary Geology*, **130**: 283-311.

Eyles, N. and Mullins, H.T., 1997. Seismic-stratigraphy of Shuswap Lake, British Columbia, Canada. *Sedimentary Geology*, **109**: 283-303.

Fitzharris, B.B., Clare, G.R. and Renwick, J., 2007. Teleconnections between Andean

and New Zealand glaciers. *Global and Planetary Change*, **59**(1-4): 159-174.
Frenot, Y., Gloaguen, J.-C., Van De Vijver, B. and Beyens, L., 1997a. Datation de quelques sediments tourbeux holocenes et oscillations glaciaires aux iles Kerguelen. *Comptes Rendus de l'Academie des Sciences - Series III - Sciences de la Vie*, **320**(7): 567-573.
Frenot, Y., Gloaguen, J.C. and Trehen, P., 1997b. Climate change in Kerguelen Islands and colonization of recently deglaciated areas by Poa kerguelensis and P. annua. In: B. Battaglia, J. Valencia and D.W.H. Walton (Editors), *Antarctic communities: species, structures and survival*. Cambridge University Press, Cambridge, pp. 358-366.
Gersonde, R., Crosta, X., Abelmann, A. and Armand, L., 2005. Sea-surface temperature and sea ice distribution of the Southern Ocean at the EPILOG Last Glacial Maximum--a circum-Antarctic view based on siliceous microfossil records. *Quaternary Science Reviews*, **24**(7-9): 869-896.
Gersonde, R. and Zielinski, U., 2000. The reconstruction of late Quaternary Antarctic sea-ice distribution - the use of diatoms as a proxy for sea-ice. *Palaeogeography Palaeoclimatology Palaeoecology*, **162**(3-4): 263-286.
Gilli, A. et al., 2005a. Seismic stratigraphy, buried beach ridges and contourite drifts: the Late Quaternary history of the closed Lago Cardiel basin, Argentina (49°S). *Sedimentology*, **52**(1): 1-23.
Gilli, A. et al., 2005b. Mid-Holocene strengthening of the Southern westerlies in South America - Sedimentological evidences from Lago Cardiel, Argentina (49°S). *Global and Planetary Change*, **49**(1-2): 75-93.
Girardclos, S., Baster, I., Wildi, W., Pugin, A. and Rachoud-Schneider, A.-M., 2003. Bottom-current and wind-pattern changes as indicated by Late Glacial and Holocene sediments from western Lake Geneva (Switzerland). *Eclogae Geologicae Helveticae*, **96**(suppl. 1): S39-S48.
Girardclos, S., Fiore, J., Rachoud-Schneider, A.-M., Baster, I. and Wildi, W., 2005. Petit-Lac (western Lake Geneva) environment and climate history from deglaciation to the present: a synthesis. *Boreas*, **34**(4): 417-433.
Giret, A., 1980. Carte géologique au 1/50.000 de la péninsule Rallier du Baty. *Comité National Français des Recherches Antarctiques*, **45**.
Håkanson, L. and Jansson, M., 1983. *Principles of Lake Sedimentology*. The Blackburn Press, Caldwell, New Jersey, USA, 316 pp.
Heirman, K. et al., in press. Detailed seismic stratigraphy of Lago Puyehue: implications for the mode and timing of glacier retreat in the Chilean Lake District. *Journal of Quaternary Science*.
Kaplan, M.R., D.C.Douglass, Singer, B.S., Ackert, R.P. and Caffee, M.W., 2005. Cosmogenic nuclide chronology of pre-last glacial maximum moraines at Lago Buenos Aires, 46°S, Argentina. *Quaternary Research*, **63**: 301-315.
Kaplan, M.R., Moreno, P.I. and Rojas, M., 2008. Glacial dynamics in southernmost South America during Marine Isotope Stage 5e to the Younger Dryas chron: a brief review with a focus on cosmogenic nuclide measurements. *Journal of Quaternary Science*, **23**(6-7): 649-658.
Lahousse, S., 2008. *Correlation of onshore and offshore Late-Glacial geomorphological features in and around Lago Villarrica, Chile*. MSc dissertation Thesis, Ghent University, Ghent, Belgium, 27 pp.
Laugenie, C., 1982. *La région des lacs, Chili méridional*, Université de Bordeaux III, Bordeaux, France, 822 pp.
Lazorek, M. et al., 2006. Late-Quaternary seismo-stratigraphy of Lake Wanapitei, Sudbury, Ontario, Canada: Arguments for a possible meteorite impact origin. *Sedimentary Geology*, **192**: 231-242.
Lønne, I. and Syvitski, J.P., 1997. Effects of the readvance of an ice margin on the seismic character of the underlying sediment. *Marine Geology*, **143**: 81-102.
Lowell, T.V. et al., 1995. Interhemispheric Correlation of Late Pleistocene Glacial

Events. *Science*, **269**(5230): 1541-1549.
McCulloch, R.D. et al., 2000. Climatic inferences from glacial and paleaoecological evidence at the last glacial termination, southern South America. *Journal of Quaternary Science*, **15**(4): 409-417.
McCulloch, R.D., Fogwill, C.J., Sugden, D.E., Bentley, M.J. and Kubik, P.W., 2005. Chronology of the last glaciation in central Strait of Magellan and Bahia Inutil, southernmost South America. *Geografiska Annaler Series a-Physical Geography*, **87A**(2): 289-312.
Mullins, H.T. and Halfman, J.D., 2001. High-resolution seismic reflection evidence for middle Holocene environmental change, Owasco Lake, New York. *Quaternary Research*, **55**: 322-331.
Nougier, J., 1970a. Carte géologique de reconnaissance au 1/200.000. *Comité National Français des Recherches Antarctiques*, **27**(2): 256.
Nougier, J., 1970b. Contribution à l'étude géologique et géomorphologique des îles Kerguelen. *Comité National Français des Recherches Antarctiques*, **27**(1): 440.
Porter, S.C., 1981. Pleistocene glaciation in the southern Lake District of Chile. *Quaternary Research*, **16**: 263-292.
Rao, D.B. and Murty, T.S., 1970. Calculation of the steady-state wind-driven circulations in Lake Ontario. *Archiv für Meteorologie, Geophysik und Bioklimatologie, Series A*, **19**: 195-210.
Schnellmann, M., Anselmetti, F.S., Giardini, D., McKenzie, J.A. and Ward, S.N., 2002. Prehistoric earthquake history revealed by lacustrine slump deposits. *Geology*, **30**(12): 1131-1134.
Seramur, K.C., Powell, R.D. and Carlson, P.R., 1997. Evaluation of conditions along the grounding line of temperate marine glaciers: an example from Muir Inlet, Glacier Bay, Alaska. *Marine Geology*, **140**: 307-327.
Schwab, D.J. and Beletsky, D., 2003. Relative effects of wind stress curl, topography, and stratification on large-scale circulation in Lake Michigan. *Journal of Geophysical Research*, **108**(C2): 3044.
Shulmeister, J., 1999. Australasian evidence for mid-holocene climate change implies precessional control of Walker Circulation in the Pacific. *Quaternary International*, **57-58**: 81-91.
Shulmeister, J. et al., 2004. The Southern Hemisphere westerlies in the Australasian sector over the last glacial cycle: a synthesis. *Quaternary International*, **118-19**: 23-53.
Shulmeister, J., Rodbell, D.T., Gagan, M.K. and Seltzer, G.O., 2006. Interhemispheric linkages in climate change: paleo-perspectives for future climate change. *Climate of the Past*, **2**: 167-185.
Shulmeister, J. et al., 2010. The stratigraphy, timing and climatic implications of glaciolacustrine deposits in the middle Rakaia Valley, South Island, New Zealand. *Quaternary Science Reviews*, **29**(17-18): 2362-2381.
Sterken, M. et al., 2008. Late Quaternary climatic changes in southern Chile, as recorded in a diatom sequence of Lago Puyehue (40°40' S). *Journal of Paleolimnology*, **39**: 219-235.
Syvitski, J.P.M. and Lee, H.J., 1997. Postglacial sequence stratigraphy of Lake Melville, Labrador. Marine *Geology*, **143**: 55-79.
USGS, 2007. *Earthquake database* http://neic.usgs.gov/neis/epic/epic.html.
Van Rensbergen, P., De Batist, M., Beck, C. and Chapron, E., 1999. High-resolution seismic stratigraphy of glacial to interglacial fill of a deep glaciogenic lake: Lake Le Bourget, Northwestern Alps, France. *Sedimentary Geology*, **128**: 99-129.
Van Rensbergen, P., De Batist, M. and Manalt, F., 1998. High-resolution seismic stratigraphy of late Quaternary fill of Lake Annecy (northwestern Alps): evolution from glacial to interglacial sedimentary processes. *Sedimentary Geology*, **117**: 71-96.

Vandergoes, M.J. et al., 2005. Regional insolation forcing of late Quaternary climate change in the Southern Hemisphere. *Nature*, **436**(7048): 242-245.

Volland, S., Sturm, M., Lukas, S., Pino, M. and Müller, J., 2007. Geomorphological and sedimentological evolution of a lake basin under strong volcano-tectonic influence: Lake Calafquén (South Central Chile). *Quaternary International*, **161**(1): 32-45.

Warren, C. and Aniya, M., 1999. The calving glaciers of southern South America. *Global and Planetary Change*, **22**: 59-77.

Warren, C.R. and Kirkbride, M.P., 2003. Calving speed and climatic sensitivity of New Zealand lake-calving glaciers, *Annals of Glaciology*, **36**: 173-178.

Williams, M., Cook, E., van der Kaars, S., Barrows, T., Shulmeister, J. and Kershaw, P., 2009. Glacial and deglacial climatic patterns in Australia and surrounding regions from 35 000 to 10 000 years ago reconstructed from terrestrial and near-shore proxy data. *Quaternary Science Reviews*, **28**(23-24): 2398-2419.

V. High-resolution Climate Variability through Time

As soon as you go into the real details of any process, you discover it is open-ended in terms of what needs to be found out about it. Details help in perceiving the essential nature of a system. And this knowledge of an apparently trivial detail quite often makes it possible to see into the depth of things.

Climatic variability is reflected in the lacustrine record. As a result, lake sediments show a considerable stratigraphic variability reflected in its physical, geochemical and biological parameters. In contrast to the metre or sometimes decimetre scale analysis of environmental changes in the lake basin determined with high-resolution reflection seismic techniques, sediment core analysis can go to centimetre or even millimetre resolutions allowing the reconstruction of changes in the sedimentary environment on a much finer scale. These spatial scales can be translated into time, consequently the reflection seismic time-scale spans a longer time period, but has a lower resolution, while a sediment core spans a shorter period of time, but on a much higher time-resolution. Sediment cores, on the other hand, do not have the same spatial coverage as high-resolution seismic techniques. All information logged in the sediment record is obtained from one location in the lake. High-resolution seismic techniques come in hand to determine this optimal location.

V.1. Lago Villarrica

V.1.1. Bulk Organic Geochemistry of Modern Villarrica Lake and Catchment Samples

V.1.1.1. Terrestrial Organic Material

TOC and LOI_{550} were measured of the surface sediment of Lago Villarrica at 9 different locations (Table V-1 and Figure V-4). The values are lowest in VB1 and VB10 (Table V-1). These low values can be explained by the proximity of the sample location to one of the three most important, permanent inflows: Río Trancura, Río Correntoso and Río Molco (Volland, 2006) (Figure V-4). VB1 is located close to both inlets of the Río Trancura, the largest river entering Lago Villarrica and draining most of the lake's catchment. VB10's low TOC and LOI_{550} values can be attributed to its closeness to Río Correntoso and the Río Molco. Both rivers drain the Volcán Villarrica flank. These riverbeds have also been the pathway of several lahar flows (Figure II-10). Although the rivers transport also organic matter from the catchment, the low TOC and LOI_{550} values close to the river mounts indicate that the majority of the influx is detrital and of a non-organic origin.

The C/N ratio is used to distinguish between the amount of organic matter that originates from aquatic sources as opposed to land sources (Meyers and Teranes, 2001). A distance to river and shore index was calculated. This index is a summation of the log(distance to Río Trancura) and the 0.5 log(average distance to Río Correntoso and Molco) and the 0.5 log(distance to shore) (adapted from Bertrand et al., 2010). Distances to Río Molco and Correntoso and shores were given half weighting to account for their smaller contribution to the total sediment supply compared to Río Trancura. We used the logarithm of the distance to account for the globally exponential decrease of sediment accumulation rate with increasing distance to the source (Schiefer, 2006). The C/N ratios of the 9 surface sediment samples show a very good correlation (Pearson correlation coefficient r = -0.934 and the probability $p < 0.001$) between the C/N ratios of the surface sediment samples and the distance to the distance to river and shore index (Figure V-1). This demonstrates that the lake sediment further away from the rivers mouths and the shores contains more aquatic and less terrestrial organic matter. A similar conclusion can be drawn when plotting the C/N ratio versus the $\delta^{13}C$ values (Figure V-2). Here we see that the surface sediment at the locations of VB8, VB9, VB11 and VILL

Table V-1: The measurement results of the sediment samples. The first 9 are lake-sediment surface samples, the last one is a soil sample. ALST=annual lake-water surface temperature, MAAT=mean annual air temperature

Sample name	LOI_{550} (%)	$\delta^{13}C$ (‰)	TOC (%)	C/N (atomic)	TEX_{86}	BIT	MBT	CBT	Calculated parameters using the GDGT measurements		
									ALST (°C)	Soil pH	MAAT (°C)
VB1	4.12	-27.9	1.78	17.65	0.407	0.612	0.223	0.963	12.05	6.23	-3.98
VB2	6.42	-28.7	2.78	15.22	0.421	0.336	0.194	0.789	12.85	6.69	-3.79
VB3	9.59	-28.4	4.07	13.81	0.431	0.230	0.190	0.704	13.38	6.91	-3.20
VB4	9.41	-28.5	3.86	14.59	0.423	0.267	0.186	0.674	12.96	6.99	-3.09
VB8	13.57	-29.6	4.94	10.13	0.441	0.147	0.162	0.702	13.95	6.92	-4.56
VB9	12.69	-29.	4.61	10.58	0.434	0.170	0.160	0.700	13.55	6.92	-4.64
VB10	4.07	-27.8	1.36	13.13	0.445	0.175	0.204	0.805	14.16	6.64	-3.45
VB11	11.74	-28.7	4.03	10.01	0.444	0.149	0.159	0.755	14.13	6.78	-5.22
VILL	12.51	-28.3	3.82	9.55	0.417	0.312	0.153	0.622	12.63	7.13	-4.27
Soil	9.68	-26.1	2.60	17.81	0.587	0.973	0.637	0.814		6.62	18.13

Table V-2: The measurement results of the suspended matter present in the river-water and lake-water samples

Sample name	TEX_{86}	BIT	MBT	CBT	Calculated parameters using the GDGT measurements			Parameters of the water measured with a multimeter		
					ALST (°C)	Soil pH	MAAT (°C)	Water temperature (°C)	pH	Conductivity (µS)
Río Trancura	0.464	0.958	0.268	1.068		5.95	-2.69	9.80	6.67	20.17
Río Trancura 2	0.520	0.972	0.257	1.053		5.99	-3.08	9.30	6.45	23.55
Río Trancura 3	0.525	0.976	0.305	1.012		6.10	-0.29	9.90	6.71	19.68
Río Maichín	0.490	0.984	0.255	0.979		6.19	-2.49	8.80	6.66	19.40
Ojos de Caburgua	0.481	0.915	0.287	0.863		6.49	0.16	10.30	6.74	53.10
Río Liucura	0.449	0.986	0.267	1.053		5.99	-2.60	9.80	6.75	26.42
Río Claro	0.481	0.960	0.282	0.975		6.20	-1.12	9.70	7.07	22.44
Estéro Molco	0.513	0.951	0.286	0.988		6.16	-1.01	10.30	7.00	93.20
Estéro Carmelito	0.560	0.877	0.372	0.973		6.20	3.40	12.10	6.55	13.10
Estéro Las Ranas	0.542	0.985	0.259	1.053		5.99	-3.02	13.30	6.45	34.70
Lake surface water	0.394	0.169	11.345	0.333	11.35	6.42	2.22	14.50	7.12	48.70
-5m	0.358	0.118	9.315	0.360	9.31	6.85	5.12	14.70	7.25	48.40
-10m	0.354	0.127	9.092	0.292	9.09	6.11	-0.92	14.60	7.31	45.30
-15m	0.373	0.132	10.163	0.428	10.16	6.74	8.12	14.30	7.17	47.40
-20m	0.369	0.119	9.969	0.332	9.97	6.59	2.79	14.40	7.20	38.50
-25m	0.366	0.117	9.775	0.348	9.78	6.61	3.67	14.40	7.20	38.30
-30m	0.356	0.078	9.238	0.337	9.24	6.66	3.28	13.80	7.04	37.60
-40m	0.370	0.081	10.003	0.294	10.00	no value	no value	13.70	7.03	36.70
-60m	0.417	0.085	12.590	0.196	12.59	6.25	-5.25	14.30	7.30	38.40
-80m	0.413	0.054	12.370	0.274	12.37	6.11	-1.81	10.80	7.11	35.30

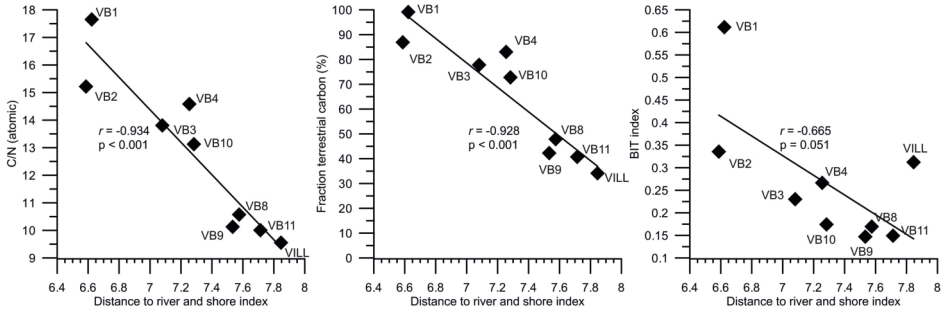

Figure V-1: Relation between the fraction of terrestrial carbon contained in the surface sediment samples of Lago Villarrica and the distance to river and shore index

only contains organic matter of aquatic origin. The data from the other locations indicate a mixture of organic matter from land vegetation with organic matter derived from phytoplankton. Organic matter originating from land vegetation has a less negative $\delta^{13}C$ value than phytoplankton, but a higher C/N ratio than the organic matter from the phytoplankton.

Having measured the C/N ratio of the lake sediment at different locations and also the C/N ratio of a soil sample in the Lago Villarrica catchment, a mixing equation (Equation V-1) can be constructed to estimate the relative contribution of the aquatic and terrestrial sources of organic matter. It is better to use the N/C ratio in this equation, because by using the C/N ratio the terrestrial fraction of organic carbon tends to be overestimated (Perdue and Koprivnjak, 2007).

To apply this equation an aquatic and a terrestrial end member need to be selected. For Lago Puyehue Bertrand et al (2010) opted to select the N/C value (0.069) of the palaeosol as the terrestrial end member. Consequently, for Lago Villarrica we use the N/C ratio (0.056) of the soil sample. Following Bertrand et al (2010) for the aquatic end member, the N/C value of VILL (0.104) would be chosen as the aquatic end member. On the other hand, the BIT index of VILL indicates that some terrestrial material reaches this location, implying the organic input at this side is not entirely of aquatic origin. Lago Puyehue and Lago Villarrica are lakes with very similar settings: 1) both lake basins have a comparable size and shape; 2) both lakes have a catchment area of a similar dimension; 3) these lakes also have a lake catchment with a similar geology, vegetation and climate. The Lago Puyehue aquatic end member has a higher N/C ratio (and consequently a lower C/N ratio) indicating a lesser influence of terrestrial carbon, than is the case for the surface sediment sample VILL in Lago Villarrica. Consequently, the value of the aquatic end member of Lago Puyehue (0.13) was chosen as the aquatic end member in Lago Villarrica.

$$F_T = \frac{(N/C)-(N/C)_A}{(N/C)_T-(N/C)_A}$$

(Equation V-1)

F_T = fraction of terrestrial organic carbon
$(N/C)_A$= aquatic end member
$(N/C)_T$= terrestrial end member

Since the calculation of the fraction of terrestrial organic carbon is based on the C/N values of the samples, it is logical that the correlation between this fraction and the distance of samples from the shore and rivers is also very good (r = -0.928 and $p < 0.001$) (Figure V-1).

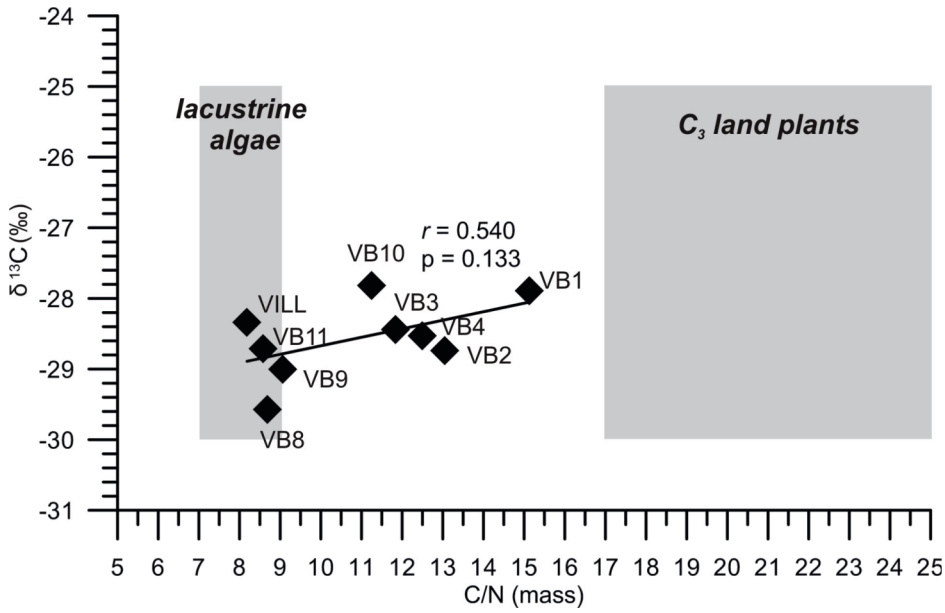

Figure V-2: Scatterplot of C/N (mass ratio) versus $\delta^{13}C$ of the surface sediment (the boundaries of the organic matter sources are according to Meyers and Teranes, 2001)

V.1.1.2. Biomarkers: TEX_{86} and BIT

The BIT index was measured on the same surface sediment samples, but also on the suspended matter in river and lake water samples. The BIT values of the river water samples are all high (>0.87) (Table V-2). The length of the river (short or long), size of the catchment (large or small) or the type of area they drain (a volcano flank or a moraine) do not seem to influence the BIT value. The Río Trancura effluents tend to have a slightly higher BIT index than the Río Trancura water where it is about to enter the lake. Although the BIT index of the surface samples should represent, like the C/N ratio, a proxy for the fluvial input of terrestrial organic matter (Hopmans et al., 2004), the correlation (r = -0.665 and p = 0.051) between this index and the distance to river and lake shore index is not as good as the correlation with the C/N ratio or the fraction of terrestrial carbon (Figure V-1). The probability of this correlation is ca. 5%, which is on the limit of being statistically significant. Branched GDGTs, which are used in the calculation of the BIT index are thought to be produced by anaerobic terrestrial bacteria (Sinninghe Damsté et al., 2000; Weijers et al., 2006a; Weijers et al., 2006b; Weijers et al., 2009), and therefore considered to be of a terrestrial origin. It has, however, recently been brought up by other researchers that there might be an in-lake production of branched GDGTs, leading to incorrect interpretation of the BIT index (Tierney and Russell, 2009).

The BIT index and the TEX_{86} index show a linear relationship with both C/N and the fraction of terrestrial carbon, calculated by Equation V-1 (Figure V-3). Although the correlation between the BIT index and the C/N values is good (Pearson correlation coefficient r = 0.747 and the probability p = 0.021), the correlations of the BIT index with the fraction terrestrial carbon is less reliable. The correlation between TEX_{86} and C/N and fraction terrestrial carbon is not reliable as well. Data from the VILL sample are always outliers (Figure V-3). VILL is also the only lake sediment sample that was from the western part of the Villarrica lake basin, which is

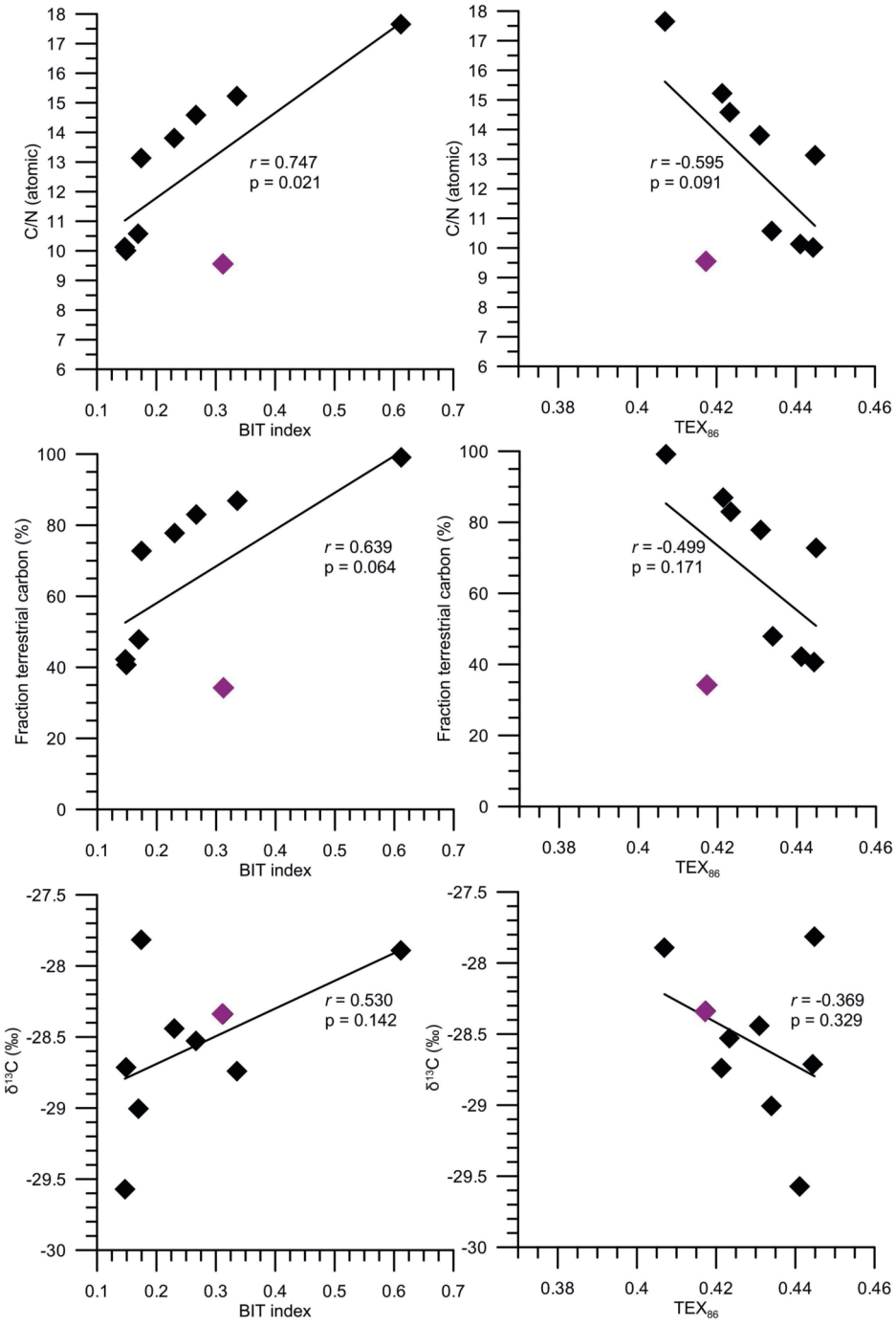

Figure V-3: Scatterplots of the BIT and TEX_{86} index of the surface sediment samples versus C/N, fraction terrestrial carbon and $\delta^{13}C$. The purple diamond represents the surface sample VILL taken on the location of the long sediment core. The trend line and its r and p value were calculated using all surface sediment samples.

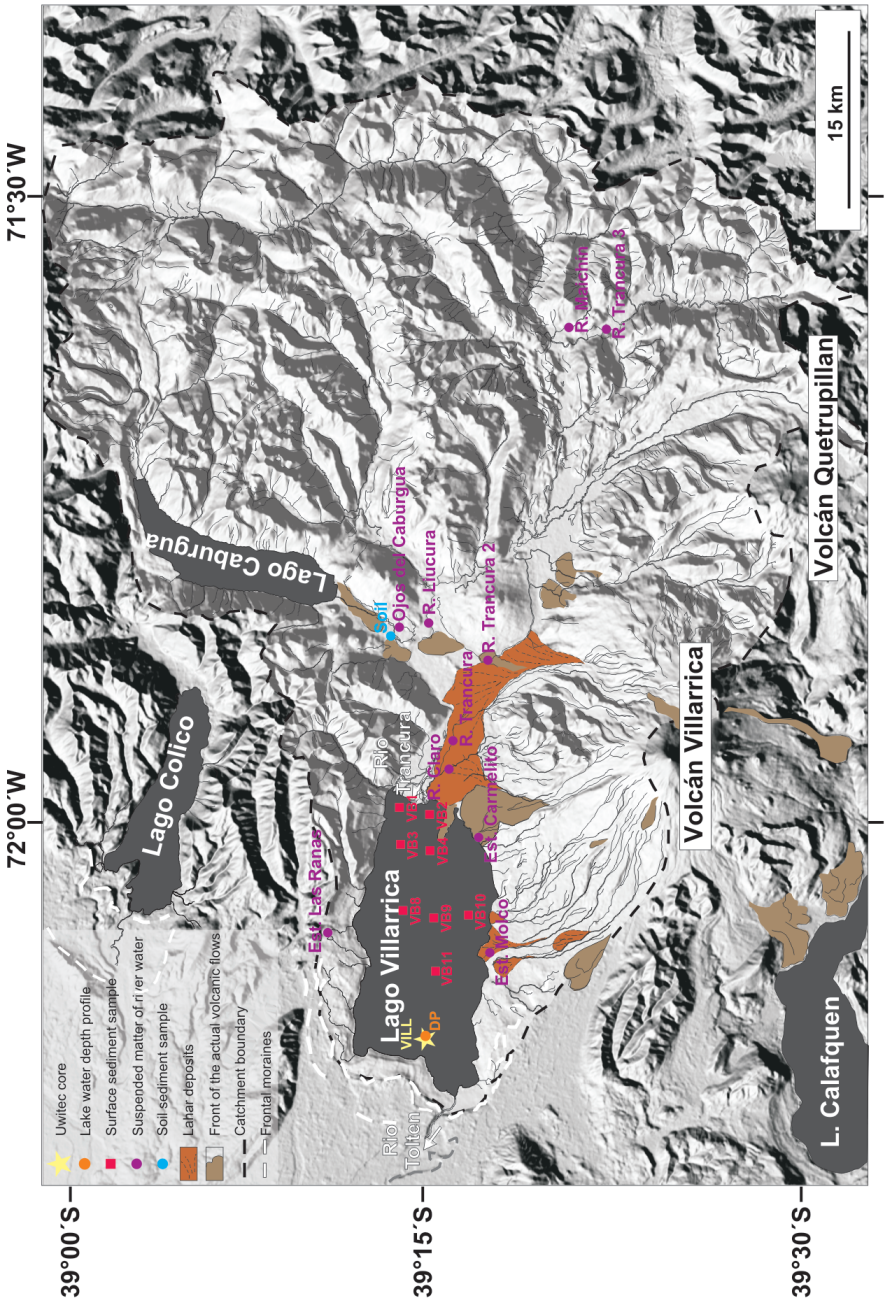

Figure V-4: Location of the surface sediment samples, soil sample and river and lake water samples taken in Lago Villarrica and its catchment. The three main, permanent rivers are indicated in black.

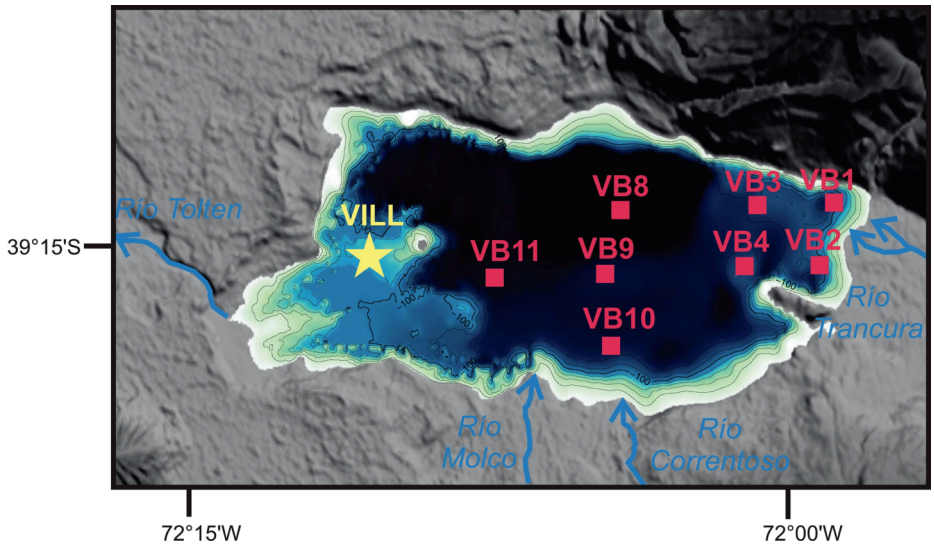

Figure V-5: Bathymetric map of Lago Villarrica (combination of SHOA data and bathymetry derived from seismic data) with the location of the surface sediment samples and the main, permanent rivers. Detailed information on the bathymetry and the scale can be found in Figure II-10

much shallower and has a more complex morphology than the rest of the basin (Figure II-10 and Figure V-5). Although there are no rivers flowing into the lake in this area, which could bring more terrigenous material to the VILL site, there might be some coastal erosion caused by wave action. Generally, the prevailing winds are from the WSW, but occasionally, strong easterly winds, known as *Puelche*, flow down the Andean slopes affecting the foothills, including the Villarrica area (Meruane et al., 2005). *Puelches* occur mostly in summer and have high wind speeds. The maximum observed speed value in the austral summer of 2003-2004 was 13 m/s (Meruane et al., 2005). They strongly affect the lake's thermal structure (Meruane et al., 2005) and the large waves created by these *Puelche* winds have a significant impact on the western coast line of Lago Villarrica as was observed in the field. It is thus not unlikely that the sediment released by this coastal erosion are transported into the lake and deposited on the western plateau.

There is no clear correlation between $\delta^{13}C$ and the BIT index or the TEX_{86} index (Figure V-3). Considering the 0.56‰ error on the $\delta^{13}C$ measurements and the limited spread of the $\delta^{13}C$ results of the samples (ca. 1.5‰), the significance of these correlations is questionable.

Campos et al. (1983) measured an annual lake-water temperature of the surface water of Lago Villarrica of ca. 14°C. The lake-water temperature reconstruction based on the TEX_{86} values of the surface sediment samples is broadly similar to measured values (Table V-1), with reconstructed temperatures ranging between 12.05 and 14.16°C. When comparing this value to the observed value of Campos et al. (1983) this seems a correct estimate, especially since the calibration equation for lake-water temperature reconstruction range between 3 and 5°C (Powers et al., 2010). In this study, we used the calibration equation of Blaga et al. (2009) (Equation III-6), since the calibration equation of Powers et al. (2010) tends to underestimate the lake temperature by 5°C or more. The lake

data set of Blaga et al. (2009) incorporates many European Alpine lakes, which are located in a very similar setting as Lago Villarrica, whereas the data set of Powers et al. (2010) includes lakes from all over the world with a wide variety of temperature regimes.

Samples with a lower BIT index tend to give a better estimate of the lake-water temperature. Nevertheless, the reconstructed, estimated lake water temperature of VB1 (12.05°C), which has a very high BIT index, is not that exotic. It gives about the same value as samples with a BIT value between 0.3 and 0.35 (12.6 and 12.9°C). Although it is advised not to use samples with a BIT index of >0.4 to reconstruct the surface-water temperature (Weijers et al., 2006), here we consider all lake-water temperature reconstructions, independent from the BIT index, in good in agreement with instrumental observations and well within the range of the error. The temperature reconstruction based on the suspended matter in the lake-water taken at different depths at the VILL location tend to underestimate the lake water temperature, even though their BIT values are very low (Table V-2). Furthermore, GDGT compounds measured from the VILL site tend to differ from the other GDGT-based measurements elsewhere in the lake. Again, the difference between the VILL site and all other sampling sites is probably related to the location of this site, on an elevated platform with complex morphology.
Since no soil pH was directly measured, we do not know if the GDGT-based pH reconstructions are reliable.

Almost all the mean annual air temperature (MAAT) reconstructions derived from the lake-sediment samples and from the suspended matter from lake and river water differs significantly from the observed mean annual air temperature which is known to be ca. 12°C (Table V-1 and Table V-2). Only the MAAT reconstruction of the soil sample approaches the real value (Table V-1). In lake sediments the straightforward application of MBT/CBT as palaeoproxies for soil pH and MAAT may be difficult given the uncertainties regarding the source and origin of branched GDGTs (Blaga et al., 2010). Branched GDGTs might not only be formed in soils and these branched GDGTs which reach the rivers and finally the lake can thus be a mixture of a soil source and an unknown other source.

V.1.2. VILL Core Lithological Description

The sediment of the VILL long core is mostly silt sized and of a greyish-olive colour. It is generally medium to finely laminated or faintly laminated (Figure V-6). Intercalated within the silty sediment are 62 black, sandy tephra layers/laminae of which 49 are thinner than 1 cm. The tephras are more or less equally distributed all over the core. Because of the proximity of Volcán Villarrica, which is considered one of the most historically active volcanoes of the entire Andean chain (>30 reported eruptions since 1552), it is not unlikely that most of the tephras can be attributed to a Villarrica eruption. Except for one thick tephra sequence at 535-600 cm, the eruptions do not seem to affect the lake sedimentation process directly above the tephra deposit. The deposit between 535 and 600 cm is probably the result of the Pucón Ignimbrite eruption (Silva Parejas et al., 2010). This eruption is considered to be the largest volcanic event of this volcano in the Holocene and has been associated with the partial collapse of the stratocone and the generation of pyroclastic flows (Clavero and Moreno, 1994; Silva Parejas et al., 2010). The assumption that this deposit represents the Pucón ignimbrite eruption is based on the facts that i) it is the thickest tephra present in the core, and that ii) a similar sequence has been found on land (Silva Parejas et al., 2010) and in a very small lagune (Laguna Las Ranas) just north of Lago Villarrica (Abarzúa et al., 2010) and that iii) the radiocarbon date of the bulk sediment sample fits in the time frame of the eruption (ca. 3510

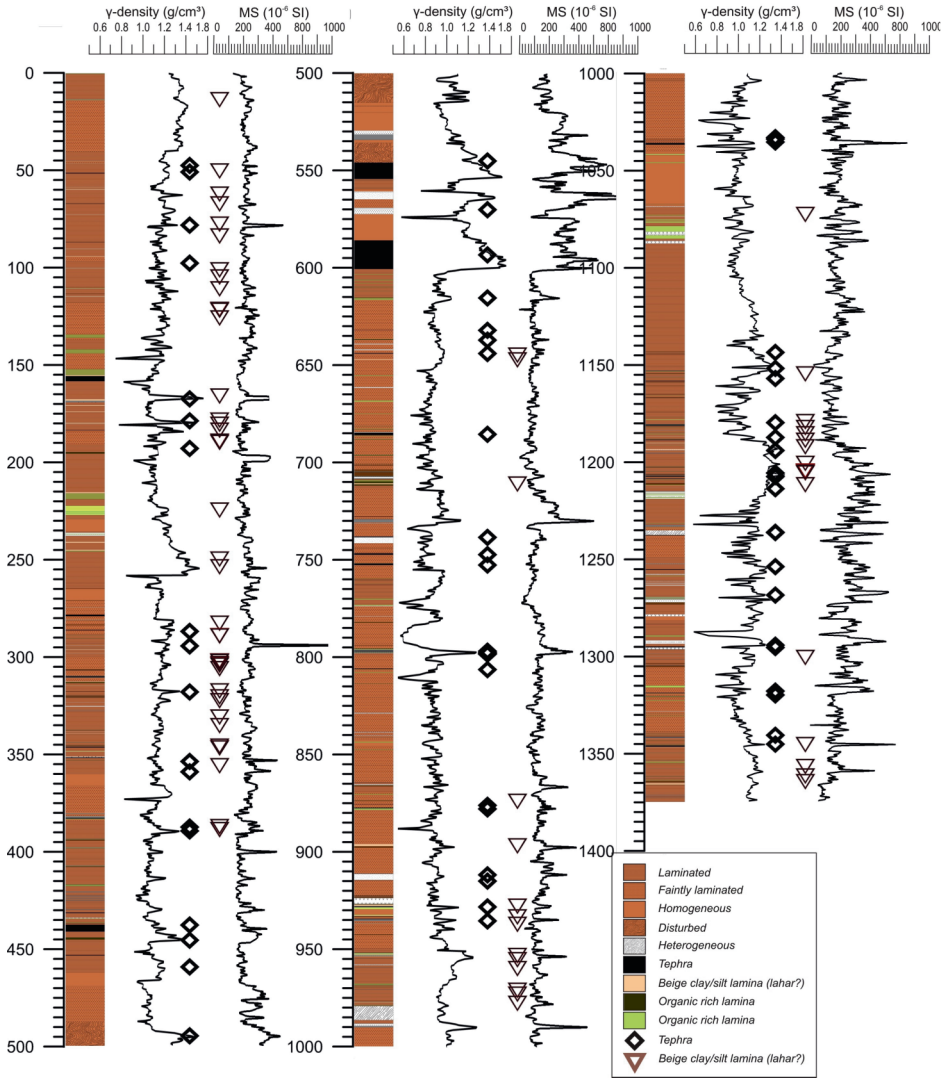

Figure V-6: Litholog of the VILL sediment core and the graph of variations in the density and magnetic susceptibility (MS) of the sediment.

± 60 ^{14}C cal a BP) (Silva Parejas et al., 2010).

Another remarkable aspect in the lithology of the VILL core is the presence of 72 beige coloured, silt to silt-clay sized laminae. Van Daele et al. (2010) identified these laminae as traces of lahars that originated from the Volcán Villarrica, by linking their characteristics and their stratigraphic position with historically reported lahar events. Unlike the tephras, these laminae are only present in certain intervals. They are very abundant between 0 and 390 cm, 644 to 710 cm, 873 and 987, 1155 and 1213 cm, 1301 and 1366 cm.

Smear-slide analysis revealed that the silty sediment mostly consists of diatoms (minimum 80%). The remainder of the material consists of volcanic glass shards, a very low amount of mineral grains (pyroxenes, quartz, ...) and organic matter and some clay minerals. The bulk XRD analysis of the Villarrica sediment was not successful. The XRD measurements were too close to the detection limit to be considered as a quantitative tool. They do, however, indicate the dominance of an amorphous material (e.g. volcanic glass or biogenic silica), making up min. 70% of the sediment, and this is probably even an underestimation of the real value, thereby confirming the smear-slide results.

V.1.3. Age-Depth Model

Eighteen samples (16 bulk sediment samples and 2 pieces of wood) were sent off for radiocarbon dating (Table III-2 and Table V-3).

The age discrepancy between the radiocarbon ages of the wood samples and the bulk sediment samples at the same core depth identified certain issues. If we assume the ages of the wood samples to be correct, the radiocarbon ages of the bulk sediment samples are too old. The assumption of the correctness of the wood samples was corroborated by the VILL core (VILLSC02 is a gravity core taken at the same location as the VILL long core) with the VILLSC01 gravity core, which was taken in another location in the lake in the context of a for palaeoseismological study (Moernaut, 2010). VILLSC01 contains a series of event deposits related to historical earthquakes, with horizons representing the mega-earthquakes of

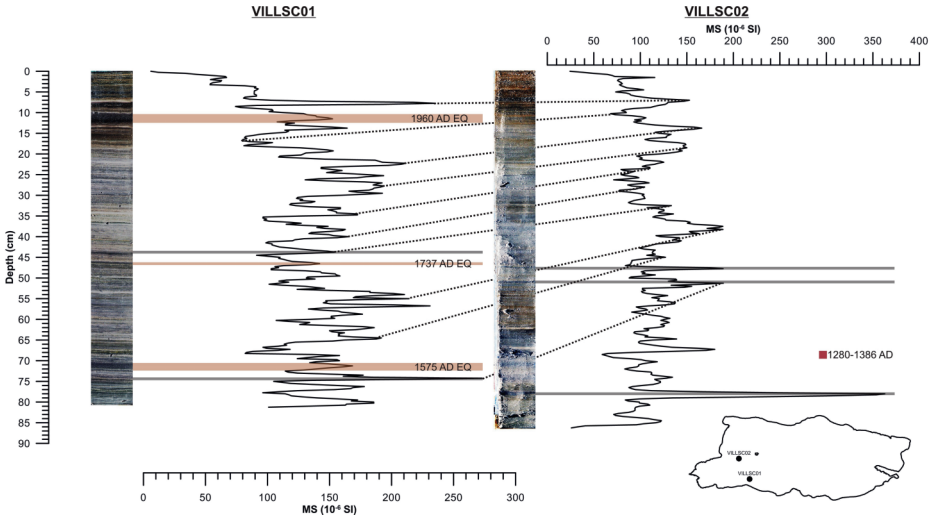

Figure V-7: Correlation between VILLSC02 (gravity core of the VILL core sequence) and VILLSC01

Table V-3: The radiocarbon ages of the 18 samples and their minimum and maximum calibrated value (2σ range) using the ShCal04 curve (McCormac et al., 2004). The samples with an asterisk (*) are wood samples, these radiocarbon ages were not corrected. The remaining 16 samples are bulk sediment samples, a correction term of 834 ^{14}C a was subtracted of their radiocarbon age and the error of the correction term of 186 ^{14}C a was added to the error of the radiocarbon ages. The sample printed in a grey colour is considered an outlier was excluded from the age-depth model.

Sample name	Sample depth (cm)	Radiocarbon age (^{14}C a BP)	Error (1σ) (^{14}C a BP)	Corrected radiocarbon age (^{14}C a BP)	Corrected error (1σ) (^{14}C a BP)	2σ error range calibrated ages (cal a BP)
VILL VSC1-0	0.5	225	100	modern	286	-286–502
VILLSC02-68*	*68.5*	*720*	*25*	*720**	*25**	*560–666*
VILLSC02-68	68.5	1360	25	526	211	-2–797
VILL1-TEST-I-59	84.05	2350	30	1516	216	958–1865
VILL TESTI-73	98.05	2600	30	1766	216	1183–2290
VILL1-TEST-II-49	156.8	2670	35	1836	221	1291–2305
VILL2B-I-102	279	3160	35	2326	221	1741–2842
VILL1C-I-105	390.45	4140	40	3306	226	2887–4084
VILL1C-II-56	448.7	4380	35	3546	221	3265–4419
VILL1D-I-66	616.6	4530	30	3696	216	3413–4571
VILL2D-II-57	770.25	6620	35	5786	221	6017–7156
VILL1E-I-12	779.4	5260	45	4426	231	4411–5593
VILL 1EI-W*	*779.9*	*4445*	*35*	*4445**	*35**	*4851–5260*
VILL1E-II-32	890.9	5290	50	4456	236	4416–5604
VILL 1EII-93	951.9	5450	90	4616	276	4525–5898
VILL1F-I-89	1039.4	6560	45	5726	231	5939–7147
VILL1G-I-7	1196.45	7370	45	6536	231	6806–7826
VILL 1GII-93	1374.55	9330	110	8496	296	8649–10200

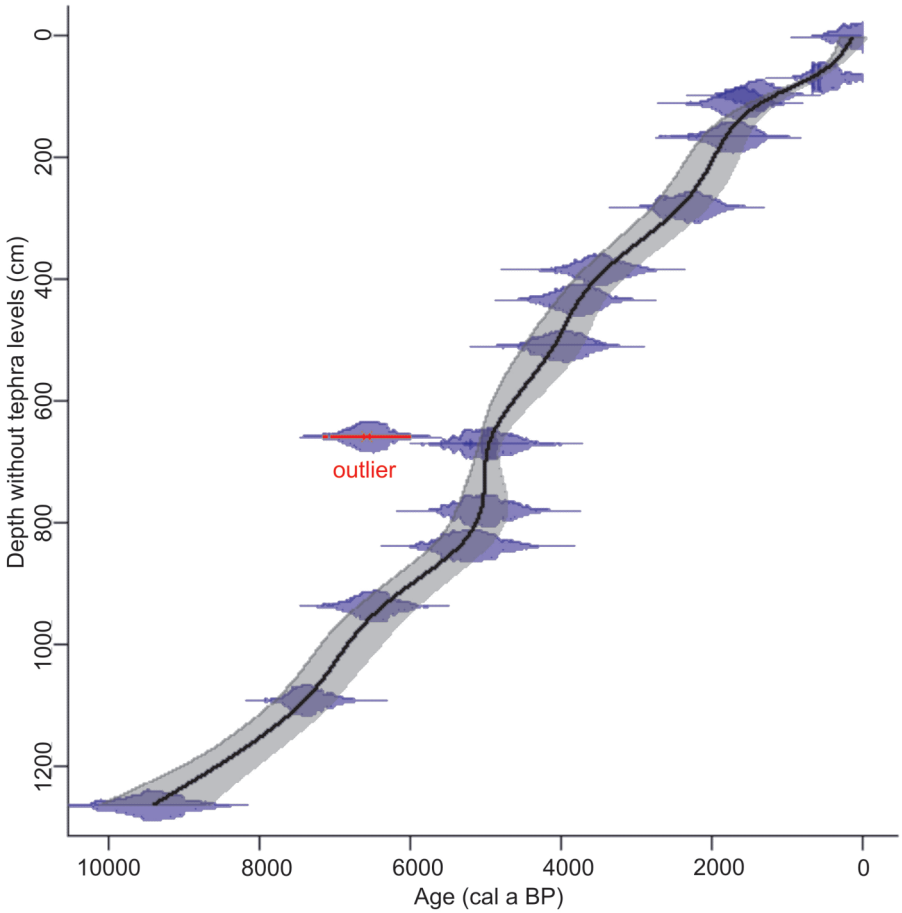

Figure V-8: Age-depth model of the VILL sediment core using Blaauw's Clam software (2010). To calculate this model all tephra levels were first removed, therefore reducing the core length with more than 1 m. One radiocarbon age was considered an outlier. The grey band around the black age-depth model, indicates the 2σ error.

1960 and 1575 AD. Using these events horizons and the tephra layers as markers, the radiocarbon age from the wood sample at 68.5 cm could be confirmed (Figure V-7).

Another time marker is the thick tephra deposit between 535 cm and 600 cm. This is the largest tephra deposit present in the core. It corresponds most likely to the Pucón eruption, the largest, explosive outburst of Volcán Villarrica in the Holocene (Silva Parejas et al., 2010). Silva Parejas et al. (2010) dated this eruption at several locations around Lago Villarrica at ca. 3510 ± 60 ^{14}C a BP. This same tephra deposit is also present in Laguna Las Ranas, where it was dated to be at 3670 ± 20 ^{14}C a BP (Abarzúa et al., 2010). To assess the ^{14}C offset of the bulk sediments, the age difference between the two wood-bulk sample levels was calculated, as well as the age difference between the bulk sediment age of the Pucón tephra in the VILL core and the available ^{14}C ages of Silva Parejas et al. (2010) and Abarzúa et al. (2010). The four age differences, ranging between 640 and 1020 year, resulted in an averaged age difference of 834 ± 186 ^{14}C years. This difference was used as a local reservoir correction from bulk sediment ages and was subtracted from all the bulk sediment

age data.

The bulk sediment ages are most likely too old, because of 'old' carbon from soil material and decayed organic matter washed into the lake (Björck and Wohlfarth, 2001). In addition, the constant release of volcanic CO_2 in the atmosphere may affect the isotopic carbon values of plants nearby the volcanic centre, resulting in radiocarbon ages which can be up to 5000 years too old (Calderoni and Turi, 1998).
All tephra levels were removed when constructing the final age-depth model, since ash-fall deposits can be considered as (quasi) instantaneous deposits, likely deposited in a few days to weeks. All radiocarbon ages were calibrated using the SHCal04 Southern Hemisphere calibration curve (McCormac et al., 2004) using the Clam software of Blaauw (2010). The same software was used to create the age-depth model. One radiocarbon age was considered an outlier, since the radiocarbon age created an age reversal in the age-depth model. The model was generated using a smooth spline (error-weighted with smoothness set at 0.3) (Figure V-8 and Figure V-9). This age-depth model was chosen, because it respects the age ranges of most of the radiocarbon samples best. Since all the ages (except one) are in stratigraphic order, the sudden shifts in sedimentation rate resulting from the age-depth model can be considered real.

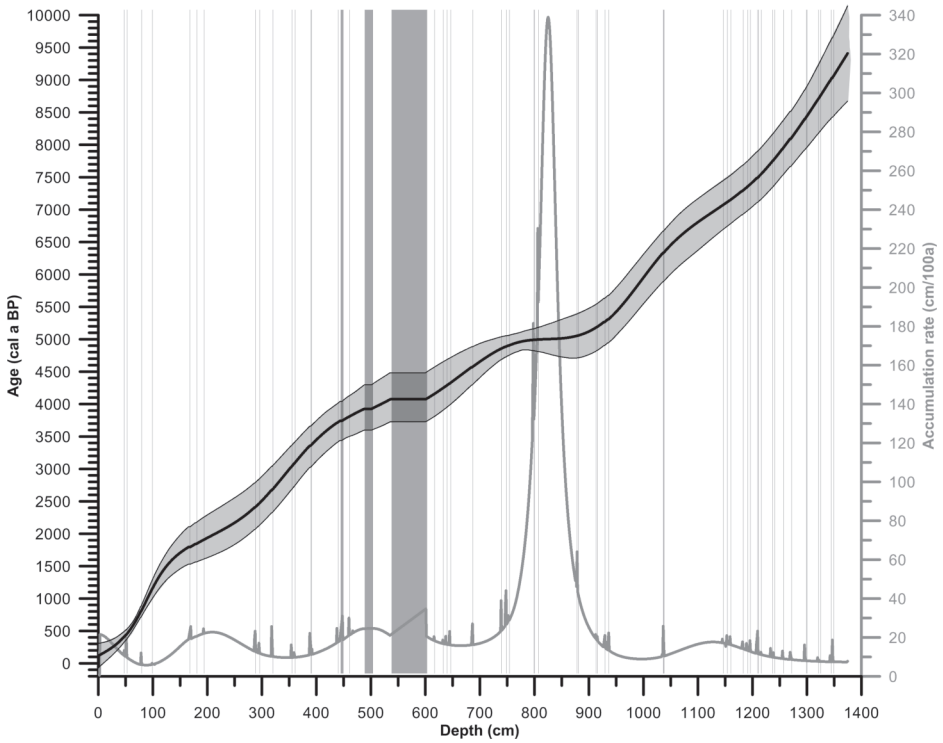

Figure V-9: The age-depth model with the previously removed tephra levels (grey bars). There is also a plot of the accumulation rate which demonstrates the variations in sedimentation rate throughout the core. The very sudden peaks can all be linked to the presence of a tephra deposit. The grey band around the black age-depth model, indicates the 2σ error.

V.1.4. Relative Palaeomagnetic Intensity Changes

V.1.4.1. Reliability of Sediments as Recorders of the Palaeointensity of the Geomagnetic Field

The successful extraction of a palaeointensity record from sedimentary cores depends on the fidelity of the NRM directional record, magnetic mineralogy and concentration, and grain size of the remanence carriers (Tauxe, 1993).

First, reliable palaeointensity estimates require uniformity of concentration of magnetic grains and magnetic mineralogy (Tauxe, 1993). The type of magnetic carrier was determined visually under a binocular. This revealed that magnetite is the dominant carrier of magnetic remanence in this core (Matthys, 2010). The variation in the concentration of magnetic minerals can typically be monitored by changes in the S-value (Equation III-7). The S-value indicates the quantity of high coercivity remanence versus low coercivity remanence. An S-value close to 1 indicates an important contribution of low coercivity minerals (e.g. magnetite), while a value close to 0 indicates the dominance of high coercivity minerals (e.g. hematite) (Evans and Heller, 2003). In the case of the VILL core the value approaches 1 very closely (Figure V-11). The S-value, however, is also dependent on the grain size of the magnetic minerals. When the grain size increases, the S-value will decrease (Stockhausen and Zolitschka, 1999).

Down-core homogeneity in grain size is an important factor for reliable estimation of the relative changes of palaeointensity of the geomagnetic field (King et al., 1983; Tauxe, 1993). The extent of the grain-size variations can be determined with a Banerjee plot (Banerjee et al., 1981) or a King plot (King et al., 1982) (Figure V-10). The steepness of the slope of the trend line in these plots estimates the average grain size, with steeper slopes representing finer grain sizes (Figure V-10). Palaeointensity studies are preferably performed on sediments with fine magnetic grains (Evans and Heller, 2003).

Both plots indicate that the majority of the magnetic grains has a grain size between ~5 and ~25 µm. If we plot the k_{ARM}/SIRM which were determined in

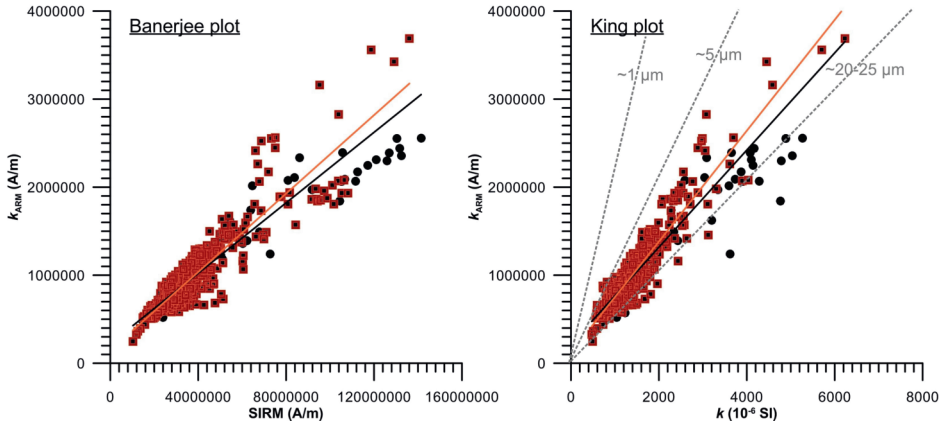

Figure V-10: Banerjee plot of the anhysteretic susceptibility (k_{ARM}) against the saturated isothermal remanent magnetisation (SIRM) and King plot of the anhysteretic susceptibility (k_{ARM}) against volume susceptibility (k). Lines of magnetic grain size estimates are based on experimental work by King et al. (1982)

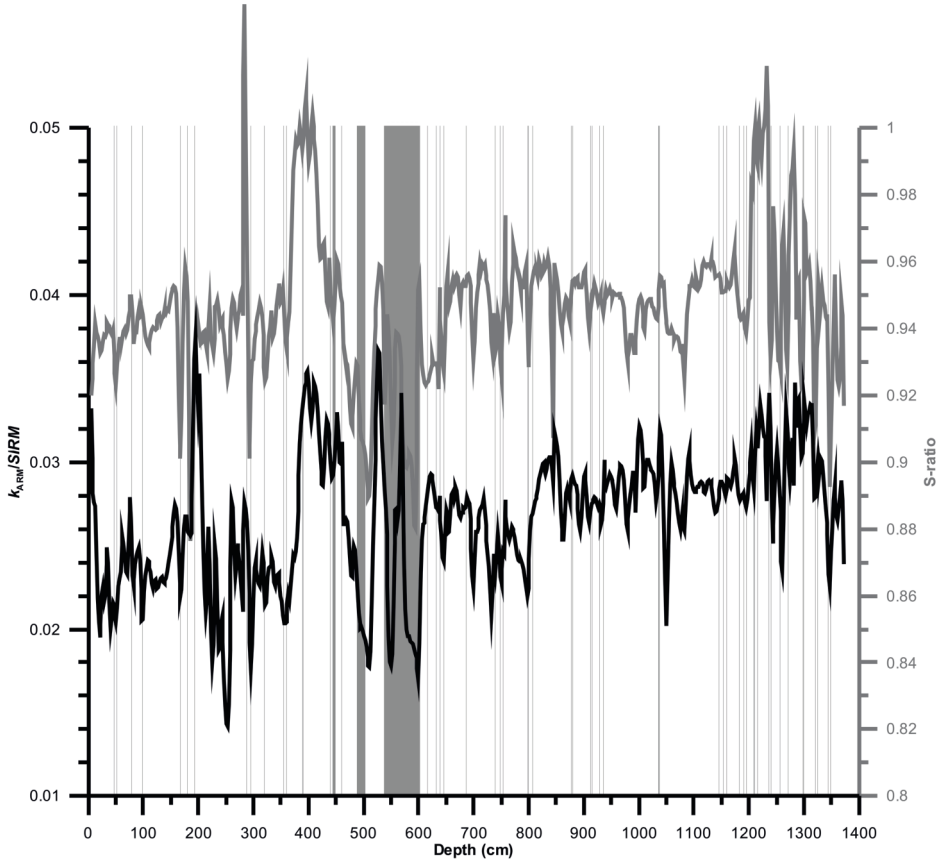

Figure V-11: Variation of the S-ratio and the k_{ARM}/SIRM ratio in relation to its depth in the Villarrica sediment core

the Banerjee plot versus depth, together with the S-value, the lower S-values correspond to lower k_{ARM}/SIRM values and both correspond most of the time to tephra levels (Figure V-11). In general, the tephra levels have a coarser grain size. The high S-ratio peak at 1200 cm corresponds to an interval with a higher clay percentage. The other S-ratio peak at 420 cm corresponds to the sediments deposited right after the Pucón Ignimbrite eruption.

The stability of the NRM was investigated by alternating field (AF) demagnetization. When the demagnetization curve approaches a straight line, the NRM is most likely carried by a detrital phase with a high magnetic stability and the NRM is defined by a remanence vector with only one component (Tauxe, 1998). The sequence of NRM values between 15 and 50 mT approaches this condition best (Figure V-12). Consequently, NRM values measured at 25 mT were used to determine the RPI. Furthermore, Zijderveld plots of this step-wise demagnetization show no changes in inclination and declination, except for minor changes associated with the Pucón Ignimbrite tephra (Figure V-13). Therefore, we consider that the Villarrica sediment records the geomagnetic field particularly well.

Not all tephra layers are good recorders of magnetic field directions (Gogorza et al., 1999; Gogorza et al., 2000a). Therefore, after identification of the tephra layers, and determination of the quality of their NRM values, they were

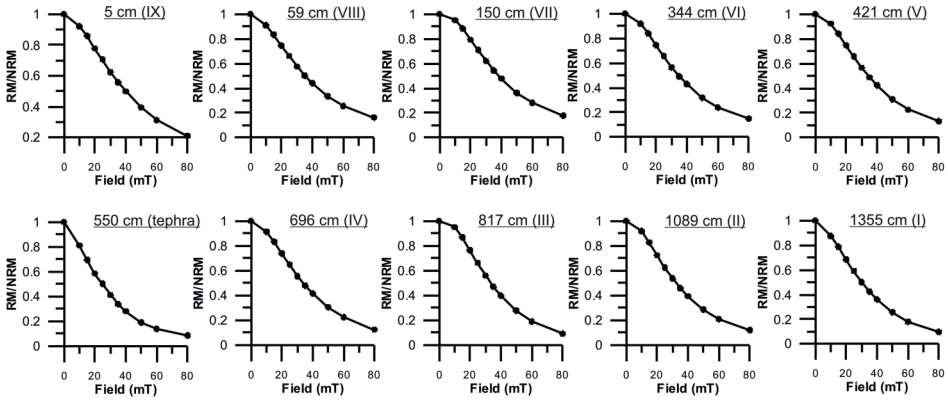

Figure V-12: Curves of progressive demagnetisation of representative samples from the Villarrica sediment core. Demagnetisation peak field steps are 10, 15, 20, 25, 30, 35, 40, 60 and 80 mT

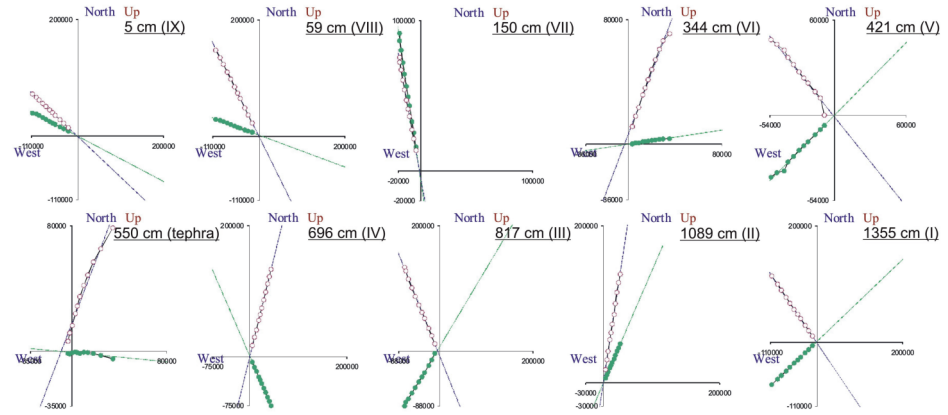

Figure V-13: Zijderveld diagrams of progressive demagnetisation of representative samples from the Villarrica sediment core. The orange, open and green, closed circles represent vector end points projected on the vertical and horizontal plane, respectively. Demagnetisation peak field steps are 10, 15, 20, 25, 30, 35, 40, 60 and 80 mT.

removed from the sequence if necessary.

The NRM_{25mT}, k and k_{ARM} values have very similar variations with increasing depth (Figure V-14). The highest values correspond to the sediments deposited immediately after the Pucón Ignimbrite eruption. Maximum angular deviation (MAD), which was calculated to monitor the quality of the NRM component directions, varies little. Most of the time the deviation is less than 3°. The levels were it is larger than 4° correspond to tephra layers. The relative declination and the inclination have clearly varied through time. (Figure V-14).

V.1.4.2. Relative Palaeointensity (RPI) Record

The Villarrica sediment fulfils the requirements for a successful extraction of a palaeomagnetic record. To construct the relative palaeointensity (RPI) variability the NRM_{25mT} values

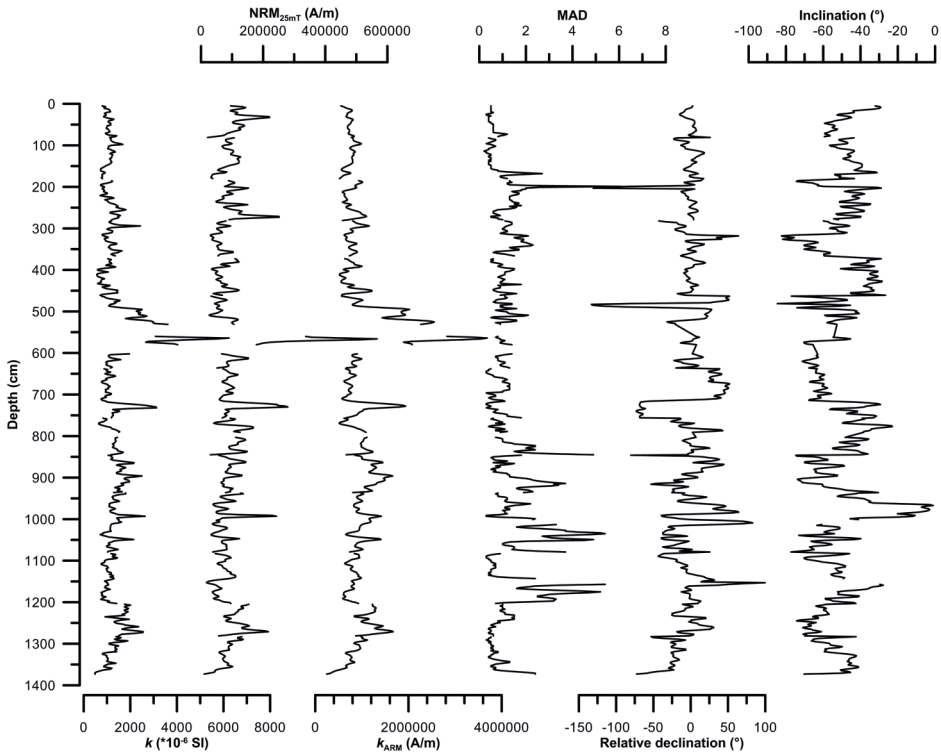

Figure V-14: Magnetic parameters (volume susceptibility k, intensity of NRM_{25mT} and anhysteretic susceptibility k_{ARM}) and directional data (maximum angular deviation MAD, relative declination and inclination) versus depth

were normalised by k_{ARM}. In fine-grained sediments, which is the case for the Villarrica sediments, kARM is the more appropriate normaliser (Gogorza et al., 2004).

The evolution of the RPI signal, defined by the relative declination and inclination is in good agreement with the overall trend of existing palaeomagnetic lake records from the region, i.e. from Lago El Trébol (41°S), Lago Escondido (41°S) and Lago Moreno (41°S) in Argentina (Figure V-15) (Gogorza et al., 2006; Gogorza et al., 2004; Gogorza et al., 1999; Gogorza et al., 2002; Gogorza et al., 2000a; Gogorza et al., 2000b; Irurzun et al., 2006). The average sedimentation rate in these three lakes is three times lower (0.5 mm/a), than the average sedimentation rate in Lago Villarrica (1.5 mm/a). Consequently the geomagnetic records of Lago Villarrica show a much higher variability. The changes observed in the Argentinian records always precede the changes in Lago Villarrica. The age-depth models of these three Argentinian lakes are also based on radiocarbon dating and the majority of the ages are obtained from bulk sediment (Gogorza et al., 2006; Gogorza et al., 1999; Gogorza et al., 2000a). The Lago El Trébol record is tuned to the record of Lago Escondido (Gogorza et al., 2006).

The Lago Villarrica record and the records of the Argentinian lakes can also be compared with RPI records of marine sediments in Antarctica (Brachfeld et al., 2000; Willmott et al., 2006) in order to expand the comparison of changes in RPI from a local to a regional scale. Geomagnetic changes are often

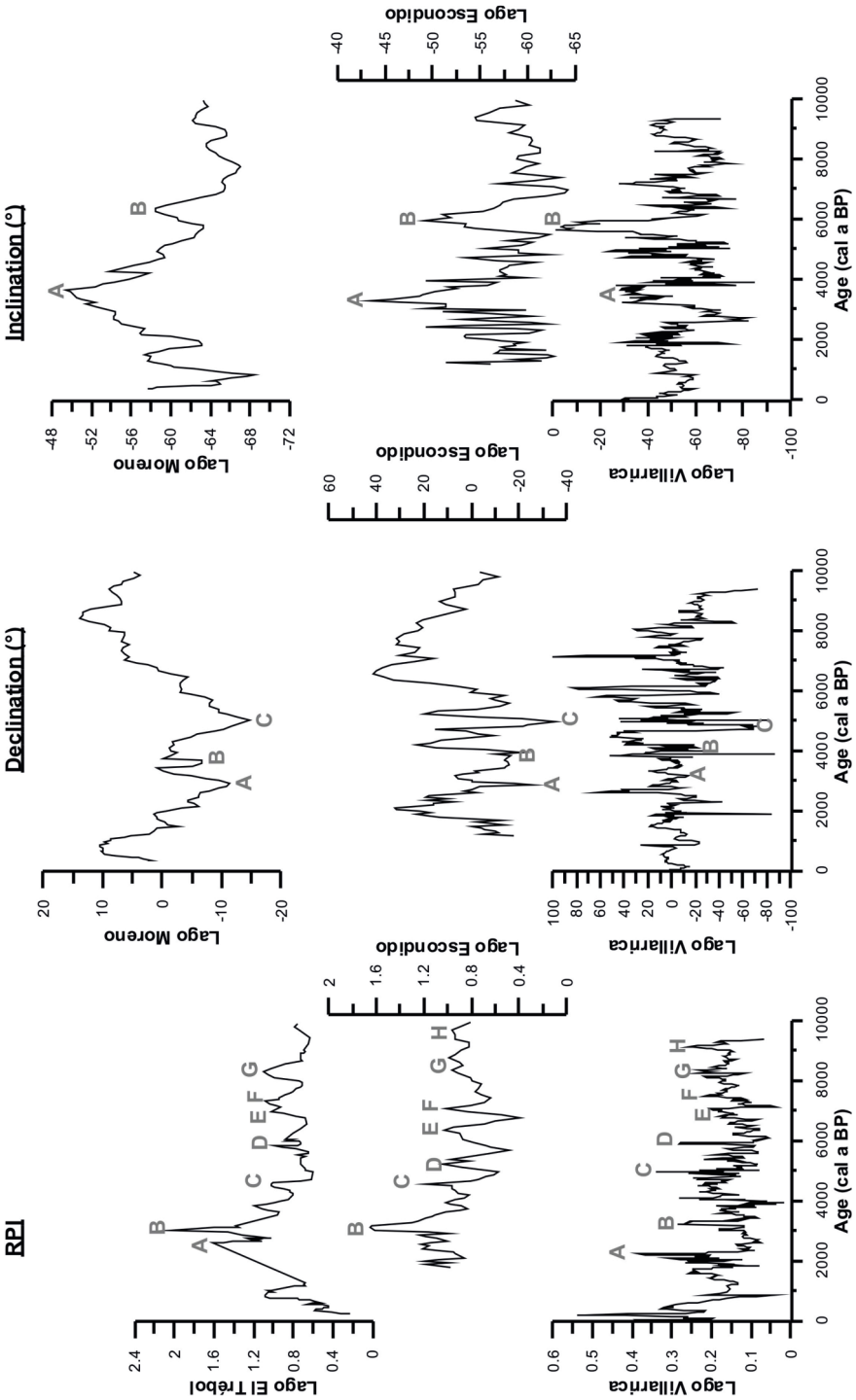

Figure V-15: Comparison of the Lago Villarrica RPI, relative declination and inclination records with the records of Lago Escondido (Gogorza et al., 1999; Gogorza et al., 2002), Lago Moreno (Gogorza et al., 2000a) and Lago El Trébol (Irurzun et al., 2006)

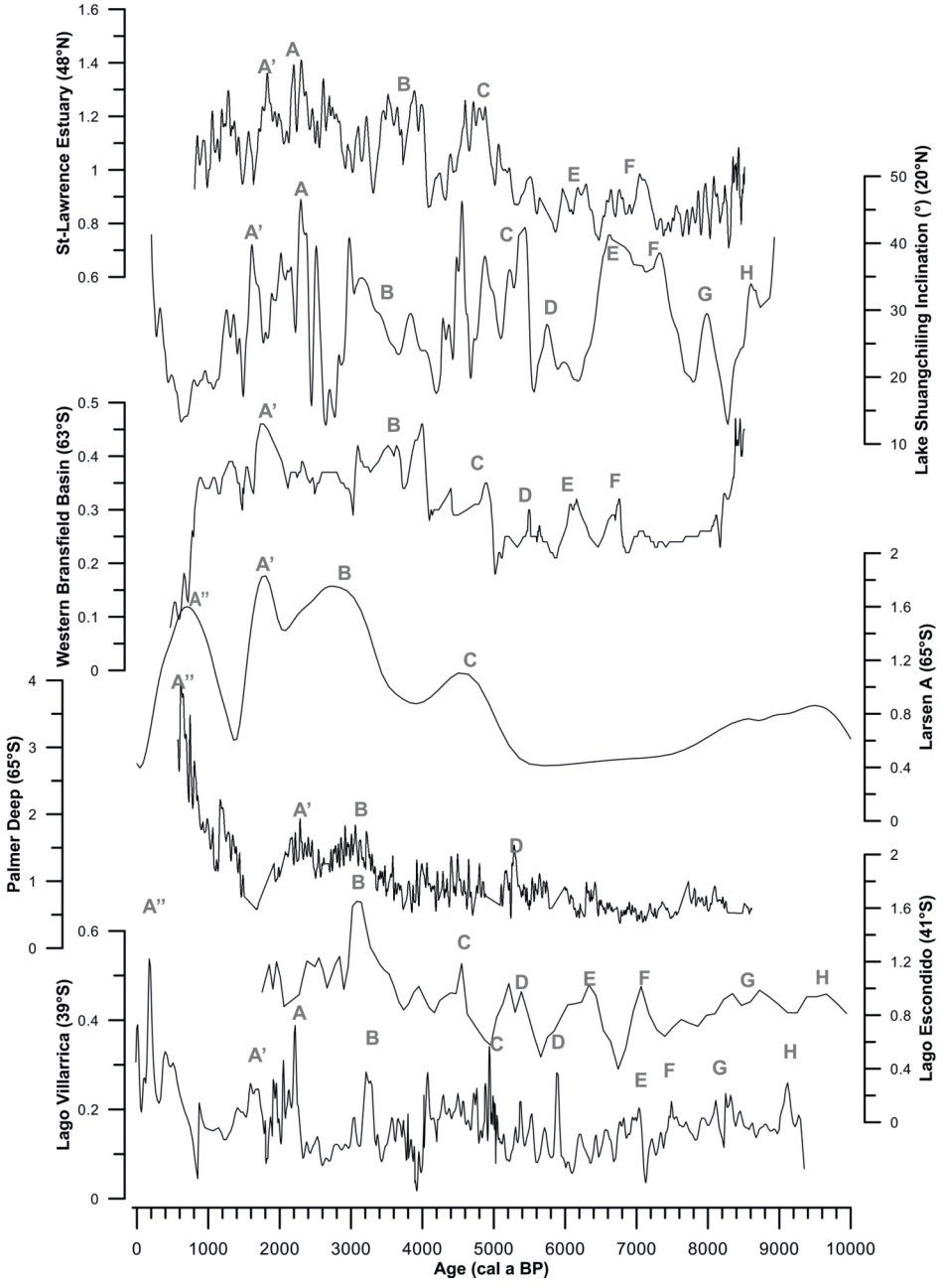

Figure V-16: Comparison of the Lago Villarrica RPI record (39°S) with RPI records from Lago Escondido (Argentina, 41°S) (Gogorza et al., 1999; Gogorza et al., 2002), of Palmer Deep (Antarctic Peninsula, 65°S) (Brachfeld et al., 2000), Larsen A area (Antarctic Peninsula, 65°S) (Willmott et al., 2006), Western Bransfield Basin (Antarctic Peninsula, 63°S) (Willmott et al., 2006), the inclination record of lake Shuangchiling (China, 20°N) (Yang et al., 2009) and the RPI record of the Saint-Lawrence Estuary (Canada, 48°N) (St-Onge et al., 2003)

considered to be global, so the Villarrica RPI record was also compared to the inclination record of lake Shuangchiling in China (Yang et al., 2009), a high-resolution record from lake sediments, and to the RPI record of the Saint-Lawrence Estuary (St-Onge et al., 2003), which is considered to be one of the best dated Holocene records (Figure V-16). The Antarctic records show an drastic RPI increase from a low value in the Early Holocene to high values in the Late Holocene. The Saint-Lawrence Estuary record shows a similar trend, but with a smaller amplitude. In all the lake records, both in South America and in China, this trend is less clear.

V.1.4.3. Possible Linkages between RPI and Cosmogenic Radionuclide Production

Geomagnetic field intensity together with solar activity plays a crucial role in the formation of cosmogenic radionuclides (e.g. Beer et al., 2002). Galactic cosmic ray particles produce radionuclides in the upper Earth's atmosphere by particle interaction, but the production rate is strongly modulated by the geomagnetic field and solar activity. The conditions for the cosmogenic radionuclide production are well understood (Masarik and Beer, 1999) and therefore past solar activity can be reconstructed knowing the production of the radionuclides and the geomagnetic field intensity through time (e.g. Vonmoos et al., 2006). It is widely accepted that long term fluctuations in geomagnetic field intensity significantly affect cosmogenic radionuclide production. It has, however, also been proposed that geomagnetic field changes on centennial time scales could contribute to the variability of the radionuclide production rate (Snowball and Sandgren, 2002; St-Onge et al., 2003). A possible linkage between geomagnetic palaeointensity and the production of cosmogenic radionuclides was investigated. The Villarrica RPI record is compared with the ^{10}Be record of the GISP2 ice core (Finkel and Nishiizumi, 1997). The RPI record was also plotted against the stacked drift ice index of Bond et al (2001). In this study they claim a persistent solar influence on the North Atlantic climate through a close correlation between the radionuclide production rate and percentages in ice rafted debris. Subsequently also the reconstructed, Holocene solar irradiance using the ^{10}Be measurements in ice cores (uncorrecting for geomagnetic variations) (Steinhilber et al., 2009) and an estimation of the 14C production rate based on the Δ^{14}C record of tree rings and a simple box model (Marchal, 2005) were added to the composite graph (Figure V-17).

The Villarrica RPI record correlates well with the above mentioned records. A decrease in RPI can be linked to higher ^{10}Be measurements in Greenland, to a higher ^{14}C production rate, to an increase in North-Atlantic IRD and a lower solar irradiance (Figure V-17). Especially the higher radionuclide production between 5000 and 800 cal a BP, corresponds to a period with low palaeointensities in Lago Villarrica. If the Villarrica RPI record truly reflects changes in the intensity of the Earth's magnetic field, then the assumption that millennial- and even some centennial-scale variations within the cosmogenic isotope production rate records are solely a function of solar variability (e.g. Bond et al., 2001; Muscheler et al., 2005; Steinhilber et al., 2009; van Geel et al., 1999) may have to be re-examined. Bond et al. (2001) showed that changes in drift-ice proxies within North Atlantic deep-sea cores correlate with changes in the production rate of cosmogenic nuclides during the Holocene. They suggested that the North Atlantic's millennial-scale climate variations were influenced and perhaps forced by solar changes. The Villarrica data show that variations of the geomagnetic field may have contributed to cause these cosmogenic nuclide changes and therefore might play a role in climate.

During recent years, considerable efforts have been made for compiling all

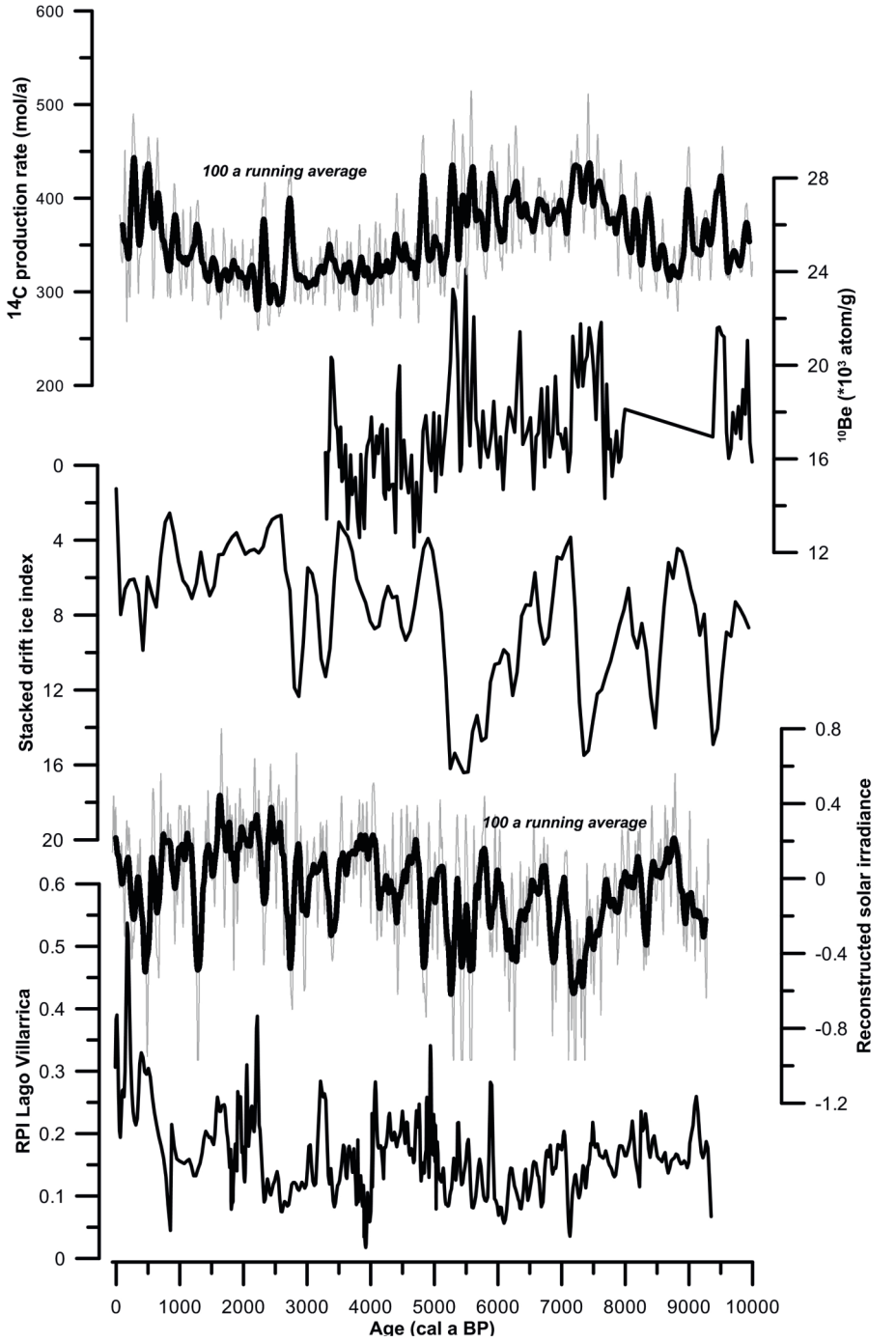

Figure V-17: Comparison between the estimated ^{14}C production rate (Marchal, 2005), the ^{10}Be concentrations in the GISP2 ice core (Finkel and Nishiizumi, 1997), the stacked drift ice index from the North Atlantic (this record is plotted inverse) (Bond et al., 2001), the reconstructed, Holocene solar irradiance (Steinhilber et al., 2009) and the Lago Villarrica RPI record

available data in order to construct a model of the global geomagnetic field behaviour during the Holocene (Korte and Constable, 2005; Korte et al., 2009). Thanks to these compilations it has been possible to overcome - to a certain extent - some of the problems typically associated with local records - such as local effects due to higher moments of the geomagnetic field, which influence individual records, 'analytical' noise in the reconstructions and random dating errors (Muscheler et al., 2007). The Southern Hemisphere is under-represented in these compilations compared to the Northern Hemisphere. Records like the Villarrica RPI record, help to fill that void, especially if the current age-depth model with its dating problems (e.g. 'old' carbon effects) could be improved in the future by involving additional dating methods (e.g. varve counting or tephrochronology).

V.1.5. VILL Long Core Sediment Proxy Variations

V.1.5.1. Bulk Organic Geochemistry of Modern Villarrica Lake Samples versus VILL Downcore Record

In general the $\delta^{13}C$ and C/N values of the VILL long core sediment point toward a predominantly aquatic origin of the organic matter (Meyers, 1997; Meyers and Teranes, 2001) (Figure V-18). This is corroborated by the smear-slide analysis, which shows that the Villarrica sediment mostly consists of diatom frustules. Although the surface sediment sample of the VILL site has the lowest, and therefore most aquatic, C/N value, its BIT index is higher than some of the surface sediment samples taken in the deep basin. When plotting the VILL long core sediment samples on the same plots as the surface sediment samples, they are almost always outliers (Figure V-19). This highlights again the concern that the location of the VILL core in the western, morphologically complex part of the basin, might influence the sedimentation pattern.

V.1.5.2. Particle Size Variations

The smear slide analysis already indicated the strong dominance of diatom frustules in the sediment of the Villarrica long core. The geometric mean particle size varies almost constantly between 20 and 25 µm and likely reflects the average size of the diatom frustules (Figure V-20). Overall, the particle-size distribution varies with depth (Figure V-21 and Figure V-20). The sediments' first mode shifts towards higher values between 760 and 80 cm. Between 760 and 600 cm and between 280 and 390 cm there is a shift of the first a hibher value, but within the interval the mode's value remains constant. The first mode's value is highly variable between 600 and 390 cm and 280 and 80 cm (Figure V-22). The interval between 600 and 390 cm comprised the Pucón Ignimbrite tephra and two other thick tephras. Most likely

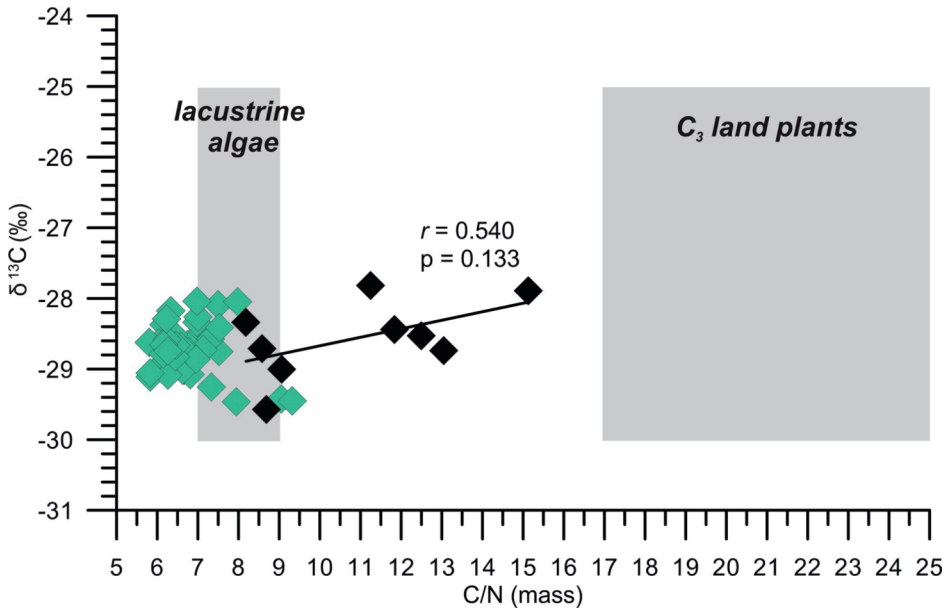

Figure V-18: Scatterplot of C/N (mass ratio) versus $\delta^{13}C$ of the surface sediment samples (black diamonds) and the VILL long core sediment samples (green diamonds) (the boundaries of the organic matter sources are according to Meyers and Teranes, 2001). The trend line has been calculated using only the surface sediment samples (black diamonds).

the volcanic eruption supplied a large amount of terrigenous material by airfall and later on by run-off, as the eruption likely affected the entire Lago Villarrica catchment (Silva Parejas et al., 2010). Due to this volcanic overprint, it is hard to deduce palaeoclimatic changes at these depths. Consequently the changes in this part of the core are not considered relevant to this study and are never discussed in great detail.

Using the changes in the first mode of the PSA distribution, the long core can be subdivided in 9 different units (Figure V-20 and Figure V-22). Unit I and II have about the same geometric mean PSA, and they both have an important clay and sand fraction (Figure V-22). The latter results even in the creation of a secondary mode in the PSA distribution (Figure V-20). Unit III has the lowest geometric mean particle size. The PSA distribution is very symmetrical (Figure V-20). In Unit IV, the geometric mean PSA and the first mode of the PSA distribution are no longer the same. The PSA distribution is slightly skewed towards coarser grains (Figure V-20). The particle-size distribution is very variable in Unit V (Figure V-20). In Unit VI, the first mode of the particle size distribution has shifted towards higher values, but there is evidence of another dominant particle size group indicated by the bulge on the finer size side (Figure V-20). This same bulge is present in Unit VII, but sometimes the transition between both peaks is more smooth (Figure V-20). Both Unit VI and VII have the highest sand-size content, excluding Unit V (Figure V-22). Unit VIII and IX have a very symmetrical particle size distribution (Figure V-20).

V.1.5.3. Organic Proxy Variations

The variation in the values of the organic proxies of the sediment of Lago Villarrica is small, except in the proximity of a thick tephra layer (>1 cm) or when many lamina of lahar origin are present (Figure V-23). Although LOI_{550} values should be about twice the TOC

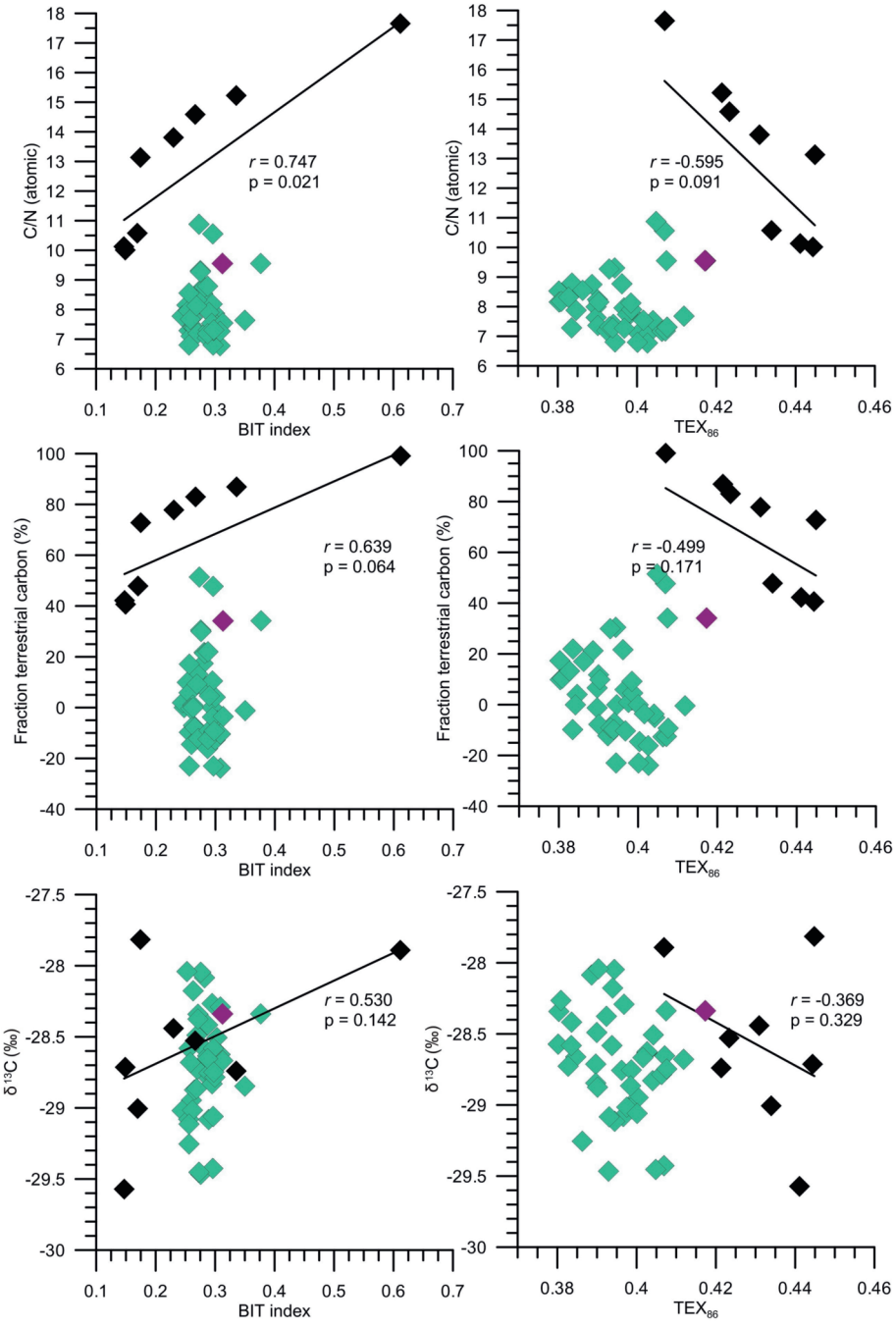

Figure V-19: Scatterplots of the BIT and TEX_{86} index of the surface sediment samples (black and purple diamonds) and the VILL long core sediment samples (green diamonds) versus C/N, fraction terrestrial carbon and $\delta^{13}C$. The purple diamond represents the surface sample VILL, which was taken on the location of the VILL long core. The trend lines have been calculated using only the surface sediment samples (black and purple diamonds).

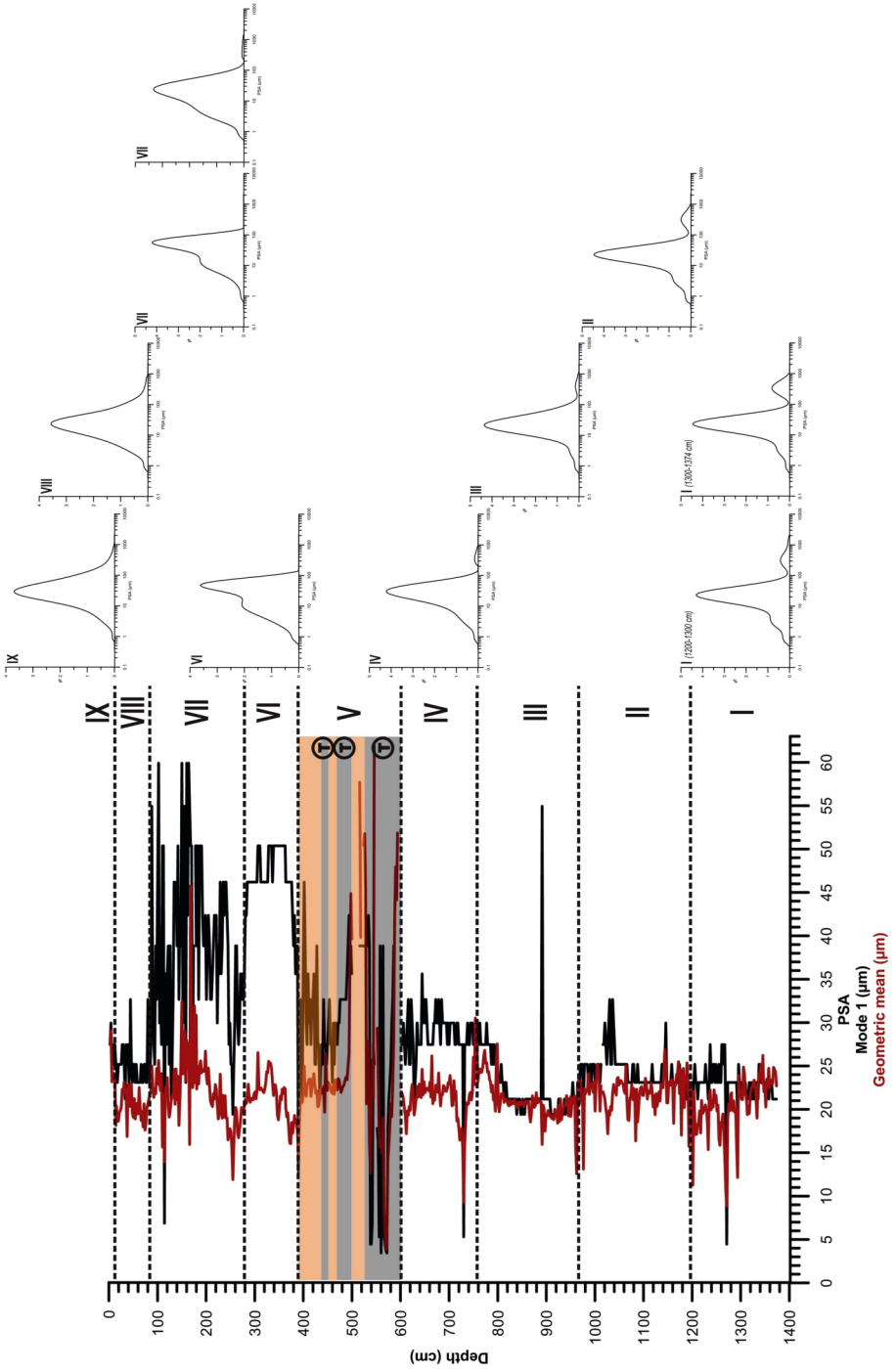

Figure V-20: A graph of the geometric mean and the first mode of the particle size analysis and indication of the division of the core in 9 units. Per unit a particle size distribution graph is shown to demonstrate the general particle size distribution of the sediment in each unit.

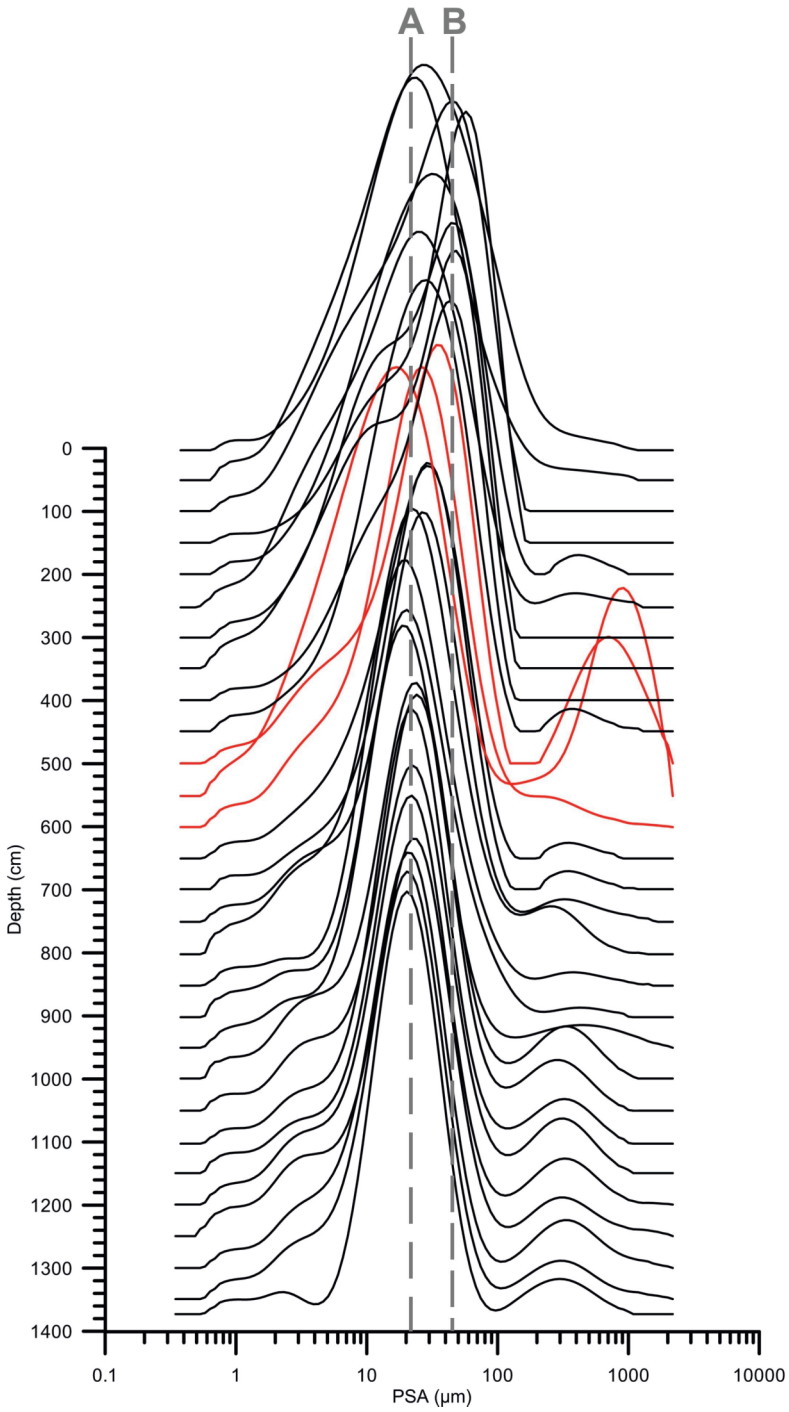

Figure V-21: Variation of the particle size distribution throughout the VILL core. The red lines indicate the particle size distribution of the Pucón ignimbrite tephra.

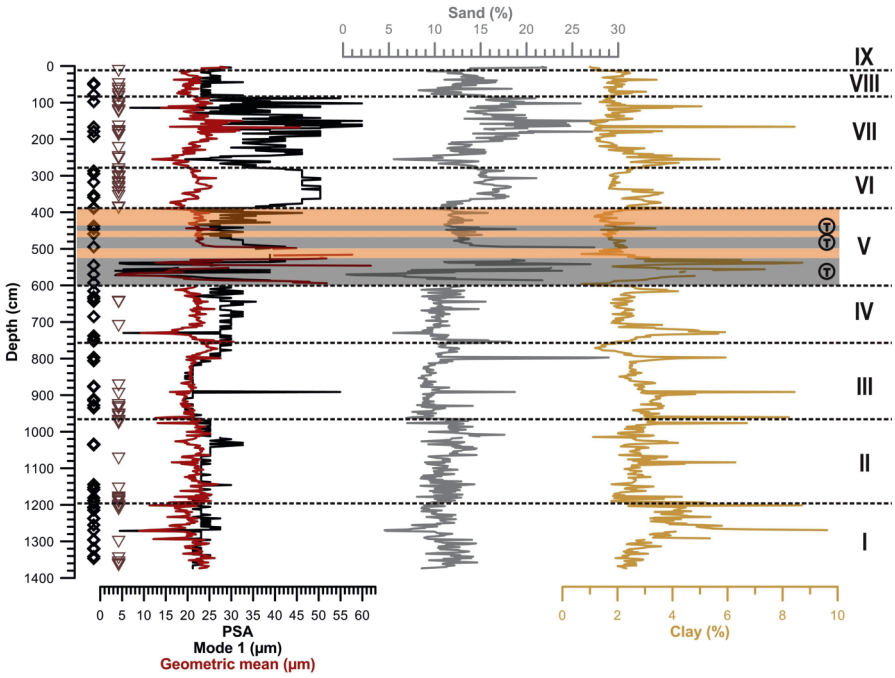

Figure V-22: Graph of the geometric mean and the first mode of the particle size analysis, and the percentages of clay and sand present in the sediment of VILL. The black diamonds are tephra levels, the brown triangles are lahar levels

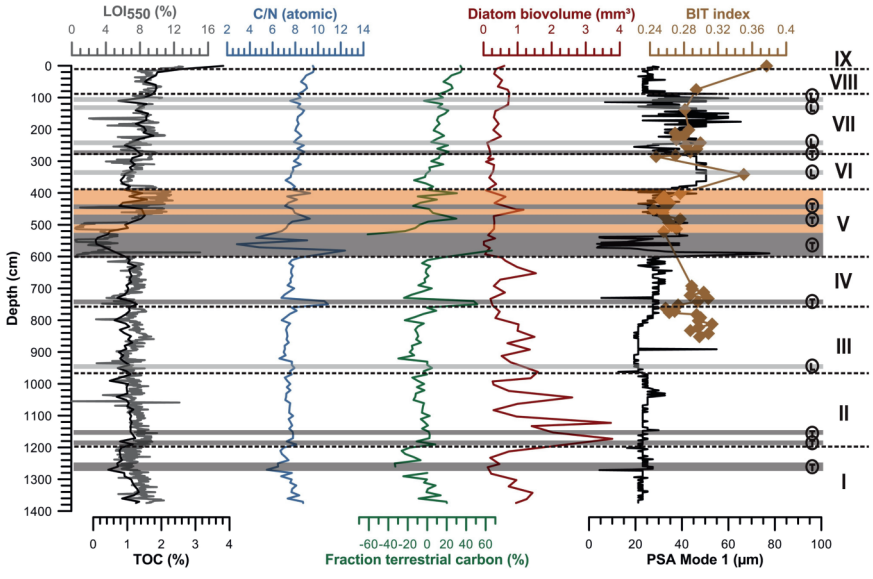

Figure V-23: Graph of the organic proxies (LOI_{550}, TOC, C/N, fraction of terrestrial carbon and the diatom biovolume) and the first mode of the particle size analysis and the BIT index of the VILL sediment core.

value, here they are much larger. Variable amounts of volatile non-carbon sediment components can increase LOI_{550} values and cause inflated organic matter concentrations (Meyers and Teranes, 2001).

There is a slight decrease in the TOC, C/N and fraction terrestrial carbon in Unit I. In Unit II, III and IV all proxies remain really stable until the Pucón ignimbrite deposit in Unit V (Figure V-23). Unit II and III have the highest amount of diatom biovolume. This biovolume was calculated using the abundance and average size of the three main planktonic species present in the sediment (Aulacoseira granulata var. angustissima, Aulacoseira granulata, Discostella sp.) (Van de Vyver, pers. comm.). Directly above the Pucón ignimbrite deposit, the TOC, C/N and fraction terrestrial carbon values are slightly higher. From Unit VI to the top there is a slow, but steady increase in TOC, C/N and fraction terrestrial carbon (Figure V-23).

In general, there is no major variability in the organic proxies prior to the last major eruption of Volcán Villarrica. This eruption lead to the collapse of the Volcán Villarrica cone and the formation of a large ignimbrite, the Pucón ignimbrite, which covers almost the entire Villarrica catchment (Clavero and Moreno, 1994). Very shortly after this eruption two other thick tephras were deposited as well. The TOC, C/N and fraction terrestrial carbon values vary significantly after this event. The lake and its catchment probably needed a certain amount of time to recover from the effects of this large volcanic eruption. The higher TOC values and slightly higher C/N values indicate that there was probably a larger influx of terrestrial organic matter. At 400 cm depth the TOC and C/N values slightly rise until the top of the core. This rise is synchronous with a change in the particle size distribution, i.e. an increases in the sand fraction (Figure V-22). In general, the C/N ratios of organic matter in fine-sized sediments are lower than those of coarse sediments (Meyers, 1997). Coarse sediment fractions contain a larger proportion of intact land-plant debris than the fine fraction and thereby have elevated C/N ratios. Fine sediment fractions contain larger proportions of clay minerals, which tend to absorb ammonia well, consequently more nitrogen is preserved in clay-sized sediment compared to coarser sediment. A decrease in C/N probably caused by a larger amount of clay minerals can be seen at a depth of 1200-1300 cm in Unit I (Figure V-22 and Figure V-23). The fact that the higher content of sand in Units VI and VII does not significantly affect the TOC, CN and fraction terrestrial carbon, probably indicates that the sand fraction does not contain a lot of organic carbon, but is mostly detrital. Therefore although the sediment's particle size might have an influence on the organic matter content, this effect seems to be subdued in Lago Villarrica.

The BIT index remains constant, except for the core top sample and one sample taken just above a lahar lamina.

V.1.5.4. Geochemical Proxy Variations

The log(Si/Al) XRF variations correspond well with changes in the quantity of clay minerals. The Si content is most likely determined by the biogenic silica of the diatom frustules, while the Al content is determined by the quantity of clay minerals. Unit I is characterised by the lowest log(Si/Al) values of the entire core (Figure V-24). This Unit has the highest clay content. There is a sudden shift to higher values in Unit II (Figure V-24). In Unit II the diatom biovolume is the highest. The log(Si/Al) values remain rather constant in Unit II, III and IV. The log(Si/Al) values are low and do not vary much in Unit VI and IX. There is a gradual increase in Unit VII, this continues in Unit VIII with an important peak at the top of this unit. The biovolume is lower in Unit VI, VII, VIII and IX (Figure V-24), and with little variation The variations that are present in these units are likely induced by changes in clay mineral content and

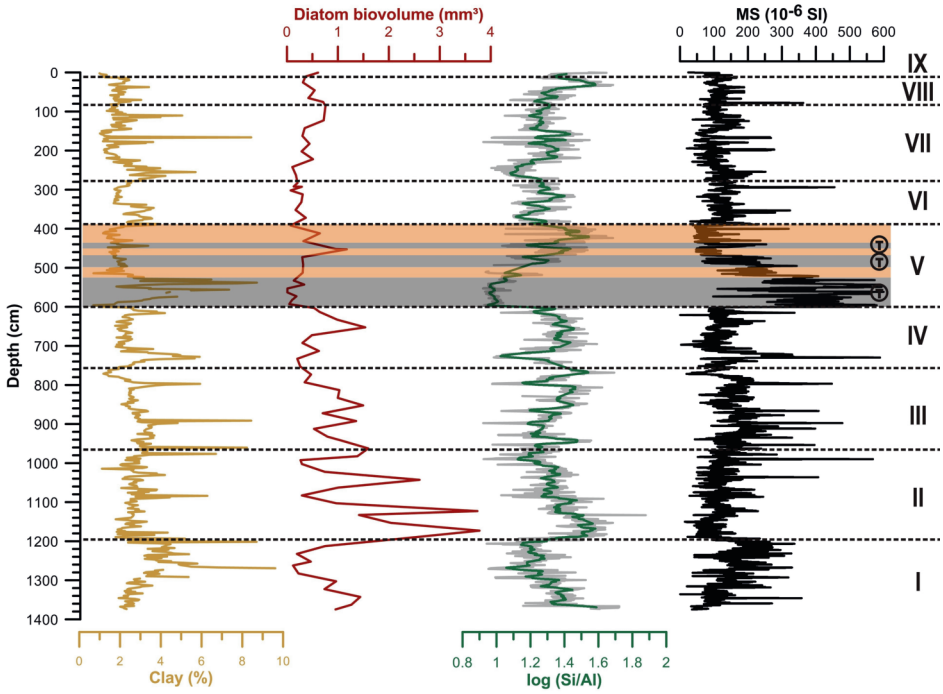

Figure V-24: Graph of the percentage clay of the sediment, the diatom biovolume, the log (Si/Al) and the magnetic susceptibility (MS)

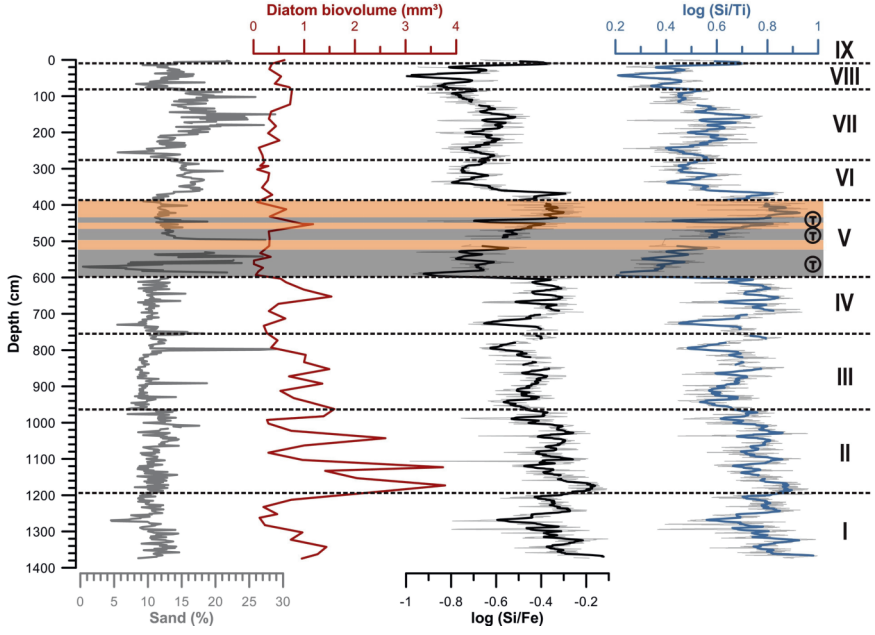

Figure V-25: Graph of the percentage sand of the sediment, the diatom biovolume, the log(Si/Fe) and the log(Si/Ti)

abundances.

The log(Si/Fe) and log(Si/Ti) variations correspond well with changes in the sand grain-size fraction. The Fe and Ti content is linked to the abundance of sand grain-size fraction, since the Si content is most likely determined by the biogenic silica of the diatom frustules. Below Unit V, the log(Si/Fe) and log(Si/Ti) gradually decrease with a slight hick-up in the middle and higher values to the top of Unit VI (Figure V-25). Log(Si/Fe) and log(Si/Ti) have in general the same trend as the biovolume content. There is a sudden drop in log(Si/Fe) and log(Si/Ti) at the beginning of Unit VI (Figure V-25). This drop can be linked to the increase in sand and the decrease in diatom biovolume. The values remain low until the top of the core (Figure V-25).

V.1.5.5. Diatom Species and LST Variations

In the sediment of Lago Villarrica four planktonic diatom species are dominant: *Aulacoseira granulata var. angustissima*, *Aulacoseira granulata*, *Discostella sp.* and *Urosolenia eriensis* (Van de Vyver, pers. comm.). The abundance of these species varies throughout the core. The variations in the absolute abundance of *Urosolenia eriensis* correlates with the number of lahar laminae (Figure V-26). This diatom species is especially highly abundant in Unit II and III and Unit VII and VIII. In these units there is also a higher occurrence of the lahar laminae. The variation of the first axis of a PCA analysis conducted on the diatom assemblages by Evelien Van de Vyver shows an important shift at the limit between Unit III and IV. Changes in the

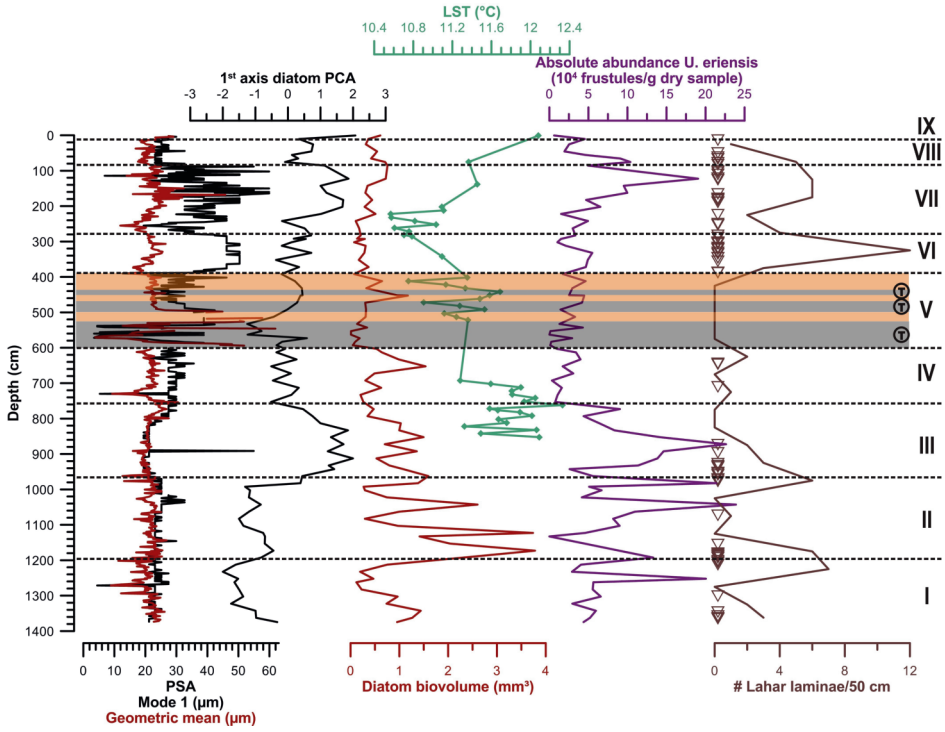

Figure V-26: Graph of the geometric mean and the first mode of the particle size analysis, the first axis of the PCA analysis on the diatom assemblage, the diatom biovolume, the lake-water surface temperature calculated using the TEX_{86} values, the absolute abundance of the diatom species Urosolenia eriensis, the lahar levels and the amount of these lahar levels per 50 cm of sediment core.

value of this PCA axis correspond well to changes in the first mode of the particle size distribution (Figure V-26), implying that the diatom community has a large influence on the sediment grain size changed. Therefore, variations in the environmental conditions of Lago Villarrica will control the diatom community and consequently the grain size of the lake sediment.

The reconstruction of the lake-water surface temperature (LST) from the measured TEX_{86} values indicate higher lake-water temperatures in Unit III and IV, lower temperatures in Unit VI and VII and higher temperatures in Unit VIII and IX (Figure V-27). The LST values vary highly in Unit V, but this disturbance might be created by the presence of the thick tephra layers.

V.1.6. Environmental Change in the Region of Lago Villarrica

Tephra layers are present almost everywhere in the long sediment core, whereas the lahar laminae are confined to certain intervals. A lahar is a type of mudflow or debris flow composed of volcanic material and water. This substance flows down from a volcano flank, typically along a pre-existing river valley. The lahar flows of Volcán Villarrica tend to follow the river valleys carved in the volcano flank (Figure III-10). Lahars can occur without any real volcanic activity, as long as the conditions are right to cause the collapse and movement of material originating from existing volcanic ash deposits. Only 10 of the 72 lahar laminae appear to be directly linked to a tephra

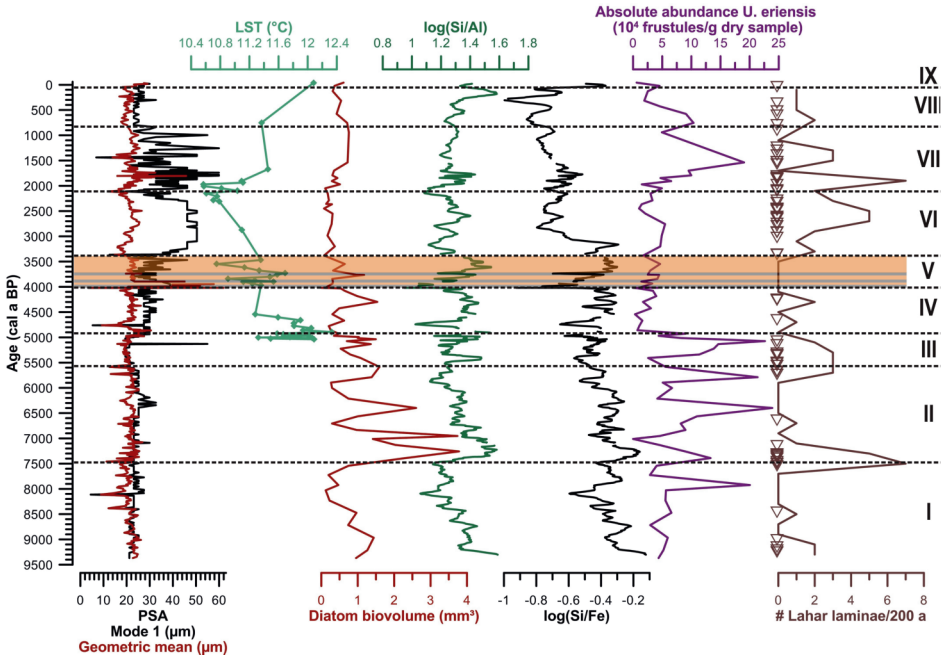

Figure V-27: Graph of the geometric mean and the first mode of the particle size analysis, the lake-water surface temperature calculated using the TEX_{86} values, the diatom biovolume, the log(Si/Al) and log(Si/Fe), the absolute abundance of the diatom species Urosolenia eriensis, the lahar levels and the amount of these lahar levels per 200 years. This time all proxies were plotted versus the sediment age.

layer, shown by a tephra layer immediately underlying such a lahar lamina. This does, however, not exclude that the other lahar could not have been triggered by an eruption and that maybe the tephra layer is missing in the sediment core, because the wind blew the volcanic ash towards the east, away from the Villarrica lake basin. The good correlation between the occurrence of the lahar laminae and the abundance of *Urosolenia eriensis* suggests that there might be another external factor in play, which controls the formation of the lahars. This other external factor could be climate. There also seems to be a seasonality in the volcanic eruptions of Chilean volcanoes and other volcanoes in the Pacific 'Ring of Fire'. There is a higher occurrence of eruptions during austral summer (Mason et al., 2004).

Urosolenia eriensis is a diatom species that grows in late summer in a well-stratified water column (Van de Vyver, pers. comm.; Campos et al., 1983). Such stratification is typically created during warm summers, which cause the surface water to be warmer. On the other hand, the higher abundance of *Urosolenia eriensis* is also associated with higher abundances of *Aulacoseira granualata sp.*, which occur in autumn, winter and spring and which need a well-mixed water column (Van de Vyver, pers. comm.; Campos et al., 1983). The occurrence of both points to seasonality differences. Such climatic seasonality might be important to trigger lahars. Colder winters would cause more snow to accumulate on the volcano flanks and warmer summers would cause the accumulated snow to melt and this sudden snow melt could create a lahar flow. A current climate phenomenon which creates such seasonality differences is the El Niño Southern Oscillation (ENSO). However, it is also possible that the lahar deposits influence the diatom community by adding for example extra nutrients to the lake water.

Most sedimentary proxies (grain size, elemental composition, geochemistry) do not vary substantially and it is difficult to determine significant palaeo-environmental changes from them. However, the pollen and diatom data do indicate environmental changes. The boundaries of the pollen (Abarzúa, pers. comm.) and diatom zones (Van de Vyver, pers. comm.) are generally at the same depth as the unit divisions based on the sedimentological parameters.

In Unit I (9369-7450 cal a BP) the pollen record indicates warm and dry conditions (Abarzúa, pers. comm.). The warmer temperatures can also be inferred from the high charcoal content, indicating increased wildfire activity (Abarzúa, pers. comm.). In many pollen records in the region a similar climate has been detected during that period (Abarzúa et al., 2010; Abarzúa and Moreno, 2008; Abarzua et al., 2004; Moreno, 2004; Vargas et al., 2008), which is also known as the Early Holocene climate optimum in the Southern Hemisphere with the highest temperatures recorded in the entire Holocene in Antarctica (Barbante et al., 2006; Masson et al., 2000; Steig et al., 2000). This is also the period with the lowest summer insolation in the Southern Hemisphere, and with the least seasonal insolation differences between summer and winter (Berger, 1978). A warmer, and probably more arid, climate could have caused the sediment in the catchment to be less fixated by vegetation and consequently to be eroded more easily, hence the higher clay and sand content of the sediment. In this unit some lahar laminae are present (Figure V-27).

Unit II (7450-5565 cal a BP) is still warm, as indicated by the pollen record (Abarzúa, pers. comm.) and the higher diatom productivity (Van de Vyver, pers. comm.). Conditions became increasingly wetter (Abarzúa, pers. comm.). The increased seasonality of the warm, and increasingly more humid, climate could have been responsible for the increased frequency of lahars. Similar conditions probably existed during Unit III (5565-4886 cal a

BP). Here, the warmer climate is confirmed by the LST reconstruction (Figure V-27).

Unit IV (4886-4020 cal a BP) shows a drop in lake temperature and a lower abundance of *Urosolenia eriensis* and of lahar laminae. The pollen record indicates a sudden increase in humidity (Abarzúa, pers. comm.). There is also a shift in the first axis of the diatom PCA, which suggests a change to better mixing of the water column (Van de Vyver, pers. comm.). The increase of humidity could have been caused by a northward shift of the Southern Westerlies, bringing more precipitation to the area, but also more wind and thus better mixing of the lake's water column. A northward shift of the Southern Westerlies has also been proposed by pollen studies and a marine study (Abarzúa et al., 2010; Abarzúa and Moreno, 2008; Abarzua et al., 2004; Lamy et al., 2001; Lamy et al., 2010; Lamy et al., 2002). The timing of this shift at ca. 5500 cal a BP is, however, 1500 years earlier than proposed by Lamy et al. (2001; 2002).

It is difficult to define the environmental conditions of Unit V (4022-3364 cal a BP), because the sediments indicate that the lake system was still recovering from sedimentary inputs associated with the large eruption of the Villarrica Volcano, which lead to the formation of the Pucón ignimbrite.

The pollen of Unit VI (3364-2273 cal a BP) and VII (2273-842 cal a BP) still indicate a high humidity, but also a large seasonal variability (Abarzúa, pers. comm.). This seasonal variability is also confirmed by the diatom record (Van de Vyver, pers. comm.). This period also has a high occurrence of lahar laminae (Figure V-27). The greater seasonal variability could have been caused by the increase in ENSO strength which has been detected in several records in South America around 3000-4000 cal a BP (Conroy et al., 2008; Moy et al., 2002; Rein et al., 2005). The reconstructed lake-water temperature is at its lowest and high amounts of non-organic terrigenous, sandy material are brought into the lake basin. This could be caused by more intensive coastal erosion due to higher wind strengths. These higher wind strengths could be the result of an increased intensity of the Southern Westerlies or due to a higher occurrence of the Easterly Puelche winds, which typically occur during hot summer days, and more frequently during an El Niño period.

Unit VIII (842-20 cal a BP) and IX (20--50 cal a BP) show clear evidence of an anthropogenic influence. There is the occurrence of exotic species in the pollen record (Abarzúa, pers. comm.) and a sudden increase in *Asterionella formosa* and *Fragilaria crotonensis* diatom species, indicating increased nutriënt levels (Van de Vyver, pers. comm.). In these two units there is also a very sudden increase in total nitrogen (TN) causing lake eutrophication.

V.1.7. Palaeoclimatic Implications

V.1.7.1. Lago Villarrica and ENSO

As mentioned above, the changes in the occurrence of the lahar laminae and the abundance of Urosolenia eriensis can be interpreted as linked to ENSO activity. A comparison of ENSO proxies from Lago Villarrica (i.e. lahar laminae, abundance of *Urosolenia eriensis*) with other palaeo-ENSO records, reveals striking similarities (Figure V-28). The abundance of *Urosolenia eriensis* can be linked to similar changes in the Laguna Pallcacocha record (Moy et al., 2002) (Van de Vyver, pers. comm.). The lahar record corresponds to a lesser extent to the Laguna Pallcacocha record, but matches well with the Lago El Junco record (Conroy et al., 2008). The lahar record shows an increase in ENSO activity in the Early Holocene (Figure V 28), which is not detected in the Laguna Pallcacocha record (Moy et al., 2002), but which is present in the Lago El Junco (Conroy et al., 2008) and Peru margin record (Rein et al., 2005). An

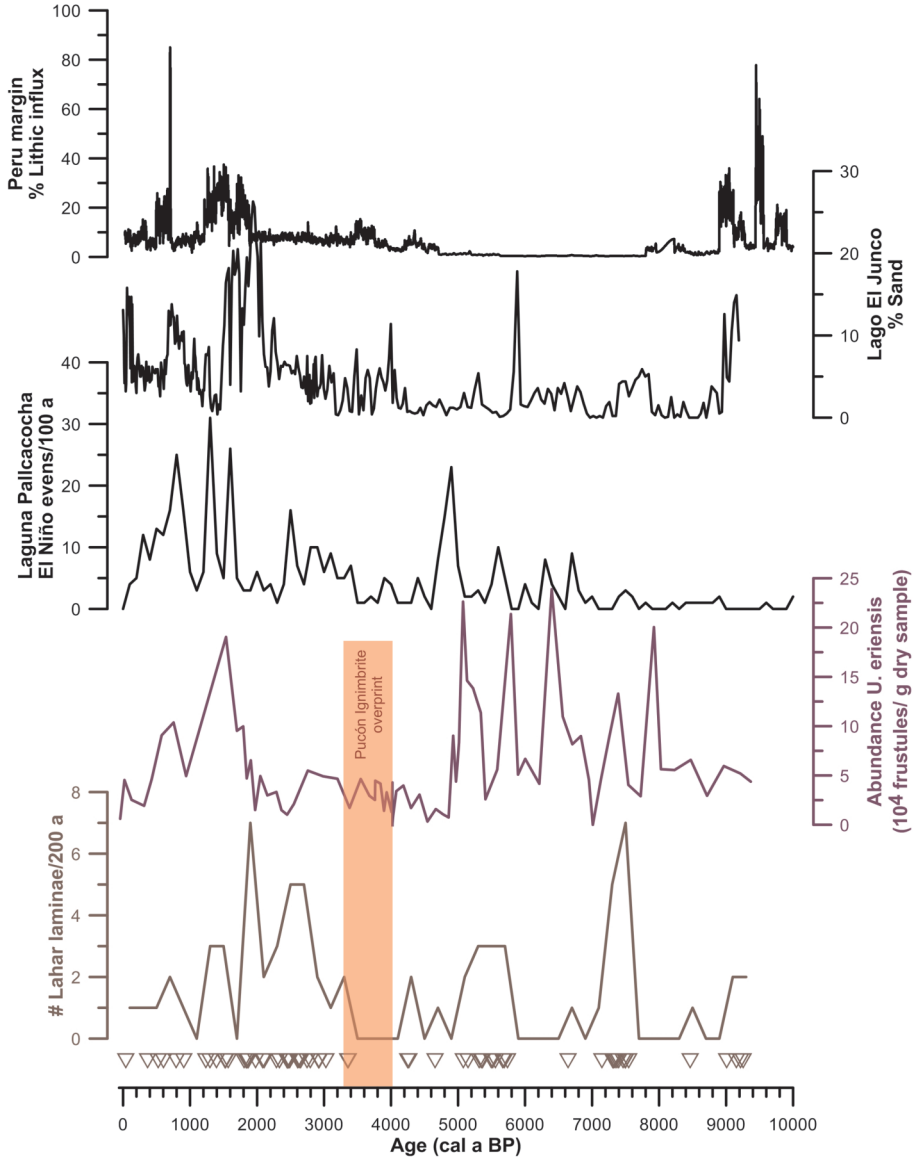

Figure V-28: Comparison of the absolute abundance of the diatom species Urosolenia eriensis, the lahar levels and the amount of these lahar levels per 200 years with records of the ENSO intensity in the Holocene: the Laguna Pallcacocha record in southern Ecuador (2°S) (Moy et al., 2002), the Lago El Junco record in the Galápagos Islands (1°S) (Conroy et al., 2008) and the Peru margin, marine record (12°S) (Rein et al., 2005).

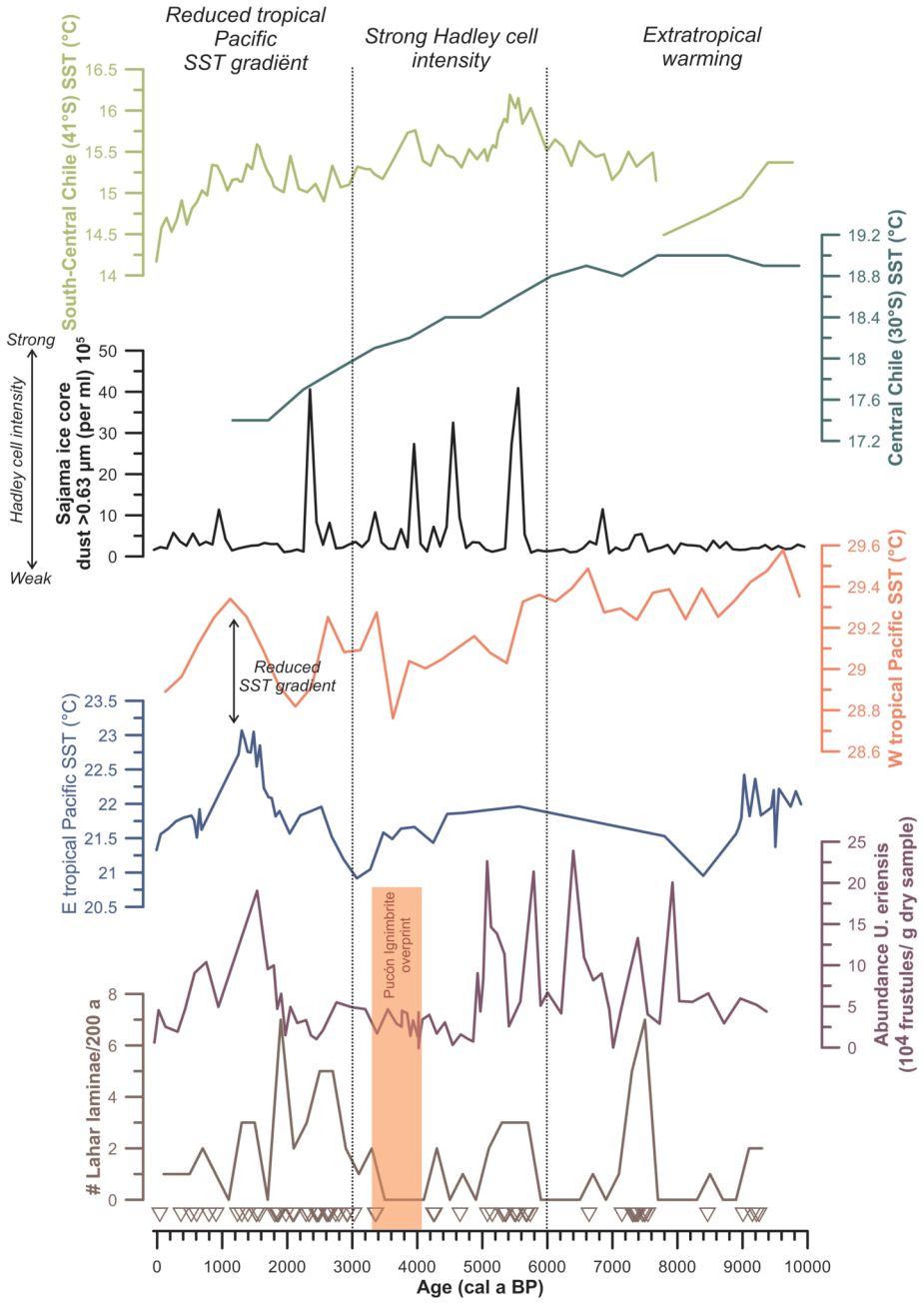

Figure V-29: Factors influencing the ENSO record of Lago Villarrica: the tropical Pacific SST gradient determined by the temperature difference between the Eastern tropical Pacific (Peru margin 12°S) (Rein et al., 2005) and the Western tropical Pacific (Stott et al., 2004), the intensity of the Hadley cell reconstructed from changes in the amount of dust present in the Sajama ice core in Bolivia (18°S) (Thompson et al., 1998) and the changes in SST of the Pacific ocean off the Chilean coast at 30°S (Kaiser et al., 2008) and 41°S (Lamy et al., 2004; Lamy et al., 2002)

isotopic study on Early Holocene, Peruvian sea shells does also indicate the presence of strong ENSO events between 9000 and 7900 cal a BP (Carré et al., 2005). Remarkably, indications for an Early Holocene ENSO has only been identified on the Eastern side of the Pacific.

ENSO activity was probably reduced during the Mid-Holocene as can be inferred from several palaeorecords (Moy et al., 2002; Shulmeister, 1999) and from modelling studies (Clement et al., 1999; Clement et al., 2000). ENSO events were, however, not absent between 8000 and 3000 cal a BP, but greatly reduced in amplitude (McGregor and Gagan, 2004; Tudhope et al., 2001; Woodroffe et al., 2003; Woodroffe and Gagan, 2000). Many records along the Pacific point toward a sudden strengthening of ENSO activity around 3000-4000 cal a BP (Conroy et al., 2008; Gagan et al., 2004; Moy et al., 2002; Rein et al., 2005; Sandweiss et al., 2001; Woodroffe et al., 2003; Woodroffe and Gagan, 2000).

How can these changes in ENSO amplitude be explained? Currently the occurrence of ENSO events depends on changes in the Walker circulation. The Walker circulation is an ocean-based system of air circulation. It is the result from a difference in surface pressure and temperature over the Western and Eastern tropical Pacific Ocean. A weak Walker circulation corresponds to an El Niño event, while a strong Walker circulation corresponds to a La Niña event. A stronger Walker circulation can also be linked to greater Hadley cell intensity and a stronger SW Asian monsoon (Webster et al., 1998). A reduced SST gradient between the Eastern and Western tropical Pacific may lead to a weakened Walker circulation and favour the development of more frequent El Niño events (Koutavas et al., 2006). The comparison of an Eastern tropical Pacific SST record (Rein et al., 2005) with a Western tropical Pacific SST record (Koutavas et al., 2002) shows that this SST gradient weakened about 3000 years ago, synchronous with the onset of a higher ENSO frequency in Lago Villarrica (Figure V-29).

A stronger Hadley cell strengthens the Walker circulation. The dust record of the Sajama ice core in the Bolivian Andes (Thompson et al., 1998) indicates a much stronger Hadley cell between 6000 and 3000 cal a BP. In this period ENSO events occurred less frequently in Lago Villarrica (Figure V-29). This interplay between Hadley cell intensity and ENSO activity in the Mid and Late Holocene has also been documented in a marine sediment core just of the Chilean coast (41°S) (Verleye and Louwye, 2010).

It is harder to explain the occurrence of ENSO in the Early Holocene. During that time period Asian monsoon was at its strongest (Dykoski et al., 2005; Wang et al., 2005), indicating a strong Walker circulation. A modelling study shows, however, that extratropical warming of the ocean weakens the Hadley cell and consequently slows down the shallow meridional overturning circulation of the upper Pacific and therefore reduces upwelling (Zhang et al., 2005). Such oceanic behaviour is typical for an El Niño event. The amplitude of the ENSO events is reduced, but this reduction is smaller on the Eastern Pacific coast, than on the Western (Zhang et al., 2005). SST records of the extratropical Pacifc waters in front of the Chilean coast at 41°S (Lamy et al., 2004; Lamy et al., 2002) and 30°S (Kaiser et al., 2008) indicate much warmer temperatures in the Early Holocene (Figure V-29). Can it be surmised that this extratropical warming may have lead to the sporadic occurrence of ENSO events during that time period?

V.1.7.2. Lago Villarrica and the Position and Intensity of the Southern Westerlies

Around 6000 cal a BP, the Southern Westerlies likely shifted northward affecting the Lago Villarrica region as can be deduced from the pollen and

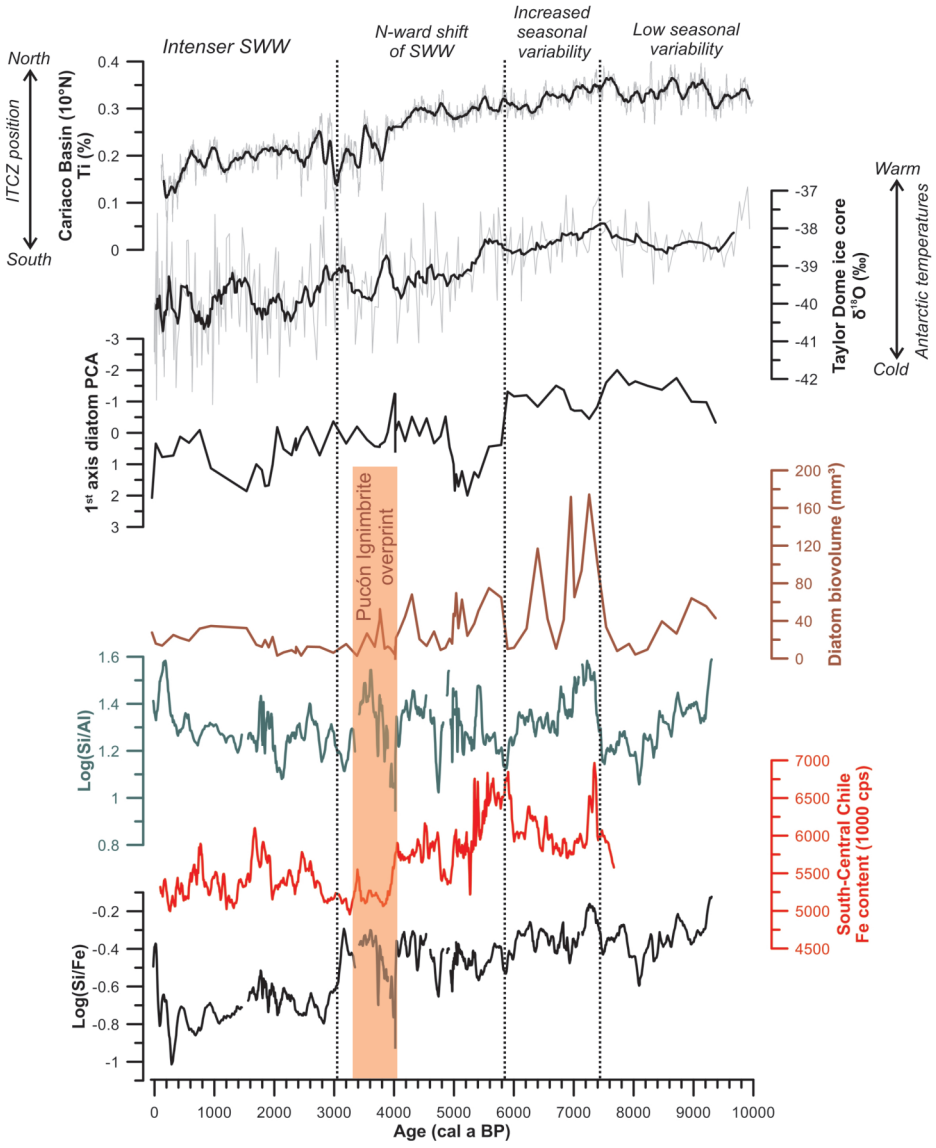

Figure V-30: The changing climate in the Lago Villarrica region created by shift in the position and intensity of the Southern Westerly winds (SWW) compared to changes in the Fe content of South-Central Chilean marine sediment (41°S) (Lamy et al., 2002), in the position of the ITCZ (Haug et al., 2001) and Antarctic temperatures at Taylor Dome in the Ross Sea sector (Steig et al., 2000).

diatom record. This onset of Westerly activity in the region is synchronous with other records in the region (Abarzúa et al., 2010; Abarzúa and Moreno, 2008; Abarzua et al., 2004; Lamy et al., 2001; Lamy et al., 2010; Lamy et al., 2002).

The position and intensity of the Southern Westerlies is controlled by the atmospheric pressure gradient between the SE Pacific high and the Antarctic low. Cooling of Antarctica increases this gradient. A similar effect is caused by a southward shift of the ITCZ, which will push the SE Pacific high towards the south.

In the Early Holocene, the ITCZ was located further north (Haug et al., 2001; Hodell et al., 2008) and Antarctica was experiencing its Early Holocene climatic optimum (Masson et al., 2000; Steig et al., 2000) (Figure V-30). Consequently the pressure gradient was shallow and the Southern Westerlies were weak. Because the strength of the Southern Westerlies was greatly reduced in the Early Holocene it might well be that the Lago Villarrica region was influenced by the Southern Westerlies, but its effects were less noticeable. Currently, the Southern Westerly belt shifts ca. 3-4° towards the north in winter (Lamy et al., 2001). During the Early Holocene, the Southern Hemisphere had its lowest solar seasonal variability (Berger, 1978), perhaps reducing the seasonal shifts of the Southern Westerlies.

Between 7500 and 6000 cal a BP, solar seasonality increased. This might have caused the first incursion of the Southern Westerly belt during winter periods, causing the local climate to become increasingly humid as shown by the pollen record at this time. It could also be that there were seasonal changes in the intensity of the Southern Westerlies, which would have the same effects as a shift. At the same time, Antarctica slowly cools down and the ITCZ slowly drifts southward, increasing the pressure gradient (Figure V 30). Winter incursions of the Southern Westerlies would also explain the increased seasonality picked up in the diatom record. Maybe these winter excursions of the Westerlies in an overall warmer climate resulted in the peaks in abundance of *Urosolenia eriensis* and the amount of lahar laminae and not an increase in ENSO activity.

Around 6000 cal a BP, the Southern Westerlies shifted northward or they increased in strength (Figure V-30). Between 5000 and 6000 cal a BP sea ice expanded around Antarctica (Divine et al., 2010; Hodell et al., 2001), indicating drastic cooling of the Antarctic climate. Such cooling increases the pressure gradient between the SE Pacific high and the Antarctic low, consequently increasing the Southern Westerlies' strength. In addition, sea-ice expansion pushed the Polar Front, the southern limit of the Southern Westerly belt towards the north, consequently shifting the entire system northward.

Around 3000 cal a BP, Southern Westerly wind intensity increased further. Antarctica was still cooling and the ITCZ continued to move southward, slowly increasing the pressure gradient responsible for the Southern Westerly wind's strength (Figure V-30).

The log(Si/Fe) and Fe content record of Lamy et al. (2001; 2002) show a significant change at this time. Lamy et al. (2001; 2002) interprets this shift at 4000 cal a BP as the northward shift of the Southern Westerlies. The increase in Fe in Villarrica lags the marine record, but the period between 4000 and 3000 years is the re-equilibration period of Lago Villarrica after the Pucón ignimibrite eruption. Consequently the palaeoclimatic signal might have been overprinted.

In Lago Villarrica proxies other than the log(Si/Fe) indicate this might have been 2000 years earlier. It is possible that the shift in Fe content in the marine record and in the Villarrica record is the result of more intense Westerly winds or from the sudden increase in ENSO activity.

V.2. Laguna Parrillar

V.2.1. Laguna Parrillar Basin

A bathymetry was constructed for Laguna Parrillar. The lake is rather shallow with a maximum depth of 25 m (Figure V-31). The semi-elliptical basin has very shallow shores, only the central part of the basin has a depth larger than 10 m. It is unknown how this lake basin was formed.

Around the lake shores, traces a higher lake terrace, ca. 10 m above the current lake level were observed during field work. This terrace was formed sometime in the past when the lake level was higher.

V.2.2. Lithological Description

Lithologically the PAR1 core can be divided in three major units. A first unit from 695 to 195 cm, a second unit from 195 to 96 cm and a third unit from 96 to 0 cm.

Unit I (695-195 cm) consists of very clearly laminated clays and silt with an occasional thin, sand lamina (Figure V-32). The gamma-density and the magnetic susceptibility of this part of the core is very stable. The amount and the thickness of these sand laminae increases between 540 and 650 cm. At the same depth there is a very slight increase in gamma-density.

The unit II (195-96 cm) is composed of very fine laminae which contain a greater proportion of sand, than the laminae further downcore (Figure V-32). Unit II has the highest gamma-density of the entire core and the beginning and the end of the unit are marked by a sudden shift. Gamma-density and magnetic susceptibility do not vary significantly within this unit.

Unit III (96-0 cm) is the most variable unit of all (Figure V-32). Its laminations are mostly faint or even absent. Remarkable about this unit is the presence of black pellets, which disintegrate when you rub them between your fingers. The majority of these pellets are found in the top 50 cm of the core. They disappear deeper down. Where these pellets are present, the sediment is more rust coloured. The gamma-density decrease steadily towards the top.

The transition from unit I into unit II is diffuse and marked by rusty colouring of the laminae. Similar 'rust-coloured' patches are also present between 215 and 220 cm, but here the type of lamination remains similar above and below the patches, while the thickness of the laminations decreases gradually towards the transition from unit I into unit II.

The transition from unit II into unit III is again marked by rust colouring. This time the colour change is sudden, marked by a clear stratigraphic boundary. This rusty sediment has no visible internal structures (e.g. laminae) and is a mixture of clay, silt and sand.

The white tephra layer at 52 to 54 cm corresponds to the highest magnetic susceptibility measured in the entire core. There are some more high magnetic peaks in this unit, but a smear slide investigation did not show higher amounts of volcanic glass or different mineralogical components.

All levels with high magnetic susceptibility were screened for the presence of volcanic glass. Only the with tephra layer between 52 and 54 cm had plenty of glass. This same marker horizon is present in PAR1-liv, a 50 cm long livingstone core taken in a more shallow part of the lake (Figure III-7). The shards of both white tephras were analysed geochemically. These results were compared with geochemical measurements of other marker tephras found in the region. Geochemically this tephra is most similar to the Mount Burney 2 (MB2) eruption (Figure V-33).

V.2.3. Organic Proxies

Clear shifts in the sediment composition

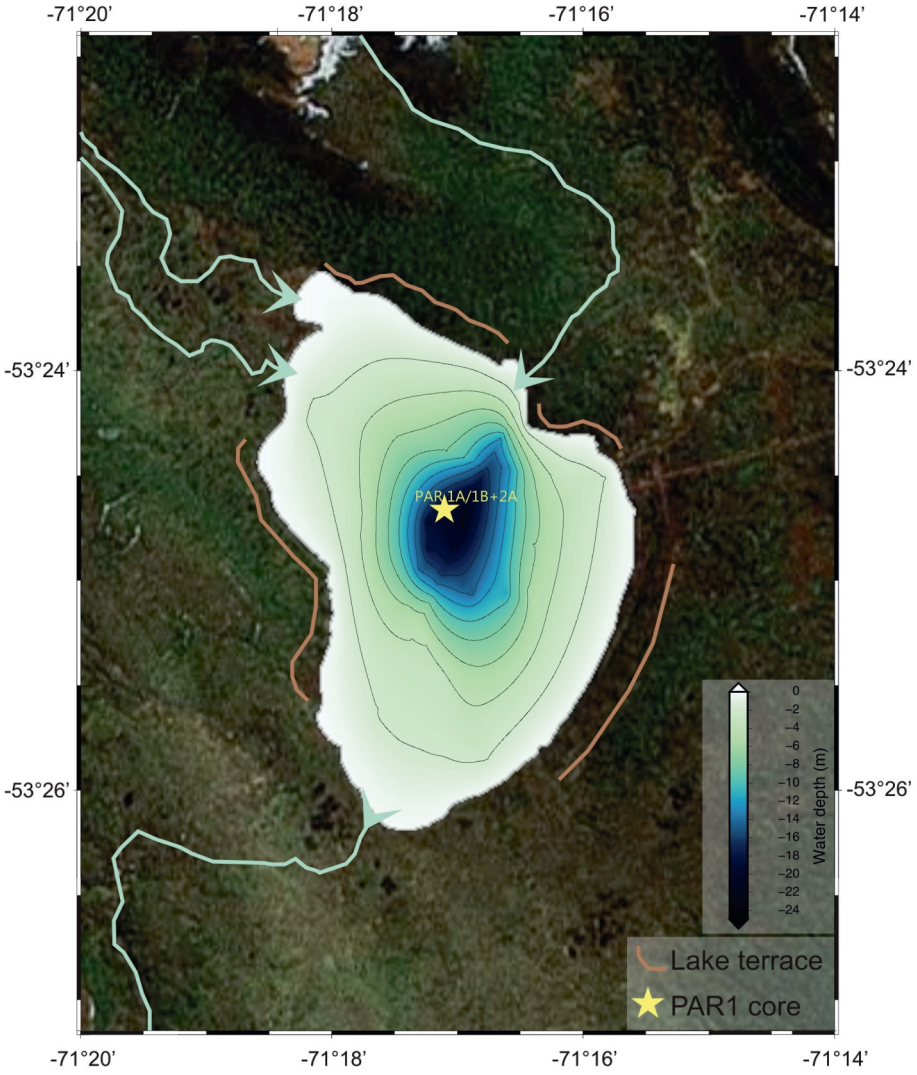

Figure V-31: Bathymetry of Laguna Parrillar with the location of the PAR1 core and the occurrence of palaeolake terraces around the lake as they were observed in the field.

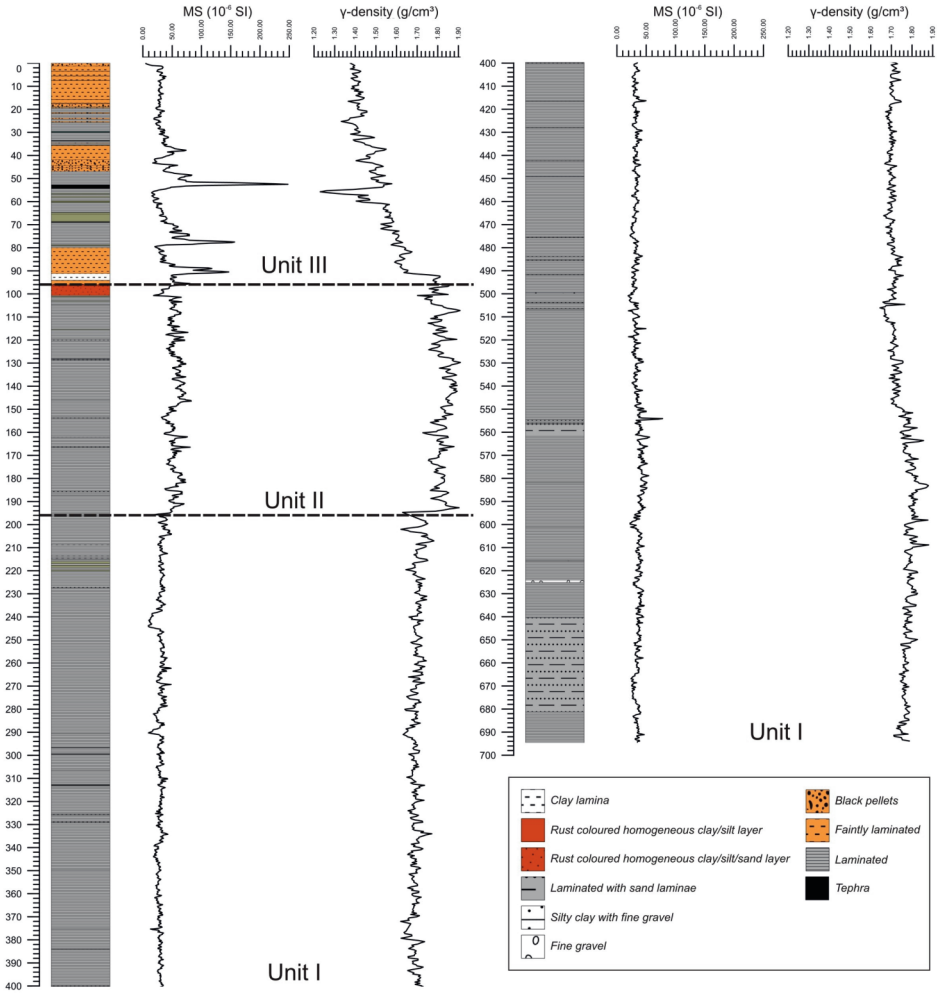

Figure V-32: Litholog of the PAR1 sediment core and the graph of variations in the density and magnetic susceptibility (MS) of the sediment.

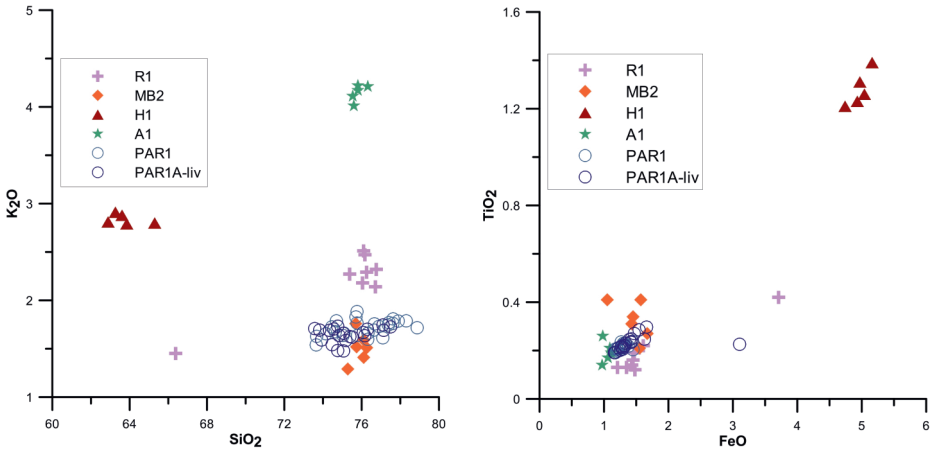

Figure V-33: Geochemical comparison of the white tephra layer in PAR1 and PAR1A-liv with other geochemical measurements of well-known tephra deposits in the area (data from Haberzettl et al., 2007; Kilian et al., 2003; Naranjo and Stern, 1998; Stern, 2008; Stern and Kilian, 1996). R1 = Volcán Réclus eruption of 12693 ± 192 ^{14}C a BP (McCulloch and Davies, 2001), MB2 = Volcán Mount Burney eruption of 3860 ± 50 ^{14}C a BP (McCulloch and Davies, 2001), H1 = Volcán Hudson eruption of 6725 ± 65 ^{14}C a BP (McCulloch and Davies, 2001), A1 = Volcán Aguillera eruption of 3000 ±100 ^{14}C a BP (Stern, 2008). For a location of the volcanic centres see Figure II-15

are reflected clearly in changes in organic parameters and water content (Figure V-34). Changes in water content are especially clear at the boundaries between Unit I, II and III. The area in Unit I with sandy laminae is also expressed in the water content.

Unit I has a low water content, which is lower in the interval with more sand laminae. The TOC level remains constant at 0.5%, as is the case for the C/N ratio (8) and the δ^{13}C value (-26‰). In Unit II, the water content is the lowest. The TOC remains constant at ca. 0.5%. The C/N ratio and the δ^{13}C value vary a little bit more with a very sudden shift between 136 and 138 cm. This shift is based on two measurements, and it is unclear whether it represents a faulty measurement or a real event, because lithologically this interval does not look different from the rest of the Unit II sediment.

Unit III shows a gradual increase in both water content, TOC and C/N, while the δ^{13}C values decrease. The water content has a sudden shift downwards at 53 cm, associated with the presence of the white tephra layer. The TOC and the C/N have a sudden positive shift in their gradual increase around 50 cm, this shift is followed by a drop in their values. After this drop, the values increase again.

The C/N values of Unit I and II are typical for lacustrine algae (Meyers and Teranes, 2001) and, currently, the inflowing rivers cut across peat bogs. The soil organic matter of a peat bog has a C/N atomic ratio of 17 and a δ^{13}C value of -28.7‰ (Ertel and Hedges, 1984). Increases in C/N and the lowering in δ^{13}C could be linked with the establishment of the moorland vegetation.

No pollen grains are preserved in the Laguna Parrillar sediment (Abarzúa, pers. comm.). A very low quantity of diatom remains was found in the surface sediment, but no other diatom frustules were found deeper down in the core (Van de Vyver, pers. comm.). The few diatom valves found show clear signs of dissolution. pH measurements of the lake water in 2007 noted a value of 7.9 to 8.0. Such a pH is not high

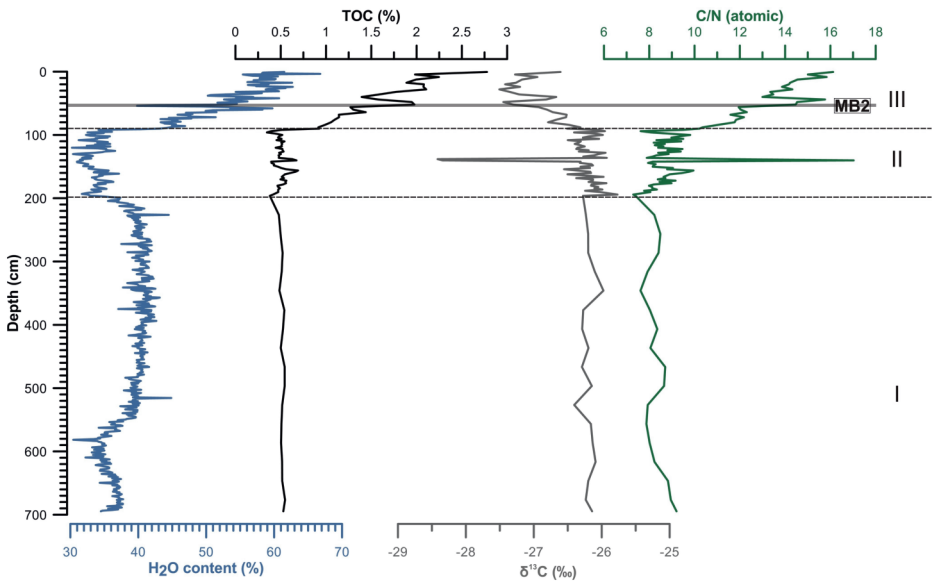

Figure V-34: Water content, TOC, C/N atomic ratio and δ13C values of the PAR1 sediment core

enough to cause dissolution of pollen or diatoms. The Si content of the modern lake water is low, possibly too low to sustain a large diatom community, and large wave action could cause physical corrosion of the diatom valves. In a windy setting, tree pollen are often extremely underrepresented even if large areas of woodland are present (Gearey and Gilbertson, 1997). Windy conditions are certainly not uncommon, but it does not explain the total absence of pollen.

V.2.4. Mineralogical, Elemental and Particle Size Variations

The variation in mineralogical composition of the Laguna Parrillar sediment is relatively minor throughout the core (Figure V-35). The changes in mineralogy are induced by changes in particle size, particularly changes in the percentage of clay. Notably, amphiboles are only present in the upper two metres and there are two sudden peaks in the pyroxene content, one at 170 cm and one at 64 cm depth. These peaks cannot be linked to any clear change in the lithology of the sediment, indicating that the sediment source remained local, i.e., within the lake's catchment, throughout and likely did not change significantly over time.

Overall, the minerals measured can be linked to the local bedrock of argillites and sandstones (Dollenz, 1983; SERNAGEOMIN, 2003). The clays consist in general of about 40-60% illite with variable amounts of chlorite (15-25%) and kaolinite (10-20%).

The particle size distributions and the XRF data show greater variability than the mineralogical composition (Figure V-36).

In Unit I the sediment is dominanted by a clay size fraction. The amount of sand increases from ca. 5 to ca. 10 % between 540 and 650 cm, and can be linked to a visible change in the lithology associated with an increase in sand laminae. Apart from the log(Al/Fe) data most XRF measurements show little variations in Unit I. The log(Fe/Mn) decreases slightly towards the top of the unit and shows a sudden shift between 210 and 220 cm. The log(Fe/Zr)

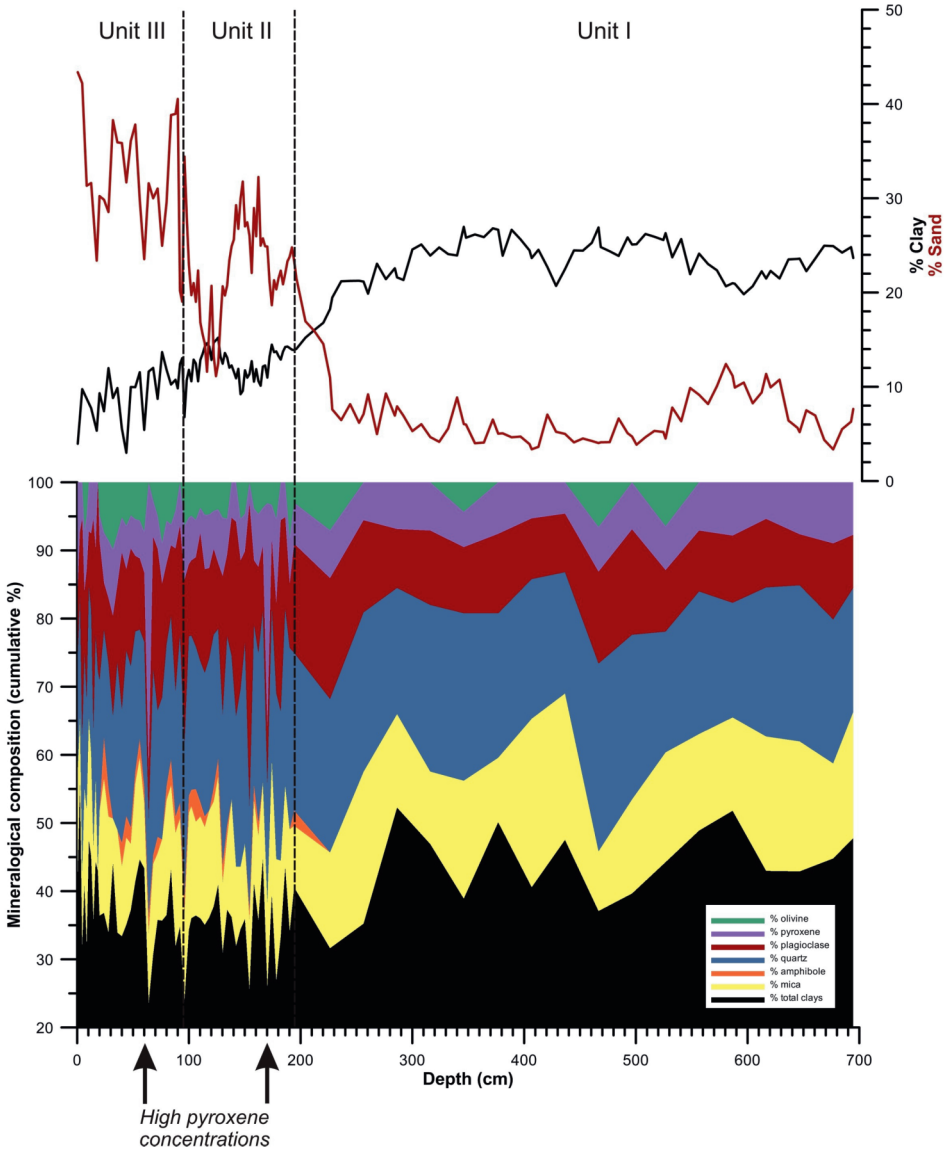

Figure V-35: Bulk XRD measurements of and percentages sand and clay present in the sediment of PAR1

Table V-4: The radiocarbon ages of the 10 samples and their 2σ calibrated error range using the IntCal09 calibration curve (Reimer et al., 2009) . The sample with an asterisk (*) is the radiocarbon sample taken just below the MB2 tephra., The four Holocene samples were corrected by 1683 ^{14}C a, a value of 37 ^{14}C a was added to their error. The sample printed in a gray colour is considered an outlier was excluded from the age-depth model.

Sample name	Sample depth (cm)	Radiocarbon age (^{14}C a BP)	Error (1σ) (^{14}C a BP)	Corrected radiocarbon age (^{14}C a BP)	Corrected error (1σ) (^{14}C a BP)	2σ error range calibrated ages (cal a BP)
PARSCI-0	0.5	1050	30	modern	67	-67–268
PARSCIII-21	21.5	2670	30	987	67	742–1052
PAR1A-I-46*	55	5550*	40	3867*	77	4031–4517
PAR1A-I-65	74	9150	40	7467	77	8060–8415
PAR1A-I-83	92	16400	120	not corrected	not corrected	19299–20008
PAR1A-II-29	130.2	20800	95	not corrected	not corrected	24462–25080
PAR1A-II-90	191.2	24300	190	not corrected	not corrected	28554–29513
PAR1A-III-94	290.3	30800	310	not corrected	not corrected	34759–36284
PAR1B-II-41	548.6	37500	840	not corrected	not corrected	41078–43670
PAR1B-III-93	694.6	36600	570	not corrected	not corrected	40685–42510

data shows a sudden increase at the top of the unit, associated with rust patches visible on the sediment at this interval.

Unit II has a much higher sand content and all XRF data vary more than in Unit I. The sudden positive shift in log(Fe/Zr) at the top of this unit, is again related to the change to a more 'rusty coloured' sediment.
Unit III has the highest variability both in particle size distribution and XRF data variability. Both the log(Al/Fe) and log(Al/Zr) decrease until ca. 30 cm depth. In the top 30 cm of the core, both values increase again with the log(Fe/Zr) exhibiting very sudden peaks. The largest of these peaks correspond to the levels with high magnetic susceptibility, such as the MB2 tephra and also to parts of the core with a high pellet content. The log(Fe/Mn) values are slightly lower than Unit II in the bottom of Unit III, but after decreasing until a core depth of ca. 50 cm, they subsequently increase gradually towards the top of Unit III. The large drops in the log(Fe/Mn) curve and large peaks in the log(Fe/Zr) curve in Unit III correspond to levels in the sediment core with a higher pellet concentration and more 'rust'-colouring of the sediment.

Variations in the log(Al/Fe) and log(Al/Zr) ratios are a good proxy for the sand content of the sediment. High log(Al/Fe) and log(Al/Zr) values indicate generally a lower sand content. The log(Fe/Zr) is a good indicator for increased Fe content, or were the Fe has been oxidised with higher log(Fe/Zr) values always corresponding to a 'rust-coloured' sediment.

SEM analysis of the sand fraction revealed that the grains have the typical characteristics of chemical weathering (Mahaney, 2002). Like the XRD analysis this implies a similar source of the material throughout the entire core and that the distance that the grains have been transported from their source area into the lake basin was always relatively short.

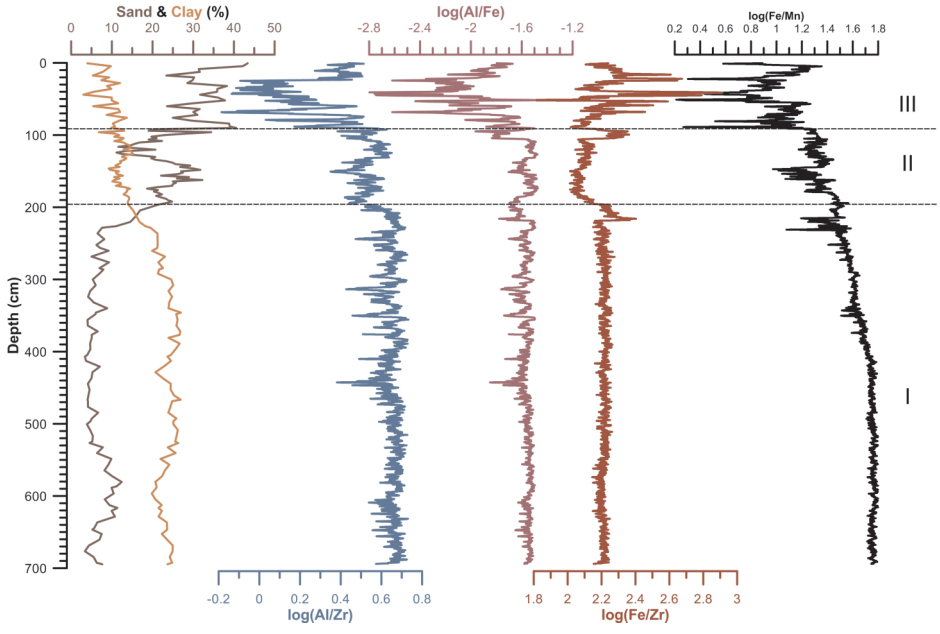

Figure V-36: Changes in sand and clay (%) and XRF variations of the PAR1 core

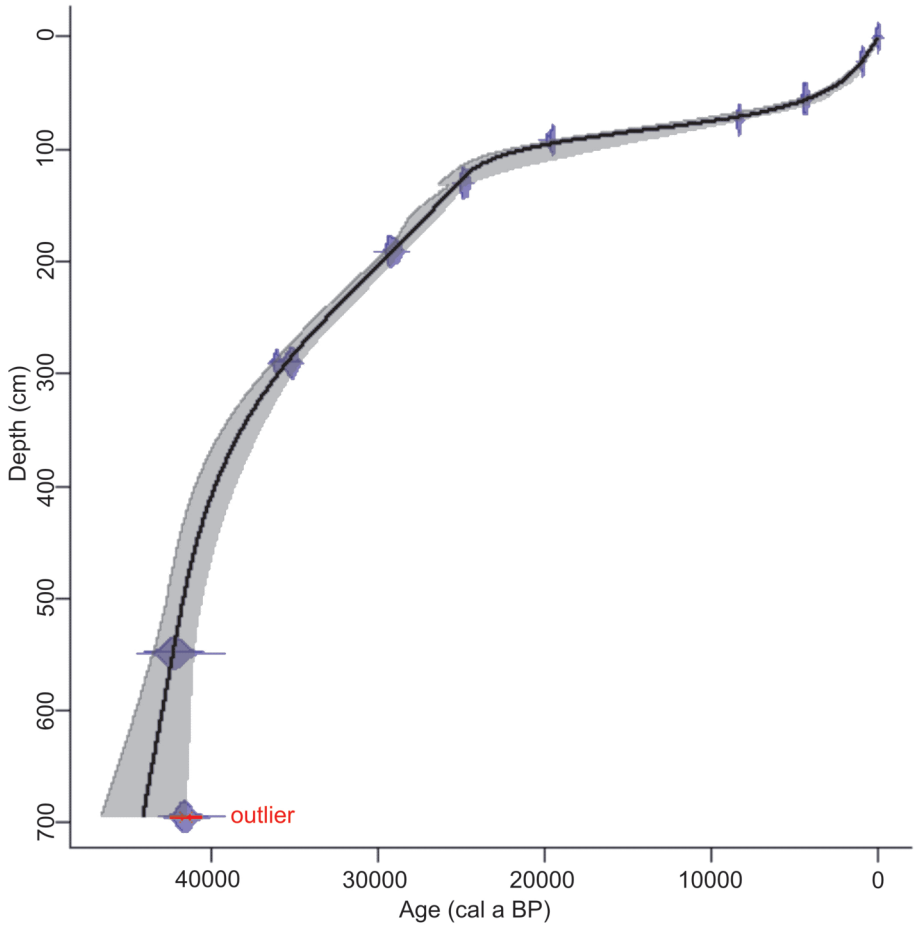

Figure V-37: Age-depth model of the PAR1 sediment core using Blaauw's clam software (2010). One radiocarbon age was considered an outlier. The grey band around the black age-depth model, indicates the 2σ error.

V.2.5. Age-Depth Model

Ten samples were sent for radiocarbon dating (Table III-2 and Table V-4).
To create the age-depth model, all radiocarbon ages were calibrated using the IntCalo9 calibration curve (Reimer et al., 2009) using the Clam software of Blaauw (2010). The model was generated using a smooth spline (error-weighted with smoothness set at 0.3) (Figure V-37 and Figure V-38), chosen because it encompasses the age ranges of most of the radiocarbon samples. The radiocarbon age from 694.6 cm depth is considered to be an outlier because the radiocarbon age created an age reversal in the age-depth model. Nevertheless, the age-depth curve is still within the 2σ error of the calibrated radiocarbon age for this sample.

The well-established tephrochronology of Southern Patagonia (Stern, 2008) meant that the tephra at 52-54 cm depth could be used as a 'known-age' maker horizon. One radiocarbon date was taken directly below this tephra. Major elemental geochemical data indicate this tephra is related to an eruption from Mount Burney, most likely the MB2 tephra. The MB2 eruption has been dated by several other investigators to 3830-3910 ^{14}C a BP (Kilian et al., 2003; McCulloch and

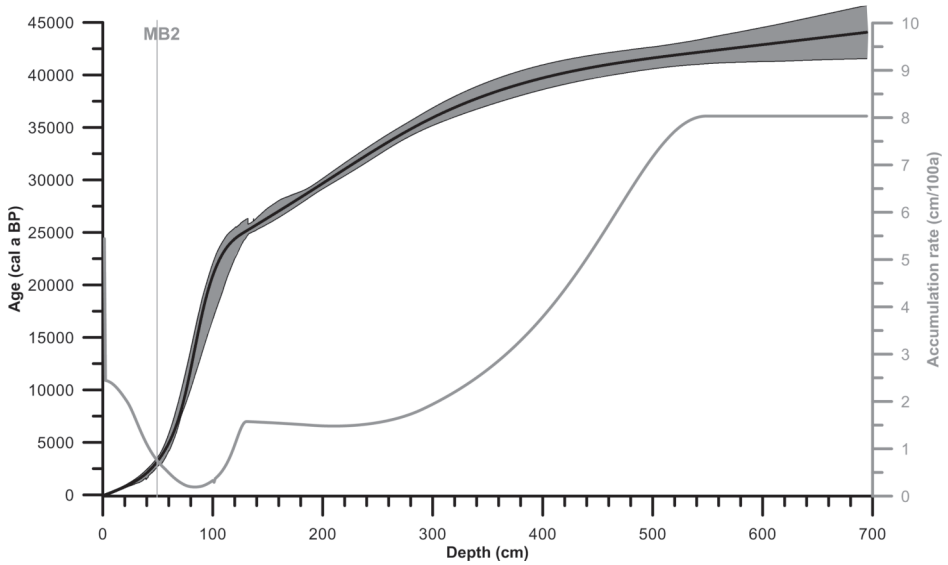

Figure V-38: The age-depth model of PAR1. There is also a plot of the accumulation rate which demonstrates nicely the variations in sedimentation rate throughout the core. The grey band around the black age-depth model, indicates the 2σ error.

Davies, 2001; Stern, 2008). The ^{14}C age of the sample below the tephra is, however, much older. Organic material from soils and peats in lake sediments can vary between 1600 and 5400 years in age (Björck and Wohlfarth, 2001). Since Laguna Parrillar has a moorland catchment it is possible that the 'old' carbon retained in the peat has influenced the radiocarbon ages of the sediments.

An average of all published radiocarbon ages of MB2 was taken and the difference between this age and the radiocarbon sample below the MB2 tephra was calculated (age difference of 1683 ± ^{37} ^{14}C years). This correction was only applied to the Holocene samples, because there was probably no peat present in the catchment prior to the Holocene. However, it is possible that the pre-Holocene OIS 2 and OIS 3 radiocarbon ages of the PAR1 sediment core could also be too old since bulk samples with little organic carbon (<2%) are more subject to several dating errors (Björck and Wohlfarth, 2001). Radiocarbon ages from OIS2 and OIS3 sediments of Laguna Parrillar were obtained from sediment which contains about 0.5% organic carbon. Furthermore, if the lake remained frozen for a prolonged periods during OIS 2 and perhaps OIS 3, the perennial ice cover would have sealed off the lake water from the atmosphere, preventing isotopic equilibrium between the lake water and the atmosphere and, potentially, creating a 'reservoir effect' of between 1600 and 10000 years, similar to that found in some Antarctic lakes (Doran et al., 1999).

V.2.6. Environmental Change in Laguna Parrillar

During the Last Glacial Maximum (LGM), the majority of this regions was covered by the Patagonian Ice Sheet (Bentley et al., 2005; Glasser et al., 2008; Hulton et al., 2002; Kaplan et al., 2007; McCulloch et al., 2005b; Sugden et al., 2009). The sediment recovered from Laguna Parrillar represents the complete Oxygen Isotope Stages (OIS) 1 and 2 and a large part of OIS 3 (Figure V-39 and Figure V-41), and suggests that the Laguna Parrillar area was not glaciated in the build up to, and during,

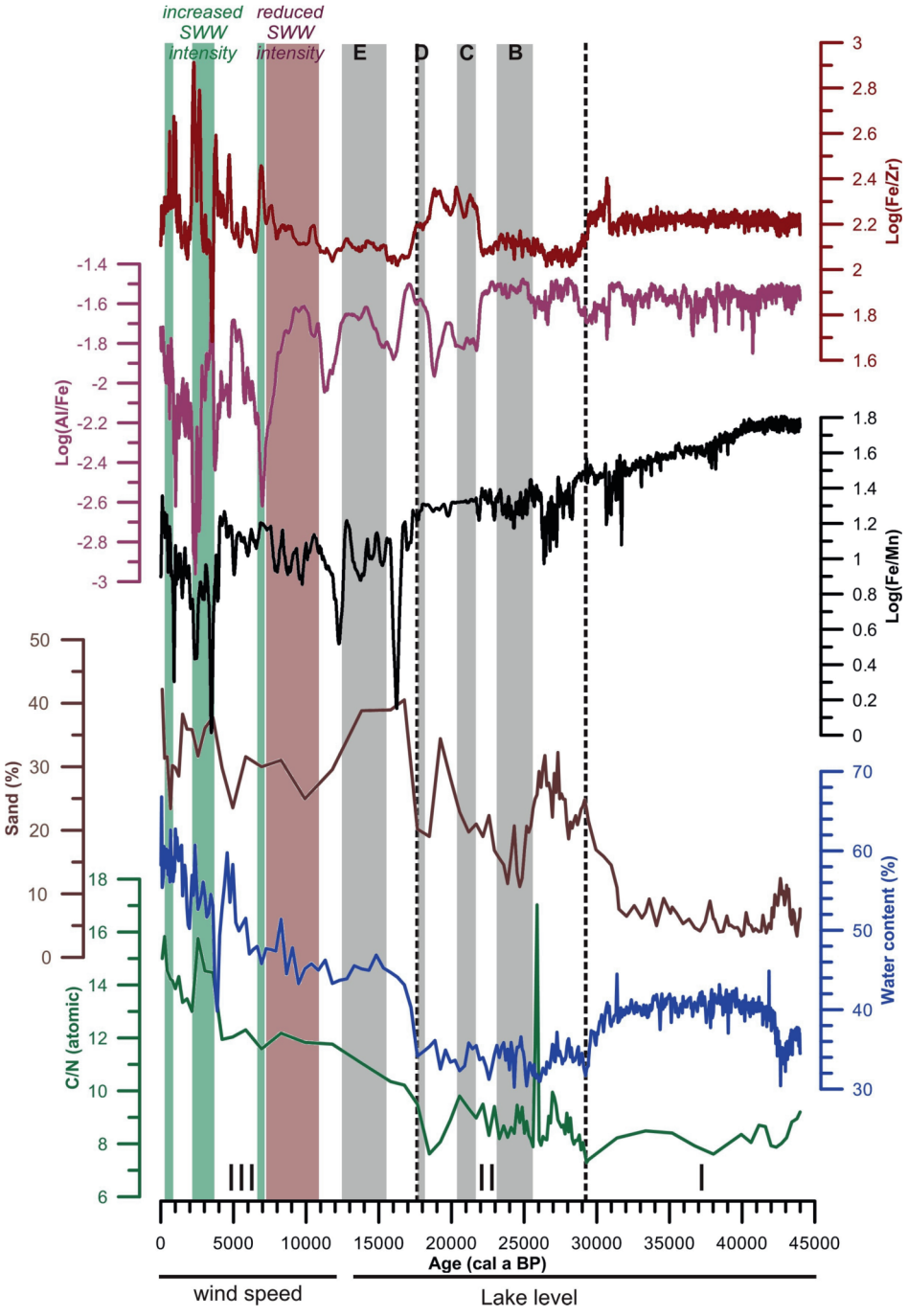

Figure V-39: Variations in the sediment proxies of Laguna Parrillar versus the age of the sediment. The gray bars indicate the age of the four different glacial stages in the Magellan area (Bentley et al., 2005; Kaplan et al., 2007; McCulloch and Bentley, 1998; McCulloch et al., 2005b; Sugden et al., 2009). The red bar indicates a period of reduced Southern Westerly wind intensity (Fletcher and Moreno, 2011; Moreno et al., 2010)

the LGM.

As each sedimentary unit in the core represents a OIS, the Laguna Parrillar sediment record is one of only a few sediment records to date from this region which document the palaeoenvironmental conditions of OIS 2 and OIS 3.

Unit I corresponds to OIS 3. The onset of Unit II or OIS 2 is at 29600 cal a BP, earlier than the onset of OIS 2 in the Greenland ice core (NGRIP) at 27780 cal a BP (Andersen et al., 2006) or the Antarctic ice cores (EDC and EDML) (Barbante et al., 2006; Blunier and Brook, 2001) and could reflect dating errors mentioned above. Nevertheless, the onset of Unit III at 17500 cal a BP is broadly synchronous with the retreat of the entire Patagonian Ice Sheet over a region with a length of 16° of latitude (McCulloch et al., 2000) and also corresponds to the retreat of the Magellan ice lobe from moraine D (Figure V-40) (Bentley et al., 2005; Kaplan et al., 2007; Sugden et al., 2005).

Although no glaciers covered Laguna Parrillar at the LGM, the level of the lake was probably controlled by fluctuations in the volume of ice present in this part of Southern Patagonia. Currently, the Río San Juan connects the lake basin with the Strait of Magellan. When the Magellan ice lobe filled the Strait, this outlet would be blocked. Several moraine arcs have been documented in this Strait, representing different stages during the last glaciation (Figure V 40) (Bentley et al., 2005; Clapperton et al., 1995; Kaplan et al., 2007; McCulloch and Bentley, 1998; McCulloch et al., 2005a; McCulloch et al., 2005b; Sugden et al., 2005; Sugden et al., 2009). During all the stages of glaciation represented by these moraines, the outlet of Laguna Parrillar would have been blocked (Figure V 40), resulting in higher lake levels as drainage of the lake was effectively dammed.

The higher solubility of Mn versus Fe in the sediment (Wetzel, 1983) has been suggested as a key to the interpretation of the Fe/Mn-ratio (Cohen, 2003). Dissolution of Mn compounds occurs if the redox potential (EH) decreases below 600 mV because of reduction of Mn^{4+} to Mn^{2+} (Sigg and Stumm, 1996). For iron the critical EH for reduction of Fe^{3+} compounds to more soluble Fe^{2+} compounds is 100 mV (Sigg and Stumm, 1996). Therefore, if the redox potential drops to values between 100 and 600mV, Fe/Mn ratios will be increasing. Rising Fe/Mn ratios are hence indicative for the beginning of reducing conditions (Cohen, 2003) and can be used as a 'palaeo-redox indicator' for lacustrine sediments (Granina et al., 2004; Schaller and Wehrli, 1997). Higher log(Fe/Mn) values can therefore be interpreted as more reducing conditions, this can be due to a higher lake level, prolonged ice cover and/or a lower wind speed, which prevent a good mixing of the complete water column.

During a higher lake level, coarse material will less likely accumulate in the centre of the lake basin, since the distance between the lake edge and the deepest part of the basin will be greater. This is visible in the variations in the sand content and in the variations of the log(Al/Fe) graph. Higher log(Al/Fe) probably indicates a higher lake level and/or during glacial times a longer period of ice cover would have created calm conditions in which the deposition of Al rich fine material such as clays, could settle. A lower log(Al/Fe) indicates a lower lake level or a less prolonged period of ice cover during glacial times. During the 'glacial interval' the length of ice cover must have had an impact as well.

The higher sand content between 44000-42000 cal a BP, coincident with rising log(Fe/Mn) (Figure V-39) values could indicate a prolonged ice cover of the lake, or that the lake level at that time was too high to allow a complete mixing of the water column, therefore not affecting the oxygen levels at the bottom of the lake.

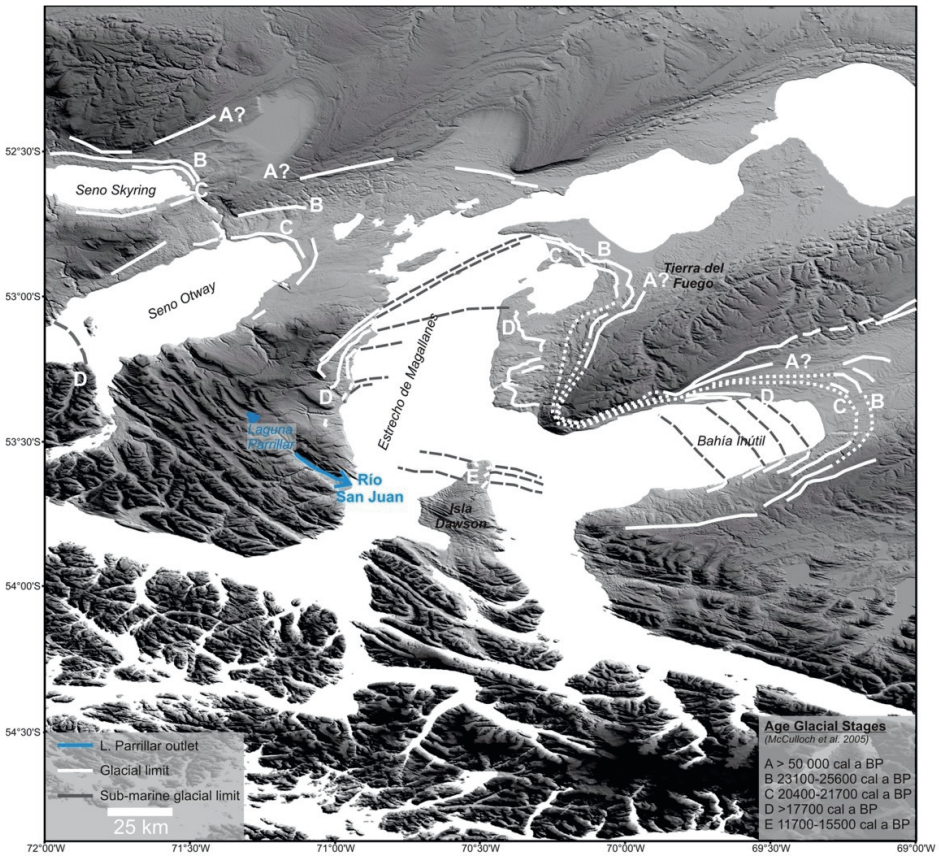

Figure V-40: Location of the MIS 2 and 3 glacial limits (e.g. A, B, C, D and E) in the Magellan area (Bentley et al., 2005; Clapperton et al., 1995; Kilian et al., 2007; McCulloch et al., 2000) and how their position prevents the outflowing water of Laguna Parrillar to reach the ocean.

Between ca. 44000-20000 cal a BP, the log(Fe/Mn) record suggests the lake level gradually reduced. The two sharp declines in the log(Fe/Mn) between 32000-31000 cal a BP and 28000-26000 cal a BP (Figure V-39) could indicate a rapid drop in lake level or simply a period with less prolonged ice cover or higher wind speeds. These two periods coincide with a higher input of sand, and the combination of higher sand content and the lower log(Fe/Mn) is perhaps indicative of better mixing within the water column, either due to a lower lake level, higher wind speeds and/or because of less prolonged winter ice cover. Except for glacial stage E (11700-15500 cal a BP) (McCulloch et al., 2005b) (Unit III: 88-80 cm depth), the other glacial stages identified by McCulloch et al. (2005b) in the Magellan Strait region are zones which contain less sand (Figure V-39). This might indicate a more prolonged period of ice cover on Laguna Parrillar.

Traces of an old shoreline at ca. 10 m above the current lake level (Figure V-31) exist, and log(Fe/Mn) variations until ca. 81 cm, ca. 12500 cal a BP, suggest higher lake levels occurred during the LGM-Holocene transition (Figure V-39). By 11700 cal a BP at the latest, the Magellan ice lob is thought to have retreated from moraine limit E (Figure V-40) (McCulloch et al., 2005b). The Laguna Parrillar record indicates retreat

from this limit might have occurred ca. 1000 years earlier.

After the retreat of the Magellan Strait glacier from limit E (McCulloch et al., 2005b), wind speed most likely controlled the log(Fe/Mn) variations in the Laguna Parrillar sediment record, since the lake's outlet was no longer blocked by the glacier. A higher wind speed will guarantee a better mixing of the water and therefore higher oxygen levels at the bottom of the lake. The wind speed in this area is highly depended of the intensity of the Southern Westerlies. More intense Westerly winds also bring more precipitation. Between 11000 and 7500 cal a BP, less intense winds would have led to a drier climate and prevented complete mixing of the lake water, resulting in a lower input of coarser grained material and higher log(Al/Fe) values (Figure V-39).

Higher Fe levels in the sediment can also be linked to the development of a moorland catchment. Iron concentration in peat-draining rivers are known to be 10-50 times higher (Krachler et al., 2010). The more developed peatbogs allowed a higher input of this enriched Fe water into the lake. Around 7000 cal a BP the first pellets, and higher log(Fe/Zr) values appear (Figure V-39). At this time, the wind was probably not sufficiently intense to allow complete mixing of the water column, which would have lowered the log(Fe/Mn) values in the sediment. Between 4000 and 2000 cal a BP, increasing log(Fe/Zr) levels and a drop in log(Fe/Mn) suggest the Westerly wind intensity increased (Figure V-39). The amount of pellets in the sediment increases at the same time. Most likely the sediment pellets are created by wave action. At this time, there is also a sudden peak in C/N which could indicate a rapid expansion of the peat vegetation, which could, in turn, be linked to the increased Westerly wind strength and resulting increase in precipitation. A similar event occurs between 1000 and 600 cal a BP (Figure V 39). Between 600 and 150 cal a BP the Westerly wind strength decreased (Figure V 39). The last 150 years the wind strength increased again (Figure V-39) and remained so until this day.

V.2.7. Palaeoclimatic Implications and Global Linkages

As mentioned previously the onset of Unit III is synchronous with the retreat of the Patagonian Ice Sheet (McCulloch et al., 2000) and the retreat of the Magellan ice lobe from the moraine limit D (McCulloch et al., 2005b; Sugden et al., 2009) in this region (Figure V-39 and Figure V-41). This event is also synchronous with the onset of the Last Termination warming in the Antarctic ice cores (Barbante et al., 2006) and the first warming pulse in the Northern Hemisphere (Rasmussen et al., 2006) (Figure V 41).

Glacial stages B to D occurred during the most cold conditions in Antarctica (Barbante et al., 2006) and during periods of less intense Southern Westerlies recorded on New Zealand's South Island (Whittaker et al., 2011) (Figure V-41).

After retreat from moraine D, the Magellan ice lobe must have retreated beyond the location of the Río San Juan outlet, allowing Laguna Parrillar's lake level to drop as is indicated by the sudden shift in log(Fe/Mn). Glacial advance E corresponds to the Antarctic Cold Reversal, and a higher lake level in Laguna Parrillar when the outflow was blocked once again. McCulloch et al. (2005b) showed that the Magellan glacier retreated from the E moraine ridge by 11700 cal a BP. The Laguna Parrillar records suggests that this might have been earlier as it requires the outflow to have been unblocked by 12500 cal a BP (Figure V-41). Therefore, during the Younger Dryas interval, the Magellan glacier could have retreated allowing reactivation of the outflow, causing the a lake level in Laguna Parrillar to drop and creating higher

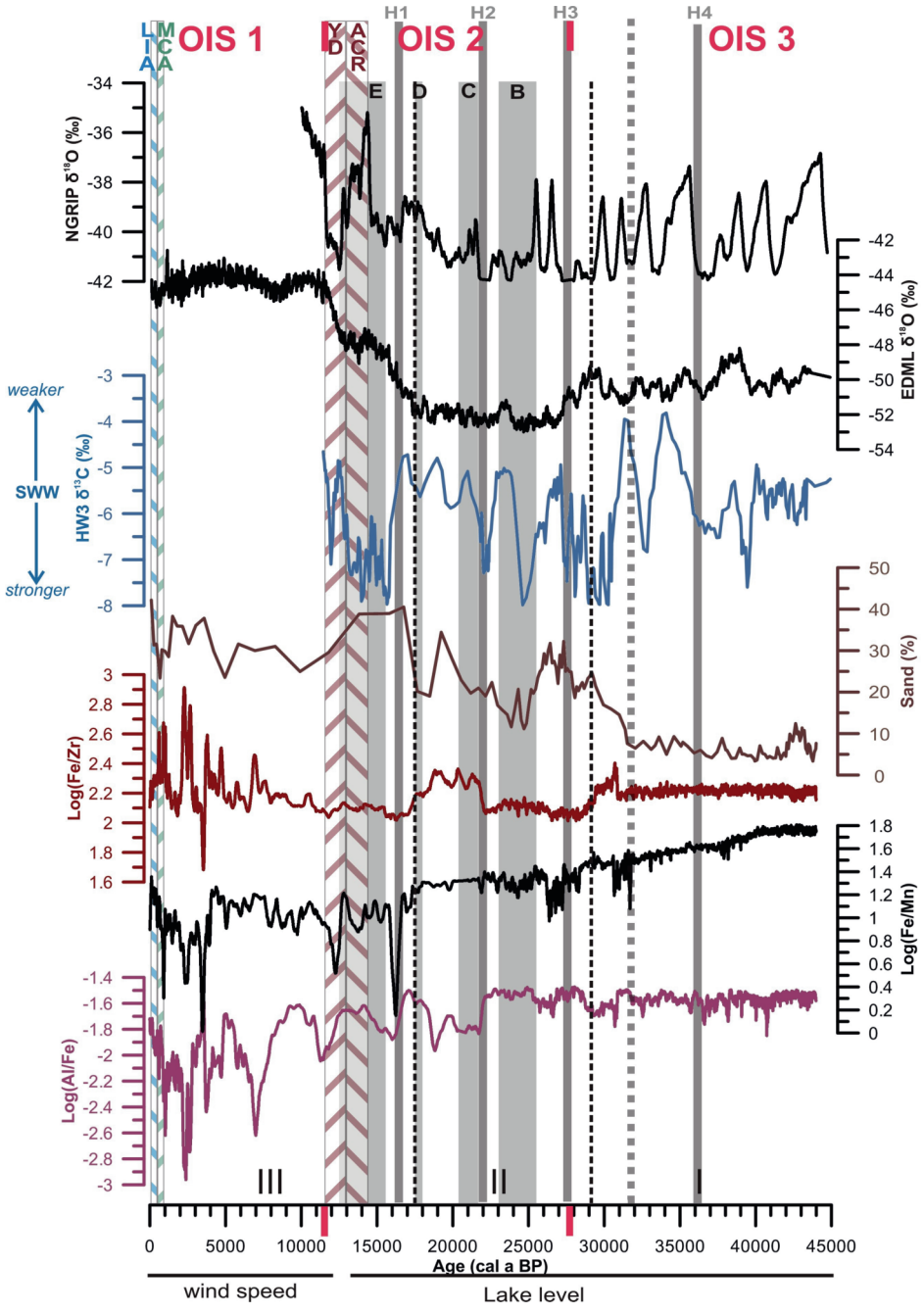

Figure V-41: Comparison to the Parrillar climate record with the oxygen isotope records of the Antarctic EDML ice core (Barbante et al., 2006), the Arctic NGRIP ice core (Rasmussen et al., 2006), both representing temperature changes and the HW3 speleothem record from the South Island in New Zealand, which records changes in the intensity of the Westerlies over this position (Whittaker et al., 2011).

oxygen levels at the bottom of the lake.

The Laguna Parrillar lake record appears to be synchronous with the Antarctic signal if we consider the start of the first warming and the climate conditions during the ACR and the YD. There are, however, indications that Northern Hemisphere Heinrich events affect local climate as well. Wang et al. (Wang et al., 2001) has already shown that the climatic impact of Heinrich events can be considered to be global in reach and rapidly transmitted through the atmosphere. Anderson et al. (2009) argues that a Heinrich event increases southern mid-latitudinal wind stress, by pushing the ITCZ southward, therefore steepening the gradient between the Tropical Pacific high pressure cell and the Antarctic low pressure cell, which will increase the Westerly wind intensity. In Laguna Parrillar, log(Fe/Mn) values fall and sand content rises directly after Heinrich Events H1 and H3, ca. 16800 and 28000 cal a BP respectively (Hemming, 2004) (Figure V-41). As a lake level drop would indicate drier conditions, it is more likely that reduced open water conditions at these times allowed more intense winds to mix the water column. Similarly, another decline in log(Fe/Mn) values at 32000 cal a BP is synchronous with a strong DO event in the Northern Hemisphere (Figure V-41).

In common with other terrestrial Holocene records using pollen (Fletcher and Moreno, 2011; Moreno et al., 2010), the early Holocene period to ca. 7000 cal a BP in Laguna Parrillar is characterised by less intense Westerly winds (Figure V-39 and Figure V-41). All these records contradict a marine record from the region, which records an increase in Westerly wind strength during this period (Lamy et al., 2010).
The onset of the Southern Westerly wind intensification at 7000 cal a BP in the Laguna Parrillar record is synchronous with many records from southern South America, whose proxy records suggest 7000-6000 cal a BP marks a phase of more intense wind (Anselmetti et al., 2009; Fletcher and Moreno, 2011; Gilli et al., 2005; Moreno et al., 2010). The wind force of the Southern Westerlies seem to be particularly strong between 4000 and 2000 cal a BP (Figure V-39 and Figure V-41). The Lago Fagnano, a large lake in Tierra del Fuego (55°S), sediment record also infers strengthening of the Westerlies at 4000 cal a BP (Moy et al., 2011).

The last event of strong Westerly winds before the current strong conditions occurs between 1000 and 600 cal a BP and corresponds to the Medieval Climate Anomaly (MCA) (Figure V-41). This period has been linked to the dominance of la Niña like conditions (Mohtadi et al., 2007; Rein et al., 2004). Periods of la Niña dominance have been linked with an intensification of the Southern Westerlies (Montecinos and Aceituno, 2003). This could be expected since an intenser Hadley cell circulation, which is associated with a La Niña phase (O'Hare et al., 2005) will push the ITCZ southward, increasing the pressure gradient between the Tropical high and the Antarctic low. Stronger Westerlies would imply more precipitation as seen in the Laguna Parrillar record at this time, and drier conditions further east, as is found in the Laguna Potrok Aike (Haberzettl et al., 2005) and the Laguna Azul (Mayr et al., 2005) records. Other records in the region record, however, drier conditions and subsequently less intense Westerlies (Moy et al., 2008; Waldmann et al., 2008) suggesting more complex and local climatological influences exist and/or that more reliable and more inter-linked sediment chronologies are needed for this region.

Opposite conditions were likely true for the period between 600 and 150 cal a BP, which corresponds to the Little Ice Age (LIA) (Figure V-41). This period is associated with a northward shift of the ITCZ (Haug et al., 2001), which would reduce the pressure gradient between the Tropical high and the Antarctic low, consequently decrease the intensity of the Southern Westerlies.

References

Abarzúa, A.M., Adán, L., De Batist, M. and Maldonado, A., 2010. Glacial to Holocene paleoclimate reconstruction based on Laguna Las Ranas record in south-central Chile (39°S), *18th International Sedimentological Congress*, Mendoza, Argentina.

Abarzúa, A.M. and Moreno, P.I., 2008. Changing fire regimes in the temperate rainforest region of southern Chile over the last 16,000 yr. *Quaternary Research*, **69**(1): 62-71.

Abarzua, A.M., Villagran, C. and Moreno, P.I., 2004. Deglacial and postglacial climate history in east-central Isla Grande de Chiloe, southern Chile (43 degrees S). *Quaternary Research*, **62**(1): 49-59.

Andersen, K.K., Svensson, A., Johnsen, S.J., Rasmussen, S.O., Bigler, M., Rothlisberger, R., Ruth, U., Siggaard-Andersen, M.L., Steffensen, J.P., Dahl-Jensen, D., Vinther, B.M. and Clausen, H.B., 2006. The Greenland Ice Core Chronology 2005, 15-42 ka. Part 1: constructing the time scale. *Quaternary Science Reviews*, **25**(23-24): 3246-3257.

Anderson, R.F., Ali, S., Bradtmiller, L.I., Nielsen, S.H.H., Fleisher, M.Q., Anderson, B.E. and Burckle, L.H., 2009. Wind-driven upwelling in the southern ocean and the deglacial rise in atmospheric CO2. *Science*, **323**: 1443-1448.

Anselmetti, F.S., Ariztegui, D., De Batist, M., Gebhardt, A.C., Haberzettl, T., Niessen, F., Ohlendorf, C. and Zolitschka, B., 2009. Environmental history of southern Patagonia unravelled by the seismic stratigraphy of Laguna Potrok Aike. *Sedimentology*, **56**(4): 873-892.

Banerjee, S.K., King, J. and Marvin, J., 1981. A rapid method for magnetic granulometry with applications to environmental studies. *Geophysical Research Letters*, **8**: 333-336.

Barbante, C., Barnola, J.-M., Becagli, S., Beer, J., Bigler, M., Boutron, C., Blunier, T., Castellano, E., Cattani, O., Chappellaz, J., Dahl-Jensen, D., Debret, M., Delmonte, B., Dick, D., Falourd, S., Faria, S., Federer, U., Fischer, H., Freitag, J., Frenzel, A., Fritzsche, D., Fundel, F., Gabrielli, P., Gaspari, V., Gersonde, R., Graf, W., Grigoriev, D., Hamann, I., Hansson, M., Hoffmann, G., Hutterli, M.A., Huybrechts, P., Isaksson, E., Johnsen, S., Jouzel, J., Kaczmarska, M., Karlin, T., Kaufmann, P., Kipfstuhl, S., Kohno, M., Lambert, F., Lambrecht, A., Lambrecht, A., Landais, A., Lawer, G., Leuenberger, M., Littot, G., Loulergue, L., Lüthi, D., Maggi, V., Marino, F., Masson-Delmotte, V., Meyer, H., Miller, H., Mulvaney, R., Narcisi, B., Oerlemans, J., Oerter, H., Parrenin, F., Petit, J.-R., Raisbeck, G., Raynaud, D., Röthlisberger, R., Ruth, U., Rybak, O., Severi, M., Schmitt, J., Schwander, J., Siegenthaler, U., Siggaard-Andersen, M.-L., Spahni, R., Steffensen, J.P., Stenni, B., Stocker, T.F., Tison, J.-L., Traversi, R., Udisti, R., Valero-Delgado, F., Broeke, M.R.v.d., Wal, R.S.W.v.d., Wagenbach, D., Wegner, A., Weiler, K., Wilhelms, F., Winther, J.-G. and Wolff, E., 2006. One-to-one coupling of glacial climate variability in Greenland and Antarctica. *Nature*, **444**(7116): 195-198.

Beer, J., Muscheler, R., Wagner, G., Laj, C., Kissel, C., Kubik, P.W. and Synal, H.-A., 2002. Cosmogenic nuclides during Isotope Stages 2 and 3. *Quaternary Science Reviews*, **21**(10): 1129-1139.

Bentley, M.J., Sugden, D.E., Hulton, N.R.J. and McCulloch, R.D., 2005. The landforms and pattern of deglaciation in the Strait of Magellan and Bahia Inu'til, southernmost South America. *Geografiska Annaler Series A - Physical Geography*, **87A**(2): 313-333.

Berger, A.L., 1978. Long-Term Variations of Caloric Insolation Resulting from Earths Orbital Elements. *Quaternary Research*, **9**(2): 139-167.

Bertrand, S., Sterken, M., Vargas-Ramirez, L., De Batist, M., Vyverman, W., Lepoint, G. and Fagel, N., 2010. Bulk organic geochemistry of sediments from

Puyehue Lake and its watershed (Chile, 40°S): Implications for paleoenvironmental reconstructions. *Palaeogeography, Palaeoclimatology, Palaeoecology*, **294**(1-2): 56-71.

Björck, S. and Wohlfarth, B., 2001. 14C chronostratigraphic techniques in paleolimnology. In: W.M. Last and J.P. Smol (Editors), *Tracking Environmental Change Using Lake Sediments. Volume 1: Basin Analysis, Coring and Chronological Techniques.* Kluwer Academic Publishers, Dordrecht, The Netherlands, pp. 205-245.

Blaauw, M., 2010. Methods and code for `classical' age-modelling of radiocarbon sequences. *Quaternary Geochronology*, **5**(5): 512-518.

Blaga, C., Reichart, G.-J., Heiri, O. and Sinninghe Damsté, J., 2009. Tetraether membrane lipid distributions in water-column particulate matter and sediments: a study of 47 European lakes along a north–south transect. *Journal of Paleolimnology*, **41**(3): 523-540.

Blaga, C.I., Reichart, G.-J., Schouten, S., Lotter, A.F., Werne, J.P., Kosten, S., Mazzeo, N., Lacerot, G. and Sinninghe Damsté, J.S., 2010. Branched glycerol dialkyl glycerol tetraethers in lake sediments: Can they be used as temperature and pH proxies? *Organic Geochemistry*, **41**(11): 1225-1234.

Blunier, T. and Brook, E.J., 2001. Timing of millennial-scale climate change in Antarctica and Greenland during the last glacial period. *Science*, **291**(5501): 109-112.

Bond, G., Kromer, B., Beer, J., Muscheler, R., Evans, M.N., Showers, W., Hoffmann, S., Lotti-Bond, R., Hajdas, I. and Bonani, G., 2001. Persistent solar influence on North Atlantic climate during the Holocene. *Science*, **294**: 2130-2136.

Brachfeld, S., Acton, G.D., Guyodo, Y. and Banerjee, S.K., 2000. High-resolution paleomagnetic records from Holocene sediments from the Palmer Deep, Western Antartic Peninsula. *Earth and Planetary Science Letters*, **181**(3): 429-441.

Calderoni, G. and Turi, B., 1998. Major constraints on the use of radiocarbon dating for tephrochronology. *Quaternary Internationa*l, **47/48**: 153-159.

Campos, H., Steffen, W., Román, C., Zúñiga, L. and Agüero, G., 1983. Limnological studies in Lake Villarrica: Morphometric, physical, chemical, planktonical factors and primary productivity. *Archiv für Hydrobiologie Supplement*, **65**(4): 371-406.

Carré, M., Bentaleb, I., Fontugne, M. and Lavallée, D., 2005. Strong El Niño events during the early Holocene: stable isotope evidence from Peruvian sea shells. *The Holocene*, **15**(1): 42-47.

Clapperton, C.M., Sugden, D.E., Kaufman, D.S. and McCulloch, R.D., 1995. The Last Glaciation in Central Magellan-Strait, Southernmost Chile. *Quaternary Research*, **44**(2): 133-148.

Clavero, J. and Moreno, H., 1994. Ignimbritas Licán y Pucón: Evidencias de erupciones explosivas andesítico-basálticas postglaciales del Volcán Villarrica, Andes del Sur, 39°25'S, *Actas VII Congreso Geológico Chileno*, Concepción, Chile, pp. 250-254.

Clement, A.C., Seager, R. and Cane, M.A., 1999. Orbital controls on the El Niño/Southern Oscillation and the tropical climate. *Paleoceanography*, **14**(4): 441-456.

Clement, A.C., Seager, R. and Cane, M.A., 2000. Suppression of El Niño during the mid-Holocene by changes in the Earth's orbit. *Paleoceanography*, **15**(6): 731-737.

Cohen, A.S., 2003. *Paleolimnology - The History and Evolution of Lake Systems*. Oxford University Press, Oxford, 500 pp.

Conroy, J.L., Overpeck, J.T., Cole, J.E., Shanahan, T.M. and Steinitz-Kannan, M., 2008. Holocene changes in eastern tropical Pacific climate inferred from a Galápagos lake sediment record. *Quaternary Science Reviews*, **27**: 1166-1180.

Divine, D.V., Koc, N., Isaksson, E., Nielsen, S., Crosta, X. and Godtliebsen, F., 2010. Holocene Antarctic climate variability from ice and marine sediment cores: Insights on ocean-atmosphere interaction. *Quaternary Science Reviews*, **29**(1-2): 303-312.

Dollenz, O.A., 1983. Fitosociologia de la Reserva Forestal "El Parrillar", Peninsula de Brunswick, Magallanes. *Anales del Instituto de la Patagonia*, **14**: 109-118.

Doran, P.T., Berger, G.W., Lyons, J., Wharton, R.A., Davisson, M.L., Southon, J. and Dibb, J.E., 1999. Dating Quaternary lacustrine sediments in the McMurdo Dry Valleys, Antarctica. *Palaeogeography Palaeoclimatology Palaeoecology*, **147**: 223-239.

Dykoski, C.A., Edwards, R.L., Cheng, H., Yuan, D., Cai, Y., Zhang, M., Lin, Y., Qing, J., An, Z. and Revenaugh, J., 2005. A high-resolution, absolute-dated Holocene and deglacial Asian monsoon record from Dongge Cave, China. *Earth and Planetary Science Letters*, **233**(1-2): 71-86.

Ertel, J.R. and Hedges, J.I., 1984. The lignin compenent of humic substances: Distribution among soil and sedimentary humic, fulvic, and base-insoluble fractions. *Geochimica Et Cosmochimica Acta*, **48**: 2065-2074.

Evans, M.E. and Heller, F., 2003. Environmental Magnetism: Principles and Applications of Enviromagnetics. International Geophysics series, Volume 86. Academic Press, San Diego, 295 pp.

Finkel, R.C. and Nishiizumi, K., 1997. Beryllium 10 concentrations in the Greenland Ice Sheet Project 2 ice core from 3-40 ka. *Journal of Geophysical Research*, **102**: 26699-26706.

Fletcher, M.-S. and Moreno, P.I., 2011. Zonally symmetric changes in the strenght and position of the Southern Westerlies drove atmospheric CO2 variations over the past 14 k.y. *Geology*, **39**(5): 419-422.

Gagan, M.K., Hendy, E.J., Haberle, S.G. and Hantoro, W.S., 2004. Post-glacial evolution of the Indo-Pacific Warm Pool and El Niño-Southern oscillation. *Quaternary International*, **118-119**: 127-143.

Gearey, B. and Gilbertson, D., 1997. Pollen taphonomy of trees in windy climate: Northbay Plantation, Barra, Outer Hebrides. *Scottish Geographical Journal*, **113**(2): 113-120.

Gilli, A., Ariztegui, D., Anselmetti, F.S., McKenzie, J.A., Markgraf, V., Hajdas, I. and McCulloch, R.D., 2005. Mid-Holocene strengthening of the Southern westerlies in South America - Sedimentological evidences from Lago Cardiel, Argentina (49°S). *Global and Planetary Change*, **49**(1-2): 75-93.

Glasser, N.F., Jansson, K.N., Harrison, S. and Kleman, J., 2008. The glacial geomorphology and Pleistocene history of South America between 38°S and 56°S. *Quaternary Science Reviews*, **27**(3-4): 365-390.

Gogorza, C.S.G., Irurzun, M.A., Chaparro, M.A.E., Lirio, J.M., Nunez, H., Bercoff, P.G. and Sinito, A.M., 2006. Relative paleointensity of the geomagnetic field over the last 21,000 year BP from sediment cores, Lake El Trébol (Patagonia, Argentina). *Earth Planets Space*, **58**: 1323-1332.

Gogorza, C.S.G., Lirio, J.M., Nunez, H., Chaparro, M., Bertorello, H.R. and Sinito, A.M., 2004. Paleointensity studies on holocene-pleistocene sediments from Lake Escondido, Argentina. *Physics of the Earth and Planetary Interiors*, **145**(1-4): 219-238.

Gogorza, C.S.G., Sinito, A.M., Di Tommaso, I., Vilas, J.F., Creer, K.M. and Nuñez, H., 1999. Holocene geomagnetic secular variations recorded by sediments from Escondido Lake (south Argentina). *Earth Planets Space*, **51**(2): 93-106.

Gogorza, C.S.G., Sinito, A.M., Lirio, J.M., Nunez, H., Chaparro, M. and Vilas, J.F., 2002. Paleosecular variations 0-19,000 years recorded by sediments from Escondido Lake (Argentina). *Physics of the Earth and Planetary Interiors*, **133**(1-4): 35-55.

Gogorza, C.S.G., Sinito, A.M., Tommaso, I.D., Vilas, J.F., Creer, K.M. and Nunez, H.,

2000a. Geomagnetic secular variations 0-12 kyr as recorded by sediments from Lake Moreno (southern Argentina). *Journal of South American Earth Sciences*, **13**(7): 627-645.

Gogorza, C.S.G., Sinito, A.M., Vilas, J.F., Creer, K.M. and Nunez, H., 2000b. Geomagnetic secular variations over the last 6500 years as recorded by sediments from the lakes of south Argentina. *Geophysical Journal International*, **143**(3): 787-798.

Granina, L., Müller, B. and Wehrli, B., 2004. Origin and dynamics of Fe and Mn sedimentary layers in Lake Baikal. *Chemical Geology*, **205(**1-2): 55-72.

Haberzettl, T., Corbella, H., Fey, M., Janssen, S., Lücke, A., Mayr, C., Ohlendorf, C., Schäbitz, F., Schleser, G.H., Wille, M., Wulf, S. and Zolitschka, B., 2007. Lateglacial and Holocene wet-dry cycles in southern Patagonia: chronology, sedimentology and geochemistry of a lacustrine record from Laguna Potrok Aike, Argentina. *The Holocene*, **17**: 297-310.

Haberzettl, T., Fey, M., Lucke, A., Maidana, N., Mayr, C., Ohlendorf, C., Schabitz, F., Schleser, G.H., Wille, M. and Zolitschka, B., 2005. Climatically induced lake level changes during the last two millennia as reflected in sediments of Laguna Potrok Aike, southern Patagonia (Santa Cruz, Argentina). *Journal of Paleolimnology*, **33**(3): 283-302.

Haug, G.H., Hughen, K.A., Sigman, D.M., Peterson, L.C. and Rohl, U., 2001. Southward migration of the intertropical convergence zone through the Holocene. *Science*, **293**(5533): 1304-1308.

Hemming, N.G., 2004. Heinrich events: massive late Pleistocene detritus layers of the North Atlantic and their global climate imprint. *Review of Geophysics*, **42**: RG1005.

Hodell, D.A., Anselmetti, F.S., Ariztegui, D., Brenner, M., Curtis, J.H., Gilli, A., Grzesik, D.A., Guilderson, T.J., Müller, A.D., Bush, M.B., Correa-Metrio, A., Escobar, J. and Kutterolf, S., 2008. An 85-ka record of climate change in lowland Central America. *Quaternary Science Reviews*, **27**(11-12): 1152-1165.

Hodell, D.A., Kanfoush, S.L., Shemesh, A., Crosta, X., Charles, C.D. and Guilderson, T.P., 2001. Abrupt cooling of Antarctic surface waters and sea ice expansion in the South Atlantic sector of the Southern Ocean at 5000 cal yr B.P. *Quaternary Research*, **56**(2): 191-198.

Hopmans, E.C., Weijers, J.W.H., Schefuß, E., Herfort, L., Sinninghe Damsté, J.S. and Schouten, S., 2004. A novel proxy for terrestrial organic matter in sediments based on branched and isoprenoid tetraether lipids. *Earth and Planetary Science Letters*, **224**(1-2): 107-116.

Hulton, N.R.J., Purves, R.S., McCulloch, R.D., Sugden, D.E. and Bentley, M.J., 2002. The last glacial maximum and deglaciation in southern South America. *Quaternary Science Reviews*, **21**: 233-241.

Irurzun, M.A., Gogorza, C.S.G., Chaparro, M.A.E., Lirio, J.M., Nunez, H., Vilas, J.F. and Sinito, A.M., 2006. Paleosecular variations recorded by Holocene-Pleistocene sediments from Lake El Trebol (Patagonia, Argentina). *Physics of the Earth and Planetary Interiors*, **154**(1): 1-17.

Kaiser, J., Schefuss, E., Lamy, F., Mohtadi, M. and Hebbeln, D., 2008. Glacial to Holocene changes in sea surface temperature and coastal vegetation in north central Chile: high versus low latitude forcing. *Quaternary Science Reviews*, **27**: 2064-2075.

Kaplan, M.R., Coronato, A., Hulton, N.R.J., Rabassa, J.O., Kubik, P.W. and Freeman, S.P.H.T., 2007. Cosmogenic nuclide measurements in southernmost South America and implications for landscape change. *Geomorphology*, **87**: 284-301.

Kilian, R., Hohner, M., Biester, H., Wallrabe-Adams, H.J. and Stern, C.R., 2003. Holocene peat and lake sediment tephra record from the southernmost Chilean Andes (53-55 degrees S). *Revista geológica de Chile*, **30**(1): 23-37.

Kilian, R., Schneider, C., Koch, J., Fesq-Martin, M., Biester, H., Casassa, G., Arévalo, M., Wendt, G., Baeza, O. and Behrmann, J., 2007. Palaeoecological constraints on late Glacial and Holocene ice retreat in the Southern Andes (53°S). *Global and Planetary Change*, **59**(1-4): 49-66.

King, J., Banerjee, S.K., Marvin, J. and Özden, Ö., 1982. A comparison of different magnetic methods for determining the relative grain size of magnetite in natural materials: some results from lake sediments. *Earth and Planetary Science Letters*, **59**(2): 404-419.

King, J.W., Banerjee, S.K. and Marvin, J., 1983. A new rock-magnetic approach to selecting sediments for geomagnetic paleointensity studies: application to paleointensity for the last 4000 years. *Journal of Geophysical Research*, **88**(B7): 5911-5921.

Korte, M. and Constable, C.G., 2005. Continuous geomagnetic field models for the past 7 millennia: 2. CALS7K. *Geochemistry Geophysics Geosystems*, **6**(2): Q02H16.

Korte, M., Donadini, F. and Constable, C.G., 2009. Geomagnetic field for 0-3 ka: 2. A new series of time-varying global models. *Geochemistry Geophysics Geosystems*, **10**(6): Q06008.

Koutavas, A., deMenocal, P., Olive, G.C. and Lynch-Stieglitz, J., 2006. Mid-Holocene El Niño-Southern Oscillation (ENSO) attenuation revealed by individual foraminifera in eastern tropical Pacific sediments. *Geology*, **34**: 993-996.

Koutavas, A., Lynch-Stieglitz, J., Marchitto, T.M.J. and Sachs, J.P., 2002. El Niño-like pattern in Ice Age tropical Pacific sea surface temperature. *Science*, **297**: 226-230.

Krachler, R., Krachler, R.F., von der Kammer, F., Süphandag, A., Jirsa, F., Ayromlou, S., Hofmann, T. and Keppler, B.K., 2010. Relevance of peat-draining rivers for the riverine input of dissolved iron into the ocean. *Science of the Total Environment*, **408**(11): 2402-2408.

Lamy, F., Hebbeln, D., Röhl, U. and Wefer, G., 2001. Holocene rainfall variability in southern Chile: a marine record of latitudinal shifts of the Southern Westerlies. *Earth and Planetary Science Letters*, **185**: 369-382.

Lamy, F., Kaiser, J., Ninnemann, U., Hebbeln, D., Arz, H.W. and Stoner, J., 2004. Antartic timing of surface water changes off Chile and Patagonian Ice Sheet response. *Science*, **304**: 1959-1962.

Lamy, F., Kilian, R., Arz, H.W., Francois, J.-P., Kaiser, J., Prange, M. and Steinke, T., 2010. Holocene changes in the position and intensity of the Southern Westerly wind belt. *Nature Geoscience*, **3**: 695-699.

Lamy, F., Ruhlemann, C., Hebbeln, D. and Wefer, G., 2002. High- and low-latitude climate control on the position of the southern Peru-Chile Current during the Holocene. *Paleoceanography*, **17**(2): 1028.

Mahaney, W.C., 2002. *Atlas of sand grain surface textures and applications.* Oxford University Press, Oxford, England, 237 pp.

Marchal, O., 2005. Optimal estimation of atmospheric 14C production over the Holocene: paleoclimate implications. *Climate Dynamics*, **24**(1): 71-88.

Masarik, J. and Beer, J., 1999. Simulation of particle fluxes and cosmogenic nuclide production in the Earth's atmosphere. *Journal of Geophysical Research - Atmospheres*, **104**(D10): 12099-12111.

Mason, B.G., Pyle, D.M., Dade, W.B. and Jupp, T., 2004. Seasonality of volcanic eruptions. *Journal of Geophysical Research*, **109**: B04206.

Masson, V., Vimeux, F., Jouzel, J., Morgan, V., Delmotte, M., Ciais, P., Hammer, C., Johnsen, S., Lipenkov, V.Y., Mosley-Thompson, E., Petit, J.R., Steig, E.J., Stievenard, M. and Vaikmae, R., 2000. Holocene climate variability in Antarctica based on 11 ice-core isotopic records. *Quaternary Research*, **54**(3): 348-358.

Matthys, A., 2010. *Relatieve paleomagnetische-intensiteitmetingen op Holocene*

sedimenten uit het Villarricameer (Chili, Zuid-Amerika) - Bijdrage tot de mastercorrelatiecurve voor de zuidelijke hemisfeer. MSc Thesis, Ghent University, Ghent, 143 pp.

Mayr, C., Fey, M., Haberzettl, T., Janssen, S., Lucke, A., Maidana, N.I., Ohlendorf, C., Schabitz, F., Schleser, G.H., Struck, U., Wille, M. and Zolitschka, B., 2005. Palaeoenvironmental changes in southern Patagonia during the last millennium recorded in lake sediments from Laguna Azul (Argentina). *Palaeogeography Palaeoclimatology Palaeoecology*, **228**(3-4): 203-227.

McCormac, F.G., Hogg, A.G., Blackwell, P.G., Buck, C.E., Higham, T.F.G. and Reimer, P.J., 2004. SHCal04 Southern Hemisphere calibration, 0-11.0 cal kyr BP. *Radiocarbon*, **46**(3): 1087-1092.

McCulloch, R.D. and Bentley, M.J., 1998. Late glacial ice advances in the Strait of Magellan, southern Chile. *Quaternary Science Reviews*, **17**(8): 775-787.

McCulloch, R.D., Bentley, M.J., Purves, R.S., Hulton, N.R.J., Sugden, D.E. and Clapperton, C.M., 2000. Climatic inferences from glacial and paleaoecological evidence at the last glacial termination, southern South America. *Journal of Quaternary Science*, **15**(4): 409-417.

McCulloch, R.D., Bentley, M.J., Tipping, R.M. and Clapperton, C.M., 2005a. Evidence for late-glacial ice dammed lakes in the central Strait of Magellan and Bahia Inutil, southernmost South America. *Geografiska Annaler Series a-Physical Geography*, **87A**(2): 335-362.

McCulloch, R.D. and Davies, S.J., 2001. Late-glacial and Holocene palaeoenvironmental change in the central Strait of Magellan, southern Patagonia. *Palaeogeography Palaeoclimatology Palaeoecology*, **173**(3-4): 143-173.

McCulloch, R.D., Fogwill, C.J., Sugden, D.E., Bentley, M.J. and Kubik, P.W., 2005b. Chronology of the last glaciation in central Strait of Magellan and Bahia Inutil, southernmost South America. *Geografiska Annaler Series a-Physical Geography*, **87A**(2): 289-312.

McGregor, H.V. and Gagan, M.K., 2004. Western Pacific coral d18O records of anomalous Holocene variability in the El Niño-Southern Oscillation. *Geophysical Research Letters*, **31**: L11204.

Meruane, C., Niño, Y. and Garreaud, R., 2005. *Response of the thermal structure of lake Villarrica (Chile) to strong foehn like wind: field study and numerical simulations, MECOM*. Universidad de Chile, Santiago de Chile, pp. 37.

Meyers, P.A., 1997. Organic geochemical proxies of paleoceanographic, paleolimnologic, and paleoclimatic processes. *Organic Geochemistry*, **27**(5-6): 213-250.

Meyers, P.A. and Teranes, J.L., 2001. Sediment organic matter. In: W.M. Last and J.P. Smol (Editors), *Tracking environmental change using lake sediments. Volume 2: Physical and geochemical methods.* Kluwer Academic Publishers, Dordrecht, The Netherlands, pp. 239-269.

Moernaut, J., 2010. *Sublacustrine landslide processes and their paleoseismological significance: Revealing the recurrence rate of giant earthquakes in South-Central Chile*. PhD Thesis, Ghent University, Ghent, 274 pp.

Mohtadi, M., Romero, O.E., Kaiser, J. and Hebbeln, D., 2007. Cooling of the southern high latitudes during the Medieval Period and its effect on ENSO. *Quaternary Science Reviews*, **26**: 1055-1066.

Montecinos, A. and Aceituno, P., 2003. Seasonality of the ENSO-Related Rainfall Variability in Central Chile and Associated Circulation Anomalies. *Journal of Climate*, **16**(2): 281-296.

Moreno, P.I., 2004. Millennial-scale climate variability in northwest Patagonia over the last 15000 yr. *Journal of Quaternary Science*, **19**(1): 35-47.

Moreno, P.I., Francois, J.-P., Moy, C.M. and Villa-Martínez, R., 2010. Covariability of the Southern Westerlies and atmospheric CO2 during the Holocene.

Geology, **38**: 727-730.
Moy, C.M., Dunbar, R.B., Guilderson, T.P., Waldmann, N., Mucciarone, D.A., Recasens, C., Ariztegui, D., Austin, J.A. and Anselmetti, F.S., 2011. A geochemical and sedimentary record of high southern latitude Holocene climate evolution from Lago Fagnano, Tierra del Fuego. *Earth and Planetary Science Letters*, **302**(1-2): 1-13.
Moy, C.M., Dunbar, R.B., Moreno, P.I., Francois, J.-P., Villa-Martínez, R., Mucciarone, D.M., Guilderson, T.P. and Garreaud, R.D., 2008. Isotopic evidence for hydrologic change related to the westerlies in SW Patagonia, Chile, during the last millenium. *Quaternary Science Reviews*, **27**: 1335-1349.
Moy, C.M., Seltzer, G.O., Rodbell, D.T. and Anderson, D.M., 2002. Variability of El Niño/Southern Oscillation activity at millennial timescales during the Holocene epoch. *Nature*, **420**: 162-165.
Muscheler, R., Beer, J., Kubik, P.W. and Synal, H.A., 2005. Geomagnetic field intensity during the last 60,000 years based on 10Be and 36Cl from the Summit ice cores and 14C. *Quaternary Science Reviews*, **24**(16-17): 1849-1860.
Muscheler, R., Joos, F., Beer, J., Müller, S.A., Vonmoos, M. and Snowball, I., 2007. Solar activity during the last 1000 yr inferred from radionuclide records. Quaternary Science Reviews, 26(1-2): 82-97.
Naranjo, J.A. and Stern, C., R., 1998. Holocene explosive activity of Hudson Volcano, southern Andes. *Bulletin of Volcanology*, **59**: 291-306.
O'Hare, G., Sweeney, J. and Wilby, R., 2005. *Weather, Climate and Climate Change - Human Perspectives*. Pearson Prentice Hall, Harlow, England.
Perdue, E.M. and Koprivnjak, J.-F., 2007. Using the C/N ratio to estimate terrigenous inputs of organic matter to aquatic environments. *Estuarine, Coastal and Shelf Science*, **73**(1-2): 65-72.
Powers, L., Werne, J.P., Vanderwoude, A.J., Sinninghe Damsté, J.S., Hopmans, E.C. and Schouten, S., 2010. Applicability and calibration of the TEX86 paleothermometer in lakes. *Organic Geochemistry*, **41**(4): 404-413.
Rasmussen, S.O., Andersen, K.K., Svensson, A.M., Steffensen, J.P., Vinther, B.M., Clausen, H.B., Siggaard-Andersen, M.L., Johnsen, S.J., Larsen, L.B., Dahl-Jensen, D., Bigler, M., Rothlisberger, R., Fischer, H., Goto-Azuma, K., Hansson, M.E. and Ruth, U., 2006. A new Greenland ice core chronology for the last glacial termination. *Journal of Geophysical Research - Atmospheres*, **111**(D6): D06102.
Reimer, P., Baillie, M., Bard, E., Bayliss, A., Beck, J., Blackwell, P., Bronk Ramsey, C., Buck, C., Burr, G., Edwards, R., Friedrich, M., Grootes, P., Guilderson, T., Hajdas, I., Heaton, T., Hogg, A., Hughen, K., Kaiser, K., Kromer, B., McCormac, F., Manning, S., Reimer, R., Richards, D., Southon, J., Talamo, S., Turney, C., van der Plicht, J. and Weyhenmeyer, C., 2009. IntCal09 and Marine09 radiocarbon age calibration curves, 0-50,000 years cal BP. *Radiocarbon*, **51**(4): 1111-1150.
Rein, B., Lückge, A., Reinhardt, L., Sirocko, F., Wolf, A. and Dullo, W.-C., 2005. El Niño variability off Peru during the last 20,000 years. *Paleoceanography*, **20**(4): PA4003.
Rein, B., Lückge, A. and Sirocko, F., 2004. A major Holocene ENSO anomaly during the Medieval period. *Geophysical Research Letters*, **31**: L17211.
Sandweiss, D.H., Maasch, K.A., Burger, R.L., Richardson, J.B., Rollins, H.B. and Clement, A., 2001. Variation in Holocene El Nino frequencies: Climate records and cultural consequences in ancient Peru. *Geology*, **29**(7): 603-606.
Schaller, T. and Wehrli, B., 1997. Geochemical focusing of manganese in lake sediments - An indicator of deep-water oxygen conditions. *Aquatic Geochemistry*, **2**: 359-378.
Schiefer, E., 2006. Contemporary sedimentation rates and depositional structures in

a montane lake basin, southern Coast Mountains, British Columbia, Canada. *Earth Surface Processes and Landforms*, **31**: 1311-1324.

SERNAGEOMIN, 2003. *Mapa Geológico de Chile: versión digital*. Servicio Nacional de Geología y Minería, Publicación Geológica Digital, No. 4, Santiago.

Shulmeister, J., 1999. Australasian evidence for mid-holocene climate change implies precessional control of Walker Circulation in the Pacific. *Quaternary International*, **57-58**: 81-91.

Sigg, L. and Stumm, W., 1996. *Aquatische Chemie*. B.G. Teubner, Stuttgart.

Silva Parejas, C., Druitt, T.H., Robin, C., Moreno, H. and Naranjo, J.-A., 2010. The Holocene Pucón eruption of Volcán Villarrica, Chile: deposit architecture and eruption chronology. *Bulletin of Volcanology*, **72**(6): 677-692.

Sinninghe Damsté, J.S., Hopmans, E.C., Pancost, R.D., Schouten, S. and Geenevasen, J., 2000. Newly discovered non-isoprenoid dialkyl diglycerol tetraether lipids in sediments. *Journal of the Chemical Society - Series Chemical Communications*: 1683-1684.

Snowball, I. and Sandgren, P., 2002. Geomagnetic field variations in northern Sweden during the Holocene quantified from varved lake sediments and their implications for cosmogenic nuclide production rates. *The Holocene*, **12**(5): 517-530.

St-Onge, G., Stoner, J.S. and Hillaire-Marcel, C., 2003. Holocene paleomagnetic records from the St. Lawrence Estuary, eastern Canada: centennial- to millennial-scale geomagnetic modulation of cosmogenic isotopes. *Earth and Planetary Science Letters*, **209**(1-2): 113-130.

Steig, E.J., Morse, D., Waddington, E.D., Stuiver, M., Grootes, P., Mayewski, P., Twickler, M.S. and Whitlow, S., 2000. Wisconsinan and Holocene climate history from an ice core at Taylor Dome, western Ross Embayment, Antarctica. *Geografiska Annaler*, **82A**: 213-235.

Steinhilber, F., Beer, J. and Fröhlich, C., 2009. Total solar irradiance during the Holocene. *Geophysical Research Letters*, **36**: L19704.

Stern, C., 2008. Holocene tephrochronology record of large explosive eruptions in the southernmost Patagonian Andes. *Bulletin of Volcanology*, **70**(4): 435-454.

Stern, C. and Kilian, R., 1996. Role of the subducted slab, mantle wedge and continental crust in the generation of adakites from the Andean Austral Volcanic Zone. *Contributions to Mineralogy and Petrology*, **123**: 263-281.

Stockhausen, H. and Zolitschka, B., 1999. Environmental changes since 13.000 cal BP reflected in magnetic and sedimentological properties of sediments from lake Holzmaar (Germany). *Quaternary Science Reviews*, **18**: 913-925.

Stott, L.D., Cannariato, K.G., Thunell, R.C., Haug, G.H., Koutavas, A. and Lund., S.P., 2004. Decline of surface temperature and salinity in the western tropical Pacific Ocean in the Holocene epoch. *Nature*, **431**: 56-59.

Sugden, D.E., Bentley, M.J., Fogwill, C.J., Hulton, N.R.J., McCulloch, R.D. and Purves, R.S., 2005. Late-glacial glacier events in southernmost South America: A blend of 'northern'and 'southern' hemispheric climatic signals? *Geografiska Annaler Series a-Physical Geography*, **87A**(2): 273-288.

Sugden, D.E., McCulloch, R.D., Bory, A.J.-M. and Hein, A.S., 2009. Influence of Patagonian glaciers on Antarctic dust deposition during the last glacial period. *Nature Geoscience*, **2**: 281-285.

Tauxe, L., 1993. Sedimentary Records of Relative Paleointensity of the Geomagnetic-Field - Theory and Practice. *Reviews of Geophysics*, **31**(3): 319-354.

Tauxe, L., 1998. *Paleomagnetic principles and practice*. Kluwer Academic Publishers, Dordrecht, 299 pp.

Thompson, L.G., Davis, M.E., Mosley-Thompson, E., Sowers, T.A., Henderson, K.A., Zagorodnov, V.S., Lin, P.N., Mikhalenko, V.N., Campen, R.K., Bolzan, J.F., Cole-Dai, J. and Francou, B., 1998. A 25,000-year tropical climate history from Bolivian ice cores. *Science*, **282**(5395): 1858-1864.

Tierney, J.E. and Russell, J.M., 2009. Distributions of branched GDGTs in a tropical lake system: Implications for lacustrine application of the MBT/CBT paleoproxy. *Organic Geochemistry*, **40**(9): 1032-1036.

Tudhope, A.W., Chilcott, C.P., McCulloch, M.T., Cook, E.R., Chappell, J., Ellam, R.M., Lea, D.W., Lough, J.M. and Shimmield, G.B., 2001. Variability in the El Niño-Southern Oscillation Through a Glacial-Interglacial Cycle. *Science*, **291**(5508): 1511-1517.

Van Daele, M., Moernaut, J., Heirman, K., Silversmit, G., Wolff, C., Pino, M., Brümmer, R., Urrutia, R., Roberts, S., Vincze, L., Brauer, A. and De Batist, M., 2010. Impact of the 1960 earthquake and older historical earthquakes on the sedimentary record of lakes in South-Central Chile, *18th International Sedimentological Congress "Sedimentology at the foot of the Andes"*, Mendoza, Argentina.

van Geel, B., Raspopov, O.M., Renssen, H., van der Plicht, J., Dergachev, V.A. and Meijer, H.A.J., 1999. The role of solar forcing upon climate change. *Quaternary Science Reviews*, **18**(3): 331-338.

Vargas, L., Roche, E., Gerrienne, P. and Hooghiemstra, H., 2008. A pollen-based record of late glacial–Holocene climatic variability in the southern lake district, Chile. *Journal of Paleolimnology*, **39**: 197-217.

Verleye, T.J. and Louwye, S., 2010. Late Quaternary environmental changes and latitudinal shifts of the Antarctic Circumpolar Current as recorded by dinoflagellate cysts from offshore Chile (41°S). *Quaternary Science Reviews*, **29**(1025-1039).

Volland, S., 2006. *Sediment dynamics in Lago Calafquén and Lago Villarica (Northern Patagonia - Chile): A baseline study on sedimentological processes and considerations in assessing palaeoenvironmental change*, Technischen Universität München, München, 341 pp.

Vonmoos, M., Beer, J. and Muscheler, R., 2006. Large variations in Holocene solar activity: Constraints from 10Be in the Greenland Ice Core Project ice core. *Journal of Geophysical Research*, **111**: A10105.

Waldmann, N., Ariztegui, D., Anselmetti, F.S., Austin, J.A.J., Dunbar, R., Moy, C.M. and Recasens, C., 2008. Seismic stratigraphy of Lago Fagnano sediments (Tierra del Fuego, Argentina) - A potential archive of paleoclimatic change and tectonic activity since the Late Glacial. *Geologica Acta*, **6**(1): 1-10.

Wang, Y.J., Cheng, H., Edwards, R.L., An, Z.S., Wu, J.Y., Shen, C.C. and Dorale, J.A., 2001. A high-resolution absolute-dated Late Pleistocene monsoon record from Hulu Cave, China. *Science*, **294**(5550): 2345-2348.

Wang, Y.J., Cheng, H., Edwards, R.L., He, Y.Q., Kong, X.G., An, Z.S., Wu, J.Y., Kelly, M.J., Dykoski, C.A. and Li, X.D., 2005. The Holocene Asian monsoon: links to solar changes and North Atlantic climate. *Science*, **308**: 854-857.

Webster, P.J., Magana, V.O., Palmer, T.N., Shukla, J., tomas, R.A., Yanai, M. and Yasunari, T., 1998. Monsoon: processes, predictability, and the prospects for prediction. *Journal of Geophysical Research - Oceans*, **103**(C7): 14451-14510.

Weijers, J.W.H., Schouten, S., Hopmans, E.C., Geenevasen, J.A.J., David, O.R.P., Coleman, J.M., Pancost, R.D. and Sinninghe Damsté, J.S., 2006a. Membrane lipids of mesophilic anaerobic bacteria thriving in peats have typical archaeal traits. *Environmental Microbiology*, **8**: 648-657.

Weijers, J.W.H., Schouten, S., Spaargaren, O.C. and Sinninghe Damsté, J.S., 2006b. Occurrence and distribution of tetraether membrane lipids in soils: Implications for the use of the TEX86 proxy and the BIT index. *Organic Geochemistry*, **37**(12): 1680-1693.

Weijers, J.W.H., Panoto, E., van Bleijswijk, J., Schouten, S., Balk, M., Stams, A.J.M., Rijpstra, W.I.C. and Sinninghe Damsté, J.S., 2009. Constraints on the biological source(s) of the orphan branched tetraether membrane lipids. *Geomicrobiology Journal*, **26**: 402-414.

Wetzel, R.G., 1983. *Limnology*. Saunders College Publishing, Philadelphia, USA.

Whittaker, T.E., Hendy, C.H. and Hellstrom, J.C., 2011. Abrupt millenial-scale changes in intensity of Southern Hemisphere winds during marine isotope stage 2-4. *Geology*, **39**(5): 455-458.

Willmott, V., Domack, E.W., Canals, M. and Brachfeld, S., 2006. A high resolution relative paleointensity record from the Gerlache-Boyd paleo-ice stream region, northern Antarctic Peninsula. *Quaternary Research*, **66(**1): 1-11.

Woodroffe, C.D., Beech, M.R. and Gagan, M.K., 2003. Mid-late Holocene El Niño variability in the equatorial Pacific from coral microatolls. *Geophysical Research Letters*, **30**(7): 1358.

Woodroffe, C.D. and Gagan, M.K., 2000. Coral microatolls from the central Pacific record late Holocene El Niño. *Geophysical Research Letters*, **27**(10): 1511-1514.

Yang, X., Heller, F., Yang, J. and Su, Z., 2009. Paleosecular variations since ~9000 yr BP as recorded by sediments from maar lake Shuangchiling, Hainan, South China. *Earth and Planetary Science Letters*, **288**: 1-9.

Zhang, Q., Yang, H., Zhong, Y. and Wang, D., 2005. An idealized study of the impact of extratropical climate change on El Niño–Southern Oscillation. *Climate Dynamics*, **25**(7): 869-880.

VI. Changes in the Southern Westerlies' Position and Intensity

"The pessimist complains about the wind;
the optimist expects it to change;
the realist adjusts the sails."
(William Arthur Ward)

The Southern Westerly Winds (SWW) are an important component of the global climate system. In conjunction with the Antarctic Circumpolar Current (ACC), westerly flow regulates meridional heat flux and the concentration of atmospheric carbon dioxide (Toggweiler et al., 2006), and is able to rapidly transmit climatic signals like El Niño-Southern Oscillation (ENSO) (Bertler et al., 2006). Changes in Westerly intensity over time will enhance or diminish these climatic controls. Changes in the intensity of this wind system can be inferred from the Laguna Parrillar record for the last 40000 years. Since the Lago Villarrica record only spans the Holocene, comparison of both lake records (Lago Villarrica and Laguna Parrillar) are only possible in this time period. Due to the same reason, the Holocene is also the only period were it is possible to determine if the Southern Westerlies have shifted north or south through time. Since no time frame is available for the seismic records, only assumptions can be made on the possible timing of the environmental changes detected in these seismic stratigraphies.

VI.1. Modern Southern Westerlies

The Southern Westerlies are the prevailing winds in the southern mid-latitudes of Earth's atmosphere, blowing from west to east between the high-pressure areas of the subtropics and the low-pressure areas near Antarctica. This wind system exhibits considerable variability on intra- and inter-annual time scales.

The track and intensity of the Southern Westerlies are controlled by the strength and latitudinal position of the subtropical anticyclone in the Southeast Pacific and the circum-Antarctic low pressure belt. The position of the Southeast Pacific anticyclone is controlled by the position of the Intertropical Convergence Zone (ITCZ). The ITCZ shifts south during austral summer (December-January-February), consequently pushing the Southeastern Pacific anticyclone south (Figure VI-1). This results in a strengthening of the

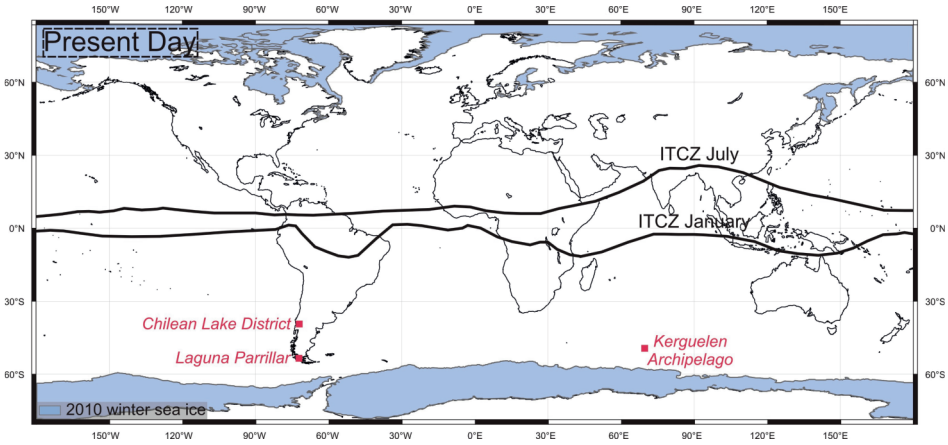

Figure VI-1: Current January and July position of the ITCZ (Iriondo, 1999) and the expansion of the polar sea ice during boreal and austral winter (NOAA, 2010)

Southern Westerlies. During the austral winter (June-July-August) the ITCZ shifts north (Figure VI-1). This decreases the pressure gradient between the subtropical high and the Antarctic low, reducing the intensity of the Southern Westerlies. Colder temperatures in Antarctica and Antarctic sea-ice expansion during the austral winter will, however, push the southern limit of the Westerly belt slightly north, therefore affecting the pressure gradient.

The climate of southern Chile is controlled by the frequent passage of cyclonic storms originating from the Southern Westerlies. The area north of 42°S is characterized by gradually decreasing summer rain towards the north, changing to the Mediterranean-type summer dry conditions in central Chile. The seasonal north-south movement of the ITCZ has a major influence in this area. South of 42°S a year-round supply of moist Pacific air masses results in extraordinary high precipitation (> 6000 mm/a). The location of the maximum storm tracks of the Southern Westerlies is related to the steepest SST gradients within the Polar Front, which is located near 45°S off the coast of Chile (Streten and Zillman, 1984).

The Southern Westerlies have strengthened and shifted poleward over the past 50 years, due to a positive phase of the Antarctic Oscillation (AAO), and possibly in response to warming from rising concentrations of atmospheric carbon dioxide (CO_2) (Gillett et al., 2006; Shindell and Schmidt, 2004).

VI.2. Glacial Southern Westerlies

Until the early 1990s, the Westerlies were generally not regarded as a particularly important component of the global climate system. Early attempts to locate the glacial Southern Westerlies with biological proxies were equivocal; with one school arguing for equatorward shifted Southern Westerlies (Heusser, 1989) and another supporting poleward shifted Southern Westerlies (Markgraf, 1989).

The poleward shifts in the Southern Westerlies over the last 50 years (Gillett et al., 2006) and the evidence tying these shifts to greenhouse warming (Shindell and Schmidt, 2004) suggest that the Southern Westerlies also shifted poleward as CO_2 increased and

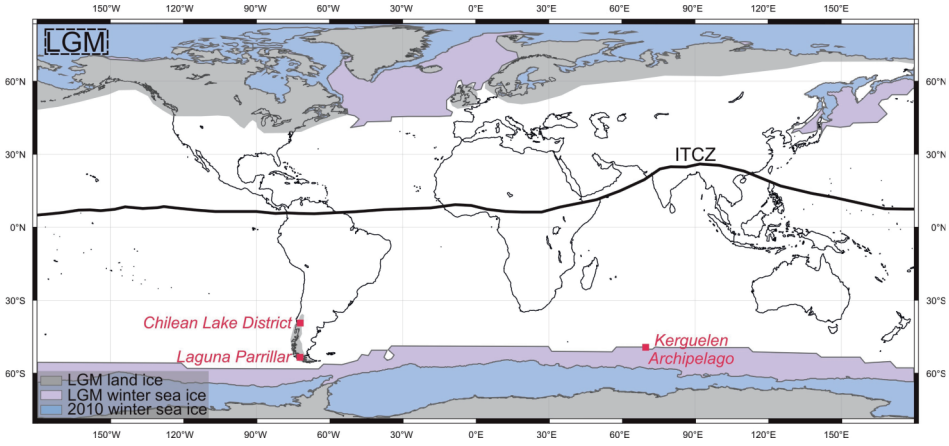

Figure VI-2: Position of the ITCZ (the modern July position is used as a possible northern location of the ITCZ) (Iriondo, 1999), location of the major ice sheets (Chiang and Bitz, 2005) and expansion of the polar sea ice during the Last Glacial Maximum (LGM) (Wyrwoll et al., 2000)

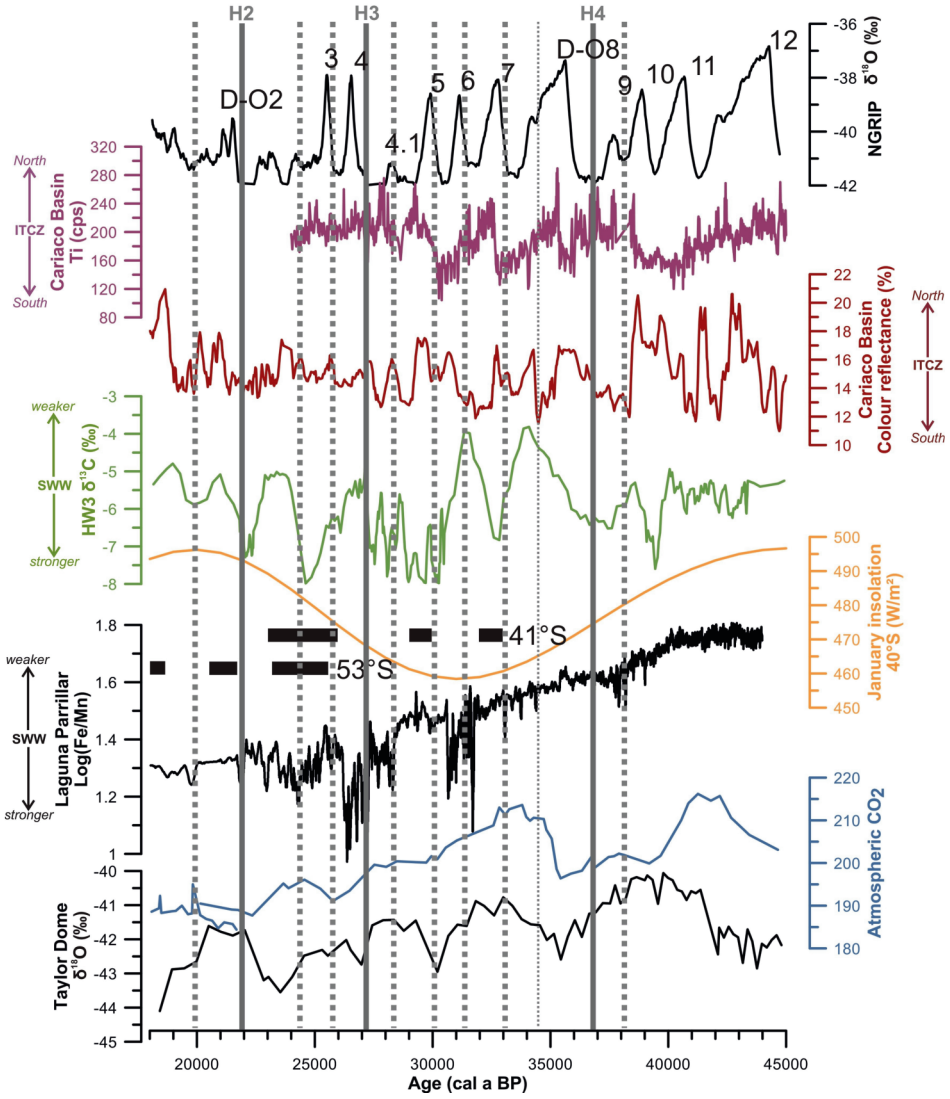

Figure VI-3: Comparison of the Laguna Parrillar log(Fe/Mn) record with $\delta^{18}O$ temperature record of the Greenland NGRIP ice core (Rasmussen et al., 2006), the titanium and colour reflectance record of the Cariaco Basin (10°N) (Peterson and Haug, 2006), the New Zealand HW3 speleothem record (41°S) (Whittaker et al., 2011), the periods of Patagonian moraine formation (black bars) at 41°S (Denton et al., 1999; Lowell et al., 1995) and 53°S (McCulloch et al., 2005b), austral summer solar irradiance at 40°S (Berger, 1978), the atmospheric CO_2 (Indermühle et al., 1999a) record and the $\delta^{18}O$ temperature record of the Antarctic Taylor Dome ice core (Steig et al., 2000) during the last glaciation. The grey bars indicate the location in time of the H2, H3 and H4 Heinrich event (Hemming, 2004). The dotted lines indicate the periods when a D-O event corresponds to a disturbance in the log(Fe/Mn) record of Laguna Parrillar.

the climate warmed at the end of the last ice age. This implies that the Southern Westerlies at the Last Glacial Maximum (LGM) were equatorward of their Holocene position (Anderson et al., 2009; Lamy et al., 2007; Toggweiler et al., 2006).

The key process is the ventilation of the deep Southern Ocean and its relationship to the Southern Westerly winds in the atmosphere. Strong Southern Westerlies over the ACC bring deep water laden with respired CO_2 directly up to the surface where the respired CO_2 is rapidly vented to the atmosphere. Southern Westerlies shifted away from the ACC shut down this process by allowing a low-salinity cap and thick sea ice to develop over the Southern Ocean (Anderson et al., 2009). The Southern Westerlies over the Southern Ocean seem to be stronger and/or shift poleward in warmer climates and weaker and/or shift equatorward in cool climates (Ahn and Brook, 2008; Anderson et al., 2009).

Some modelling studies suggest that a southward shift in the ITCZ is a robust feature of atmospheric reorganisation during cold climates, regardless of whether cold Northern Hemisphere conditions are induced by imposing sea ice (Chiang and Bitz, 2005) or fresh water (Dahl et al., 2005; Zhang and Delworth, 2005) on the North Atlantic Ocean (Figure VI-2). Both will cause the Atlantic Meridional Overturning Circulation (AMOC), to slow down (McManus et al., 2004).

Evidence from marine sediment proxies of a core in the Southern Ocean indicates that CO_2 concentration rose most rapidly when AMOC slowed down and stratification in the Southern Ocean was reduced (Ahn and Brook, 2008).

Studies have presented evidence for a global reorganization of atmospheric circulation during Northern Hemisphere cold events such as Heinrich Events (H) and the Younger Dryas (YD). Heinrich events are believed to represent glacial ice sheet instabilities that have triggered major reorganizations of the AMOC (Hemming, 2004). Palaeoproxy evidence for a southward shift in the ITCZ during H and/or the YD is found in records from Africa (Tierney and Russell, 2007; Verschuren et al., 2009),

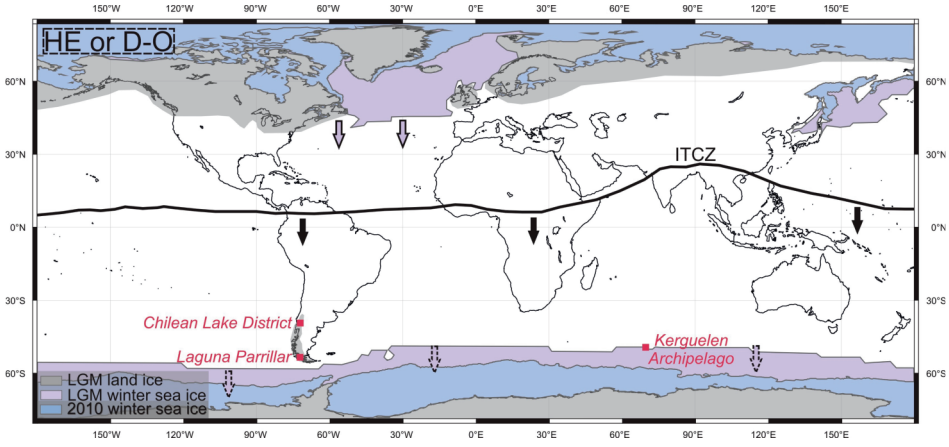

Figure VI-4: Position of the ITCZ (the modern July position is used as a possible northern location of the ITCZ) (Iriondo, 1999), location of the major ice sheets (Chiang and Bitz, 2005) and expansion of the polar sea ice (Wyrwoll et al., 2000) during a Heinrich event (HE) or Dansgaard-Oeschger event. The arrows indicated the direction in which the sea-ice limits and the ITCZ changed. of the polar sea ice during the Last Glacial Maximum (LGM) (Wyrwoll et al., 2000)

Asia (Wang et al., 2001), and South America (Haug et al., 2001; Peterson and Haug, 2006) (Figure VI-4 and Figure VI-5).

The Laguna Parrillar record contains proxy indications of Southern Westerly wind intensification during the last glaciation (Figure VI-3). Lower log(Fe/Mn) values suggest better mixing of the lake water, implying that stronger winds were stirring up the water column, and that the lake did not have a year round ice-cover. A common trend emerges when the timing of these changes are compared with proxies for Northern Hemisphere ice sheet expansion (NGRIP ice core) (Rasmussen et al., 2006), for ITCZ movement in the Cariaco Basin (10°N) (Peterson and Haug, 2006), for atmospheric CO_2 levels (Indermühle et al., 1999a; Indermühle et al., 1999b) and for Southern Hemisphere ice sheet expansion (Taylor Dome ice core) (Steig et al., 1998; Steig et al., 2000). The start of a Southern Westerly wind intensification is synchronous with a southward movement of the ITCZ, a Dansgaard-Oeschger (D-O) event in Greenland, increased temperatures over the Antarctic and increased atmospheric CO_2 levels (Figure VI-3). Some of these intensifications are synchronous with Heinrich events (e.g. H2, H3 and H4), but apparently almost every other D-O event can cause the ITCZ to shift southward and therefore affect the intensity of the Southern Westerlies. Even a minor cold pulse in the Greenland interstadial between D-O7 and D-O8 leaves its mark in the Laguna Parrillar record (Figure VI-3).

The reconstructed Southern Westerly behaviour, using the Laguna Parrillar record, is similar to another Southern Westerly record from the HW3 speleothem from New Zealand's Southern Island (Whittaker et al., 2011) (Figure VI-3). Before 40000 cal a BP the Southern Westerlies were less variable. Although the Northern Hemisphere ice sheet already fluctuated, the Ti record of the Cariaco Basin shows reduced ITCZ latitudinal fluctuations and reduced temperature in Antarctica. Similarly, the HW3 speleothem record in New Zealand also show less Southern Westerlies variability.

Laguna Parrillar is located within the belt of the Southern Westerlies, regardless if they occur in their most poleward or most equatorward position. Therefore, it is not straightforward to reconstruct changes in the Southern Westerlies' position from the Laguna Parrillar record and to infer whether a latitudinal shift of the position of the Southern Westerlies occurred or whether simply an expansion of the region in where the influence of the Southern Westerlies operated.

During the twentieth century, retreats (advances) of glaciers in the Southern Alps of New Zealand and in the Southern Andes are all associated with weaker (stronger) Westerlies (Fitzharris et al., 2007). Consequently it is not unreasonable to assume that the same mechanism was acting during glacier advances in OIS 2 and 3. The largest changes in the Southern Westerly intensity occurred between 23000 and 33000 cal a BP in the Laguna Parrillar record and the HW3 speleothem record (Whittaker et al., 2011). This is also the time frame in OIS 2 during which many moraine formation in Southern (53°S) and Northern (41°S) Patagonian were formed (Denton et al., 1999; Kaplan et al., 2005; Lowell et al., 1995; McCulloch et al., 2005b). Austral summer insolation was at its lowest (Berger, 1978) (Figure VI-3). This might indicate that three of the four erosional unconformities (UC2, UC3 and UC4) seen in the seismic stratigraphy of four lakes in the Chilean Lake District were formed sometime during this period. These unconformities indicate glacial advances of the northern edge of the Patagonian ice sheet. UC4 might be of a younger (16500-17500 cal a BP) age, when using the deglaciation sequence constructed from dating moraines bordering the lakes in the Chilean Lake District (Denton et al., 1999; Lowell et al., 1995). But, UC4 might well be older,

when considering the seismic stratigraphy of Lago Puyehue (Charlet et al., 2008; Heirman et al., in press).

The rapid and large changes in the Southern Westerlies' intensity between 33000 and 23000 cal a BP might explain why the Chilean Lake District glaciers did not completely remove all previously deposited sediments from the lake basins. The duration of the more intense Southern Westerlies was probably not long enough to sustain a glacier with a large erosional force. Consequently, it is likely that the erosional surface UC1 was made prior to 40000 cal a BP in period when the Westerlies fluctuated less.

VI. 3. Last Termination Southern Westerlies

The Last Termination until the start of the Holocene saw major global reorganization of atmospheric and oceanic circulation patterns. Both poles started to warm, ice sheets retreat and the AMOC's intensity started to increase.

The effects of this reorganisation are reflected in the record of Laguna Parrillar, in which they are evidenced by fluctuations in the log(Fe/Mn) values, which are interpreted to mark variations in the intensity of wind induced mixing of the lake water (Figure VI-6). A first evidence for a strong increase in the intensity of the Southern Westerlies starts at 17500 cal a BP. This is synchronous with the proposed age of the retreat of the Patagonian ice sheet across all latitudes by McCulloch et al (2000). At this time, temperatures in Antarctica were slightly higher (Steig et al., 2000), the ITCZ was in a more southward position (Peterson and Haug, 2006) and atmospheric CO_2 levels started to increase (Indermühle et al., 1999b) (Figure VI-6). The period with the most intense increase in Southern Westerlies' activity is synchronous with H1, ca. 16800 cal a BP (Hemming, 2004). A large discharge of ice bergs in the North Atlantic had a major influence on the AMOC, subsequently affecting the Southern Hemisphere (Anderson et al., 2009). At ca. 16000 cal a BP the Southern Westerly wind was weaker possibly due to a northward shift of the ITCZ. Weak Southern Westerly winds persisted into the Antarctic Cold Reversal (ACR) (Figure VI-6). This is also the case in the HW3 speleothem record from New Zealand (Whittaker et al., 2011) (Figure VI-6). During the Younger Dryas (YD) the Southern Westerly wind

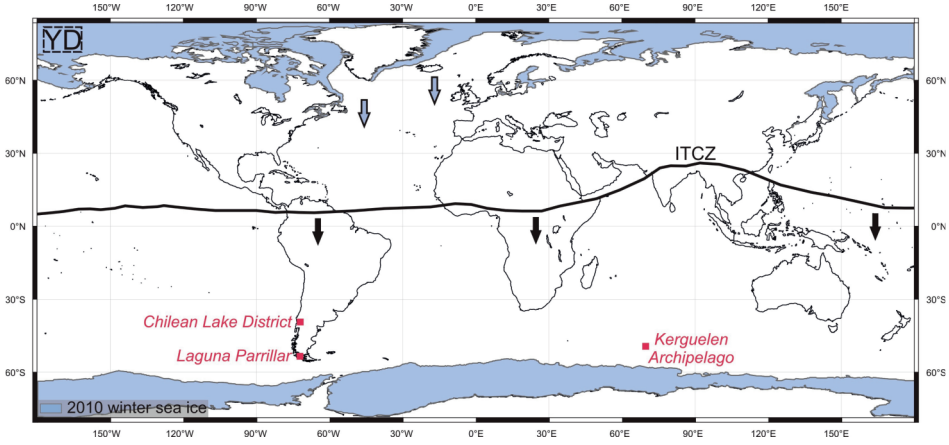

Figure VI-5: Position of the ITCZ (the modern July position is used as a possible northern location of the ITCZ) (Iriondo, 1999) and expansion of the polar sea ice (NOAA, 2010) during the Younger Dryas (YD). The arrows indicated the direction in which the sea-ice limits and the ITCZ changed.

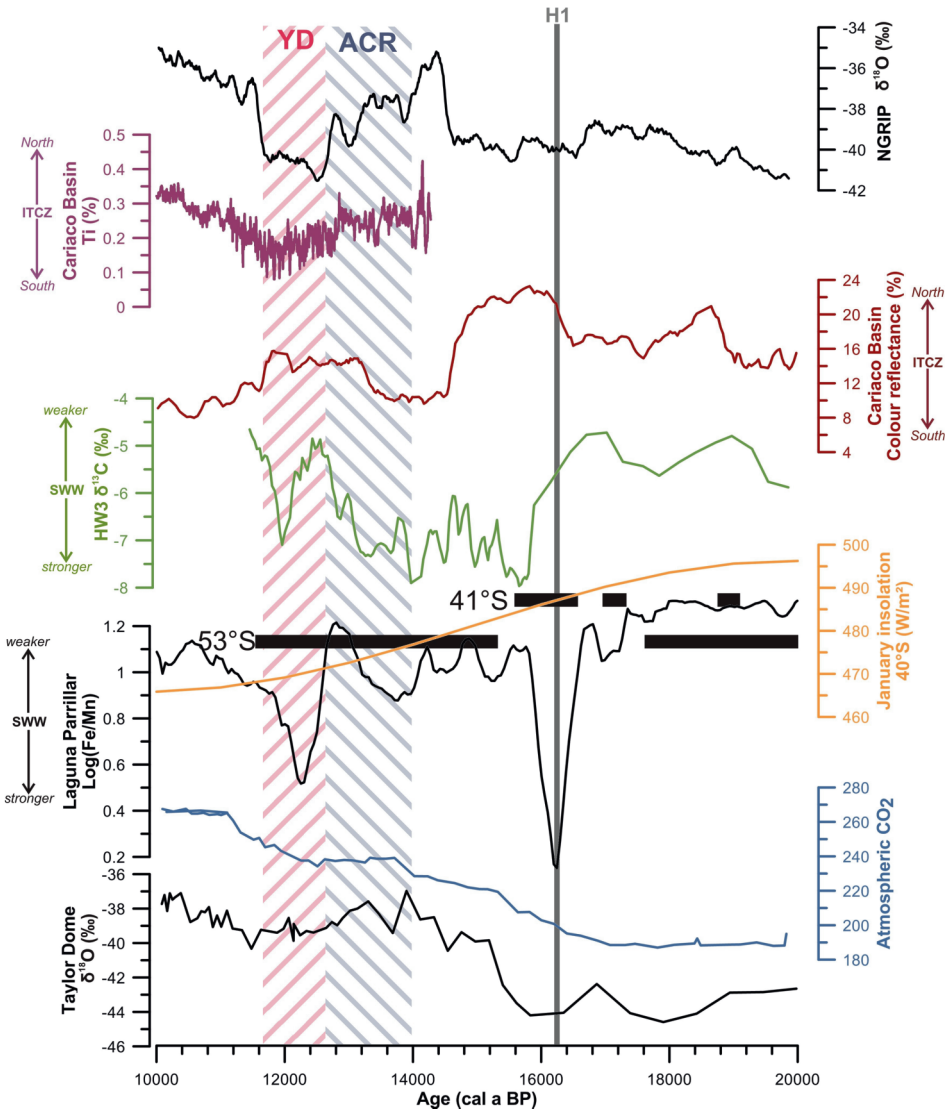

Figure VI-6: Comparison of the Laguna Parrillar log(Fe/Mn) record with $\delta^{18}O$ temperature record of the Greenland NGRIP ice core (Rasmussen et al., 2006), the titanium (Haug et al., 2001) and colour reflectance (Peterson and Haug, 2006) record of the Cariaco Basin (10°N), the New Zealand HW3 speleothem record (41°S) (Whittaker et al., 2011), the periods of Patagonian moraine formation (black bars) at 41°S (Denton et al., 1999; Lowell et al., 1995) and 53°S (McCulloch et al., 2005b), austral summer solar irradiance at 40°S (Berger, 1978), the atmospheric CO_2 (Indermühle et al., 1999a) record and the $\delta^{18}O$ temperature record of the Antarctic Taylor Dome ice core (Steig et al., 2000) during the Last Terminaton. The grey bar indicates the timing of H1 (Hemming, 2004).

strength increased again, broadly synchronous with Northern Hemisphere ice sheet advances which pushed the ITCZ southward (Figure VI-5 and Figure VI-6). When the Northern Hemisphere started to warm at the end of the YD, the ITCZ moved northward again, and the pressure gradient between the Southeast Pacific high and the Antarctic low reduced, inducing weaker Southern Westerlies.

Glacial retreat most likely started around 17500 cal a BP. If this retreat was indeed synchronous at both the northern and southern edge of this ice sheet, it would imply that the Southern Westerlies' intensity changed synchronously both at its northern and southern edge. In Southern Patagonia, there was a major glacier standstill between ca. 15000 and 11000 cal a BP (McCulloch et al., 2005a). No large moraines have been dated in this period at the northern edge of the ice sheet, but there are geomorpholgoical traces of glacier standstill (Bentley, 1997; Denton et al., 1999). As there are records in this region which indicate a much earlier retreat (Charlet et al., 2008; Heirman et al., in press; Sterken et al., 2008), it remains debatable whether or not the youngest erosional unconformity in the seismic stratigraphy in the Chilean Lake District (UC4) was formed during the Last Termination.

VI. 4. Holocene Southern Westerlies

When examined together, the Lago Villarrica and Laguna Parrillar sediment records can provide key new constraints on the Holocene variability of the Southern Westerlies (Figure VI-9).

Since the position and the intensity of the Southern Westerlies have changed during the last 50 years (Gillett et al., 2006), it is not unreasonable to assume that this happened in other periods of the Holocene.

During the Holocene the ITCZ has gradually moved southward (Haug et al., 2001), which should have resulted in a gradual increase in intensity of the Southern Westerlies. After the warm, Early Holocene Optimum, sea-ice cover increased again (Divine et al., 2010), affecting the latitudinal gradient in atmospheric pressure and resulted in an intensification of the Westerlies. Furthermore changes in insolation at this time likely caused a general strengthening of the Southern

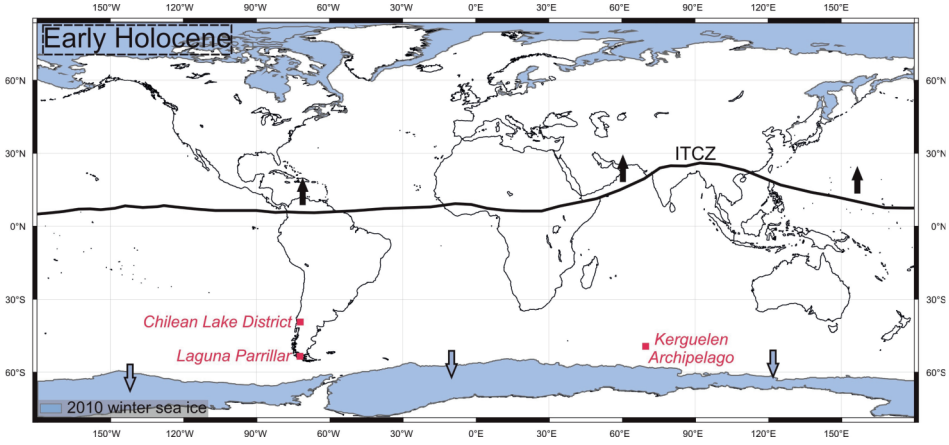

Figure VI-7: Position of the ITCZ (the modern July position is used as a possible northern location of the ITCZ) (Iriondo, 1999) and expansion of the polar sea ice (NOAA, 2010) in the Early Holocene. The arrows indicated the direction in which the sea-ice limits and the ITCZ changed.

Westerlies (Markgraf et al., 1992).

Both Lago Villarrica (39°S) and Laguna Parrillar (53°S) contain records of the Southern Westerlies variability during the Holocene (Figure VI-9). For this time window, it is possible to determine whether this variability affected the entire Westerly belt in a synchronous fashion.

There is an overall southward trend present in most of the compared records (Figure VI-9). The ITCZ gradually moves southward, and temperatures decrease steadily in Antarctica, the Lago Villarrica records (log(Si/Fe) and first diatom PCA axis) have this same trend. This large trend is less obvious in the Laguna Parrillar record.

The Southern Westerly winds were relatively weak in the Early Holocene (Figure VI-7). The first signs of intensification are around 7800 cal a BP (Figure VI-9). In Laguna Parrillar, this is best reflected in the log(Al/Fe) proxy record (Figure VI-9). In Lago Villarrica there is a slight drop in the log(Si/Fe) record and an increase in the first diatom PCA axis, which indicates a better mixing of the water column. This intensification did not last very long and was most probably linked to a decrease in temperature in Antarctica. The ITCZ position did not change. This increased intensity is synchronous with Chilean pollen records (Fletcher and Moreno, 2011; Moreno et al., 2010).

Around 6000 cal a BP, there is a clear increase in Southern Westerly activity in Lago Villarrica according to the diatom record (Figure VI-8 and Figure VI-9). There is also a small drop in log(Si/Fe). Laguna Parrillar, however, records weak Westerlies at that time. At this moment the ITCZ started to shift south and temperatures in Antarctica decreased further, synchronous with Antarctic sea-ice expansion (Divine et al., 2010). It is remarkable that Laguna Parrillar does not record this intensification, especially since other lake records in Southern Patagonia started to develop a mounded drift sedimentation around 6800 cal a BP in Lago Cardiel (Gilli et al., 2005) and around 6000 cal a BP in Laguna Potrok Aike (Anselmetti et al., 2009). The latter one is located only 200 km east of Laguna Parrillar. The onset of the build-up of the sediment drift in Lac d'Armor in the Kerguelen Archipelago could have started around this time as well.

There is a clear intensification of the Southern Westerlies around 4000 cal a

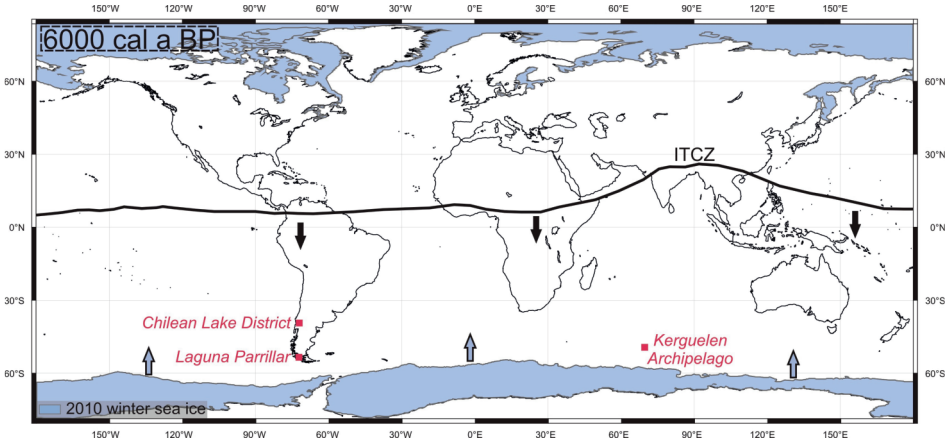

Figure VI-8: Position of the ITCZ (the modern July position is used as a possible northern location of the ITCZ) (Iriondo, 1999)and expansion of the polar sea ice (NOAA, 2010) at 6000 cal a BP. The arrows indicated the direction in which the sea-ice limits and the ITCZ changed.

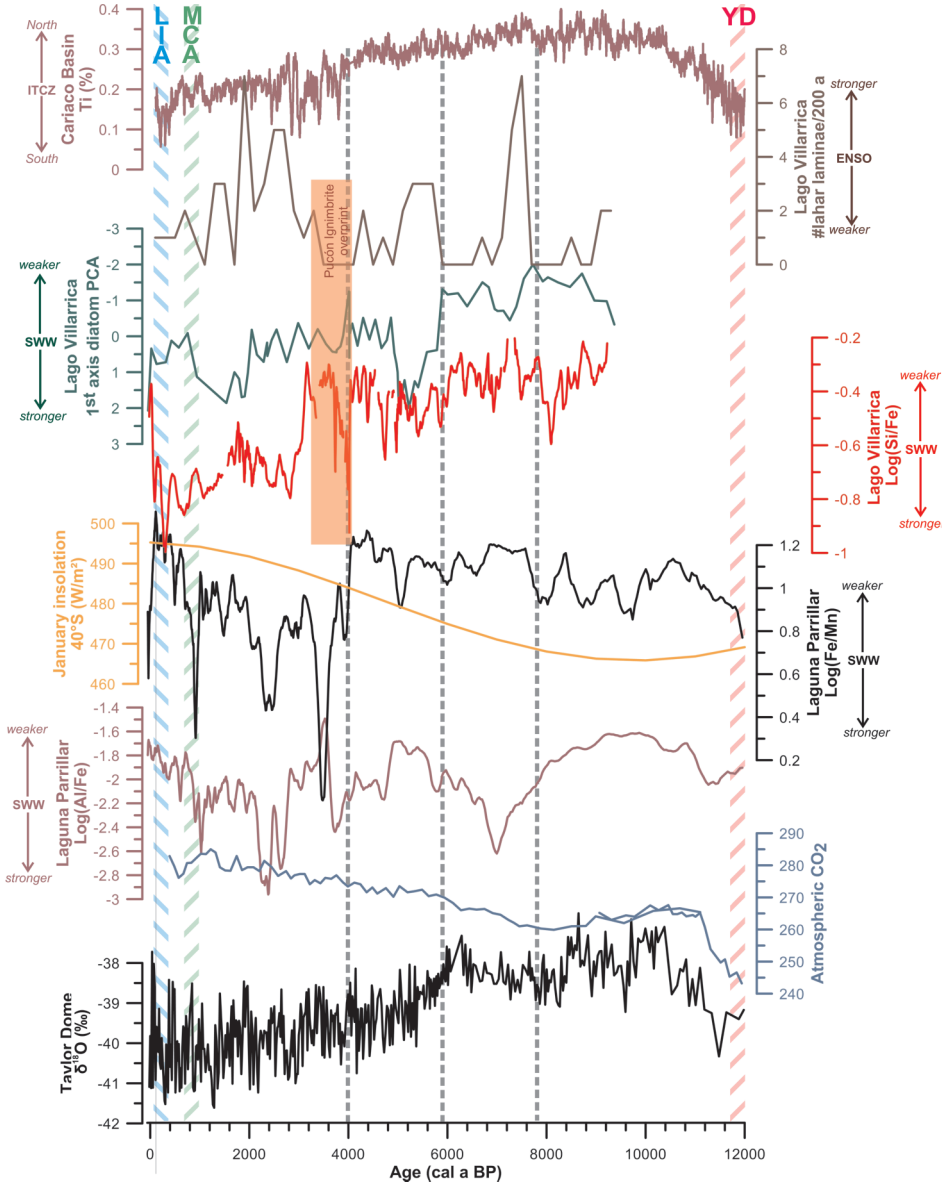

Figure VI-9: Comparison of the Laguna Parrillar log(Fe/Mn) record and the Lago Villarrica log(Si/Fe), the Lago Villarrica first axis of the diatom PCA and the Lago Villarrica record of the quantity of lahar laminae per 200 a with the titanium record of the Cariaco Basin (10°N) (Haug et al., 2001), austral summer solar irradiance at 40°S (Berger, 1978), the atmospheric CO_2 (Indermühle et al., 1999a) record and the $\delta^{18}O$ temperature record of the Antarctic Taylor Dome ice core (Steig et al., 2000) during the Holocene. The dashed lines indicate the onset of a period with more intense Southern Westerlies

BP (Figure VI-9). There is a clear drop in the log(Fe/Mn) record of Laguna Parrillar and the log(Si/Fe) of Lago Villarrica starts to drop as well. The Lago Villarrica record between 4000 and 3000 cal a BP reflects a period of intense volcanic activity. Most likely, the climatic signal has been overprinted by the volcanic signal during this interval. At 4000 cal a BP there is a clear southern shift of the ITCZ (Haug et al., 2001). This second intensification of the Westerly winds could be the start of an even stronger build-up of drift deposits in Lac d'Armor, Kerguelen Archipelago.

During the Medieval Climate Anomaly (MCA) the records of Laguna Parrillar and Lago Villarrica contradict each other (Figure VI-9). The MCA is a period of increased wind stress and most likely precipitation in Southern Patagonia according to the Laguna Parrillar record. Lago Villarrica, on the other hand, seems to have recorded drier conditions and therefore less influence of the Southern Westerlies. The reverse is true for the Little Ice Age (LIA) with drier conditions in Laguna Parrillar and more humid conditions in Lago Villarrica.

The MCA and LIA conditions of Laguna Parrillar are the reverse of Laguna Potrok Aike (Haberzettl et al., 2005) and Laguna Azul (Mayr et al., 2005), both located towards the east, but roughly at the same latitude. Since moisture supply for these two latter lakes depend on easterly wind incursion, they should be in antiphase with Laguna Parrillar, where precipitation is regulated by the Westerlies. Strong Westerlies prevent the incursion of moisture bearing easterlies towards Laguna Potrok Aike and Laguna Azul. The climatic conditions of Laguna Parrillar are, however, also the opposite of those at Lago Guanaco (Moy et al., 2008), another South Patagonian lake that should have recorded the same climate conditions as in Laguna Parrillar as its moisture supply is also regulated by the Southern Westerlies. Since both Lago Villarrica and Laguna Parrillar have issues with their radiocarbon ages, it is possible that this conflicting correlation is the result of inadequate age-depth models. The findings for the MCA and LIA in Lago Villarrica are supported by similar findings in Lago Puyehue (Bertrand et al., 2005; Boës and Fagel, 2008) and off the South-Central Chilean coast (Lamy et al., 2001; Lamy et al., 2002).

Large changes in the Westerlies' intensity seem to be synchronous at both edges of the Westerly belt during the Holocene. Short-term variations, like the MCA and LIA, seem to indicate that this is not the case. Since 4000 cal a BP El Niño-Southern Oscillation (ENSO) activity has increased drastically as can be seen in the increase of lahar laminae in the Lago Villarrica record and in other records around the South Pacific (Conroy et al., 2008; Gagan et al., 2004; Moy et al., 2002; Rein et al., 2005). Perthaps the increased ENSO caused the Westerlies to behave in antiphyase between northern and southern Patagonia.

VI. 5. Future Southern Westerlies

Model simulations from the mid 1990s hinted that there might be a small intensification and a poleward shift of the Southern Westerlies in our greenhouse future (Watson et al., 2001). Current coupled models produce much more substantial poleward shifts in their greenhouse warming scenario runs (Stouffer et al., 2006).

In the projections of future climate (Russell et al., 2005), Southern Westerly winds over the Southern Ocean will intensify as the climate warms. This leads to more divergence, greater ventilation, and the potential for enhanced storage of heat and anthropogenic carbon dioxide by the ocean. If continuing intensification of the Southern Westerlies outpaces the ocean warming and stratification associated with increases in

atmospheric carbon dioxide, the deep ocean has the potential to slow the warming of the atmosphere through the increased storage of heat and carbon.

VI.6. Southern Westerlies and ENSO

Modern data show a strong influence of ENSO on both the behaviour of Antarctic sea-ice (Simmonds and Jacka, 1995) and on the latitudinal position of the Southern Westerlies in South America (Cerveny, 1998; Karoly, 1989).

During the warm phase of ENSO (El Niño years), a weakening of the Southeast Pacific anticyclone results in a northward shift of the Southern Westerlies leading to wet anomalies in central Chile (30-38°S). Conversely, a strengthening and southward expansion of the anticyclone results in more poleward located westerly storm tracks reducing winter rain in the Mediterranean climate zone of Chile (30-38°S) , while the region between 38-41°S will receive much more rain during the La Niña state.

Rein et al. (2004) and Mohtadi et al. (2007) claim the MCA was a period of reduced ENSO activity. Consequently the region of Lago Villarrica should receive more rain (Montecinos and Aceituno, 2003). This is, however, in contradiction with the Lago Villarrica and Lago Puyehue record (Bertrand et al., 2005; Boës and Fagel, 2008), which indicate drier conditions. The peak in lahar laminae during the MCA might indicate more a stronger ENSO signal (Figure VI-9). The same contradiction is valid for the LIA (Figure VI-9). Such contradictions only point out how little we understand of the world's climate system.

References

Ahn, J. and Brook, E.J., 2008. Atmospheric CO2 and climate on millennial time scales during the last glacial period. *Science*, **322**: 83-85.

Anderson, R.F., Ali, S., Bradtmiller, L.I., Nielsen, S.H.H., Fleisher, M.Q., Anderson, B.E. and Burckle, L.H., 2009. Wind-driven upwelling in the southern ocean and the deglacial rise in atmospheric CO2. *Science*, **323**: 1443-1448.

Anselmetti, F.S., Ariztegui, D., De Batist, M., Gebhardt, A.C., Haberzettl, T., Niessen, F., Ohlendorf, C. and Zolitschka, B., 2009. Environmental history of southern Patagonia unravelled by the seismic stratigraphy of Laguna Potrok Aike. *Sedimentology*, **56**(4): 873-892.

Bentley, M.J., 1997. Relative and radiocarbon chronology of two former glaciers in the Chilean Lake District. *Journal of Quaternary Science*, **12**: 25-33.

Berger, A.L., 1978. Long-Term Variations of Caloric Insolation Resulting from Earths Orbital Elements. *Quaternary Research*, **9**(2): 139-167.

Bertler, N.A.N., Naish, T.R., Oerter, H., Kipfstuhl, S., Barrett, P.J., Mayewski, P.A. and Kreutz, K.J., 2006. The effects of joint ENSO-Antarctic Oscillation forcing on the McMurdo Dry Valleys, Antarctica. *Antarctic Science*, **18**: 507-514.

Bertrand, S., Boes, X., Castiaux, J., Charlet, F., Urrutia, R., Espinoza, C., Lepoint, G., Charlier, B. and Fagel, N., 2005. Temporal evolution of sediment supply in Lago Puyehue (Southern Chile) during the last 600 yr and its climatic significance. *Quaternary Research*, **64**(2): 163-175.

Boës, X. and Fagel, N., 2008. Relationship between southern Chilean varved lake sediments, precipitation and ENSO for the last 600 years. *Journal of Paleolimnology*, **39**(2): 237-252.

Cerveny, R.S., 1998. Present climates of South America. In: J.E. Hobbs, J.A. Lindesay and H.A. Bridgman (Editors), *Climates of the southern continents: Present, past and future*. John Wiley & Sons, Chichester, pp. 107-135.

Charlet, F., Chapron, E., De Batist, M., Pino, P. and Urrutia, R., 2008. Seismic stratigraphy of Lago Puyehue (Chilean Lake District): new views on its deglacial and Holocene evolution. *Journal of Paleolimnology*, **39**: 163-177.

Chiang, J.C.H. and Bitz, C.M., 2005. Influence of high latitude ice cover on the marine Intertropical Convergence Zone. *Climate Dynamics*, **25**(5): 477-496.

Conroy, J.L., Overpeck, J.T., Cole, J.E., Shanahan, T.M. and Steinitz-Kannan, M., 2008. Holocene changes in eastern tropical Pacific climate inferred from a Galápagos lake sediment record. *Quaternary Science Reviews*, **27**: 1166-1180.

Dahl, K.A., Broccoli, A.J. and Stouffer, R.J., 2005. Assessing the role of North Atlantic freshwater forcing in millennial scale climate variability: a tropical Atlantic perspective. *Climate Dynamics*, **24**(4): 325-346.

Denton, G.H., Lowell, T.V., Heusser, C.J., Schlüchter, C., Andersen, B.G., Heusser, L.E., Moreno, P.I. and Marchant, D.R., 1999. Geomorphology, stratigraphy, and radiocarbon chronology of Llanquihue drift in the area of the southern Lake District, Seno Reloncaví, and Isla Grande de Chiloé, Chile. *Geografiska Annaler*, **81A**(2): 167-229.

Divine, D.V., Koc, N., Isaksson, E., Nielsen, S., Crosta, X. and Godtliebsen, F., 2010. Holocene Antarctic climate variability from ice and marine sediment cores: Insights on ocean-atmosphere interaction. *Quaternary Science Reviews*, **29**(1-2): 303-312.

Fitzharris, B.B., Clare, G.R. and Renwick, J., 2007. Teleconnections between Andean and New Zealand glaciers. *Global and Planetary Change*, **59**(1-4): 159-174.

Fletcher, M.-S. and Moreno, P.I., 2011. Zonally symmetric changes in the strenght and position of the Southern Westerlies drove atmospheric CO2 variations over the past 14 k.y. *Geology*, **39**(5): 419-422.

Gagan, M.K., Hendy, E.J., Haberle, S.G. and Hantoro, W.S., 2004. Post-glacial

evolution of the Indo-Pacific Warm Pool and El Niño-Southern oscillation. *Quaternary International*, **118-119**: 127-143.

Gillett, N.P., Kell, T.D. and Jones, P.D., 2006. Regional climate impacts of the Southern Annular Mode. *Geophysical Research Letters*, **33**(23): L23704.

Gilli, A., Ariztegui, D., Anselmetti, F.S., McKenzie, J.A., Markgraf, V., Hajdas, I. and McCulloch, R.D., 2005. Mid-Holocene strengthening of the Southern westerlies in South America - Sedimentological evidences from Lago Cardiel, Argentina (49°S). *Global and Planetary Change*, **49**(1-2): 75-93.

Haberzettl, T., Fey, M., Lucke, A., Maidana, N., Mayr, C., Ohlendorf, C., Schabitz, F., Schleser, G.H., Wille, M. and Zolitschka, B., 2005. Climatically induced lake level changes during the last two millennia as reflected in sediments of Laguna Potrok Aike, southern Patagonia (Santa Cruz, Argentina). *Journal of Paleolimnology*, **33**(3): 283-302.

Haug, G.H., Hughen, K.A., Sigman, D.M., Peterson, L.C. and Rohl, U., 2001. Southward migration of the intertropical convergence zone through the Holocene. *Science*, **293**(5533): 1304-1308.

Heirman, K., De Batist, M., Charlet, F., Moernaut, J., Chapron, E., Brümmer, R., Pino, M. and Urrutia, R., in press. Detailed seismic stratigraphy of Lago Puyehue: implications for the mode and timing of glacier retreat in the Chilean Lake District. *Journal of Quaternary Science*.

Hemming, N.G., 2004. Heinrich events: massive late Pleistocene detritus layers of the North Atlantic and their global climate imprint. *Review of Geophysics*, **42**: RG1005.

Heusser, C.J., 1989. Southern westerlies during the last glacial maximum. *Quaternary Research*, **31**: 423-425.

Indermühle, A., Monnin, E., Stauffer, B., Stocker, T.F. and Wahlen, M., 1999a. Atmospheric CO2 concentration from 60 to 20 kyr BP from the Taylor Dome ice core, Antarctica. *Geophysical Research Letters*, **27**: 735-738.

Indermühle, A., Stocker, T.F., Joos, F., Fischer, H., Smith, H.J., Wahlen, M., Deck, B., Mastroianni, D., Tschumi, J., Blunier, T., Meyer, R. and Stauffer, B., 1999b. Holocene carbon-cycle dynamics based on CO2 trapped in ice at Taylor Dome, Antarctica. *Nature*, **398**: 121-126.

Kaplan, M.R., D.C.Douglass, Singer, B.S., Ackert, R.P. and Caffee, M.W., 2005. Cosmogenic nuclide chronology of pre-last glacial maximum moraines at Lago Buenos Aires, 46°S, Argentina. *Quaternary Research*, **63**: 301-315.

Karoly, D.J., 1989. Southern Hemisphere Circulation Features Associated with El Niño-Southern Oscillation Events. *Journal of Climate*, **2**(11): 1239-1252.

Lamy, F., Hebbeln, D., Röhl, U. and Wefer, G., 2001. Holocene rainfall variability in southern Chile: a marine record of latitudinal shifts of the Southern Westerlies. *Earth and Planetary Science Letters*, **185**: 369-382.

Lamy, F., Kaiser, J., Arz, H.W., Hebbeln, D., Ninnemann, U., Timm, O., Timmermann, A. and Toggweiler, J.R., 2007. Modulation of the bipolar seesaw in the Southeast Pacific during Termination I. *Earth and Planetary Science Letters*, **259**: 400-413.

Lamy, F., Ruhlemann, C., Hebbeln, D. and Wefer, G., 2002. High- and low-latitude climate control on the position of the southern Peru-Chile Current during the Holocene. *Paleoceanography*, **17**(2): 1028.

Lowell, T.V., Heusser, C.J., Andersen, B.G., Moreno, P.I., Hauser, A., Heusser, L.E., Schluchter, C., Marchant, D.R. and Denton, G.H., 1995. Interhemispheric Correlation of Late Pleistocene Glacial Events. *Science*, **269**(5230): 1541-1549.

Markgraf, V., 1989. Reply to C.J. Heusser's "Southern westerlies during the last glacial maximum". *Quaternary Research*, **31**: 426-432.

Markgraf, V., Dodson, J.R., Kershaw, P.A., McGlone, M.S. and Nicholls, N., 1992. Evolution of late Pleistocene and Holocene climates in the circum-South

Pacific land areas. *Climate Dynamics*, **6**: 193-211.
Mayr, C., Fey, M., Haberzettl, T., Janssen, S., Lucke, A., Maidana, N.I., Ohlendorf, C., Schabitz, F., Schleser, G.H., Struck, U., Wille, M. and Zolitschka, B., 2005. Palaeoenvironmental changes in southern Patagonia during the last millennium recorded in lake sediments from Laguna Azul (Argentina). *Palaeogeography Palaeoclimatology Palaeoecology*, **228**(3-4): 203-227.
McCulloch, R.D., Bentley, M.J., Purves, R.S., Hulton, N.R.J., Sugden, D.E. and Clapperton, C.M., 2000. Climatic inferences from glacial and paleaoecological evidence at the last glacial termination, southern South America. *Journal of Quaternary Science*, **15**(4): 409-417.
McCulloch, R.D., Bentley, M.J., Tipping, R.M. and Clapperton, C.M., 2005a. Evidence for late-glacial ice dammed lakes in the central Strait of Magellan and Bahia Inutil, southernmost South America. *Geografiska Annaler Series A - Physical Geography*, **87A**(2): 335-362.
McCulloch, R.D., Fogwill, C.J., Sugden, D.E., Bentley, M.J. and Kubik, P.W., 2005b. Chronology of the last glaciation in central Strait of Magellan and Bahia Inutil, southernmost South America. *Geografiska Annaler Series A - Physical Geography*, **87A**(2): 289-312.
McManus, J.F., Francois, R., Gherardi, J.M., Keigwin, L.D. and Brown-Leger, S., 2004. Collapse and rapid resumption of Atlantic meridional circulation linked to deglacial climate changes. *Nature*, **428**(6985): 834-837.
Mohtadi, M., Romero, O.E., Kaiser, J. and Hebbeln, D., 2007. Cooling of the southern high latitudes during the Medieval Period and its effect on ENSO. *Quaternary Science Reviews*, **26**: 1055-1066.
Montecinos, A. and Aceituno, P., 2003. Seasonality of the ENSO-Related Rainfall Variability in Central Chile and Associated Circulation Anomalies. *Journal of Climate*, **16**(2): 281-296.
Moreno, P.I., Francois, J.-P., Moy, C.M. and Villa-Martínez, R., 2010. Covariability of the Southern Westerlies and atmospheric CO2 during the Holocene. *Geology*, **38**: 727-730.
Moy, C.M., Dunbar, R.B., Moreno, P.I., Francois, J.-P., Villa-Martínez, R., Mucciarone, D.M., Guilderson, T.P. and Garreaud, R.D., 2008. Isotopic evidence for hydrologic change related to the westerlies in SW Patagonia, Chile, during the last millenium. *Quaternary Science Reviews*, **27**: 1335-1349.
Moy, C.M., Seltzer, G.O., Rodbell, D.T. and Anderson, D.M., 2002. Variability of El Niño/Southern Oscillation activity at millennial timescales during the Holocene epoch. *Nature*, **420**: 162-165.
Peterson, L.C. and Haug, G.H., 2006. Variability in the mean latitude of the Atlantic Intertropical Convergence Zone as recorded by riverine input of sediments to the Cariaco Basin (Venezuela). *Palaeogeography Palaeoclimatology Palaeoecology*, **234**(1): 97-113.
Rasmussen, S.O., Andersen, K.K., Svensson, A.M., Steffensen, J.P., Vinther, B.M., Clausen, H.B., Siggaard-Andersen, M.L., Johnsen, S.J., Larsen, L.B., Dahl-Jensen, D., Bigler, M., Rothlisberger, R., Fischer, H., Goto-Azuma, K., Hansson, M.E. and Ruth, U., 2006. A new Greenland ice core chronology for the last glacial termination. *Journal of Geophysical Research - Atmospheres*, **111**(D6): D06102.
Rein, B., Lückge, A., Reinhardt, L., Sirocko, F., Wolf, A. and Dullo, W.-C., 2005. El Niño variability off Peru during the last 20,000 years. *Paleoceanography*, **20**(4): PA4003.
Rein, B., Lückge, A. and Sirocko, F., 2004. A major Holocene ENSO anomaly during the Medieval period. *Geophysical Research Letters*, **31**: L17211.
Russell, J.L., Dixon, K.W., Gnanadesikan, A., Stouffer, R.J. and Toggweiler, J.R., 2005. The Southern Hemisphere Westerlies in a warming world: Propping open the door to the deep ocean. *Journal of Climate*, **19**: 6382-6390.

Shindell, D.T. and Schmidt, G.A., 2004. Southern Hemisphere climate response to ozone changes and greenhouse gas increases. *Geophysical Research Letters*, **31**(18): L18209.

Simmonds, T. and Jacka, H., 1995. Relationship between the interannual variability of Antarctic sea-ice and the Southern Oscillation index. *Journal of Climate*, **8**: 637-647.

Steig, E.J., Brook, E.J., White, J.W.C., Sucher, C.M., Bender, M.L., Lehman, S.J., Morse, D.L., Waddington, E.D. and Clow, G.D., 1998. Synchronous climate changes in Antarctica and the North Atlantic. *Science*, **282**(5386): 92-95.

Steig, E.J., Morse, D., Waddington, E.D., Stuiver, M., Grootes, P., Mayewski, P., Twickler, M.S. and Whitlow, S., 2000. Wisconsinan and Holocene climate history from an ice core at Taylor Dome, western Ross Embayment, Antarctica. ***Geografiska Annaler***, **82A**: 213-235.

Sterken, M., Verleyen, E., Sabbe, K., Terryn, G., Charlet, F., Bertrand, S., Boës, X., Fagel, N., Batist, M.D. and Vyverman, W., 2008. Late Quaternary climatic changes in southern Chile, as recorded in a diatom sequence of Lago Puyehue (40°40' S). *Journal of Paleolimnology*, **39**: 219-235.

Stouffer, R.J., Yin, J., Gregory, J.M., Dixon, K.W., Spelman, M.J., Hurlin, W., Weaver, A.J., Eby, M., Flato, G.M., Hasumi, H., Hu, A., Jungclaus, J.H., Kamenkovich, I.V., Levermann, A., Montoya, M., Murakami, S., Nawrath, S., Oka, A., Peltier, W.R., Robitaille, D.Y., Sokolov, A., Vettoretti, G. and Weber, S.L., 2006. Investigating the causes of the response of the Thermohaline Circulation to past and future climate changes. *Journal of Climate*, **19**: 1365-1387.

Streten, N.A. and Zillman, J.W., 1984. Climate of the South Pacific. In: H. van Loon (Editor), *Climates of the Oceans*. Elsevier, Amsterdam, The Netherlands, pp. 26-429.

Tierney, J.E. and Russell, J.M., 2007. Abrupt climate change in southeast tropical Africa influenced by Indian monsoon variability and ITCZ migration. *Geophysical Research Letters*, **34**: L15709.

Toggweiler, J.R., Russell, J.L. and Carson, S.R., 2006. Midlatitude westerlies, atmospheric CO2, and climate change during the ice ages. *Paleoceanography*, **21**(2): PA2005.

Verschuren, D., Sinninghe Damste, J.S., Moernaut, J., Kristen, I., Blaauw, M., Fagot, M. and Haug, G.H., 2009. Half-precessional dynamics of monsoon rainfall near the East African Equator. *Nature*, **462**(7273): 637-641.

Wang, Y.J., Cheng, H., Edwards, R.L., An, Z.S., Wu, J.Y., Shen, C.C. and Dorale, J.A., 2001. A high-resolution absolute-dated Late Pleistocene monsoon record from Hulu Cave, China. *Science*, **294**(5550): 2345-2348.

Watson, R.T., Albritton, D.L., Barker, T., Bashmakov, I.A., Canziani, O., Christ, R., Cubasch, U., Davidson, O., Gitay, H., Griggs, D., Halsnaes, K., Houghton, J., House, J., Kundzewicz, Z., Lal, M., Leary, N., Magadza, C., McCarthy, J.J., Mitchell, J.F.B., Moreira, J.R., Munasinghe, M., Noble, I., Pachauri, R., Pittock, B., Prather, M., Richels, R.G., Robinson, J.B., Sathaye, J., Schneider, S., Scholes, R., Stocker, T., Sundararaman, N., Swart, R., Taniguchi, T. and Zhou, D., 2001. *Climate Change 2001: Synthesis Report, IPCC*. Cambridge University Press, Cambridbe.

Whittaker, T.E., Hendy, C.H. and Hellstrom, J.C., 2011. Abrupt millenial-scale changes in intensity of Southern Hemisphere winds during marine isotope stage 2-4. *Geology*, **39**(5): 455-458.

Zhang, R. and Delworth, T.L., 2005. Simulated Tropical Response to a Substantial Weakening of the Atlantic Thermohaline Circulation. *Journal of Climate*, **18**(12): 1853-1860.

VII. Conclusions

"A conclusion is the place where you got tired thinking."
(Martin H. Fischer)

Palaeoclimate research is one of the few reliable tools to reconstruct climate conditions in the past and to evaluate how fast natural systems can change. The analysis of sediment is one of the most powerful means to reconstruct the history of the Quaternary period. In this thesis lake basins were analysed on a large spatial and temporal scale, using high-resolution reflection seismic surveying, and a smaller spatial and temporal scale, using lake sediment cores. Both techniques revealed important past climatic changes, which could all be linked to changes in the behaviour of the Southern Westerly winds.

VII.1. Low-resolution Climate Variability through Space and Time

VII.1.1. Chilean Lake District

The high-resolution reflection seismic profiles of four lakes (Lago Villarrica, Lago Calafquén, Lago Panguipulli and Lago Riñihue) revealed the presence of four important seismic unconformities in each lake basin. The occurrence of these unconformities makes the seismic stratigraphy of these Chilean, glacigenic lakes different from the common seismic stratigraphy of glacigenic lakes in other parts of the world (e.g. the European Alps or North America). Generally only two of these unconformities are present, one delimiting the boundary between the acoustic basement and the lake-basin infill and the second one between the glacial/ice-contact deposits and the glaciolacustrine deposits. Similar to the two unconformities in the general model, all four unconformities in the Chilean lakes were probably created by glacial activity. The fact that more of these unconformities are present indicates that the last advances and retreats of the glaciers in each of these four basins were less extensive, less powerful and probably not as long lasting than the glacial advances which created the oldest unconformity. The smaller size of these glaciers during the last advances is supported by geomorphological studies around these lakes (Laugenie, 1982). This information can be considered as a sign that the climatic situations in the mid-latitudes of the Southern Hemisphere were different from the Northern Hemisphere were the glacier advances during OIS 2 were the most extensive of the entire last glacial period.

Since no absolute ages are available for the four unconformities, it is difficult to create a time frame for these events. Few records of absolutely dated pre-Last Glacial Maximum glacial advances are available in the mid-latitudes of the Southern Hemisphere. Most of them indicate that the most extensive advances of the last glacial period occurred during OIS 3. The advances during OIS 2 were less extensive and most of them took place between 25000 and 35000 cal a BP.

VII.1.2. Kerguelen Archipelago

The seismic stratigraphy of Lac d'Armor, compared to the Chilean lakes, does not differ from the general model, only two unconformities are present. The most remarkable feature of the seismic stratigraphy in this lake is the formation of sediment drift deposits during the deposition of the youngest seismic unit. Such a construction indicates the presence of strong bottom currents. A likely creator of such currents is wind. Currently the force of the Southern Westerly wind in Kerguelen should not be underestimated. The sudden onset of these sediment drifts argues for a sudden strengthening of the Southern Westerlies somewhere in the Holocene. Again an absolutely dated time frame is missing for this seismic records, so only estimates can be made for its timing.

Lake seismic stratigraphic studies at similar latitudes in South America have dated the onset of their drift deposits somewhere between 7000 and 6000 cal a BP (Anselmetti et al., 2009; Gilli et al., 2005). This can be used as a lead to date the strengthening of the Southern Westerlies around Kerguelen.

VII.2. High-resolution Climate Variability through Time

VII.2.1. Lago Villarrica

A Holocene sediment record of Lago Villarrica disclosed information about Holocene changes in the strength and position of the Southern Westerlies. During the Early Holocene the Southern Westerlies' strength was weakened and/or the Westerlies had shifted more poleward. Around 6000 cal a BP the Southern Westerlies' influence increased in the area, but the largest intensification occurred around 4000 cal a BP.

The Lago Villarrica record is not only a good record for the Southern Westerlies, but contain also traces of changes in the activity of the El Niño Southern Oscillation (ENSO). There is a strong increase in ENSO activity around 4000 cal a BP. This is synchronous with other ENSO records in the South Pacific. The Villarrica record reveals also older periods of increased ENSO strength or an ENSO-type climate signal between 5000 and 9000 cal a BP. Atmospheric conditions were very different from today with lower seasonal solar irradiance variability and stronger Hadley cell activity.

VII.2.2. Laguna Parrillar

The 44000 year long sediment record of Laguna Parrillar revealed drastic changes in the Southern Westerly wind's intensity. From 44000 cal a BP until ca. 12500 cal a BP the lake environment and lake level was mostly controlled by the thickness of its glacial dam, since the main outlet was blocked by the Magellan Strait glacier. When the Magellan Strait glacier receded the lake level would have been lower. As glacier advances are largely controlled by Westerly wind intensity, a retreat of the glacier dam reflected a decrease in the Southern Westerly wind strength. Another important factor affecting the lake sedimentation during this period is the duration of the ice cover of the lake. During cold periods, probably associated with strong Westerlies, the lake was completely frozen during the entire year. In times of weaker Southern Westerlies, there might have been periods when the lake was ice free. After 12500 cal a BP the sedimentation in the lake basin became controlled by the wind, the Southern Westerly wind. The strong, persistent wind creates waves and induces bottom currents in the lake which highly affect the lake sedimentation. A first sign of Holocene Westerly wind strengthening appears around 7800 cal a BP. Shortly after this the wind strength appears to decrease again. A more obvious strengthening of the Southern Westerlies occurred at ca. 4000 cal a BP, since then the intensity of the Westerly winds remained high.

VII.3. Changes in the Southern Westerlies' Intensity and Position

Advances of the glaciers in the Southern Andes during the last century have been linked to periods of more intense Southern Westerlies (Fitzharris et al., 2007). Increased Southern Westerly wind strength has also been used as an argument for glacial advances in the Holocene and during the last glacial period in the Southern Alps of New Zealand (Putnam et al., 2010; Schaefer et al., 2009; Shulmeister et al., 2010). The Southern Westerlies control the amount of precipitation in the southern mid-latitudes. Stronger and more intense Westerlies will cause an increase in the precipitation amount in this

region. The behaviour of the temperate glaciers in the southern mid-latitudes is largely dependent of the amount of precipitation supplied to the ablation area and therefore dependent of the Southern Westerly wind strenght.

The lack of an absolutely dated age frame in the seismic records in both the Chilean Lake District and the Kerguelen Archipelago does not allow these records to be linked to other records of climate change on a regional or global scale. They only tell us that there is evidence of change in the Westerly winds' strength.

The two sediment core records of Lago Villarrica and Laguna Parrillar, which are absolutely dated, were linked to existing palaeoclimate records. Since the Lago Villarrica record only spans the Holocene, this is the only time period during which the shifting position of the Southern Westerlies can be evaluated. The millenial changes in both Laguna Parrillar and Lago Villarrica are broadly synchronous, both recording changes in the intensity of the Southern Westerlies. Because of this synchronous behaviour, the debate surrounding shifts in the position of the Southern Westerlies remains. Possibly only the core of the Southern Westerlies shifts and the boundaries of the Westerly wind cell contract or expand north- or southward.

On a centennial time scale the changes in both lakes are not synchronous. The climate conditions during the Medieval Climate Anomaly (MCA) were probably wetter in Laguna Parrillar, but drier in Lago Villarrica. The reverse is true during the Little Ice Age (LIA). In South America MCA and LIA have also been linked to changes in the El Niño Southern Oscillation (ENSO) activity, a decrease and increase respectively. Maybe the strength of the ENSO signal influences how effectively the Southern Westerlies will affect climate at its northern edge (e.g. the Lago Villarrica area) of the wind belt. The Early Holocene ENSO(-type) signal recorded in Lago Villarrica does not seem to affect the Southern Westerly winds' behaviour as strongly. Still the Lago Villarrica record shows that ENSO variability was not absent in the Early Holocene and that there is still a lot to learn about climate dynamics inducing ENSO variability.

In general it seems that changes in the Southern Westerlies' strength can be linked to changes in the position of the ITCZ and the sea-ice extent both in the Arctic and Antarctic. This illustrates the importance of a global perspective on climate change, since all the different climate components are connected, and can induce and/or transmit climatic changes in each others behaviour.

References

Anselmetti, F.S. et al., 2009. Environmental history of southern Patagonia unravelled by the seismic stratigraphy of Laguna Potrok Aike. *Sedimentology*, **56**(4): 873-892.

Fitzharris, B.B., Clare, G.R. and Renwick, J., 2007. Teleconnections between Andean and New Zealand glaciers. *Global and Planetary Change*, **59**(1-4): 159-174.

Gilli, A. et al., 2005. Mid-Holocene strengthening of the Southern westerlies in South America - Sedimentological evidences from Lago Cardiel, Argentina (49°S). *Global and Planetary Change*, **49**(1-2): 75-93.

Laugenie, C., 1982. *La région des lacs, Chili méridional*, Université de Bordeaux III, Bordeaux, France, 822 pp.

Putnam, A.E. et al., 2010. Glacier advance in southern middle-latitudes during the Antarctic Cold Reversal. *Nature Geoscience*, **3**: 700-704.

Schaefer, J.M. et al., 2009. High-frequency Holocene glacier fluctuations in New Zealand differ from the northern signature. *Science*, **324**: 622-625.

Shulmeister, J. et al., 2010. The stratigraphy, timing and climatic implications of glaciolacustrine deposits in the middle Rakaia Valley, South Island, New Zealand. *Quaternary Science Reviews*, **29**(17-18): 2362-2381.

VIII. Outlook

This thesis addressed certain scientific questions about the climate of the Southern Hemisphere mid-latitudes and the Southern Westerlies in the Late Quaternary. These result will be a contribution to a better understanding of these topics. But as always, answers raise more questions. It's digging into those never-ending layers of questions beneath answers that keeps science going.

VIII.1. Low-resolution Climate Variability through Space and Time

The most important thing missing in both seismic stratigraphic lake-basin studies is the lack of an absolutely dated time frame.

In the Chilean Lake District, it will not be easy to obtain sediment cores penetrating through the different seismic unconformities. They are located very deep into the sediment. Most lake coring devices are not equipped to drill down to such depths. Another possible issue is that most of these unconformities are capped by glacial/ice-contact deposits like till. Such deposits contain a lot of rocks and are often hard due to compaction by the weight of the overriding glacier. The penetration of such deposits before reaching the unconformity surface itself will greatly increase the difficulty of the sediment coring. However, if these surfaces could be dated this would add a great value to the understanding of the Patagonian ice sheet behaviour and glacial conditions in the Southern Hemisphere in general.

A way around the coring issues would be dating the moraines around the four lakes, since this has never been done before, only the moraines of the southern lakes of the Chilean Lake District have been dated. Another option is to core, analyse and date sediments of peat bogs and/or small ponds located in between the different moraines or just outside the moraine limits.

Currently there is a large discrepancy in Lago Puyehue between the ages obtained from moraines and the timing of climatic change recorded in the lake sediment itself. It should be tested if this is also the case in and around other Chilean lakes.

A long sediment core from Lac d'Armor, Kerguelen Archipelago, will definitely add value to the seismic stratigraphy as it will allow to construct a time frame for the events recorded in the seismic stratigraphy. Also there are hardly any long climate records available for this group of islands, making any dated climate record a valuable addition to the current gap of information that currently exists in this area.

VIII.2. High-resolution Climate Variability through Time

Both lake records, Laguna Parrillar and Lago Villarrica have radiocarbon age issues since bulk sediment had to be used to obtain the radiocarbon ages. Alternative techniques like varve counting and/or the development of a reliable tephrochronology will allow the construction of a much better age-depth model.
Since the Lago Villarrica record only spans the Holocene, it would be good to obtain records of changes in the Westerlies' intensity that span a larger period of time. This will also allow a better understanding of the term shift. Maybe Lago Villarrica is located not far enough north to truly detect the effects of changes in the position of the Southern Westerlies. It might be a good idea to obtain high resolution and long records of more northern latitudes.

The very exploratory seismic survey of Laguna Parrillar revealed there is more sediment present below the 7 m that was recovered. This implies that there is even an older record of changes of the Southern Westerlies available in this lake basin.

To evaluate the behaviour of the Southern Westerlies through time, Westerly wind records should be constructed on different locations scattered along the mid-latitudes of the Southern Hemisphere with extra attention to locations at the edges of

the Westerly belt. This is the only way to estimate the conduct of this wind system and how it is affected by and influences global atmospheric circulation patterns.

The driver behind ENSO activity in the Late Holocene has already been studied in detail and although it is not yet fully understood, much attention is given to ENSO changes in this period of time. The occurrence of ENSO in the Early Holocene, however, is documented, but it is still not understood why ENSO events occurred, since the climate conditions were very different from the Late Holocene conditions. It is also remarkable that Early Holocene ENSO records have only been reported on the eastern side of the Southern Pacific.